

Large Break LOCA Code Applicability Report for US-APWR

Non-Proprietary Version

March 2014

**© 2014 Mitsubishi Heavy Industries, Ltd.
All Rights Reserved**

February 24, 2014

Mr. Yoshiki Ogata, General Manager
APWR Promoting Department
Mitsubishi Heavy Industries, Ltd.
16-5, Konan 2-Chome, Minato-Ku
Tokyo, 108-8215 Japan

SUBJECT: UNITED STATES - ADVANCED PRESSURIZED WATER REACTOR REVISED
FINAL TOPICAL REPORT SAFETY EVALUATION FOR TOPICAL REPORTS
MUAP-07011-P, "LARGE BREAK LOCA CODE APPLICABILITY REPORT FOR
US-APWR," REVISION 4; AND MUAP-07013-P, "SMALL BREAK LOCA
METHODOLOGY FOR US-APWR," REVISION 3

Dear Mr. Ogata:

The U.S. Nuclear Regulatory Commission (NRC) staff issued final Topical Report Safety Evaluations (TRSEs) for Topical Reports MUAP-07011-P, "Large Break LOCA Code Applicability Report for US-APWR," Revision 3; and MUAP-07013-P, "Small Break LOCA Methodology for US-APWR," Revision 2 on May 14, 2013. This action was supported by Advisory Committee on Reactor Safeguards (ACRS) letter dated April 29, 2013 (Agencywide Documents Access and Management System (ADAMS) accession number ML13105A219), whereby the ACRS agrees with the NRC staff's conclusions, within the limits and conditions that are specified in the TRSE.

Both topical reports describe the codes and methods (calculation framework) used to calculate the emergency core cooling acceptance parameters given in Title 10 of the *Code of Federal Regulations* Section 50.46, "Acceptance criteria for emergency core cooling systems for light-water nuclear power reactors." The final comparison of the calculated and acceptance criteria values is given in the United States - Advanced Pressurized Water Reactor, Design Certification Document (DCD), Section 15.6.5, "Loss-of-Coolant Accidents Resulting from Spectrum of Postulated Piping Breaks within the Reactor Coolant Pressure Boundary."

Consistent with conclusions made in the February 5, 2014, final TRSE for Topical Report MUAP-07001-P, "The Advanced Accumulator," Revision 5, the staff's larger scaling biases are applied to the DCD Section 15.6.5 loss of coolant (LOCAs) analyses. This is supported by the ACRS in a letter dated January 6, 2014, (ADAMS accession number ML13352A413), Mitsubishi Heavy Industries, Ltd. (MHI) has agreed to the staff's (larger) scaling biases (large and small flow rates) and has since issued MUAP-07011, Revision 4 on December 4, 2013, and MUAP-07013, Revision 3 on December 5, 2013, to reflect these conclusions.

The changes reflected in MUAP-07011, Revision 4 and MUAP-07013, Revision 3 are editorial in nature as no changes to the calculation framework presented in MUAP-07011, Revision 3 and MUAP-07013, Revision 2 were necessary because the scaling biases are model inputs. The effects of the revised scaling biases will be reflected in a revision to the Tier 2, DCD Section 15.6.5 LOCA analyses results. Therefore, the staff's enclosed TRSEs, associated with

Y. Ogata

- 2 -

MUAP-07011, Revision 3 and MUAP-07013, Revision 2, also apply to MUAP-07011, Revision 4 and MUAP-07013, Revision 3 unchanged from their May 14, 2013, issuance.

The staff requests that MHI publish the accepted proprietary and non-proprietary versions of MUAP-07011, Revision 4 and MUAP-07013, Revision 3 within one month of receipt of this letter. The accepted versions shall incorporate this letter and the enclosed final TRSEs after the title page. Also, they must contain historical review information, including NRC requests for additional information and your responses. The accepted versions of the topical reports shall include an "-A" (designated accepted) following the report identification number.

If the NRC's criteria or regulations change, so that its conclusion that the accepted topical report is invalidated, MHI and/or the applicant referencing the topical report will be expected to revise and resubmit its respective documentation, or submit justification for continued applicability of the topical report without revision of the respective documentation.

If you have any questions or comments concerning this matter, I can be reached at (301) 415-1383 or via e-mail address at Perry.Buckberg@nrc.gov.

Sincerely,

/RA/

Perry Buckberg, Senior Project Manager
Licensing Branch 2
Division of New Reactor Licensing
Office of New Reactors

Docket No. 52-021

Enclosures:
As stated

cc: See next page

MUAP-07011, Revision 3 and MUAP-07013, Revision 2, also apply to MUAP-07011, Revision 4 and MUAP-07013, Revision 3 unchanged from their May 14, 2013, issuance.

The staff requests that MHI publish the accepted proprietary and non-proprietary versions of MUAP-07011, Revision 4 and MUAP-07013, Revision 3 within one month of receipt of this letter. The accepted versions shall incorporate this letter and the enclosed final TRSEs after the title page. Also, they must contain historical review information, including NRC requests for additional information and your responses. The accepted versions of the topical reports shall include an "-A" (designated accepted) following the report identification number.

If the NRC's criteria or regulations change, so that its conclusion that the accepted topical report is invalidated, MHI and/or the applicant referencing the topical report will be expected to revise and resubmit its respective documentation, or submit justification for continued applicability of the topical report without revision of the respective documentation.

If you have any questions or comments concerning this matter, I can be reached at (301) 415-1383 or via e-mail address at Perry.Buckberg@nrc.gov.

Sincerely,

/RA/

Perry Buckberg, Senior Project Manager
Licensing Branch 2
Division of New Reactor Licensing
Office of New Reactors

Docket No. 52-021

Enclosures:
As stated

cc: See next page

DISTRIBUTION:

PUBLIC	RidsNroLaCSmith	RidsNroDnrl	JSchmidt, NRO
D081	RidsNroOd	PBuckberg, NRO	
LB2 R/F	RidsNroDnrlLb2	RReyes, NRO	

ADAMS Accession Nos.:

ML14050A360-pkg

ML14050A053-letter

via email*

NRO-002

OFFICE	DNRL/LB2: PM	DNRL/LB2: LA	DNRL/LB2: PM
NAME	RReyes	CMurphy*	PBuckberg
DATE	02/19/2014	02/19/2014	02/24/2014

OFFICIAL RECORD COPY

cc:

Mr. Robert E. Sweeney
IBEX ESI
4641 Montgomery Avenue
Suite 350
Bethesda, MD 20814

Mr. Gary Wright, Director
Division of Nuclear Facility Safety
Illinois Emergency Management Agency
1035 Outer Park Drive
Springfield, IL 62704

DC Mitsubishi - US APWR Mailing List

Email

acpasswater@aol.com (Al Passwater)
APH@NEI.org (Adrian Heymer)
atsushi_kumaki@mhi.co.jp (Atsushi Kumaki)
awc@nei.org (Anne W. Cottingham)
bgattoni@roe.com (William (Bill) Gattoni)
CumminWE@Westinghouse.com (Edward W. Cummins)
cwaltman@roe.com (C. Waltman)
david.hinds@ge.com (David Hinds)
david.lewis@pillsburylaw.com (David Lewis)
DeLaBarreR@state.gov (R. DeLaBarre)
donald.woodlan@luminant.com (Donald Woodlan)
eliza.seedcoalition@gmail.com (Elza Brown)
erg-xl@cox.net (Eddie R. Grant)
erin_wisler@mnes-us.com (Erin Wisler)
ewallace@nuscalepower.com (Ed Wallace)
gcesare@enercon.com (Guy Cesare)
hiroki_nishio@mhi.co.jp (Hiroki Nishio)
james1.beard@ge.com (James Beard)
jerald.head@ge.com (Jerald G. Head)
Joseph_Hegner@dom.com (Joseph Hegner)
joseph_tapia@mnes-us.com (Joseph Tapia)
jrappe@nuscalepower.com (Jodi Rappe)
jrund@morganlewis.com (Jonathan Rund)
karlg@att.net (Karl Gross)
kevin_lynn@mnes-us.com (Kevin Lynn)
KSutton@morganlewis.com (Kathryn M. Sutton)
kwaugh@impact-net.org (Kenneth O. Waugh)
lchandler@morganlewis.com (Lawrence J. Chandler)
lon.burnam@house.state.tx.us (Lon Burnam)
m.goto@mnes_us.com
maria.webb@pillsburylaw.com (Maria Webb)
mark.a.giles@dom.com (Mark Giles)
masanori_onozuka@mnes-us.com (Masanori Onozuka)
masatoshi_nagai@mnes-us.com (Masatoshi Nagai)
matias.travieso-diaz@pillsburylaw.com (Matias Travieso-Diaz)
media@nei.org (Scott Peterson)
michael_melton@mnes-us.com (Michael Melton)
MSF@nei.org (Marvin Fertel)
nirsnet@nirs.org (Michael Mariotte)
Nuclaw@mindspring.com (Robert Temple)
patriciaL.campbell@ge.com (Patricia L. Campbell)
paul.gaukler@pillsburylaw.com (Paul Gaukler)
Paul@beyondnuclear.org (Paul Gunter)

DC Mitsubishi - US APWR Mailing List

pbessette@morganlewis.com (Paul Bessette)
plarimore@talisman-intl.com (Patty Larimore)
rebecca_steinman@mnes-us.com (Rebecca Steinman)
RJB@NEI.org (Russell Bell)
ryan_sprengel@mnes-us.com (Ryan Sprengel)
sabinski@suddenlink.net (Steve A. Bennett)
sfrantz@morganlewis.com (Stephen P. Frantz)
stephan.moen@ge.com (Stephan Moen)
strambgb@westinghouse.com (George Stramback)
Tansel.Selekler@nuclear.energy.gov (Tansel Selekler)
tgilder1@luminant.com (Tim Gilder)
tmatthews@morganlewis.com (T. Matthews)
tom.miller@hq.doe.gov (Tom Miller)
Tony.Robinson@areva.com (Tony Robinson)
trsmith@winston.com (Tyson Smith)
Vanessa.quinn@dhs.gov (Vanessa Quinn)
vijukrp@westinghouse.com (Ronald P. Vijuk)
Wanda.K.Marshall@dom.com (Wanda K. Marshall)
whorin@winston.com (W. Horin)
yoshiki_ogata@mhi.co.jp (Yoshiki Ogata)



UNITED STATES
NUCLEAR REGULATORY COMMISSION
WASHINGTON, D.C. 20555-0001

May 14, 2013

Mr. Yoshiki Ogata, General Manager
APWR Promoting Department
Mitsubishi Heavy Industries, Ltd.
16-5, Konan 2-Chome, Minato-Ku
Tokyo, 108-8215 Japan

SUBJECT: UNITED STATES - ADVANCED PRESSURIZED WATER REACTOR
FINAL TOPICAL REPORT SAFETY EVALUATION FOR TOPICAL
REPORT MUAP-7011-P, REVISION 3, "LARGE BREAK LOCA CODE
APPLICABILITY REPORT FOR US-APWR"

Dear Mr. Ogata:

The U.S. Nuclear Regulatory Commission (NRC) staff has prepared a final Topical Report Safety Evaluation (TRSE) for Topical Report MUAP-07011-P, Revision 3, "Large Break LOCA Code Applicability Report for US-APWR." This action is supported by letter dated April 29, 2013 (Agencywide Documents Access and Management System accession number ML13105A219), whereby the Advisory Committee on Reactor Safeguards agrees with the NRC staff's conclusions, within the limits and conditions that are specified in the TRSE. This is also in support of the United States - Advanced Pressurized Water Reactor design certification submitted by Mitsubishi Heavy Industries, Ltd. (MHI) on December 31, 2007.

The staff requests that MHI publish the accepted proprietary and non-proprietary versions of this topical report within one month of receipt of this letter. The accepted versions of the topical report shall include an "-A" (designated accepted) following the report identification number, as well as incorporate this letter along with the enclosed final TRSE.

If the NRC's criteria or regulations change, so that its conclusion that the accepted topical report is invalidated, MHI and/or the applicant referencing the topical report will be expected to revise and resubmit its respective documentation, or submit justification for continued applicability of the topical report without revision of the respective documentation.

Y. Ogata

- 2 -

If you have any questions or comments concerning this matter, I can be reached at (301) 415-6391 or via e-mail address at Jeff.Ciocco@nrc.gov.

Sincerely,

A handwritten signature in black ink that reads "Jeffrey Ciocco". The signature is written in a cursive, flowing style.

Jeffrey Ciocco, Senior Project Manager
Licensing Branch 2
Division of New Reactor Licensing
Office of New Reactors

Docket No. 52-021

Enclosure:
As stated

cc w/o encl.: See next page

cc:

Mr. Robert E. Sweeney
IBEX ESI
4641 Montgomery Avenue
Suite 350
Bethesda, MD 20814

Mr. Gary Wright, Director
Division of Nuclear Facility Safety
Illinois Emergency Management Agency
1035 Outer Park Drive
Springfield, IL 62704

DC Mitsubishi - US APWR Mailing List

Email

acpasswater@aol.com (Al Passwater)
APH@NEI.org (Adrian Heymer)
atsushi_kumaki@mhi.co.jp (Atsushi Kumaki)
awc@nei.org (Anne W. Cottingham)
bgattoni@roe.com (William (Bill) Gattoni)
CumminWE@Westinghouse.com (Edward W. Cummins)
cwaltman@roe.com (C. Waltman)
david.hinds@ge.com (David Hinds)
david.lewis@pillsburylaw.com (David Lewis)
DeLaBarreR@state.gov (R. DeLaBarre)
donald.woodlan@luminant.com (Donald Woodlan)
eliza.seedcoalition@gmail.com (Elza Brown)
erg-xl@cox.net (Eddie R. Grant)
erin_wisler@mnes-us.com (Erin Wisler)
ewallace@nuscalepower.com (Ed Wallace)
gcesare@enercon.com (Guy Cesare)
hiroki_nishio@mhi.co.jp (Hiroki Nishio)
james1.beard@ge.com (James Beard)
jerald.head@ge.com (Jerald G. Head)
Joseph_Hegner@dom.com (Joseph Hegner)
joseph_tapia@mnes-us.com (Joseph Tapia)
jrappe@nuscalepower.com (Jodi Rappe)
jrund@morganlewis.com (Jonathan Rund)
karlg@att.net (Karl Gross)
kevin_lynn@mnes-us.com (Kevin Lynn)
KSutton@morganlewis.com (Kathryn M. Sutton)
kwaugh@impact-net.org (Kenneth O. Waugh)
lchandler@morganlewis.com (Lawrence J. Chandler)
lon.burnam@house.state.tx.us (Lon Burnam)
m.goto@mnes_us.com
maria.webb@pillsburylaw.com (Maria Webb)
mark.a.giles@dom.com (Mark Giles)
mark.beaumont@wsms.com (Mark Beaumont)
masanori_onozuka@mnes-us.com (Masanori Onozuka)
masatoshi_nagai@mnes-us.com (Masatoshi Nagai)
matias.travieso-diaz@pillsburylaw.com (Matias Travieso-Diaz)
media@nei.org (Scott Peterson)
michael_melton@mnes-us.com (Michael Melton)
MSF@nei.org (Marvin Fertel)
nirsnet@nirs.org (Michael Mariotte)
Nuclaw@mindspring.com (Robert Temple)
patriciaL.campbell@ge.com (Patricia L. Campbell)
paul.gaukler@pillsburylaw.com (Paul Gaukler)
Paul@beyondnuclear.org (Paul Gunter)

DC Mitsubishi - US APWR Mailing List

pbessette@morganlewis.com (Paul Bessette)
plarimore@talisman-intl.com (Patty Larimore)
rebecca_steinman@mnes-us.com (Rebecca Steinman)
RJB@NEI.org (Russell Bell)
ryan_sprengel@mnes-us.com (Ryan Sprengel)
sabinski@suddenlink.net (Steve A. Bennett)
sfrantz@morganlewis.com (Stephen P. Frantz)
stephan.moen@ge.com (Stephan Moen)
strambgb@westinghouse.com (George Stramback)
Tansel.Selekler@nuclear.energy.gov (Tansel Selekler)
tgilder1@luminant.com (Tim Gilder)
tmatthews@morganlewis.com (T. Matthews)
tom.miller@hq.doe.gov (Tom Miller)
Tony.Robinson@areva.com (Tony Robinson)
trsmith@winston.com (Tyson Smith)
Vanessa.quinn@dhs.gov (Vanessa Quinn)
vijukrp@westinghouse.com (Ronald P. Vijuk)
Wanda.K.Marshall@dom.com (Wanda K. Marshall)
whorin@winston.com (W. Horin)
yoshiki_ogata@mhi.co.jp (Yoshiki Ogata)

FINAL SAFETY EVALUATION BY THE OFFICE OF NEW REACTORS
TOPICAL REPORT MUAP-07011-P, REVISION 3
“LARGE BREAK LOCA CODE APPLICABILITY REPORT FOR US-APWR”
MITSUBISHI HEAVY INDUSTRIES, Ltd
DOCKET NO. 52-021

Table of Contents

1	INTRODUCTION.....	2
2	SYSTEM DESCRIPTION.....	2
3	REGULATORY BASIS.....	3
4	TECHNICAL EVALUATION	3
4.1	CSAU Issues Addressed in MUAP-07011-P(R3).....	5
4.1.1	The US-APWR PIRT	5
4.1.2	WCT-M1 Code Applicability	11
4.1.3	Scaling Effects.....	18
4.1.4	ASTRUM Methodology Applied to US-APWR.....	19
4.2	Sample Plant Analysis.....	24
4.3	Independent Analyses	29
4.3.1	RELAP5/MOD3.3 Simulations.....	29
4.3.2	WCT-M1 Simulations	30
5	CONCLUSIONS AND LIMITATIONS.....	31
6	REFERENCES	33
7	LIST OF ACRONYMS.....	35

List of Tables

Table 1	WCT-M1 Cases for RAI-3	- 23 -
Table 2	WCT-M1 Cases to Address DC boiling.....	- 28 -

1 INTRODUCTION

By letter dated July 20, 2007, Mitsubishi Heavy Industries, Ltd. (MHI), hereinafter referred to as the applicant, submitted Topical Report MUAP-07011-P(R0), "Large Break LOCA, Code Applicability Report for the US-APWR," [Ref. 1] prepared in connection with its request to the U.S. Nuclear Regulatory Commission (NRC), hereinafter referred to as the staff, for a pre-application review of the United States - Advanced Pressurized Water Reactor (US-APWR).

This report provides the staff's safety evaluation (SE) of Topical Report MUAP-07011-P(R3) [Ref. 28]. The evaluation focused on: (1) the differences between the US-APWR and currently operating plants considered in Reference 2, and (2) the applicability of the code assessment and validation described in Reference 3 to the US-APWR.

The applicant's Best Estimate Large Break Loss of Coolant Accident (BELBLOCA) methodology is based upon the Automated Statistical Treatment of Uncertainty Method (ASTRUM) methodology [Ref. 2] which has been approved by the NRC for the Westinghouse 2, 3 and 4 loop pressurized-water reactor (PWR) designs, the Combustion Engineering (CE) PWR design, and the Westinghouse AP600 and AP1000 advanced reactors. The methodology uses WCOBRA/TRAC(M1.0), hereinafter referred to as WCT-M1, as its thermal-hydraulic modeling engine. WCT-M1 is based upon the WCOBRA/TRAC computer program. The code qualification document for WCOBRA/TRAC has been approved by the NRC for the frozen code version WCOBRA/TRAC MOD7A Revision 1 [Ref. 3]. ASTRUM methodology with the frozen code version WCOBRA/TRAC MOD7A Revision 6 [Ref.2] has been also approved by the NRC. WCT-M1 is based on WCOBRA/TRAC MOD7A Revision 6. Significant differences between WCT-M1 and WCOBRA/TRAC are described and evaluated in Section 4.1.2 of this report.

2 SYSTEM DESCRIPTION

The US-APWR is a 4-loop plant with a core rated output of 4451 megawatts thermal (MWt). The reactor core consists of 257 fuel assemblies each containing 264 fuel rods, 24 guide tubes, and 1 incore instrument tube, all arranged in a 17x17 square lattice. The active fuel height is 4.201 m (13.78 ft). The core average linear heat generation rate is 15.2 kW/m (4.6 kW/ft). Local power peaking factor values in the US-APWR are similar to those in currently operating plants.

Unique design features of the US-APWR relative to currently operating PWRs are core length, a neutron reflector (NR) surrounding the core, omission of the low head safety injection (LHSI) system, an advanced accumulator, and direct vessel injection (DVI) of the high head safety injection (HHSI) system.

The NR assembly, which surrounds the core, consists of a ring of stacked stainless steel blocks perforated with vertical cooling holes. Its purpose is to improve neutron economy and reduce the fluence to the reactor pressure vessel. Because of its size, the NR may represent a significant heat source during the reflood period of a Large Break Loss of Coolant Accident (LBLOCA).

The advanced accumulators, one per reactor loop, are unique in that each contains an internal flow damper. The flow damper, a passive device, is designed to deliver a large flow rate during the refill of the reactor vessel following a LBLOCA, and then to automatically switch to a low flow rate as the accumulator water level drops. The accumulators' sustained delivery period at a low flow rate eliminates the need for a LHSI system.

There are four independent HHSI trains. Each train consists of a high pressure pump and the associated valves and piping.

The HHSI pumps are automatically started by an S-signal and supply borated water (approximately 4,000 ppm boron) from the Refueling Water Storage Pit (RWSP) to the reactor vessel. Each train is connected to a dedicated DVI nozzle for injection into the reactor downcomer. The DVI nozzles are located slightly below the centerline elevation of the reactor coolant hot and cold leg nozzles. A safety injection pad is attached to the outside of the core barrel opposite each DVI nozzle. The pad directs the injected flow downward. The HHSI pumps are sized so that two of the four systems can supply adequate flow to keep the core cooled following the 180 second time period of accumulator injection.

3 REGULATORY BASIS

Title 10 of the *Code of Federal Regulations* (10 CFR), Part 50, Section 46, Paragraph (a) specifies that each boiling or pressurized light-water nuclear power reactor fueled with uranium oxide pellets within cylindrical Zircaloy or ZIRLO™ cladding must be provided with an Emergency Core Cooling System (ECCS) designed so that the calculated cooling performance following a postulated loss-of-coolant accident (LOCA) conforms to the criteria set forth in 10 CFR 50.46(b). 10 CFR 50.46(a) also stipulates that the requirement can be met through an evaluation model for which an uncertainty analysis has been performed as follows:

...the evaluation model must include sufficient supporting justification to show that the analytical technique realistically describes the behavior of the reactor system during a loss-of-coolant accident. Comparisons to applicable experimental data must be made and uncertainties in the analysis method and inputs must be identified and assessed so that the uncertainty in the calculated results can be estimated. This uncertainty must be accounted for, so that, when the calculated ECCS cooling performance is compared to the criteria set forth in paragraph (b) of this section, there is a high level of probability that the criteria would not be exceeded.

10 CFR 50.46(b) specifies that: (1) the Peak Cladding Temperature (PCT) must not be calculated to exceed 1204°C (2200°F), (2) the maximum Local Cladding Oxidation (LCO) must not exceed 0.17 times the total cladding thickness before oxidation, (3) the maximum hydrogen generation from Core Wide Oxidation (CWO) must not exceed 0.01 times the hypothetical amount that would be generated if all of the metal in the cladding surrounding the fuel pellets were to react, and (4) the core must remain in a coolable geometry. Also, the core temperature shall be maintained at an acceptably low level and decay heat shall be removed for the extended period of time required by the long-lived radioactivity remaining in the core.

The NRC has provided guidance on how the above regulatory criteria can be met. Regulatory Guide (RG) 1.157 [Ref. 4] and NUREG/CR-5249 [Ref. 5] describe acceptable approaches to determine the calculated uncertainty in the 10 CFR 50.46(b) parameters.

4 TECHNICAL EVALUATION

Prediction of the 10 CFR 50.46(a)(1)(i) key safety parameters (PCT, LCO, and CWO) with a high level of probability requires that distribution of uncertainty in the models and correlations be

determined. The first step in this process is to identify the important phenomena via construction of a Phenomena Identification and Ranking Table (PIRT).

The applicant's BELBLOCA methodology is based on the NRC Code, Scaling, Applicability, and Uncertainty (CSAU) methodology [Ref. 5] as applied and approved for Westinghouse PWRs [Refs. 2 and 3].

The methodology consists of two best estimate codes, WCT-M1 for simulating reactor system response, and HOTSPOT for hot rod analysis. A third component of the methodology is ASTRUM, an automated method of conducting a set of LBLOCA calculations and extracting the uncertainty and confidence limits of the key safety parameters. The staff's review of the applicant's BELBLOCA methodology focuses on whether the CSAU methodology has been properly applied, in particular CSAU Steps 3, 6, 10, and 11 through 14.

CSAU Step 1, scenario specification, is clearly the LBLOCA for this application. Step 2, nuclear power plant selection, is the US-APWR. For CSAU Step 3, the construction of a PIRT, the applicant has relied heavily on Reference 3. This is acceptable to the staff because of the similarities between a Westinghouse 4-loop PWR and the US-APWR. In those areas where the plants are different the applicant has augmented the Reference 3 PIRT. The applicant's PIRT is evaluated in Section 4.1.1 below.

The CSAU methodology (Step 4) requires the use and identification of a frozen code. The applicant's response to the first LBLOCA Request for Additional Information (RAI) set, Question 1 [Ref. 9] noted that its system code, WCT-M1, is based on a previously approved code, WCOBRA/TRAC MOD7A Revision 6 [Ref. 3]. WCT-M1 has three significant changes from the approved code version: The incorporation of models for the advanced accumulator, allowing the neutron reflector component to use existing hot wall flow regime models, and replacement of the fuel thermal conductivity model. These changes are described in Section 3.5 of References 1 and 28. The applicant's version of HOTSPOT was properly modified to the version already approved by the staff and is therefore acceptable.

CSAU Step 5 requires proper documentation of the computer programs being used, including user manuals, assessment reports, and a demonstration of the applicability of the computer models to the US-APWR. In its response to the second LBLOCA RAI set, Question 37 [Ref. 11], the applicant noted that it fulfilled CSAU Step 5 by supplying the staff with the WCT-M1 code input manuals [Refs. 26 and 27], the subject topical report (TR), and References 2 and 3, which document the applicability of WCOBRA/TRAC and the ASTRUM methodology to the US-APWR. The staff agrees that CSAU Step 5 has been fulfilled.

Determination of code applicability, CSAU Step 6, is addressed in Section 3.5 of the subject TR. The applicant has relied on Reference 3 as proof of the applicability of WCT-M1 to simulate non-unique features of the US-APWR during a LBLOCA. The code's applicability to simulate the unique features of the US-APWR is addressed in Section 3.5 of the subject TR, and evaluated in Section 4.1.2 of this report.

CSAU Step 7 calls for the establishment of an assessment matrix for the applicant's computer program. The applicant has fulfilled this step for the US-APWR NR and advanced accumulator [Refs. 7 and 8] and has referenced the WCOBRA/TRAC assessment matrix [Ref. 3] for all other features.

Step 8 of the CSAU methodology concerns plant model nodalization. The subject TR (Section 3.6.1, "Nodalization of Plant Analysis") discusses the nodalization used in the WCT-M1 model of the US-APWR. The staff's review of the TR and its evaluation of the applicant's responses to numerous RAIs (Section 4.2 below) have led it to conclude that the applicant has satisfactorily fulfilled the requirements of CSAU Step 8.

The applicant has addressed CSAU Step 9, definition of code and experimental accuracy, in two ways. For the non-unique features of the US-APWR, the applicant has relied on [Ref. 3].

For the NR and the advanced accumulator, the applicant has conducted experiments and assessed WCT-M1 against those experiments. Uncertainty parameters have been developed for the advanced accumulator model. The staff's evaluation of the NR and advanced accumulator modeling are given in Section 4.1.2 below.

Determination of the effects of scale, CSAU Step 10, is discussed briefly in Section 3.5 of the subject TR. The most significant issue in this regard is the scalability of the advanced accumulator test results. The staff's review of this issue is not addressed here, but rather in its review of the MUAP-07001-P(R4), "The Advanced Accumulator [Ref. 29]." A limitation has been placed in this SE regarding the accumulator scaling effect as the review of MUAP-07001-P(R4) [Ref. 29] is ongoing.

Steps 11 through 14 of the CSAU process all relate to determination of code sensitivity and uncertainty. These steps are addressed in Section 3.7 of the TR. The staff's review is in Section 4.1.3 of this report.

4.1 CSAU Issues Addressed in MUAP-07011-P(R3)

The previous section has identified four main CSAU review areas for the staff: The applicant's PIRT (CSAU Step 3), the applicability of WCT-M1 (CSAU Step 6), scaling (CSAU Step 10), and the evaluation of uncertainty (CSAU Steps 11-14). The following subsections present the staff's review of these areas.

4.1.1 The US-APWR PIRT

For the purpose of PIRT and uncertainty analyses, the LBLOCA transient is subdivided into three phases. These phases are blowdown, refill, and reflood (Table 3.3-1 of MUAP-07011-P). There is a PIRT for each phase of the transient and the content of each PIRT depends upon the definition of the phases. In the CSAU and Westinghouse LBLOCA PIRT descriptions, the refilling phase starts when accumulator flow begins and ends when the lower plenum is full.

The applicant's responses to the first LBLOCA RAI set, Question 3.1 [Ref. 9] and follow-up second LBLOCA RAI set, Question 1.1 [Ref. 11] clarified the definitions of the LBLOCA phases. When describing the LBLOCA scenario, the applicant described the blowdown phase ending and the refill phase beginning when the Reactor Coolant System (RCS) pressure equaled the containment pressure. However, for the US-APWR PIRT, the definitions of the blowdown, refill, and reflood phases are identical to those used in previous PWR LBLOCA PIRTs: The blowdown phase ends and the refill phase begins when accumulator injection begins; the reflood phase begins when the lower plenum is full of liquid. The applicant's responses have provided the clarification the staff requested and assured the staff that the applicant's PIRT definitions of the LBLOCA phases are consistent with the NRC PIRT. They are therefore acceptable.

The response to the second LBLOCA RAI set, Question 22 [Ref. 11] addressed apparent inconsistencies between the description of coolant injection through the DVI nozzles and the figures and tables in Section 3.3.3. The response explained that HHSI can occur either during the refill phase or the reflood phase of a LBLOCA, depending upon whether or not offsite power is lost. The description and illustration of HHSI timing assumed no loss of offsite power (LOOP) while the sequence of events table assumed a LOOP. The staff finds the explanation of the differences between the text and tables acceptable.

The sequence of events table in Section 3.3.3 also indicated that the ECCS start signal ("S" signal) is generated by high containment pressure. The applicant explained that (in response to the second LBLOCA RAI set, Question 23 [Ref. 11]), in the plant, the "S" signal can be generated by either high containment pressure or low-low pressurizer pressure; however, in the safety analysis only the low-low pressurizer pressure signal is credited because it occurs later than the high containment pressure signal. Ignoring the high containment pressure signal conservatively delays the ECCS start signal and is therefore acceptable to the staff.

In Section 3.4 of the TR, a PIRT for the US-APWR is developed, using the same process that is described in the Westinghouse PIRT for a conventional 4-loop plant [Ref. 3]. The following phenomena were highly ranked:

- (1) critical flow
- (2) broken loop resistance
- (3) fuel rod modeling
- (4) core heat transfer
- (5) ECC bypass
- (6) entrainment/steam binding
- (7) accumulator nitrogen
- (8) condensation

There are some differences in phenomena ranking between the applicant's PIRT and the staff's CSAU PIRT [Ref. 5]. Those differences received special consideration from the staff.

The applicant's PIRT process was conducted as follows: Physical components of the RCS were considered individually and the thermal hydraulic processes related to each component were ranked in importance. The subsequent paragraphs in this section present the staff's review of each component considered by the applicant.

In Subsection 3.4.1.1 "Fuel Rod," the applicant's rankings for stored energy, decay heat, and cladding oxidation are consistent with the staff's PIRT [Ref. 5] and are therefore acceptable.

The applicant's PIRT ranked gap conductance low for all three LBLOCA phases. The CSAU PIRT [Ref. 5] had ranked it low during the blowdown and refill phases but high during the reflood phase. However, the CSAU report was documenting the PIRT process as it evolved. Subsequent analysis indicated that gap conductance was important in the blowdown phase and should be considered in the uncertainty estimate. During the blowdown phase, the stored energy is released to the clad, and is more important than the decay heat. Stored energy is rated high and the process of heat transfer from the fuel to the clad should also be rated high. The CSAU (Ref. 5, Table 16) showed that the effect of gap conductance on the blowdown PCT was large.

The first LBLOCA RAI set, Question 3.2 asked the applicant to justify the basis for rating gap conductance low in both the blowdown and the reflood phases. The response to Question 3.2 [Ref. 9] noted that the ranking of gap conductance is consistent with that of Reference 3 and the ASTRUM methodology that has been previously approved by the staff. It also noted that gap conductance is an uncertainty parameter in the US-APWR BELBLOCA analyses; therefore, even though its ranking is different from Reference 5, its impact is included in the analyses. The response to Question 3.2 is acceptable. It shows that although gap conductance is ranked low, it is treated as if it were ranked high; i.e., it is treated as an uncertainty parameter in the analysis.

In Subsection 3.4.1.2, "Core," Departure from Nucleate Boiling (DNB), post critical heat flux (CHF) heat transfer, 3-D flow, void generation, and flow reversal were all highly ranked phenomena for the blowdown phase. Only post CHF heat transfer was ranked high for the refill phase, and only reflood heat transfer and entrainment/de-entrainment were ranked high for the reflood phase. These rankings are the same as those in Reference 3. This is to be expected since the US-APWR fuel is the same, except for length, as that used in Westinghouse 4-loop plants. WCT-M1 has the same core heat transfer models as the approved WCOBRA/TRAC code; therefore, it is reasonable to conclude that it can adequately simulate all of the highly ranked phenomena in the core region. The applicant's methodology has six uncertainty parameters related to core heat transfer.

The staff has noted that DNB has been ranked high in the applicant's PIRT but it is not treated as an uncertainty parameter in the WCT-M1 model. Rather, the uncertainty is treated indirectly by modifying the blowdown heat transfer coefficient in HOTSPOT. The staff's evaluation of this methodology is given in Section 4.2 of this report.

The effect of the NR on core thermal hydraulics was ranked moderate. The NR is cooled by water flowing upward through a series of holes drilled through the structure. During reflood the NR will reflood in a manner similar to the core. Steam will be generated and entrainment of liquid into the upper plenum will occur. The flow area of the NR is very small to the core's flow area, so the effect of NR reflood on the overall reflood process is small in comparison to the core. In spite of the moderate ranking of the NR, the applicant has expended considerable effort ensuring that the reflood of the NR is adequately modeled [Ref. 8]. The staff's evaluation of the modeling of the NR is in Section 4.1.2.3 of this report.

In Subsection 3.4.1.3, "Upper Plenum," only the position of the hot assembly was ranked high; it was ranked high for blowdown only. The reason for the high ranking is that the flow draining from the upper plenum into the hot assembly during blowdown can be influenced by whether or not a guide tube sits atop the hot assembly. The staff notes that the position of the hot assembly is treated conservatively and therefore acceptably in the applicant's WCT-M1 analysis.

The entrainment/de-entrainment phenomenon was rated as moderate. It was rated high in CSAU (Ref. 5, Table 1) as it could lead to steam binding when the droplets evaporate in the steam generator (SG). In response to the first LBLOCA RAI set, Question 3.4 [Ref. 9], the applicant explained that best-estimate computer codes are less sensitive to upper plenum entrainment because they better simulate the phenomena than older conservative simulation models. The ranking of the phenomena for the US-APWR was therefore set to moderate. The staff notes that the ranking of the phenomenon is not as important as having a good simulation of the phenomenon. The ability of WCOBRA/TRAC to adequately simulate the phenomenon

has been verified by comparisons to test data [Ref. 3]. The applicant's explanation for a moderate ranking for entrainment/de-entrainment is acceptable. This issue is resolved.

In Subsection 3.4.1.4, "Hot Leg," there were no highly ranked phenomena for the hot leg. The phenomenon of entrainment/de-entrainment was rated as moderate in the reflood phase. However, if the two-phase level is at hot leg elevation then there will be a two phase mixture in the hot leg. The staff's CSAU [Ref. 5] rated it high as a continuation of upper plenum phenomenon. The first LBLOCA RAI set, Question 3.5 requested an explanation for the moderate ranking for the US-APWR. In response to LBLOCA RAI set, Question 3.5 [Ref. 9], the applicant stated that the hot leg has a small volume and any water swept into the hot leg would be entrained into the SG. It further noted that when the upper plenum two phase level reaches the hot leg elevation the core hot spot region has already quenched. The staff finds this explanation of the moderate ranking to be reasonable and acceptable.

In Subsection 3.4.1.5, "Pressurizer," the pressurizer provides coolant to the remainder of the RCS during the blowdown phase and the pressurizer pressure is the control parameter that leads to reactor trip and the safety injection signal. The first LBLOCA RAI set, Question 3.6 asked how the ranking of moderate for pressurizer phenomena was determined. In its response to LBLOCA RAI set, Question 3.6 [Ref. 9], the applicant noted that, since reactor scram is not modeled in the BELBLOCA analysis for the US-APWR, the low pressurizer pressure reactor trip signal is not needed in the analysis. The safety injection (SI) signal is modeled with a conservative delay. Therefore, the pressurizer pressure is not identified as a significant phenomenon. In its response to the second LBLOCA RAI set, Question 1.3 [Ref. 11], dated, the applicant noted that a SI signal delay time of 118 seconds is assumed. The responses to Question 3.6 and follow-up Question 1.3 are acceptable. The explanation of a moderate ranking for pressurizer pressure is reasonable. The applicant's BELBLOCA methodology places the pressurizer on the loop (intact or broken) where it is most limiting on calculated PCT. This location is determined by a sensitivity study. This placement of the pressurizer is conservative and therefore acceptable to the staff.

In Subsection 3.4.1.6, "Steam Generator," steam binding during reflood is the only highly ranked phenomenon. There is a general agreement [Refs.3 and 5] with this finding, and the ranking is acceptable to the staff.

In Subsection 3.4.1.7, "Pump," the two phase pump performance in the blowdown phase was rated as moderate. It was rated high in the staff's CSAU [Ref. 5]. The first LBLOCA RAI set, Question 3.7 asked how the ranking of moderate was determined. In its response to Question 3.7 [Ref. 9], the applicant acknowledged that the pump's two-phase behavior is important since it determines when the pumps lose their pumping capability which, in turn, determines when the flow reverses in the core. The response further noted that the most important element is the broken-loop pump resistance compared to the flow resistance through the core, downcomer, and broken loop cold leg nozzle to the break. The difference in the flow resistance between the two flow paths to the break, which is treated as an uncertainty parameter, determines the amount of down flow through the core and, accordingly, the degree of core cooling during the blowdown phase. The applicant concluded that the two-phase pump performance is less important than flow split between the two paths to the break; therefore, a moderate ranking was assigned to two-phase pump performance. The staff finds this response both reasonable and acceptable. Regardless of its ranking, two phase pump performance is modeled in WCT-M1.

In its response to the second LBLOCA RAI set, Question 1.4 [Ref. 11], the applicant discussed why the uncertainty of two-phase multipliers for the Reactor Coolant Pump (RCP) homologous

curves is not included as an uncertainty parameter in the BELBLOCA methodology. First, it was noted that there is very little scatter in two-phase data when the pump is in the pumping mode, but a large scatter in the data when the RCP is in a dissipation mode of operation. Only the pumping mode data is used to develop the two-phase multiplier used in WCT-M1. For large breaks the broken loop, the RCP may transition to the dissipation mode, but the intact loop RCPs remain in the pumping mode. In this case, the broken loop's RCP void fraction increases rapidly and the RCP becomes fully degraded. Therefore, the time spent in the two-phase regime is short. A sensitivity study was conducted in which a lower bound two-phase multiplier curve based on the dissipation mode data was used instead of the curve based on the pumping mode data. The applicant concluded that the study demonstrated that the calculated plant response was insensitive to which multiplier curve was used and it was therefore not necessary to treat the RCP two-phase multiplier as an uncertainty parameter. The staff agrees with the applicant's conclusion. This issue is resolved.

In Subsection 3.4.1.8, "Cold Leg and Accumulator," the accumulator flow mixes with the two-phase mixture in the cold leg. There will be condensation of steam during both the refill and reflood phases. The condensation is retarded if there is a non-condensable in the gas phase. The applicant ranked condensation high in the refill phase, in agreement with previous rankings [Refs. 3 and 5].

The staff's CSAU [Ref. 5] ranked the effect of non-condensable gas as high during reflood, while the applicant ranked it low. In its response to the first LBLOCA RAI set, Question 3.8 [Ref. 9], the applicant explained that the effect of non-condensable gas is ranked low during reflood because nitrogen is not released from the advanced accumulator until well after the peak cladding temperature has occurred. Based upon the applicant's response, the staff believes a ranking of low is reasonable and acceptable.

Accumulator flow was ranked high for the refill phase. This is reasonable because the accumulator flow is the main contributor to refill of the reactor pressure vessel (RPV). In the case of a LOOP, it is the only contributor during the refill phase. The accumulator flow was also ranked high during reflood, because it serves as a low pressure safety injection system until the core is nearly all quenched. The uncertainty in accumulator flow during both the high flow and low flow regimes is treated by assigning nominal values and uncertainty bands to the accumulator lines resistance coefficient. The staff agrees with the high ranking of accumulator flow.

In Subsection 3.4.1.9, "Downcomer," flashing of the fluid was rated low during the blowdown phase. In response to the first LBLOCA RAI set, Question 3.9 [Ref. 9], the applicant explained that flashing of the downcomer fluid during blowdown was ranked low because it has a very small effect on core cooling. Flashing of the downcomer fluid occurs concurrently with flashing of the lower plenum fluid. Lower plenum flashing may affect core cooling by driving fluid into the core, but downcomer flashing will not. The staff finds the applicant's explanation to be reasonable and acceptable.

Entrainment, condensation, countercurrent flow, and 3-D effects were all ranked high for the refill phase. All these rankings are consistent with the rankings for a Westinghouse 4-loop plant [Ref. 3]. This is expected because the US-APWR downcomer width is very similar to that of the Westinghouse plant, although the RPV has a larger diameter.

The effect of DVI on phenomena in the downcomer was ranked low. Steam condensation by the injected liquid is minimal because DVI is not initiated (assuming a LOOP) until after the DVI nozzles are covered with liquid that is injected by the accumulators.

Downcomer hot wall effects were ranked high for the reflood period. If the temperature of the fluid in the downcomer approaches the saturation temperature, boiling may occur, resulting in a loss of downcomer driving head and possible entrainment of downcomer fluid out the break. The staff concurs with the applicant's high ranking.

In Subsection 3.4.1.0, "Lower Plenum," the only phenomenon ranked high was the hot wall effect during reflood. The lower plenum metal structures give up their heat to the reflood liquid, thereby reducing its subcooling. This, in turn, means that more of the core will be in nucleate boiling during reflood and more steam will have to be vented through the loops. The ranking is therefore reasonable.

In Subsection 3.4.1.11, "Break," critical flow is ranked high for the blowdown phase. Break size and break discharge multipliers are both treated as uncertainty parameters in the applicant's methodology. Containment pressure is ranked high for the reflood phase.

The applicant's methodology uses a conservatively low containment pressure, an approach which is acceptable to the staff in lieu of treating it as an uncertainty parameter.

In Subsection 3.4.1.12, "Loop," only the hot leg/cold leg flow split received a high ranking. This flow split is treated as an uncertainty parameter in the applicant's methodology.

In the first LBLOCA RAI set, Question 3.11, the staff asked why the stored energy from passive heat structures was not considered in the PIRT. In response to Question 3.11 [Ref. 10], the applicant noted that it was considered under the phenomenon 'Hot Wall' for each RCS component. The response provides the clarification needed and is acceptable.

The staff requested that all of the highly ranked PIRT items be discussed, noting that several items in PIRT Table 3.4.1 were not. The information requested was provided in the response to the second LBLOCA RAI set, Question 25 [Ref. 11]. In its response, the applicant noted that fuel rod oxidation is ranked high because it can provide an additional heat source to the cladding at high temperatures. Core 3-D coolant behavior is ranked high because it directly affects cladding heat transfer. RCP head and flow losses are ranked high during reflood because they affect loop flow resistance and thereby affect core reflood. Entrainment/De-entrainment in the downcomer during the refill period is ranked high because these phenomena affect the rate at which emergency core cooling flows into the lower plenum. The foregoing response is acceptable because it makes the discussion in Section 3.4.1 address all of the highly ranked phenomena. The issue is resolved.

4.1.2 WCT-M1 Code Applicability

Step 6 in CSAU is to establish the applicability of the code to the plant and the intended transient. WCOBRA/TRAC has been approved for application to Westinghouse 3 and 4 loop plants and the AP-1000. Most of the components and the expected phenomena during LBLOCA are expected to be similar between the US-APWR and Westinghouse PWRs. Therefore, the applicability of WCT-M1 to the US-APWR reduces to an assessment of models for four components unique to the US-APWR. These are: the longer core, the advanced accumulator, an NR, and DVI.

4.1.2.1 Core Length

The 4.2-m (13.8 ft) core is about 17 percent longer than current PWR cores. The main effect of the longer core is the introduction of additional grid spacers in the fuel assembly. These additional spacers are modeled by adding additional frictional loss coefficients to the WCT-M1 model. The applicant's BELBLOCA methodology is based on a code that has been validated [Ref. 3] against the Loss-Of-Fluid Test (LOFT), which used a 1.7-m (5.6-ft) core, and against cylindrical core test facility (CCTF) and slab core test facility (SCTF) tests, which used 3.6-m (11.8-ft) cores. The validation at two different core lengths indicates the methodology is scalable to a 4.2-m (13.8-ft) core. Based on the above information, the staff finds that the methodology is applicable to the US-APWR core.

4.1.2.2 Advanced Accumulator

Subsection 3.5.1 and Appendix B of the TR describe the advanced accumulator. The advanced accumulator is a new component in the US-APWR. To properly model it, new models were added to WCT-M1. During the review of these models, 21 RAI questions were generated. Its responses are discussed in the following paragraphs. The questions are related to the effect of dissolved nitrogen, applicability of the characteristic equations derived from a full-height, ½ scale test facility, and the uncertainties associated with the characteristic equations that are implemented in the code.

The applicability of the advanced accumulator correlations to full scale is addressed in the staff's review of the topical report on the advanced accumulator (MUAP-07001-P(R4)) [Ref. 29].

In response to the first LBLOCA RAI set, Question 3.12.1 [Ref. 9], the applicant stated that nitrogen will not be released from the advanced accumulator tank until well after the peak cladding temperature has occurred. The full-height ½-scale tests of the advanced accumulator have confirmed that there is no possibility of nitrogen ingress into the standpipe during the switching from the high to low flow mode. The response also stated that the effect of dissolved nitrogen on core cooling is not significant. As part of the Advance Accumulator Topical Report review, the staff asked a similar question, under the Advanced Accumulator RAI set, Question 63 [Ref. 30], regarding the effect of dissolved nitrogen on accumulator performance. In the Advanced Accumulator Topical Report the applicant presented a ½ scale test (Test Number 5) with water-saturated nitrogen. This test indicated that switchover from large-flow to small-flow injection was delayed by up to few seconds. This switchover delay could be the effect of the dissolved nitrogen causing an increased flow resistance and a reduced flow rate. As discussed in Section 5.3 of MUAP-07001 [Ref. 29], the accumulator injection pipe loss coefficient is increased to account for any possible dissolved nitrogen effect. The basis for increase in loss coefficient is described in the Advance Accumulator Topical Report SE. To take the increase in accumulator injection pipe loss coefficient into account for the LOCA analysis is part of the

LBLOCA methodology and shall be used for licensing calculations. As the dissolved nitrogen effect has been conservatively addressed, the staff finds the response to Question 3.12.1 acceptable.

The verification of the implementation of the advanced accumulator model into WCT-M1 was done by comparing WCT-M1 simulations to the full-height 1/2-scale tests. In response to Question 3.12.2 [Ref. 9], the applicant noted that the correlations implemented are independent of scale and are therefore valid when applied to US-APWR accident simulations. As part of the Advanced Accumulator Topical Report review the staff asked in the Advanced Accumulator RAI set, Question 66 [Ref. 30], if there was any scaling effect on the flow coefficients. The Advanced Accumulator Topical Report review staff determined that a negative scaling bias shall be applied to the accumulator flow coefficients. The Advanced Accumulator Topical review is ongoing therefore; the applicant assumed bounding scaling biases as part of the LBLOCA Topical Report methodology. The assumed bounding large and small flow scaling biases to the flow rate coefficients are given in Table 3.5-7 [Ref. 28]. Therefore, a limitation exists that the final scaling biases determined in the Advanced Accumulator Topical Report are more positive than the values given in Table 3.5-7 [Ref. 28].

In its responses to the first LBLOCA RAI set, Questions 3.12.3 and 3.12.5 [Ref. 9], the applicant addressed instrument and manufacturing uncertainties. The responses noted that these uncertainties are addressed in MUAP-07001-P and the responses to the staff RAIs issued in the review of that document. The staff's Advanced Accumulator Topical report review is ongoing; therefore, a limitation exists that the final instrument and manufacturing uncertainties as determined in the Advanced Accumulator Topical Report bound those values given in Table 3.5-6 [Ref. 28].

Because the accumulator characteristics equations are least square curve fits of the test data, a dispersion uncertainty is calculated for the dispersion deviation of the flow coefficient fit. The original method of splitting the flow coefficient dispersion deviation data into two groups was clarified in the response to the first LBLOCA RAI set, Question 3.12.4 [Ref. 9]. In Advanced Accumulator Topical Report Revisions 1 through 3, the data is divided into two groups: one with values greater than the equation's values, and one with values less than the equation's value.

Separate standard deviations were than determined for data greater than (+) and less than (-) the equation values. In MUAP-07001-P (R4) [Ref. 29], the dispersion error was performed for all data points and an equal, positive and negative standard deviation determined. The revised data dispersion standard deviation is given in Table 3.5-6 [Ref. 28]. Therefore, Question 3.12.4 is no longer relevant and the dispersion standard deviation acceptability will be addressed in the review of Advanced Accumulator Topical Report. As the review of the Advanced Accumulator Topical Report is ongoing, a limitation exists that the final dispersion standard deviations in MUAP-07001 are bounded by the Table 3.5-6 [Ref. 29] values.

In its responses to the first LBLOCA RAI set, Question 3.12.6 [Ref. 9], and follow-up second LBLOCA RAI set, Question 1.7 [Ref. 11], the applicant addressed the distributions applicable for instrument error, dispersion deviation, manufacturing error, and the combination of these three distributions to form the distribution of the flow coefficient. The experimental data distribution (dispersion deviation) is assumed to be normal based upon the observed distribution of the data points. Standard engineering practice is to assume a normal distribution for the total manufacturing error, which is due to several factors; e.g., diameter of the tank, diameter of the injection pipe, height of the standpipe, etc. Finally, according to the central limit theorem, the distribution of the uncertainty made by combining independent uncertainty distributions will be a

normal distribution. Hence, the uncertainty in the flow coefficient is a normal distribution. The staff finds that the procedure followed by the applicant to obtain the uncertainty in the flow coefficient is reasonable and the assumption of a normal distribution is acceptable. The staff conducted WCT-M1 simulations to examine the sensitivity of calculated results to the flow coefficient uncertainty and determined that calculated results are relatively insensitive to the uncertainty value of the flow coefficient. Using a flow coefficient value of nominal minus one standard deviation and then nominal plus one standard deviation only changed computed PCT by 22 °F.

The flow coefficient is treated as a statistical parameter in the applicant's ASTRUM analysis. In response to the first LBLOCA RAI set, Question 3.12.9 [Ref. 9], the applicant provided a proprietary discussion of how it is implemented in ASTRUM, the type and range for the probability density function (PDF), and how the PDF is sampled. The staff reviewed the information provided in the response and found it to be technically sound, and therefore acceptable. In response to follow-up second LBLOCA RAI set, Question 1.8 [Ref. 11], the applicant clarified that there is no bias applied to the flow coefficient, and that the PDF is symmetrical about the mean value. Based on Section 5.4 of MUAP-07001-P (R4) [Ref. 29], a negative scaling bias has been added to the flow coefficient after (outside of) the ASTRUM determined value (see the discussion of Question 3.12.11 below). Therefore, the response to Question 1.8 [Ref. 11] is superseded by MUAP-07001-P (R4). The symmetry occurs as a single total (instrument, dispersion and manufacturing) standard deviation value is used for the PDF (see the discussion of Question 3.12.4 above).

The advanced accumulator switches from a high (large) flow mode to a low (small) flow mode when the top of the stand pipe uncovers. To address the uncertainty in switchover time, the accumulator water level is set conservatively low; so the high flow period is conservatively short (response to Question 3.12.10 [Ref. 9]). In response to Question 3.12.10, the applicant demonstrates a conservative treatment of switchover time and is acceptable. The response to follow-up second LBLOCA RAI set, Question 1.9 [Ref. 11], clarified that switchover time is not an uncertainty parameter; the low accumulator water level is a fixed input in WCT-M1. The clarification is acceptable; there is no need to apply uncertainty to a conservative input.

In response to the first LBLOCA RAI set, Question 3.12.11 [Ref. 9], the applicant stated that the flow coefficient uncertainty derived from the full-height ½-scale tests is applicable to the US-APWR, i.e., the uncertainty is independent of scale.

Follow-up scaling RAIs were asked as part of the Advanced Accumulator Topical Report review. Based on the applicant's response to the Advanced Accumulator RAI set, Question 66 [Ref. 30], and Advanced Accumulator Topical Report, Revision 4 [Ref. 29], the applicant assumed conservative large and small flow coefficient scaling biases in the LBLOCA methodology. Therefore, Question 66 [Ref. 30] supersedes the applicant's response to Question 3.12.11 [Ref. 9]. The staff's review of the Advanced Accumulator Topical Report is ongoing; therefore, a limitation exists that the final scaling biases determined in the Advanced Accumulator Topical Report are more positive than the values given in Table 3.5-7 [Ref. 28].

Equation B-1 of the subject TR implies that the flow damper outlet pressure must be greater than the vapor pressure if the value of the cavitation factor is to be meaningful (i.e., positive). In response to the first LBLOCA RAI set, Question 3.12.12 [Ref. 9], the applicant provided material which demonstrated that this was always the case in the full-height ½-scale tests. Therefore, equation B-1 will always yield a positive value of the cavitation factor. The staff finds this

response acceptable, pending approval of MUAP-07001-P (R4), which will address the issue of the applicability of the full-height ½-scale tests to the US-APWR.

Appendix B Equations B-4 and B-5 state that the flow coefficient becomes constant when the flow through the flow damper is small. In response to the first LBLOCA RAI set, Question 3.12.13 [Ref. 9], the applicant notes that for low flow velocities the cavitation factor becomes very large (large values are associated with little occurrence of cavitation). For large values of the cavitation factor, the exponential term in Equation B-2 and B-3 goes to zero and the equation for the flow coefficient is reduced to the first term only, which is a constant. The response properly explains how Equation B-4 and B-5 are derived and is acceptable.

The flow coefficient is converted to a form loss coefficient and then to a friction factor value for use by WCT-M1 at the outlet of the accumulator component. In response to the first LBLOCA RAI set, Question 3.12.14 [Ref. 9], the applicant explained how the loss coefficient is derived from the experimentally determined flow coefficient. The explanation is technically sound and therefore acceptable. The staff notes that the adequacy of the final FRIC values used in WCT-M1 have been verified by comparisons of WCT-M1 calculated flows to the experimental flows from the advanced accumulator tests.

In response to the first LBLOCA RAI set, Question 3.12.15 [Ref. 9], the applicant explains the apparent factor of two discrepancy between the friction factor values given in TR Appendix B, Equations B-9 and B-10, and those derived by the reviewer from Equations 4-197 and 4-256 in Reference 2. The response demonstrates that Equations B-9 and B-10 are correct and is therefore acceptable.

As explained in Appendix B of TR MUAP-07011(R0), the switch between the high and low flow modes in the advanced accumulator is modeled by changing the loss coefficient at the accumulator exit junction. Because the change in loss coefficient is large and sudden, there is a chance it may introduce numerical instability. To prevent this, Equation B-11, which slows the rate of change of the loss coefficient, is applied for ten seconds after mode switching is calculated to occur. In response to the first LBLOCA RAI set, Question 3.12.16 [Ref. 10], the applicant explains how the loss factor damping affected the results of one of the cases presented in Section 3.5 of the subject report. The explanation noted that the damping logic is active for ten seconds after mode switching, but the rate of change of the flow coefficient is determined by the rate change parameter named DKSWDT. Typically, this parameter has a large value, so the switch between flow modes is complete within three seconds. The response also demonstrated that the flow damping did not significantly alter the calculated flow being discharged by the accumulator. For this reason, the RAI response is acceptable.

In response to the first LBLOCA RAI set, Question 3.12.17 [Ref. 9], the applicant provided the values (proprietary) for parameters named QLTMIN and VDMIN. QLTMIN is the amount of water that remains in the accumulator due to the dead volume below the flow control device. VDMIN is the minimum discharge velocity used in the calculation of the cavitation factor. The discharge velocity appears in the denominator of the cavitation factor equation, so a minimum value is needed to prevent a divide by zero. The response is acceptable; it provided the requested information and justified the values used.

Heat transfer between the accumulator wall and the nitrogen gas within the accumulator is not simulated in the WCT-M1 model of the US-APWR according to the response to the second LBLOCA RAI set, Question 9 [Ref. 11]. During accumulator injection the nitrogen gas falls below the accumulator wall temperature. Simulating the wall heat transfer would result in a

slight increase in the pressure of the nitrogen gas and a slightly faster discharge of the accumulator liquid into the RCS. Ignoring this heat transfer in the US-APWR LBLOCA simulation is acceptable to the staff because it has no significant impact on the calculated core response.

Nitrogen, which is dissolved in the accumulator fluid, will not affect the operation of the advanced accumulator flow damper (response to the second LBLOCA RAI set, Question 10 [Ref. 11]). The diffusion coefficient of nitrogen is small; therefore, no significant bubble formation can occur during the short time (< 1 s) it takes fluid to traverse the flow damper. As part of the Advance Accumulator Topical Report review, the staff asked a similar question, the Advanced Accumulator RAI set, Question 63 [Ref. 30], regarding the effect of dissolved nitrogen on accumulator performance. In the Advanced Accumulator Topical Report the applicant presented a $\frac{1}{2}$ scale test (Test Number 5) with water-saturated nitrogen. This test indicated that the accumulator injection large (high flow) injection phase could be extended by up to two seconds. Based on this test, the applicant agreed to increase the accumulator injection pipe loss coefficient by 20 percent to account for any possible dissolved nitrogen effect. The basis for the 20 percent increase in injection pipe loss coefficient is described in the Advance Accumulator Topical Report SE. The 20 percent increase in accumulator loss coefficient is part of the LBLOCA methodology and shall be used for licensing calculations. Therefore, the applicant's response to Question 10 is superseded by the response to Question 63 [Ref. 30].

In response to the second LBLOCA RAI set, Question 11 [Ref. 11], the applicant explained how the uncertainty in the cavitation factor was covered by the assumed uncertainty in the flow coefficient. For large values of the cavitation factor the effect of cavitation factor uncertainty on the flow coefficient is negligibly small. For small values of the cavitation factor, the instrument uncertainties are quite small, less than half of the value assumed in the ASTRUM methodology. Therefore, the assumed instrument uncertainty for the flow coefficient already covers any uncertainty associated with the measurement of the cavitation factor. The applicant also noted that the cavitation factor is independent of scale. The staff agrees with the applicant's conclusion that the uncertainty in the cavitation factor is covered by the assumed uncertainty in the flow coefficient. The response is acceptable. The effect of scaling is being addressed in the Advanced Accumulator, MUAP-07001-P (R4) review. The Conclusion and Limitations section of this SE lists the limitations associated with the effects of accumulator scaling on the LBLOCA analyses.

The applicant was asked why N instead of N-1 was used when calculating the standard deviation of the flow coefficient equations. In response to the second LBLOCA RAI set, Question 12, [Ref. 11], the applicant replied that the size of the statistical population was large (>2500); therefore, the difference between N and N-1 is negligible. The staff agrees and accepts the applicant's response.

In its response to the second LBLOCA RAI set, Question 13 [Ref. 11], the applicant addressed the effect of surface roughness on the inception of cavitation in the throat of the flow damper's outlet nozzle. Surface roughness of the flow damper device in the full scale advance accumulator will be the same as the roughness in the $\frac{1}{2}$ scale device. Hence, the effect of surface roughness has already been accounted for in the determination of the overall uncertainty of the full-height $\frac{1}{2}$ scale tests. The staff agrees that it is reasonable to conclude that the effects of surface roughness on cavitation are covered by the uncertainty that has been assigned to the advanced accumulator flow coefficient. The applicant's response is therefore accepted.

4.1.2.3 Neutron Reflector

TR Section 3.5.3, "Neutron Reflector," describes the modeling of a new component of the US-APWR. The report did not provide any specific information about the cooling holes and stored energy of the neutron reflector. The applicant subsequently provided this information in its response to the first LBLOCA RAI set, Question 3.13.1 [Ref. 9], which partially resolved this question.

In the base version of WCOBRA/TRAC, structures in the RPV, except the fuel rods, are modeled as unheated conductors with wetted walls. This was not considered appropriate for the cooling holes in the NR. Therefore, WCT-M1 was modified to allow inverted annular flow and entrainment to be simulated in the cooling holes. This change was implemented by allowing the NR cooling channels to use the flow regime models that were previously only used by the fuel rods. These flow regimes are used whenever the local wall surface temperature is greater than the local critical heat flux temperature. Several RAI questions were issued to aid the staff in judging the applicability of the WCT-M1 model for the NR and the verification of the model. The RAIs were issued in two groups. The following discussion first addresses the responses to the first set of LBLOCA RAI Questions 3.13-1 through 3.13-4, and then the second set of LBLOCA RAI Questions 1 through 8.

In response to the first LBLOCA RAI set, Question 3.13.2 [Ref. 10], the applicant discussed the NR confirmatory tests [Ref. 8] and the WCT-M1 simulations of those tests. It was demonstrated that the switching of flow regimes in WCT-M1 correlated reasonably well with the progression of the experimental quench front, thus demonstrating the validity of the switching criterion ($T < T_{\text{CHF}}$). This response satisfactorily addressed the issue raised by Question 3.13.2 and is therefore acceptable. Follow-up to the second LBLOCA RAI set, Question 1.10 [Ref. 11] asked what caused the rapid drop in the measured temperatures shortly after reflood began in the NR tests. In its response the applicant stated that sudden drop in the measured surface temperatures at the higher elevations was likely caused by entrained droplets impinging upon the heated wall. It noted that even thermocouples at the same elevation but on opposite sides of the flow channel showed different temperature responses, indicating that the cause of the rapid cooling was very localized. WCT-M1 cannot predict such localized, asymmetric behavior because, by design, it simulates only one-dimensional axi-symmetric flow within each control volume representing the flow channel. The applicant's response is reasonable and acceptable.

Modeling of the flow in the NR cooling holes requires predicting the flow regimes in the holes. One parameter required is the void fraction, α_{critical} , above which entrainment can occur. The applicant's response to the first LBLOCA RAI set, Question 3.13.3 [Ref. 9], provided the derivation of α_{critical} . The response is acceptable because it clarifies how the onset of entrainment is calculated in WCT-M1.

In order to judge the importance of the stored energy in the NR, the staff requested a comparison of the release of energy from the NR to core decay heat for the reference LBLOCA presented in Section 3.6 of MUAP-07011(R0). In response to the first LBLOCA RAI set, Question 3.13.4 [Ref. 10], the applicant provided the requested information, which is therefore acceptable. The response showed that the NR heat release is about 10 percent of the decay heat release at the time of PCT, and less than 20 percent thereafter.

The effect of the NR regarding reflood behavior and the applicability of WCT-M1 to model the relevant thermal hydraulic phenomena were further discussed in the response to the second LBLOCA RAI set, Questions 1 through 8 of Reference 11. Adequate simulation of the NR is needed because of the large amount of stored energy in the NR. During the reflood phase of a LBLOCA the heat release from the NR will cause vapor generation in the NR cooling holes and entrainment and carryout of liquid droplets into the upper plenum. This carryout of liquid droplets to the steam generators may increase the effect of steam binding on core reflooding.

In response to the second LBLOCA RAI set, Question 1 [Ref. 11], the applicant noted that calculated reflood rates in the US-APWR are between 2 and 6 cm/s, which is well within the range of reflood rates of the experimental data base used for the assessment of WCT-M1 [Ref. 3]. The code has also been assessed against the NR reflood tests [Ref. 8], which had reflood rates ranging from 5 to 15 cm/s. The latter assessments show that WCT-M1 overpredicted the amount of entrainment at the 5 cm/s reflood rate test and agreed very well with measured wall temperatures at all elevations. For the higher reflood rate tests, WCT-M1 underpredicted entrainment and the rate of heat transfer from the wall to the fluid; however, these tests are not representative of the long term reflood rates expected during an LBLOCA in the US-APWR. The staff has reviewed the WCT-M1 simulations of the NR reflooding tests and has concluded that the code can adequately simulate the thermal hydraulic phenomena occurring in the NR during reflood. Therefore, the WCT-M1 model of the NR is acceptable.

In responses to the second LBLOCA RAI set, Questions 2 and 3 [Ref. 11], the applicant provided a detailed description of how the NR is represented in the WCT-M1 model. These responses confirmed that the noding used in the US-APWR model was the same as that used in the assessment of the NR reflood tests. This modeling issue is therefore resolved.

Responses to the second LBLOCA RAI set, Questions 4, 5, and 6 [Ref. 11], all addressed the conservatisms inherent in the treatment of the NR for LBLOCA simulations. At the beginning of each transient simulation, the temperature of the NR is set artificially high in order to maximize the heat release during the simulation. The amount of flow through the NR cooling holes is set to the minimum expected value. Heat release to the core peripheral region and the NR/core barrel region is neglected in the simulation, maximizing the heat release to the cooling holes. The staff finds all of the foregoing modeling techniques to be appropriate conservatisms in that they maximize the stored energy of the NR and result in an overprediction of the liquid entrainment in the NR holes.

The code modifications needed to activate the hot wall flow regime model for the NR were given in the response to the second LBLOCA RAI set, Question 7 [Ref. 11]; WCT-M1 simulations of one of the NR reflood tests were presented to show better agreement with the test data obtained when the hot wall model was used instead of the wetted wall model. The comparison demonstrates the appropriateness of using the hot wall flow regime model. This modeling issue is therefore closed.

MHI noted (response to the second LBLOCA RAI set, Question 8 [Ref. 11]) that the applicability of WCOBRA/TRAC to simulate an LBLOCA in the AP600 was approved by the staff [Ref. 12]. The AP600 has an NR similar to that in the US-APWR and WCT-M1 is largely the same as WCOBRA/TRAC.

Based upon its review of all of the information supplied by MHI, the staff concludes that WCT-M1 can adequately simulate the thermal-hydraulic phenomena occurring in the NR cooling holes during an LBLOCA.

In order to confirm that releasing the NR stored energy to only the NR coolant holes was conservative the staff requested the applicant to provide the results of an LBLOCA simulation in which the NR had heat transfer to both the coolant holes and its outer surface. In response to the fourth LBLOCA RAI set, Question 5 [Ref. 19], the applicant provided a comparison of the base case (heat transfer to coolant holes only) to a case with heat transfer from all of the NR surfaces. The sensitivity case resulted in more heat being released during the early reflood period, as expected. However, because the sensitivity case released much of its heat during blowdown, the overall heat released from the NR during reflood was lower than the base case heat release. The PCT of the sensitivity case was 9 °F lower than the base case PCT, demonstrating that the heat transfer modeling technique in the base case is slightly conservative. That modeling technique is therefore acceptable to the staff.

4.1.2.4 Direct Vessel Injection (DVI)

DVI in the US-APWR differs from the AP600 and AP1000 designs in that it has only the HHSI flow injected into the vessel downcomer while the others have all SI flow injected into the downcomer. In response to the second LBLOCA RAI set, Question 20 [Ref. 11], the applicant noted that the NRC approved WCOBRA/TRAC for simulating DVI in the AP600 [Ref. 12] and AP1000 [Ref. 13] because WCOBRA/TRAC conservatively predicted the experimental data obtained in CCTF Run 58 and Upper Plenum Test Facility (UPTF) 21 [Ref. 3], experiments which had DVI. Since WCT-M1 is nearly identical to WCOBRA/TRAC it is reasonable to believe it also can satisfactorily simulate DVI. The response to Question 20 is therefore accepted. The US-APWR contains safety injection pads on the outside of the core barrel opposite each of the DVI nozzles. The purpose of the pads is to direct the HHSI flow downward. The effect of these pads is ignored in WCT-M1, where the DVI is connected horizontally to the vessel (response to Question 21 [Ref. 11]). The staff notes that this treatment of DVI is conservative treatment of the momentum of the injected fluid (downward momentum is ignored) and is acceptable.

4.1.3 Scaling Effects

Conformance with NUREG/CR-5249 CSAU Step 10 requires an applicant to address the ability of a best-estimate code to scale-up the phenomena and processes. The effects of scaling are not addressed in the subject technical report. Scaling was addressed in Reference 3, which considers the base code for WCT-M1. That report addressed conventional 3 and 4 loop Westinghouse plants. The US-APWR power is some 30 percent larger than those plants and may have a different power-to-volume ratio. The staff therefore requested the applicant to evaluate scaling effects with regard to emergency core cooling (ECC) bypass, liquid entrainment, and steam binding in the SG tubes in the second LBLOCA RAI set, Question 39 [Ref. 11].

In response to Question 39, the applicant noted that the ratio of the core power for the US-APWR to a conventional 4-loop Westinghouse plant is 1.3, while the ratio of the RCS liquid volume between the two plants is 1.37. Therefore, the power to volume ratio for the US-APWR is 95 percent of the power to volume ratio of a conventional PWR. It is generally accepted [Refs. 3 and 5] that full-height, power-to-volume scaling is appropriate for LBLOCA phenomena in the blowdown and reflood phases. Since the power-to-volume ratio for the US-APWR is similar to that of a conventional PWR, it is reasonable to believe that the assessment of applicability of WCOBRA/TRAC presented in Reference 3 can be used to justify the application of WCT-M1 to the US-APWR.

Scale effects were observed for some phenomena (ECC bypass, de-entrainment in the upper plenum, and entrainment in the hot legs) in the scaling assessment of WCOBRA/TRAC. Assessments of WCOBRA/TRAC [Ref. 3] against full scale UPTF data showed that it conservatively underpredicted ECC delivery to the lower plenum.

The downcomer gap in the US-APWR is the same size as in a Westinghouse 4-loop plant, while the downcomer flow area, and the core barrel and RPV diameters are 20 percent larger. Thus, one would expect ECC delivered to the core to be smaller in the US-APWR compared to the conventional plant. It is reasonable to believe, therefore, that WCT-M1 will conservatively underpredict the delivery of ECC to the lower plenum for an LBLOCA in the US-APWR.

The applicant's response to Question 39, stated that de-entrainment in the upper plenum of the US-APWR can be expected to be greater than in a conventional PWR while entrainment into the hot legs can be expected to be smaller. A comparison of the upper plenum internals shows that there are many more surfaces upon which to de-entrain liquid in the US-APWR. Also, since the diameter of the US-APWR vessel is 20 percent greater than that of a conventional plant there will be less entrainment of liquid into the hot legs due to the longer transverse path from the core to the hot legs. Therefore, the WCT-M1 prediction liquid flow into the hot legs can be reasonably expected to be less in the US-APWR than in a conventional plant, but WCOBRA/TRAC has already been demonstrated to conservatively predict this phenomenon for a conventional plant [Ref. 3]. The foregoing observations indicate that WCT-M1 can be applied without bias to the modeling of upper plenum de-entrainment and hot leg entrainment in the US-APWR.

In response to the second LBLOCA RAI set, Question 42 [Ref. 11], the applicant noted that while the core power in the US-APWR is 30 percent greater than that of a conventional plant, the flow area of the hot leg is only 14 percent greater. For similar core steaming rates in the two plants, the velocity of the steam in the hot legs would be greater (about 15 percent) in the US-APWR. Hence, any droplets which make it to the hot leg would have a greater probability of reaching the SG tubes. This is not particularly significant, however, because the WCT-M1 simulations show that all the droplets reaching the hot legs are swept into the SG tubes until well after the time of maximum PCT.

The staff finds the analysis and arguments provided in the responses to Questions 39 and 42 form a reasonable basis for concluding WCT-M1 can adequately simulate the entrainment/de-entrainment phenomena in the upper plenum and hot legs during an LBLOCA in the US-APWR. The applicant's responses are accepted.

The staff's review of scaling issues for the advanced accumulator is considered elsewhere – they are part of the staff's review of the Advanced Accumulator Topical Report, MUAP-07001-P(R4). The dynamics of reflood in the NR have already been evaluated at full scale in Reference 8.

4.1.4 ASTRUM Methodology Applied to US-APWR

Per NRC guidelines (RG 1.157 and the CSAU methodology), any best estimate LBLOCA analysis must be accompanied by an estimate of the uncertainty of the key safety parameters: PCT, LCO, and CWO.

In TR Section 3.7, the application of the ASTRUM methodology to the US-APWR is described. ASTRUM is based on the non-parametric approach described by Wilks [Ref. 17] and later on by

Guba et al. [Ref. 18]. This step is consistent with CSAU Step 13 but differs from the CSAU demonstration in Reference 5, where a response surface method was used. In the non-parametric approach, the plant and model parameters are randomly sampled and a set of 124 calculations are performed to achieve 95/95 values for the three safety parameters. The 95/95 value means that there is a 95 percent probability at the 95 percent confidence level that the actual value of a safety parameter is less than the maximum value produced by the analysis.

ASTRUM consists of a set of computer programs and PERL scripts. The calculation of the RCS response for a set of pipe breaks is accomplished using WCT-M1. The calculation of local response for the limiting rod is accomplished using HOTSPOT. HOTSPOT takes boundary conditions (local power, heat transfer coefficient, etc.) from the WCT-M1 calculation and calculates the thermal response of the hot assembly fuel rods.

The ASTRUM methodology calls for the calculation of a WCT-M1 Reference Case. This calculation is a double-ended guillotine break (DEGB) of the cold leg which uses the best estimate values for some, and conservative values of other, uncertainty parameters used in ASTRUM. All subsequent 124 WCT-M1 and HOTSPOT calculations are perturbations to the Reference Case – uncertainty parameters are randomly changed for each run. The output from all 124 cases is sorted to identify the case that has the highest PCT, the case that has the highest LCO, and the case which gives the highest CWO. These three parameters are then compared to the corresponding safety limits, and the results are reported in Section 15.6.5 of the Design Control Document (DCD) for the US-APWR.

The applicant's ASTRUM methodology has 42 uncertainty parameters, which address the highly ranked phenomena identified in its PIRT. These parameters are either sampled or treated in a conservative fashion. Of the 42 uncertainty parameters, 38 are the same as those in Reference 2, although the PDF may differ. The other four parameters are associated with uncertainty of the advanced accumulator discharge flow coefficient, one each for the high flow and low flow regimes with either a large or small cavitation factor.

In response to the first LBLOCA RAI set, Question 3.16.1 [Ref. 9], the applicant demonstrated that the value for any uncertainty parameter is obtained by sampling the full range of the parameter's uncertainty range. The response provided the demonstration requested and is therefore acceptable.

Editorial corrections requested by the staff were made in response to the first LBLOCA RAI set, Question 3.16.2 [Ref. 9] and the second LBLOCA RAI set, Questions 32 [Ref. 11].

TR Subsection 3.16.3 describes the parameters used in the uncertainty analysis, but does not provide the connection between processes ranked high in the PIRT and the uncertainty parameters. Nor does it provide any information regarding the distribution type, range, and basis for the uncertainty parameters. The first LBLOCA RAI set, Questions 3.16.3 and 3.16.4 [Ref. 9], as well as the follow-up second LBLOCA RAI set, Questions 1.12, 30, and 31 [Ref. 11], all address this lack of information. In its responses to these RAIs, the applicant stated that the connection between important PIRT parameters and uncertainty parameters are described in the ASTRUM methodology report [Ref. 2], which is the core of the applicant's approach. It was also noted that the uncertainty distribution types and ranges are also given in that report and, for most parameters, are the same as those used for the US-APWR. Four tables were provided to show those parameters that were treated differently in the US-APWR than they were in the ASTRUM report. Since the responses to the foregoing RAIs provided the nominal value, distribution type, and distribution range for the uncertainty parameters, they are acceptable.

In response to the fourth LBLOCA RAI set, Question 2 [Ref. 19], the applicant provided justification for the nominal value, range, and distribution type for several uncertainty parameters about which the staff requested additional information. The response indicated that core power level would not be sampled below the nominal value of 100 percent. The nominal value for the cold leg nozzle coefficient was derived for the US-APWR, thus providing assurance that the value was unique to the US-APWR and not a carry-over from Reference 3. The nominal value of F_q is obtained by subtracting the uncertainties in F_q from the technical specifications (TS) limiting value.

The limiting value is then conservatively assumed to be the 95 percent value for a normal distribution centered about the nominal value. This procedure can be shown to yield values of F_q that are higher than the values expected during normal operation, and therefore conservative. Because it provided the clarifications sought, the response to Question 2 is acceptable with respect to all parameters except the accumulator temperature and the fuel burnup. The staff's concerns with those parameters are addressed elsewhere in this SE.

The applicant confirmed, in its response to the second LBLOCA RAI set, Question 14 [Ref. 11], that the accumulator nominal pressure in the ASTRUM analysis is the midpoint of the TS minimum and maximum allowed values. The range of these values is sampled uniformly. The response confirmed that a reasonable nominal value and PDF are used for the accumulator pressure; it is therefore acceptable.

The temperature of the water in the accumulator and the temperature of the high pressure SI water are both uncertainty parameters in the ASTRUM analysis. The second LBLOCA RAI set, Questions 16 and 19 [Ref. 11], requested justification of the lower bound values being used for these parameters. The response to Question 16 [Ref. 11] stated that the lower bound for the accumulator temperature was 21 °C (70 °F), which is at the lower end of the anticipated containment temperatures for normal operation. The upper bound was the maximum TS limit of 49 °C (120 °F). The liquid temperature distribution is assumed to be uniform over this range. The applicant did not supply any information justifying its choice of a lower limit. The staff therefore issued the fourth LBLOCA RAI set, Question 2 which requested further justification of the lower limit value, or a demonstration that the calculated PCT for the LBLOCA analysis is not sensitive to the value chosen for the lower bound. In an amended response to Question 2 [Ref. 23], the applicant noted that the lower bound value of 21 °C (70 °F) was chosen to be consistent with the analysis for minimum containment temperature. In addition, the response presented an evaluation of the effect of the accumulator temperature lower bound value upon computed ASTRUM results. Three ASTRUM calculations (124 cases each) were run: Case 1 had an accumulator temperature range of 21 °C – 49 °C (70 °F – 120 °F); Case 2 used a 38 °C – 49 °C (100 °F – 120 °F); and Case 3 used a fixed temperature of 49 °C (120 °F). Only the accumulator temperature was varied in the three sets of runs; the values of other uncertainty parameters were the same in each set of 124 runs. The limiting run for each of the three ASTRUM cases was run 103 and the three PCTs were all within 19 °F of one another. The PCT for Cases 1 and 2 were the same and the PCT for Case 3 was 19 °F lower. Comparison of the top five highest PCT runs from Case 1 and Case 2 revealed that the range of PCTs was the same and the average PCT was somewhat higher for Case 1, the case with the largest sampling range for the accumulator temperature. The applicant concluded that the ASTRUM results demonstrate that the choice of the lower bound temperature has little effect on the final PCT obtained by ASTRUM as applied to the US-APWR. In order to cover a wider range of possible accumulator temperature values the applicant elected to use a lower bound of 21 °C (70 °F). The staff believes it is fairly unlikely that the accumulator temperature will be near 21

°C during normal reactor operation. However, because of the low sensitivity of PCT to the lower bound choice and because the case with the larger sampling range gave a higher average PCT for the top five runs, the staff finds the applicant's choice reasonable and accepts its response to Question 2.

In response to the second LBLOCA RAI set, Question 19 [Ref. 11], the applicant stated that the RWSP water temperature was represented as a uniform distribution over the range 7 °C (45 °F) to 49 °C (120 °F), with a nominal value of 35 °C (95 °F). However, in the response to the fourth LBLOCA RAI set, Question 2 [Ref. 19], the applicant revised the lower bound to 21 °C (70 °F). The staff finds the assumed range and distribution to be reasonable and therefore acceptable. The assumed RWSP temperature will not affect the limiting PCT calculated in the applicant's ASTRUM analysis because HPSI always starts after the time of PCT for the limiting breaks.

The liquid temperatures in the US-APWR accumulator may be as high as 49 °C and is slightly out of the full-height ½ scale advanced accumulator tests range. The second LBLOCA RAI set, Question 17 requested the applicant to address the effect of higher temperatures upon the flow coefficient correlations derived from the full-height ½ scale tests. In its response [Ref. 11], the applicant observed that a water temperature difference will affect water viscosity and density and nitrogen solubility. The effect of viscosity is negligible because of the high Reynolds numbers associated with accumulator injection. The effect of fluid density is included in the calculation of the flow coefficient. The solubility of N₂ at 49 °C is about 70 percent of what it is at 20 °C. In its review, the staff has concluded that the effect of temperature upon the flow coefficient equations is encompassed by the uncertainties assigned to those equations. Therefore, the response to Question 17 is accepted.

The nominal value and sampling range of the accumulator liquid volume were verified to be in compliance with the staff's expectations in the response to the second LBLOCA RAI set, Question 18 [Ref. 11], closing that issue.

In response to the second LBLOCA RAI set, Question 36 [Ref. 11], the applicant noted that fuel manufacturing uncertainties are not treated directly in the uncertainty analysis; rather, they are included in the uncertainty of the fuel rod gap conductance. This approach is standard industry practice and acceptable to the staff.

The responses to the second LBLOCA RAI set, Questions 34, 43, and 44 [Ref. 11], address initial fuel rod stored energy issues that were raised by the staff. The fuel rod temperature at any burnup is determined using the FINE computer code. Although the fuel thermal conductivity model in WCT-M1 is the same as that in FINE, the fuel gap model is not. Therefore, the gap size is adjusted in the WCT-M1 initialization process so that the average initial pellet average temperature agrees with that calculated by FINE. All fuel rods in the WCT-M1 model are initialized at a burnup of 2.4 GWD/MTU. Fuel rod gap conductance and fuel pellet thermal conductivity are uncertainty parameters in the HOTSPOT calculation. The response to Question 43 compared the nominal fuel pellet temperature from FINE plus its maximum uncertainty to the 95/95 value computed by HOTSPOT. The comparison showed that HOTSPOT always produced the higher pellet average temperature. The applicant's responses to the forgoing RAI questions regarding stored energy have provided assurance that its uncertainty is being treated reasonably. The responses are therefore acceptable.

The response to the fourth LBLOCA RAI set, Question 3 [Ref. 19], was an attempt to demonstrate that the initial fuel stored energy in the WCT-M1 simulations was conservatively high. The response showed that for a given fuel rod the stored energy peaks at a burnup of 2.4

GWD/MTU. Therefore, the applicant uses that burnup to initialize all fuel in the core. The staff was not convinced that this procedure gives a conservative initial stored energy. The periphery fuel is low power (~3 kW/m) but high burnup (~ 45 – 62 GWD/MTU over a cycle). The applicant's response to the second LBLOCA RAI set, Question 43 [Ref. 11], shows that, for a fixed rod power, fuel average temperature at 42 GWD/MTU exceeds the fuel average temperature at 2.4 GWD/MTU and steadily increases as exposure increases. A plausible makeup of an equilibrium core is 40 percent fresh fuel, 40 percent once-burnt fuel, and 20 percent twice-burnt fuel. It is not obvious that the stored energy of this fuel combination is bounded by fuel having an exposure of 2.4 GWD/MTU. In an April 5 and 6, 2011, meeting between the staff and the applicant, the staff explained its concern with the stored energy in WCT-M1. The applicant committed to providing a supplemental response to the fourth LBLOCA RAI set, Question 3 to address the staff's concerns.

In the supplemental response to RAI-3 [Ref. 24], the applicant presented the results for the following WCT-M1 cases:

Table 1 WCT-M1 Cases for RAI-3

	Hot Assm.	Avg. Assm.	Periphery Assm.	PCT °C (°F)
Base Case ^(a)	BOL ^(b)	BOL	BOL	909 (1669)
Case 1-1	BOL	EOL ^(c)	EOL	902 (1656)
Case 1-2	BOL	BOL	EOL	903 (1657)
Case 1-3	BOL	EOL	BOL	902 (1656)

^(a) Reference Case in Chapter 15.6.5 of the US-APWR DCD Revision 3

^(b) 2.4 GWD/MTU

^(c) 62 GWD/MTU

The lower PCT in Case 1-1 was shown to be a result of an increase in lateral flow from the average core region into the hot assembly.

The applicant's results demonstrate that using a beginning of life burnup distribution for all the assemblies in the core results in the highest PCT. Therefore, the staff finds the use of that distribution in WCT-M1 to be acceptable. The initial stored energy issue is resolved.

The uncertainty in the ANSI/ANS 5.1-1979 decay heat standard is ±3 percent for time less than 20 seconds after shutdown and ±2 percent thereafter. The former uncertainty value is used for all times in the applicant's ASTRUM methodology (response to the second LBLOCA RAI set, Question 40 [Ref. 11]). This uncertainty value was previously approved by the staff in its review of ASTRUM and is therefore acceptable for the US-APWR application. The response is acceptable.

The process of running ASTRUM for the US-APWR was described in the response to the second LBLOCA RAI set, Question 45 [Ref. 11]. All of the PERL scripts (PERL is a scripting language) which control the running of the computer codes for 124 LBLOCA cases were provided to the staff. The description of how the various scripts are used is acceptable.

In response to the second LBLOCA RAI set, Question 47 [Ref. 11], the applicant confirmed that the same seed was used to generate the values of uncertainty parameters for the LBLOCA results in Revisions 1 and 2 of the US-APWR DCD. This response allows the staff to confirm that the changes in the LBLOCA results were not due to use of different uncertainty parameters. Therefore, the result is acceptable.

4.2 Sample Plant Analysis

TR Section 3.6 describes the nodalization used in WCT-M1 for the analysis of an LBLOCA in the US-APWR. The results of a sample calculation are also presented.

The first LBLOCA RAI set, Questions 3.3 and 3.15.1 [Ref. 9] and the second LBLOCA RAI set, Questions 1.2, and 1.11 [Ref. 11], all pertained to calculated core heat transfer during the blowdown period. The response to Question 3.3 [Ref. 9] explained the early, brief reversal of the temperature rise at the hot spot is due to fluid flashing at the break causing a reduction in break flow, thus allowing for a brief re-establishment of positive core flow by the RCPs. The Question 3.15.1 response [Ref. 9] explained how the cladding temperature rise during blowdown was terminated by a surge of reverse flow through the core. The response to Question 1.2 [Ref. 11] provided plots showing cladding temperature and local mass flow rate during blowdown and the response to Question 1.11 [Ref. 11] provided plots of RCP flow and void fractions. The aforementioned RAI responses have provided an adequate explanation of the blowdown core heat transfer mechanisms and are therefore acceptable.

In the second LBLOCA RAI set, Question 35 [Ref. 11], the staff requested additional information about the DNB correlation used in WCT-M1, and its applicability to the US-APWR 4.2 m long core. The response to Question 35 noted WCT-M1 uses a combination of the Biasi CHF correlation and the modified Zuber CHF correlation. Both correlations are local-condition correlations and do not depend directly on heated length. Plots of DNB time and fluid conditions at DNB occurrence for the DCD LBLOCA Reference Case were given to demonstrate that the local fluid conditions were within the experimental range of the Biasi correlation. Finally the response noted that the WCT-M1 DNB model had been validated against Oak Ridge National Laboratory (ORNL) Thermal Hydraulic Test Facility (THTF) and Loss of Fluid Test (LOFT). Those validations showed DNB locations were adequately predicted in the THTF tests and DNB occurrence times were well predicted in LOFT.

In the WCT-M1 sample plant analysis DNB occurred on the hot rod at 0.4 seconds (response to Question 35 [Ref. 11]). The staff conducted an independent WCT-M1 calculation using a 0.7 multiplier on the calculated CHF value. This WCT-M1 simulation calculated DNB to occur at 0.24 seconds and gave a PCT that was about 28 °C (50 °F) higher than the applicant's sample plant analysis value. Thus, the time of DNB is a significant parameter in the determination of PCT. The applicant has ranked DNB as a significant parameter in its PIRT, but the applicant's methodology does not treat the uncertainty in DNB in its WCT-M1 calculation. Rather, the methodology claims to account for the uncertainty in the DNB calculation via application of a blowdown heat transfer multiplier in the HOTSPOT computer code. In the ASTRUM methodology, the HOTSPOT code, not WCT-M1, yields the PCT.

The staff investigated the nature of the blowdown heat transfer multiplier distribution and its derivation. It found that the multiplier's PDF was such that in a random sampling there would be only a 5 percent chance of obtaining a value greater than unity. It was much more likely to obtain a value considerably less than unity. Therefore, the most probable effect of the multiplier is to increase the HOTSPOT PCT relative to the WCT-M1 hot spot cladding temperature. The staff's investigation found the blowdown PCT calculated by HOTSPOT was 86 °C (155 °F) greater than the WCT-M1 hot spot cladding temperature for the limiting PCT case (Case 48) reported in Revision 2 of the US-APWR DCD. This is considerably larger than the increase in PCT obtained by modifying the CHF correlation in WCT-M1 as discussed in the previous paragraph. In light of these results, the staff believes the ASTRUM method of addressing uncertainty in blowdown heat transfer is reasonable and acceptably accounts for the DNB

calculation uncertainty. Therefore, the response to Question 35 is accepted and the issue closed

TR Sections 3.6.1 to 3.6.3 describe the nodalization, calculation process, and specific models of the NR, pump, and containment. Five questions (the first LBLOCA RAI set, Questions 3.14.1 to 3.14.5) were originally issued pertaining to these sections. These are general questions and requests for better documentation. They are related to three dimensional nodalization, flow losses in azimuthal and axial direction, the friction option, and nodalization in the fuel rods.

The response to Question 3.14.1 [Ref. 9], explained how WCT-M1 calculates frictional losses in the vessel. The response demonstrated that frictional losses in the radial, azimuthal, and axial directions are properly treated; therefore, the response is acceptable. In response to RAI 3.14.2 [Ref. 9], the applicant demonstrated that the nodalization used in the model of heat conduction in the fuel rods was the same as that used in the NRC approved version of WCOBRA/TRAC. Since the US-APWR fuel rods are similar to existing fuel rods, the staff agrees that the nodalization being used is adequate and this issue is closed. The modeling of the DVI in the WCT-M1 model was described to the staff's satisfaction in the response to Question 3.14.3 [Ref. 9].

Prior to running a transient, the WCT-M1 model must be brought to steady-state. In its response to Question 3.14.4 [Ref. 9], the applicant described its steady-state acceptance criteria which determine when a satisfactory steady-state condition has been achieved. The criteria require the simulated value of each of eleven parameters be within the measurement uncertainty of the desired value of that parameter. The staff finds this to be a reasonable definition of steady state; therefore, the response is acceptable.

The two-phase performance (fully degraded homologous curves and the two-phase multiplier curve) of the US-APWR pump model in WCT-M1 is based upon 1/3 scale pump tests at low pressures. In its response to Question 3.14.5 [Ref. 10], the applicant discussed the applicability of the 1/3 scale pump data to the full scale US-APWR pump. The staff finds the arguments advanced by the applicant to be reasonable and the response acceptable. Although there is some uncertainty associated with using the 1/3 scale derived performance curves, it is conservative to do so. This is because pump degradation and its uncertainty decrease with increasing pressure and increasing pump size [Ref. 5].

An editorial change was made in response to the first LBLOCA RAI set, Question 3.15.2 [Ref. 9]: the definition of the end-of-refill was corrected to be the time at which the lower plenum refills, not the time when the downcomer is full.

The staff's request for a comparison of the plant and safety analysis logic for reactor trip, RCP trip, and main steam isolation was satisfied by the response to the second LBLOCA RAI set, Question 24 [Ref. 11], confirming that all were modeled conservatively.

The applicant uses a single containment pressure curve as the break boundary condition, regardless of break size. The applicant enumerated all the conservatisms that are in its calculation of containment pressure in its response to the second LBLOCA RAI set, Question 26 [Ref. 11]. It compared a best-estimate containment pressure calculation with the conservative one used in the LBLOCA analysis and concluded that the best estimate containment pressure response is up to 40 percent higher than the curve used in the LBLOCA analysis. The staff also conducted containment pressure response calculations which showed that the curve being used is lower than a best-estimate calculation over the range of break sizes being used in the

applicant's BELBLOCA methodology. The staff is therefore confident that the containment pressure curve used in the LBLOCA analysis is conservatively low.

Table 3.6-5, "Analysis Conditions," states that the pressurizer is on an intact loop, but Figure 3.3-3 shows it on the broken loop. This discrepancy was explained in the response to the second LBLOCA RAI set, Question 27 [Ref. 11]. As part of the BELBLOCA methodology a sensitivity study is done using the Reference Case input to determine which pressurizer location, intact or broken loop, gives the highest PCT. The pressurizer location corresponding to the highest PCT is then used in all subsequent analyses. The staff accepts this technique as a reasonable approach to establishing the location of the pressurizer for the LBLOCA analysis.

The hot rod power peaking factor, F_{RH} , is assigned a value of 1.78, while the value of 1.73 is used for the US-APWR design (response to the second LBLOCA RAI set, Question 28 [Ref. 11]). The use of a conservative value in the BELBLOCA analysis is acceptable to the staff.

The BELBLOCA methodology does not credit control rod insertion. The large amount of voiding early in the LBLOCA simulation is sufficient to quickly shut down the fission process.

In response to the second LBLOCA RAI set, Question 29 [Ref. 11], the applicant addressed an apparent discrepancy between Section 15.6.5 of the DCD and the topical report. The time of reactor trip given in the DCD only refers to the time the reactor trip signal was generated. It does not imply rod insertion. The clarification is acceptable.

Proof of temporal convergence of the WCT-M1 calculations was provided in the response to the second LBLOCA RAI set, Question 33 [Ref. 11], where it was demonstrated that essentially the same PCT was obtained when the time step sizes used in the LBLOCA simulations were cut in half. This is the usual way of demonstrating temporal convergence and is acceptable to the staff.

The noding scheme used in the WCT-M1 for the US-APWR model is the same as that used in Westinghouse's approved model for 3 and 4 loop plants. Therefore, the applicant addressed only spatial convergence for those features of the US-APWR that are unique (response to the second LBLOCA RAI set, Question 38 [Ref. 11]). The adequacy of the model of the neutron reflector was demonstrated by comparisons of WCT-M1 to the NR reflood tests. The plant model uses the same nodalization as was used in those tests. The results of the nodalization sensitivity studies for the advanced accumulator, break, and DVI region of the vessel were presented. The studies showed that doubling the number of spatial nodes in the broken cold leg, and at the ECC injection points, and near the DVI nozzles did not significantly change computed results. These results satisfactorily demonstrate that the noding in these regions is adequate to resolve the thermal-hydraulics associated with the unique features of the US-APWR. The responses to Questions 33 and 38 demonstrate fulfillment of CSAU Step 8 and are therefore acceptable.

The staff noted that Figure 3.6-18, "Downcomer Liquid Level," showed an oscillatory behavior. The first LBLOCA RAI set, Question 3.10 requested an explanation of the oscillatory behavior, in particular the role of condensation due to direct vessel injection, a phenomenon which is ranked as not applicable. The response to Question 3.10 [Ref. 10] stated that DVI related condensation was rated as not applicable because it occurred after the hot spot in the core had quenched. When DVI was initiated (125 s) the downcomer level was high enough to cover the DVI nozzles, so no steam condensation was occurring due to DVI. Only after the accumulators emptied did the downcomer level drop below the DVI nozzles, but by this time the core had

been quenched. The staff finds the applicant's response acceptable in that it explained the role of DVI-induced condensation. However, the applicant did not address the part of the RAI that requested an explanation of the downcomer oscillations. Therefore, follow-up second LBLOCA RAI set, Questions 1.5 and 41 were issued, both requesting an explanation of source of the downcomer level oscillations that occur between 40 and 125 seconds and an explanation of how the uncertainty in the prediction of the oscillations is treated.

In response to Question 1.5 [Ref. 11], the applicant stated that the ASTRUM analysis accounts for the effect of core flow oscillations on PCT through its treatment of the uncertainty in parameters that affect system behavior. It provided no information about how this is done. The response to Question 41 [Ref. 11] noted that in comparisons of WCOBRA/TRAC, the base code of WCT-M1, to integral tests it also exhibited oscillations not seen in the data. Nevertheless, the code showed adequate prediction of cladding temperatures, indicating that the oscillations did not unduly enhance the core heat transfer calculation [Ref. 3]. The response to Question 41 also presented a sensitivity study which, it claimed, showed that reducing the magnitude of the oscillations did not significantly change the calculated PCT for the WCT-M1 sample calculation presented in the LBLOCA Topical Report [Ref. 1]. The staff agrees with the applicant's conclusion; however, the applicant did not present enough information for the staff to conclude that its sensitivity study was meaningful. The applicant's response indicated that oscillations were suppressed by modifying WCT-M1. In order to judge the efficacy of the modifications the staff requested more information about the code modifications and any input modifications.

In its response to the fourth LBLOCA RAI set, Question 4 [Ref. 19], the applicant provided a discussion of the temporary changes that were made to the WCT-M1 source code and input to dampen the core flow oscillations. The applicant also provided an explanation of how the temporary code modifications led to a PCT that was slightly lower than the base case. The modifications resulted in more liquid accumulation in the bottom of the core, which led to an increased vapor generation rate and increased entrainment flow rate at the hot channel PCT location.

The response to Question 4 also noted that in the assessment of WCOBRA/TRAC against CCTF run 62 fairly large oscillations were observed in the calculation, yet the calculated PCT agreed well with the measured value, indicating that calculated core flow oscillations are benign with respect to their effect on PCT calculations.

The staff evaluated the temporary changes made to WCT-M1 and judged them to be a reasonable approach to dampen the core flow oscillations. The changes essentially introduced a dynamic loss coefficient at the core inlet. By increasing the loss when the core flow increased the magnitude of the oscillations was reduced. Based on the applicant's response to Question 4, the staff believes it is reasonable to conclude that the reflood flow oscillations in the WCT-M1 simulations do not have a large effect on the calculated PCT. The response to Question 4 is therefore acceptable.

During the staff's evaluation of Question 4, it discovered a coding error in HOTSPOT. In an April 5–6, 2011, meeting with the applicant, the staff discussed the possible impact of the error and asked the applicant to address the impact in a supplementary response to Question 4. The supplementary response to Question 4 [Ref. 24] confirmed that HOTSPOT did not correctly impose the maximum limit (HMAX) on the local heat transfer coefficient as described in the HOTSPOT documentation. The applicant corrected the coding and reran the four cases with the highest PCTs in the ASTRUM analysis for DCD Revision 3. Comparison of these four cases with their original results showed that the PCT was unaffected for all cases. The only

difference in hot spot cladding temperature response was that the new cases had a slightly higher cladding temperature just prior to cladding quench. Plots of the local cladding heat transfer coefficients showed that this was the time where the HMAX limit had been exceeded in the unmodified version of HOTSPOT. The staff is satisfied that HOTSPOT has been modified so that it properly imposes HMAX and that the code modification has no impact upon the current values of PCT reported in the DCD. Therefore, the staff accepts the supplementary response to Question 4 as it pertains to HOTSPOT.

In an April 5 – 6, 2011, meeting with the applicant, the staff discussed the need for the applicant to demonstrate the WCT-M1 model nodding was adequate to address potential downcomer boiling. The hot wall effect, which could cause downcomer boiling, was ranked high during reflood in the applicant's PIRT. The staff requested the applicant to address downcomer boiling as part of its supplementary response to Question 4.

To assess the treatment of DC boiling the applicant provided the following WCT-M1 simulations:

Table 2 WCT-M1 Cases to Address DC boiling

Parameter	Base Case	Case 1	Case 2	Case 3	Case 4
Accum . Temp.	Nominal	Maximum	Maximum	Maximum	Maximum
Accum. Flow	Nominal	Minimum	Minimum	Minimum	Minimum
SI Temp.	Nominal	Maximum	Maximum	Maximum	Maximum
SI Flow	Minimum	Minimum	Minimum	Minimum	Minimum
Azimuthal Nodes	4	4	8	4	4
Azimuthal loss coefficients	0.0	0.0	0.0	0.5	0.0
Timestep Size / DTMAX in the reflood phase	0.001/0.002	0.001/0.002	0.001/0.002	0.001/0.002	0.0005/0.002

The base case is the Reference Case in DCD Revision 3. All cases were run to 1000 seconds to see if significant downcomer boiling occurred and resulted in a second reflood heatup. All cases used the minimum containment back pressure curve used in the ASTRUM analysis. The break was a DEGB with a discharge coefficient of 1.0 for all cases. The response showed that this break type results in PCTs occurring during reflood, while split breaks generally result in blowdown PCTs. Thus, the DEGB break type is more likely to be affected by downcomer boiling.

No significant boiling of the downcomer fluid occurred in any of the five WCT-M1 simulations. The average collapsed level in the downcomer was as much as 30 cm (1 ft.) lower in the sensitivity cases because of the limiting boundary conditions used in those simulations. However, since the average collapsed downcomer level for all simulations was greater than 4.2 m, all the simulations had sufficient driving head to keep coolant flowing into the core throughout the 1000 seconds of simulation time. Thus, there was no second reflood heatup in any of the simulations.

The staff reviewed the axial nodding used in the WCT-M1 model and the radial and axial nodding used for the heat structures attached to the downcomer channels and found them sufficient to accurately capture the thermal hydraulic phenomena occurring during core reflood and the long term cooling phases of the LBLOCA. Based upon this finding and the results presented in the foregoing paragraph, the staff finds the WCT-M1 model of the downcomer to be adequate and

acceptable for LBLOCA analysis. The applicant's response is therefore accepted and the issue is resolved.

The staff noticed that the LBLOCA sample problem's upper head temperature was equal to the cold leg temperature. It requested a justification of that value. The applicant responded as a supplementary response to the fourth LBLOCA RAI set, Question 2 [Ref. 23], stating that the US-APWR is designed so that the upper head fluid remains at the temperature of the cold leg fluid. The response provided the design calculations that were made to determine what downcomer to upper head bypass flow is required to guarantee downward flow in all the Rod Cluster Control Assembly (RCCA) guide tubes, the only flow paths between the upper plenum and upper head. The staff reviewed the design calculations and concurs that the designed bypass flow from downcomer to upper head is sufficient to keep the upper head fluid temperature the same as the cold leg fluid temperature. The design calculation has considered all appropriate uncertainties.

4.3 Independent Analyses

Confirmatory calculations were conducted by the staff to provide a basis for evaluating whether the applicant's LBLOCA analysis results are reasonable, and to inform the staff of the influence of uncertainty parameters upon computed results.

4.3.1 RELAP5/MOD3.3 Simulations

The RELAP5/MOD3.3 (R5M33) US-APWR plant model employed for the small break LOCA (SBLOCA) confirmatory analyses [Ref. 14] was used as the starting point for developing a R5M33 US-APWR model for the LBLOCA confirmatory calculations.

Overall the R5M33 confirmatory calculation was in good agreement with the WCT-M results for the LBLOCA Reference Case [Ref. 15]. The calculated PCT is 940 °C (1,723 °F) with R5M33 and 970 °C (1,665 °F) with WCT-M1. Therefore, neither the R5M33 nor WCT-M1 calculations indicate a significant challenge to the 1,204 °C (2,200 °F) PCT acceptance limit. The R5M33 calculation showed the PCT occurred during blowdown while WCT-M1 calculated it to occur during the reflood period. An investigation into this discrepancy revealed the lower blowdown peak temperature in WCT-M1 was due to both a model difference and a code difference.

The model difference is that the WCT-M1 model had a large loss coefficient at the broken cold leg nozzle. The R5M33 model, being based on the applicant's SBLOCA model, did not. The LBLOCA WCT-M1 model's cold leg loss coefficient is one of the ASTRUM uncertainty parameters. When the same loss was added to the R5M33 model, its calculated blowdown PCT was in much better agreement with WCT-M1.

R5M33 does not apply any relaxation technique to either heat transfer coefficients or critical heat flux. Consequently, the R5M33 LBLOCA simulation calculated DNB to occur within 20 ms of the break opening. WCT-M1 applies an exponential relaxation to both heat transfer coefficients and the critical heat flux [Ref. 3]. DNB was calculated to occur at about 0.25 seconds in the WCT-M1 simulation. The quarter-second longer period of nucleate boiling in the WCT-M1 simulation allowed the removal of a significant amount of stored energy from the fuel rods relative to the R5M33 simulation.

The R5M33 PCT response was found to be insensitive to a 15 percent variation in the peak break flow rate, which is the magnitude of the difference between peak break flows in the WCT Reference Case and R5M33 calculations.

Fuel rod gap conductance is modeled differently in WCT-M1 than in R5M33. WCT-M1 has a dynamic gap conductance model in which the conductance varies during the LOCA transient. On the other hand, gap conductance was constant throughout the transient in the R5M33 simulations. A R5M33 gap conductance sensitivity study was conducted to see how much of the codes' difference in PCT results could be attributed to the different gap conductance models. A R5M33 gap conductance sensitivity evaluation indicated that a significantly-reduced constant gap conductance (to about 20 percent of the constant gap conductance used in the R5M33 base calculation) provided the best match to the WCT-M1 PCT results. However, this value is unrealistically low, indicating that differences in gap conductance models in the two codes could not be responsible for all of the differences in calculated PCTs in the two codes.

The R5M33 blowdown/reflood period fuel temperature response was found to be insensitive to variations in the axial location of the fuel rod peak power density. This finding indicates that effects related to the elevation of core flow stagnation are likely not major contributors to the blowdown-period PCT behavior differences between R5M33 and WCT-M1 Reference Case calculations.

4.3.2 WCT-M1 Simulations

Confirmatory WCT-M1 and HOTSPOT calculations were performed to:

- Independently verify the results reported by the applicant.
- Better understand the ASTRUM methodology.
- Identify PCT sensitivities to uncertainty parameters.
- Examine calculation details not reported by the applicant.

The Reference and limiting PCT cases reported in the DCD (Section 15.6.5, Ref. 15) were run using input files and code executables supplied by the applicant. The results of that staff's calculations were in excellent agreement with the DCD results, verifying that the files provided to the staff were those used for the DCD analysis. The results also showed that for the limiting PCT case, the PCT calculated by HOTSPOT was 68 °C (123 °F) higher than the PCT calculated by WCT-M1. The fuel rod uncertainty parameters associated with HOTSPOT are responsible for the increase. The results also showed that the hot spot cladding temperature from the WCT-M1 Reference Case was 17 °C higher than the limiting case's value. This is because the Reference Case uses the TS maximum F_q value, while the hot spot cladding temperature limiting case samples F_q from a PDF with the TS maximum as a 95 percent probability.

A WCT-M1 run was made to verify that the gravitational heads around the RCS coolant loops summed to zero. This was done by specifying the RCP speeds, core power, main feedwater flows, and steam flows as zero in the model and running a 1,500-s transient calculation under those conditions. The result of this calculation revealed that instead of decaying to zero, the flow in each coolant loop reached a steady value of 300 kg/s. This result indicates an input

error in the model. The second LBLOCA RAI set, Question 46 was issued asking the applicant to address the issue.

In response to Question 46 [Ref. 11], and in response to the fourth LBLOCA RAI set, Question 1 [Ref. 19], the applicant acknowledged the WCT-M1 result obtained by the staff. The responses demonstrated that WCT-M1 would predict zero loop flow if the elevation difference terms were set to zero for each loop. The responses do not address the relevant issue. WCT-M1 is calculating a residual flow in each loop even when the fluid density is the constant around the loop. This indicates an error in WCT-M1's treatment of the gravity head. The staff's position is that if WCT-M1 has an error in its treatment of the gravity head, it should be addressed by the applicant. In a revised response to Question 1 [Ref. 20], the applicant acknowledged that an error in the momentum source calculation in the pump component of WCT-M1 was the cause of the residual loop flow identified by the staff. The coding error was fixed and the applicant demonstrated that now the residual flow disappeared after the RCPs coasted down. The applicant then presented the results of the Reference Case and the limiting PCT case (Case 48) in the DCD using the new code version. The PCT for the Reference Case decreased 3°C and the case 48 WCT-M1 and HOTSPOT PCTs increased 2 °C and 8 °C, respectively. The staff accepts the revised response to RAI-1 because it corrects a code error and demonstrates that the error had only a small impact upon computed PCT.

The set of independent calculations showed that the dominant uncertainty parameters in the WCT-M1 are break size, break discharge coefficient, and the cold leg nozzle factor (influences the flow split in the broken loop). They also demonstrated that the uncertainty in the advanced accumulator flow coefficient had little impact on PCT. Varying the flow coefficient from nominal minus one standard deviation to nominal plus one standard deviation only changed the PCT by 12 °C (22 °F).

The results of the staff's calculations are presented in more detail in Reference 14.

5 CONCLUSIONS AND LIMITATIONS

The US-APWR is an advanced PWR design that retains many functional similarities to conventional PWRs with respect to the system response during an LBLOCA accident. The advanced features of this design will not introduce any new phenomena. The codes and methodologies that were reviewed were WCT-M1, HOTSPOT, and ASTRUM. These codes and methodologies are based on NRC-approved versions of these codes and methodology, for LBLOCA analyses of Westinghouse 3 and 4 Loop plants, and the AP1000. The applicant has described and justified the changes made to WCOBRA/TRAC and ASTRUM to be applicable to US-APWR. The US-APWR unique features are an advanced accumulator, a neutron reflector, direct vessel injection, and a longer core.

The staff finds that the applicant's use of WCT-M1, HOTSPOT, and the ASTRUM methodology for the US-APWR, as described in MUAP-07011-P (R3), is acceptable for meeting the regulatory requirements of 10 CFR 50.46 based on the following limitations:

1. The final large and small scaling biases in the Advanced Accumulator Topical Report MUAP-07001 are equal to or more positive than those given in Table 3.5.7 [Ref. 28].
2. The final dispersion standard deviation values in the Advanced Accumulator Topical Report MUAP-07001 bound (smaller absolute values) or equal those

given in Table 3.5.6 [Ref. 28].

3. The final instrument uncertainty and manufacturing error standard deviation values in the Advanced Accumulator Topical Report MUAP-07001, bound (smaller absolute values) or equal those given in Table 3.5.6 [Ref. 28].

6 REFERENCES

1. "Large Break LOCA, Code Applicability Report for the US-APWR," Mitsubishi Heavy Industries, Ltd. (MHI), Topical Report MUAP-07011-P R0, July 2007.
2. Nissley, M. E., et al., "Realistic Large-Break LOCA Evaluation Methodology Using the Automated Statistical Treatment of Uncertainty Method (ASTRUM)," WCAP-16009-P-A, January 2005.
3. Bajorek, S. M., et al., "Code Qualification Document for Best Estimate LOCA Analysis," WCAP-12945-P-A, Volume 1, Revision 2, and Volumes 2 through 5, Revision 1, 1998.
4. RG 1.157, "Best Estimate Calculation of Emergency Core Cooling System Performance," May 1989.
5. "Quantifying Reactor Safety Margins, Application of Code Applicability and Uncertainty Evaluation Methodology to Large Break LOCA," NUREG/CR-5249, December 1989.
6. NUREG-1230, "Compendium of ECCS Research for Realistic LOCA Analysis," December 1988.
7. "The Advanced Accumulator," MUAP-07001-P(R1), January 2007.
8. "Neutron Reflector Reflooding Confirmatory Test," MUAP-08008-P(R0), August 2008.
9. "MHI's Partial Response to NRC's Request for Additional Information on Topical Report MUAP-07011-P(R0), 'Large Break LOCA Code Applicability Report for US-APWR,'" UAP-HF-09173-P(R0), April, 2009.
10. "MHI's 2nd Part Responses to the NRC's Requests for Additional Information on Topical Report MUAP-07011-P(R0), 'Large Break LOCA Code Applicability Report for US-APWR,'" UAP-HF-09252, May, 2009.
11. "MHI's Responses to the NRC's Requests for 2nd Set Additional Information on US-APWR Topical Report "LARGE BREAK LOCA CODE APPLICABILITY REPORT,'" MUAP-07011-P(R0)," UAP-HF-10130, May, 2010.
12. "Final Safety Evaluation Report Related to Certification of the AP600 Standard Design," NUREG-1512, August 1998.
13. "Final Safety Evaluation Report (FSER) for the Westinghouse AP1000 Advanced Reactor Design," NUREG-1793, September 2004.
14. R. Beaton and D. Fletcher, "US-APWR LBLOCA Confirmatory Analyses," Information Systems Laboratories, Inc., ISL-NSAO-TR-10-12, Proprietary, April 2010.
15. Design Control Document for the US-APWR, Revision 2, October 2009.
16. US-APWR LBLOCA Confirmatory Analyses, ISL Technical Report (ML12024A331).

17. Wilks, S.S., "Determination of Sample Sizes for Setting Tolerance Limits," The Annals of Mathematical Statistics, Vol. 12, pp. 91-96, 1941.
18. Guba, A., Makai, M., Lenard, P., "Statistical Aspects of Best Estimate Method-I," Reliability Engineering and System Safety Vol. 80, pp. 217-232, 2003.
19. "MHI's Responses to the NRC's Request for 4th Set of Additional Information on Topical Report "LARGE BREAK LOCA CODE APPLICABILITY REPORT," MUAP-07011-P(R0)" , " UAP-HF-10247, September, 2010.
20. "Revision to MHI's RAI Responses on Topical Report MUAP-07011-P(R0) "LARGE BREAK LOCA CODE APPLICABILITY REPORT" , " UAP-HF-10299, December, 2010.
21. "MHI's Response to the NRC's Request for 5th Set of Additional Information on US-APWR Topical Report 'LARGE BREAK LOCA CODE APPLICABILITY REPORT,' MUAP-07011-P (R0)," UAP-HF-10325, December 2010.
22. "Amended Response to Question 35 in 2nd set RAIs on US-APWR Topical Report "LARGE BREAK LOCA CODE APPLICABILITY REPORT,' MUAP-07011-P," Enclosure 2 of UAP-HF-11128, April 2011.
23. "Revised Responses to RAI-2 in 4th set RAIs on US-APWR Topical Report "LARGE BREAK LOCA CODE APPLICABILITY REPORT,' MUAP-07011-P," Enclosure 3 of UAP-HF-11128, April 2011.
24. "Supplemental Responses to RAI-3 and RAI-4 in 4th set RAIs on US-APWR Topical Report "LARGE BREAK LOCA CODE APPLICABILITY REPORT,' MUAP-07011-P," UAP-HF-11178, July 2011.
25. TRACE V5.0 Assessment Manual, US NRC.
26. WCOBRA/TRAC Code Input Manual, MHI Report 6AS-1E-UAP-08007(R0), 2008.
27. WCOBRA/TRAC(M1.0) Code Supplementary Manual, MHI Report 6AS-1E-UAP-100020(R0), May 2010.
28. "Large Break LOCA, Code Applicability Report for the US-APWR," Mitsubishi Heavy Industries, Ltd. (MHI), Topical Report MUAP-07011-P R3, December 2011.
29. "The Advanced Accumulator," Mitsubishi Heavy Industries, Ltd. (MHI), Topical Report MUAP-07001-P (R4), August 2011.
30. "MHI's Response to the NRC's Request for Additional Information on Topical Report, the Advanced Accumulator, MUAP-07001," UAP-HF-11202, July 2011.

7 LIST OF ACRONYMS

ANS	American Nuclear Society
ANSI	American National Standards Institute
AP600	Advanced Passive 600 MW plant
AP1000	Advanced Passive 1000 MW plant
APWR	Advanced Pressurized Water Reactor
ASTRUM	Automated Statistical Treatment of Uncertainty Method
BELBLOCA	Best Estimate Large Break Loss of Coolant Accident
CCTF	Cylindrical Core Test Facility
CE	Combustion Engineering
CFR	Code of Federal Regulations
CHF	Critical Heat Flux
CSAU	Code, Scaling, Applicability, and Uncertainty
CWO	Core Wide Oxidation
DCD	Design Control Document
DEGB	Double-Ended Guillotine Break
DNB	Departure from Nucleate Boiling
DVI	Direct Vessel Injection
ECC	Emergency Core Cooling (or Coolant)
ECCS	Emergency Core Cooling System
HHIS	High-Head Injection System
HHSI	High Head Safety Injection
LBLOCA	Large Break Loss of Coolant Accident
LCO	Local Cladding Oxidation
LHSI	Low Head Safety Injection
LOCA	Loss of Coolant Accident
LOFT	Loss of Fluid Test
MHI	Mitsubishi Heavy Industries, LTD
MWt	Megawatts thermal
NR	Neutron Reflector
NRC	U. S. Nuclear Regulatory Commission
NUREG/CR	Nuclear Regulatory Commission Regulation/Contractor Report
ORNL	Oak Ridge National Laboratory
PCT	Peak Cladding Temperature
PDF	Probability Density Function
PIRT	Phenomena Identification and Ranking Table
PWR	Pressurized Water Reactor
RAI	Request for Additional Information
RCCA	Rod Cluster Control Assembly
RCP	Reactor Coolant Pump
RCS	Reactor Coolant System
RG	Regulatory Guide
RPV	Reactor Pressure Vessel
RWSP	Refueling Water Storage Pit
R5M33	RELAP5/MOD3.3
SBLOCA	Small Break Loss of Coolant Accident

SCTF	Slab Core Test Facility
SE	Safety Evaluation
SER	Safety Evaluation Report
SG	Steam Generator
SI	Safety Injection
THTF	Thermal Hydraulic Test Facility
TR	Topical Report
UPTF	Upper Plenum Test Facility
US-APWR	United States Advanced Pressurized Water Reactor
WCT-M1	WCOBRA/TRAC(M1.0)

1 (Cont.)	1-1	<p>Editorial corrections as follows:</p> <ul style="list-style-type: none"> • Replace “the use” to “using” in first paragraph • Replace articles “the” to “a” in first and second paragraph • Add article “the” in first paragraph • Eliminate article “the” in second paragraph • Add articles “a” in second paragraph • Replace “accumulator of the US-APWR” to “US-APWR accumulator” in second paragraph • Replace “At first” to “First” in third paragraph • Replace “appeared” to “appear” in third paragraph • Replace “results” to “corresponding results” in last paragraph • Replace “described” to “provided” in last paragraph
	2-1	<ul style="list-style-type: none"> • Replace “prevention” to “preventative” in section 2.0 • Replace “,” to “and” in section 2.0 • Replace “Comparisons” to “A comparisons” in subsection 2.2.1 • Replace articles “a” to “the” in subsection 2.2.3
	2-2	<p>Editorial corrections as follows:</p> <ul style="list-style-type: none"> • Eliminate article “the” in subsection 2.2.1 • Replace “Tinlet” to “T_{inlet}” in subsection 2.2.1
	2-4	<p>Editorial corrections as follows:</p> <ul style="list-style-type: none"> • Add article “the” in subsection 2.3.4 • Eliminate article “the” in subsection 2.3.5 <p>Technical correction</p> <ul style="list-style-type: none"> • Correct the description of Pressurizer from “The relief lines discharge through spargers in the refueling water storage pit (RWSP) inside the containment.” to “The relief lines discharge steam and water into the pressurizer relief tank inside the containment.” in subsection 2.3.5
	2-5	<p>Editorial corrections as follows:</p> <ul style="list-style-type: none"> • Replace “:” to “;” in subsection 2.4.2 • Replace “orderly” to “systematically” in subsection 2.4.2 <p>RAI Response</p> <ul style="list-style-type: none"> • Reflect the response to RAI (Request 2.2) into the description of the ECCS functions.
	2-6	<p>Editorial corrections as follows:</p> <ul style="list-style-type: none"> • Eliminate “function to” in subsection 2.4.2.1 • Replace “in” to “during” in subsection 2.4.2.1
	2-7	<p>Editorial corrections as follows:</p> <ul style="list-style-type: none"> • Replace “eliminate” to “eliminates” in subsection 2.4.2.1 • Replace “on” to “in” in subsection 2.4.2.2 • Eliminate article “the” in subsection 2.4.2.2 <p>RAI Response</p> <ul style="list-style-type: none"> • Reflect the response to RAI (Request 2.1) and add the subsection 2.4.2.3 to describe “Emergency Letdown System”
	2-8	<p>Editorial correction as follows:</p> <ul style="list-style-type: none"> • Replace “in” to “at” in subsection 2.4.3

1 (Cont.)	2-10	Editorial corrections as follows: <ul style="list-style-type: none"> • Assign numbers to the comments below the Table • Replace “Vogtle Unit #1 are referred to as a US current 4-loop PWR” to “Vogtle Unit #1 is used as the U.S. current 4-loop PWR design” • Replace “those of” to “specific to” • Add article “a” • Replace “are in” to “were retrieved from”
	2-12 through 2-24	Editorial (resolution enhancement) <ul style="list-style-type: none"> • Replace the figure in Table2-3 and Figures 2-1 through 2-12
	3-1	Editorial corrections as follows: <ul style="list-style-type: none"> • Replace “approves” to “approved ” in section 3.1 • Eliminate article “the” in section 3.1 • Replace “analysis” to “analyses ” in section 3.1 • Replace “APWR though some minor modifications should be performed” to “, taking into account some minor modifications ” in section 3.1 • Replace “supported” to “supports ” in section 3.1 • Replace “have” to “has ” in section 3.1 • Replace article “a” to “the” in section 3.2
	3-2	Editorial corrections as follows: <ul style="list-style-type: none"> • Replace “termed” to “identified as ” in section 3.3.1 • Replace article “a” to “the” in subsection 3.3.2
	3-3	Editorial corrections as follows: <ul style="list-style-type: none"> • Eliminate article “the” in subsection 3.3.2 • Add article “the” in subsection 3.3.2 • Replace “degrading” to “degraded” in section 3.3.2 • Replace “turns on” to “actuates” in subsection 3.3.3 • Replace “of DVI design” to “via the DVI nozzles” in subsection 3.3.3 • Add article “a” in subsection 3.3.3 • Replace “at the time” to “when” in subsection 3.3.4 • Replace “make” to “maintain” in subsection 3.3.4 • Add article “the” in subsection 3.3.4
	3-4	Editorial corrections as follows: <ul style="list-style-type: none"> • Replace “near to” to “nearly” in subsection 3.3.4 • Add articles “the” in subsection 3.3.4
	3-8	Editorial corrections as follows: <ul style="list-style-type: none"> • Replace “with the condition that” to “when” in subsection 3.4.1 • Replace “digital” to “numerical” in subsection 3.4.1
	3-9	Editorial corrections as follows: <ul style="list-style-type: none"> • Replace “the heat-up” to “the heat-up rate” in subsection 3.4.1.1 • Replace “usual analysis” to “standard analyses” in subsection 3.4.1.1 • Replace “degraded” to “degrades” in subsection 3.4.1.1 • Replace “is considered” to “discusses in” in subsection 3.4.1.1

1 (Cont.)	3-10	<p>Editorial corrections as follows:</p> <ul style="list-style-type: none"> • Replace “linear heat rate” to “linear heat generation rate ” in subsection 3.4.1.2 • Replace “in a bigger” to “within a larger” in subsection 3.4.1.2 • Replace “on” to “of” in subsection 3.4.1.2
	3-11	<p>Editorial corrections as follows:</p>
	3-11	<ul style="list-style-type: none"> • Replace “The entrainment” to “Entrainment” in subsection 3.4.1.2 • Replace “comes” to “goes” in subsection 3.4.1.3 • Replace “almost” to “nearly” in subsection 3.4.1.4
	3-12	<p>Editorial corrections as follows:</p>
	3-12	<ul style="list-style-type: none"> • Replace “almost” to “nearly” in subsection 3.4.1.5 • Eliminate “to” in subsection 3.4.1.6 • Replace “especially” to “particularly” in subsection 3.4.1.6 • Replace “through” to “throughout” in subsection 3.4.1.7 • Add article “the” in subsection 3.4.1.7
	3-13	<p>Editorial correction as follows:</p>
	3-13	<ul style="list-style-type: none"> • Add “traveling” in last sentence of third paragraph of subsection 3.4.1.9
	3-14	<p>Editorial corrections as follows:</p>
	3-14	<ul style="list-style-type: none"> • Replace “almost” to “nearly” in subsection 3.4.1.10 • Replace “give up their” to “release” in subsection 3.4.1.10 • Add article “the” in subsection 3.4.1.10
	3-18	<p>Technical Correction</p>
	3-18	<ul style="list-style-type: none"> • Correct the ranking indicator for “Cold leg /Accumulator Non-condensable-gas during Reflooding period” in Table 3.4-1, to adjust the explanation in subsection 3.4.1.8.
	3-21	<p>Editorial corrections as follows:</p>
	3-21	<ul style="list-style-type: none"> • Add article “the” in subsection 3.5.1.1 • Replace article “a” to “the” in subsection 3.5.1.1 • Add “and” in subsection 3.5.1.1
	3-22	<p>Editorial corrections as follows:</p>
	3-22	<ul style="list-style-type: none"> • Replace “model of the code concerning flow resistance” to “flow resistance model of the code” in subsection 3.5.1.1 • Add article “the” in subsection 3.5.1.1 • Eliminate “as” in subsection 3.5.1.2
	3-23	<p>Editorial correction as follows:</p>
	3-23	<ul style="list-style-type: none"> • Replace “include” to “includes” in subsection 3.5.1.3
	3-24	<p>Editorial correction as follows:</p>
	3-24	<ul style="list-style-type: none"> • Replace “based on user’s manual (Ref.10)” to “in the same method as plant analysis” in subsection 3.5.1.3 (4)

1 (Cont.)	3-25	Editorial corrections as follows: <ul style="list-style-type: none"> • Replace “its treatment” to “how it is treated” in subsection 3.5.1.4 • Replace “were” to “was” in subsection 3.5.1.4(1) • Replace “for the safety analysis for a LBLOCA.” to “for the LOCA safety analysis.” in subsection 3.5.1.4(1) • Re-number “Ref.11” to “Ref.10” in subsection 3.5.1.4(1) Technical Change <ul style="list-style-type: none"> • Add the description of scaling effect for the Advanced Accumulator in subsection 3.5.1.4(1)
	3-27	Technical Change <ul style="list-style-type: none"> • Correct the equation 3.5.1-7, and description corresponding to it. • Add the description how the uncertainty of dispersion deviation is treated in the statistical analysis Editorial corrections as follows: <ul style="list-style-type: none"> • Add article “the” • Replace table number “Table 3.5-5” to “Table 3.5-4” • Add “shown in Table 3.5 5”
	3-28	Editorial correction as follows: <ul style="list-style-type: none"> • Replace table number “Table 3.5-5” to “Table 3.5-6” Technical Change <ul style="list-style-type: none"> • Add the description of uncertainty range sampled in the analysis • Add the description of scaling effect for the Advanced Accumulator and how it is treated in the analysis
	3-29	Editorial corrections as follows: <ul style="list-style-type: none"> • Update the table number from “Table 3.5-7” to “Table 3.5-8” • Replace “revised” to “modified” • Eliminate “as” • Replace “was” to “has been” • Replace “On the other hand” to “In addition”
	3-34	Technical Change <ul style="list-style-type: none"> • Update Table 3.5-6 • Add Table 3.5-7
	3-41 through 3-45	Technical Change <ul style="list-style-type: none"> • Replace figures 3.5-7 through 3.5-9 re-analyzed in accordance with the code update
	3-47	Editorial corrections as follows: <ul style="list-style-type: none"> • Replace “can not” to “cannot” in subsection 3.5.3.1(5) • Replace “are rising” to “rise” in subsection 3.5.3.1(6) • Add articles “the” in subsection 3.5.3.1(6) • Replace “Thus” to “Consequently” in subsection 3.5.3.1 • Add article “the” in subsection 3.5.3.1 • Replace “model of entrainment and de-entrainment” to “entrainment and de-entrainment modeling” in subsection 3.5.3.2
	3-48	Editorial correction as follows: <ul style="list-style-type: none"> • Replace “Ref.12” to “Ref.11” in subsection 3.5.3.3 c)

1 (Cont.)	3-50	Editorial (resolution enhancement) • Replace Figures 3.5-10
	3-54	Technical Change •
	3-55	Editorial correction as follows: • Replace “as” to “to be” in subsection 3.6.11 Editorial corrections as follows: • Replace “is” to “was” in subsection 3.6.11 • Replace “the guide tube from the viewpoint of the reflooding PCT” to “an open hole” to to correspond with the sample plant analysis •
	3-57	Editorial correction as follows: • Replace “Ref.13” to “Ref.12” in subsection 3.6.1.2
	3-58	Editorial corrections as follows: • Add articles “the” in subsection 3.6.1.3 • Replace “Ref.14,15,16” to “Ref.13,14,15” in subsection 3.6.2.2
	3-59	Editorial correction as follows: • Replace “Ref.17” to “Ref.16” in subsection 3.6.3.2
	3-60	Editorial corrections as follows: • Replace “Ref.18” to “Ref.17” in subsection 3.6.3.2 • Replace “Ref.17” to “Ref.16” in subsection 3.6.3.2 • Replace “Ref.19” to “Ref.18” in subsection 3.6.3.2
	3-61	RAI Response • Reflect the response to RAI (Request 3.15.2) into subsection 3.6.5.2
	3-63 and 3-65	Technical Change • Update the Tables 3.6-1, 3.6-2 and bottom note corresponding to the sample plant analysis
	3-69	Technical Change • Update the Table 3.6-5 corresponding to the sample plant analysis
	3-70	Technical Change • Update the Table 3.6-6 corresponding to re-analysis result
	3-71	Editorial Change • Update Figure 3-6.1

1 (Cont.)	3-72 and 3-78	Technical Change • Update Figures 3.6-2 and 3.6-8 corresponding to the sample plant analysis
	3-83 through 3-89	Technical Change • Update the Figures 3.6-13 through 3.6-18 corresponding to re-analysis result
	3-90	Editorial corrections as follows: • Replace “Ref.20” to “Ref.19” • Replace “Ref.21” to “Ref.20”
	3-92	Editorial corrections as follows: • Add “in” in the last sentence of the second paragraph • Replace “almosts all” to “most of” • Re-arrange the description of subsection 3.7.2 • Replace “For most of the parameters, the nominal value was assumed for the sample calculation.” to “For most of the parameters used in the sample plant analysis, the nominal value was assumed.” • Replace “take accounted for in” to “taken into account for ”
		Technical Change • Replace “Table 3.7 1 and Table 3.7 2” to “Table 3.7 1 through Table 3.7 3” to reflect RAI response (Request 3.16.3) • Change the model related description in last paragraph of subsection 3.7.2 to reflect RAI response (Request 3.16.3)
	3-95	Technical Correction (• •)
	3-95 and 96	Technical Change • Update and correct Table 3.7-1
	3-98	Technical Change • Add Table 3.7-3 to reflect RAI response (Request 3.16.3)
	4-1	Editorial corrections as follows: • Reflect RAI response (Request 3.16.3) into the first paragraph • Replace “In conclusion, the WCOBRA/TRAC(M1.0) code and the ASTRUM methodology are available to provide the analysis results in the Design Control Documents (DCD) of the US-APWR plant. Also, the nodding model of the WCOBRA/TRAC(M1.0) code for the US-APWR plant is available for LBLOCA calculation of the US-APWR as a safety analysis.” to “In conclusion, the WCOBRA/TRAC(M1.0) code and the ASTRUM methodology are acceptable to provide analysis results for the US-APWR Design Control Documents (DCD). In addition, the nodding model of the WCOBRA/TRAC(M1.0) code for the US-APWR plant is acceptable for the LOCA safety analysis calculation.”
	5-1	Update the listing of references

<p>1 (Cont.)</p>	<p>A-1</p> <p>A-2</p> <p>B-1</p> <p>B-3</p> <p>B-6</p>	<p>Editorial corrections as follows:</p> <ul style="list-style-type: none"> • Replace “if it is taken into consideration of” to “when taking into account” • Replace “in which” to “that has” • Replace “degrading” to “degradation” • Replace “partly” to “partially” • Replace “uncertainty of stored energy” to “stored energy uncertainty” • Replace “can apply fuel of the US-APWR fuel.” to “can be applied to the US-APWR fuel.” <p>Update the revision of reference A-2</p> <p>Editorial corrections as follows:</p> <ul style="list-style-type: none"> • • <p>Technical Change</p> <ul style="list-style-type: none"> • Add the description how the scaling uncertainty is treated in the code <p>Editorial correction as follows:</p> <ul style="list-style-type: none"> • <p>Add reference B-3 for scaling uncertainty</p>
<p>2</p>	<p>2-2 and 2-11</p> <p>3-26</p> <p>3-28</p> <p>3-29</p>	<p>RAI Response</p> <ul style="list-style-type: none"> • Reflect the response to Question-2, which was provided with UAP-HF-11128, into Subsection 2.2.3 and Table 2-2 <p>Technical Change</p> <ul style="list-style-type: none"> • <p>Editorial corrections as follows:</p> <ul style="list-style-type: none"> • Replace “showns in Table 3.5-7” to “shown in Table 3.5-7” • <p>Editorial correction as follows:</p> <ul style="list-style-type: none"> • <p>RAI Response</p> <ul style="list-style-type: none"> • Add the description “(3) Treatment of Dissolved Nitrogen Gas Effect” in Subsection 3.5.1.4 to consist with Section 5.3 in the latest topical report “The Advanced Accumulator MUAP-07001 Revision 4 ” (requested in the 7th set RAIs)

<p>2 (Cont.)</p>	<p>3-34 and 3-35</p> <p>3-36</p> <p>3-62</p> <p>3-70</p> <p>3-94</p> <p>3-95</p> <p>3-96</p> <p>3-97</p> <p>5-1</p> <p>B-3</p> <p>B-6</p>	<p>Technical Change</p> <ul style="list-style-type: none"> • Update Table 3.5-4 to consist with Subsection 5.1.2 (2) in the latest topical report “The Advanced Accumulator MUAP-07001 Revision 4 ” • Update Table 3.5-5 and Table 3.5-6 to consist with Subsection 5.1.2 (1) in the latest topical report “The Advanced Accumulator MUAP-07001 Revision 4 ” <p>Editorial correction as follows:</p> <ul style="list-style-type: none"> • Correct the equation number in Table 3.5-7 from 3.5.1-10 to 3.5.1-11 <p>Editorial correction as follows:</p> <ul style="list-style-type: none"> • Update Table 3.5-8 to consist with Subsection 3.5.1.4 (2) <p>Editorial correction as follows:</p> <ul style="list-style-type: none"> • Correct the transient result to consist with Table 3.3-6 <p>Editorial correction as follows:</p> <ul style="list-style-type: none"> • Correct the values in c) and d) to consist with the sample plant analysis condition <p>Editorial correction as follows:</p> <ul style="list-style-type: none"> • Correct the description of Burn-up in Subsection 3.7.2.2 to consist with the methodology <p>RAI Response</p> <ul style="list-style-type: none"> • <p>Editorial correction as follows:</p> <ul style="list-style-type: none"> • Correct the values in c) and d) to consist with the sample plant analysis condition <p>RAI Response</p> <ul style="list-style-type: none"> • <p>Update the listing of references (Ref.4 and Ref.21)</p> <p>RAI Response</p> <ul style="list-style-type: none"> • Add the description for dissolved nitrogen gas effect to consist with Section 5.3 in the latest topical report “The Advanced Accumulator MUAP-07001 Revision 4 ” (requested in the 7^h set RAIs) <p>Update reference B-3 and add reference B-4</p>
<p>3</p>	<p>2-2 and Section3</p>	<p>Editorial corrections</p> <ul style="list-style-type: none"> • Eliminate lines above and below “Figure2-3” in the first paragraph of subsection 2.3.1 in page 2-2 • Modify indents of the third paragraph in page 2-2 and titles of subsection 3.x.x

3 (Cont.)	2-12 3-28 and 3-35 3-96	<p>Editorial correction</p> <ul style="list-style-type: none"> • Replace “165.4” for Active Fuel Length in Table 2-3 to “165.4 in.” <p>Editorial corrections</p> <ul style="list-style-type: none"> • • <p>Editorial correction</p> <ul style="list-style-type: none"> • Replace “Max.” for f) SG Plugging Level in Table 3.7-1 to “Maximum”
4	2-1 3-1 3-3, 3-11, 3-18, 3-22 3-28 and 3-29 3-35 3-29 3-95, 3-97, 3-96, 5-1 A-1 B-3 B-6	<p>Editorial correction</p> <ul style="list-style-type: none"> • Revised sentence “A comparisons of...” to read “A comparison of...” <p>Editorial correction</p> <ul style="list-style-type: none"> • Added missing comma to sentence <p>Editorial correction</p> <ul style="list-style-type: none"> • Corrected the following typographical errors: nozzls => nozzles; gose => goes; Nonequilibrium => Non-equilibrium; dependant => dependent on each page respectively <ul style="list-style-type: none"> • Revised the description and Table 3.5-7 regarding the treatment of the scaling effect according to the NRC safety evaluation report for the advanced accumulator topical report MUAP-07001(R5) <p>Editorial correction</p> <ul style="list-style-type: none"> • Corrected the following typographical errors in the first paragraph of (3) Treatment of Dissolved Nitrogen Gas Effect: “was not” => “will not be”; “designing” => “design” <p>Editorial correction</p> <ul style="list-style-type: none"> • Added a missing space and delete a space on page 3-95 • Corrected typographical error in table note: tipical => typical <p>Updated the listing of references (Ref. 4, 18, 21 and 22)</p> <p>Updated Reference A-2</p> <ul style="list-style-type: none"> • Replaced the statement and values for the scaling bias • Replaced “Ref. B-4” in the note for Kpipe with “Ref. B-3” <p>Updated the listing of references (Ref. B-3 and B-4)</p>

© 2014
MITSUBISHI HEAVY INDUSTRIES, LTD.
All Rights Reserved

This document has been prepared by Mitsubishi Heavy Industries, Ltd. ("MHI") in connection with its request to the U.S. Nuclear Regulatory Commission ("NRC") for a pre-application review of the US-APWR nuclear power plant design. No right to disclose, use or copy any of the information in this document, other than that by the NRC and its contractors in support of MHI's pre-application review of the US-APWR, is authorized without the express written permission of MHI.

This document contains technology information and intellectual property relating to the US-APWR and it is delivered to the NRC on the express condition that it not be disclosed, copied or reproduced in whole or in part, or used for the benefit of anyone other than MHI without the express written permission of MHI, except as set forth in the previous paragraph.

This document is protected by the laws of Japan, U.S. copyright law, international treaties and conventions, and the applicable laws of any country where it is being used.

Mitsubishi Heavy Industries, Ltd.
16-5, Konan 2-chome, Minato-ku
Tokyo 108-8215 Japan

ABSTRACT

In this report, the applicability of the WCOBRA/TRAC(M1.0) code and the ASTRUM method to the evaluation of Large Break Loss of Coolant Accident (LBLOCA) at the US-APWR has been evaluated. Design features specific to the US-APWR have been evaluated and required changes to the model have been identified in the WCOBRA/TRAC code.

The WCOBRA/TRAC code was also approved by the NRC to perform Large Break LOCA analyses for its 2-loop plant designs (Ref.1), and for the AP600 and AP1000 advanced plant designs (Ref.2, 3). These types of plant have some specific features that which are very similar to the US-APWR system, such as Direct Vessel Injection (DVI) and Neutron Reflector (NR).

In particular, the applicability for the advanced accumulator as the new design is confirmed by putting in the modified flow resistance model and performing model validation with a comparison between calculated results and test data. And the applicability for improved designs is confirmed by mainly investigating the model availability of WCOBRA/TRAC(M1.0). In addition to this, the plant model of the WCOBRA/TRAC(M1.0) code for the US-APWR is established and a sample calculation is performed to demonstrate the applicability of the WCOBRA/TRAC(M1.0) code to the US-APWR LBLOCA transient.

This report also presents that the ASTRUM methodology, which comprises WCOBRA/TRAC(M1.0). It has the same applicability to the US-APWR because the treatment of the uncertainty for statistical calculation of LBLOCA in the US-APWR is almost the same as conventional 4-loop PWR plants. Note from this point forward the term 'conventional plants' refers to a typical U.S. 4-loop PWR plant design.

The WCOBRA/TRAC(M1.0) code and the ASTRUM methodology can be used for the purposes of performing best estimate analysis for the US-APWR on the basis of this status. The basis for this conclusion is that when compared to conventional 3- and 4-loop plants, for Large Break LOCA events, no new phenomena are identified for the US-APWR, and the test database that supports validation of this code is applicable to the US-APWR. Also the nodding model of the US-APWR plant intended for the WCOBRA/TRAC(M1.0) code, provided in this report, is available for the US-APWR LBLOCA safety analysis calculation.

Table of Contents

List of Tables	v
List of Figures.....	vi
List of Acronyms.....	viii
1.0 INTRODUCTION.....	1-1
2.0 US-APWR PLANT DESIGN AND FEATURES.....	2-1
2.1 Main Specifications	2-1
2.2 Reactor and Core	2-1
2.2.1 General Features	2-1
2.2.2 Fuel Assemblies	2-1
2.2.3 Reactor Vessel Internals	2-1
2.3 Reactor Coolant System.....	2-2
2.3.1 General Features	2-2
2.3.2 Reactor Vessel	2-3
2.3.3 Steam Generators	2-3
2.3.4 Reactor Coolant Pumps	2-3
2.3.5 Pressurizer	2-4
2.4 Engineered Safety Features	2-4
2.4.1 General Features	2-4
2.4.2 Emergency Core Cooling System	2-5
2.4.3 Containment Spray System.....	2-7
2.4.4 Containment System.....	2-8
3.0 LBLOCA CODE AND METHODOLOGY	3-1
3.1 Introduction	3-1
3.2 US-APWR Features.....	3-1
3.3 Description of US-APWR LBLOCA Transient	3-2
3.3.1 General Description	3-2
3.3.2 Blowdown Period	3-2
3.3.3 Refilling Period	3-3
3.3.4 Reflooding Period.....	3-3
3.4 Phenomena Identification and Ranking (PIRT)	3-8
3.4.1 LBLOCA PIRT	3-8
3.4.2 Effects of US-APWR Design on Westinghouse PIRT Conclusions.....	3-15
3.5 WCOBRA/TRAC Code Applicability to US-APWR	3-21
3.5.1 Advanced Accumulator	3-21
3.5.2 Direct Vessel Injection (DVI)	3-47
3.5.3 Neutron Reflector	3-47
3.6 Sample Plant Analysis	3-55
3.6.1 Nodalization of Plant Analysis	3-55
3.6.2 Calculation Process	3-59
3.6.3 Models for Sample Plant Analysis.....	3-59
3.6.4 Analysis Conditions	3-61
3.6.5 Analysis Results	3-62
3.6.6 Sample Plant Analysis Summary	3-62
3.7 ASTRUM Methodology Applied to US-APWR	3-91
3.7.1 Statistical Methodology of ASTRUM	3-91
3.7.2 ASTRUM Methodology Applicability to US-APWR.....	3-93
4.0 CONCLUSIONS.....	4-1
5.0 REFERENCES.....	5-1

Appendix-A	Thermal Properties of Nuclear Fuel Rods	A-1
Appendix-B	Aadvanced Accumulator Model Built into WCOBRA/TRAC	B-1
Appendix-C	Resolution of Requests for Additional Information	C-1

List of Tables

Table 2-1	Comparison of Principal Parameters.....	2-10
Table 2-2	Key Parameters of Core Design.....	2-11
Table 2-3	Fuel Assembly Specification.....	2-12
Table 3.3-1	Typical Sequence of the LBLOCA of US-APWR.....	3-5
Table 3.4-1	US-APWR PIRT (1/2)	3-17
Table 3.4-1	US-APWR PIRT (2/2)	3-18
Table 3.5-1	Phenomena/Model in WCOBRA/TRAC for ACC	3-31
Table 3.5-2	Test Conditions of Full Height 1/2 Scale Test.....	3-32
Table 3.5-3	Analysis Conditions	3-33
Table 3.5-4	Instrument Uncertainties (1/2) (Large Flow)	3-34
Table 3.5-4	Instrument Uncertainties (2/2) (Small Flow).....	3-34
Table 3.5-5	Dispersion of Data from Experimental Equation	3-34
Table 3.5-6	Total Uncertainty of Flow Rate Coefficient(Experimental Equations) for Safety Analysis of US-APWR	3-35
Table 3.5-7	Additional Bias to Flow Rate Coefficient(Experimental Equations).....	3-35
Table 3.5-8	Uncertainty of Water Level for Switching Flow Rates	3-36
Table 3.5-9	Phenomena/Model in WCOBRA/TRAC for NR.....	3-50
Table 3.6-1	Channel Descriptions for US-APWR Vessel Model (1/3).....	3-63
Table 3.6-1	Channel Descriptions for US-APWR Vessel Model (2/3).....	3-64
Table 3.6-1	Channel Descriptions for US-APWR Vessel Model (3/3).....	3-65
Table 3.6-2	Gap Connections for US-APWR Vessel Model (1/3)	3-66
Table 3.6-2	Gap Connections for US-APWR Vessel Model (2/3)	3-67
Table 3.6-2	Gap Connections for US-APWR Vessel Model (3/3)	3-68
Table 3.6-3	Comparison of Rated Characteristics of Various Pumps	3-69
Table 3.6-4	Comparison of Specific Speed of Various Pumps	3-69
Table 3.6-5	Analysis Conditions for US-APWR	3-70
Table 3.6-6	Sequence of Events for US-APWR Sample Transient Analysis	3-71
Table 3.7-1	Uncertainty Treatment for US-APWR (1/2).....	3-96
Table 3.7-1	Uncertainty Treatment for US-APWR (2/2).....	3-97
Table 3.7-2	Local Model Uncertainty Treatment for US-APWR	3-98
Table 3.7-3	Global Model Uncertainty Treatment for US-APWR	3-99
Table C-1	First Set of Requests for Additional Information	C-2
Table C-2	Second Set of Requests for Additional Information.....	C-4
Table C-3	Third Set of Requests for Additional Information.....	C-5

List of Figures

Figure 2-1	Reactor General Assembly	2-13
Figure 2-2	Neutron Reflector Assembly	2-14
Figure 2-3	Reactor Coolant System.....	2-15
Figure 2-4	Reactor Vessel.....	2-16
Figure 2-5	Steam Generator	2-17
Figure 2-6	Reactor Coolant Pump	2-18
Figure 2-7	Pressurizer.....	2-19
Figure 2-8	Simplified Configuration of ECCS and CSS	2-20
Figure 2-9	Emergency Core Cooling System.....	2-21
Figure 2-10	Safety System Performance for US-APWR.....	2-22
Figure 2-11	Containment Spray System	2-23
Figure 2-12	Configuration of Containment Vessel	2-24
Figure 3.3-1	System Configuration of ECCS of US-APWR	3-6
Figure 3.3-2	ECCS Flow Injection Performance during LBLOCA.....	3-6
Figure 3.3-3	Transient of LBLOCA in US-APWR.....	3-7
Figure 3.4-1	Location of Direct Vessel Injection Nozzle	3-19
Figure 3.4-2	Safety Injection Pad of Direct Vessel Injection	3-20
Figure 3.5-1	Principle of Advanced Accumulator	3-37
Figure 3.5-2	Flow Characteristics of Flow Damper.....	3-38
Figure 3.5-3	Schematic Drawing of Full Height 1/2 Scale Test Facility	3-39
Figure 3.5-4	Outline Drawing of Full Height 1/2 Scale Test Facility	3-39
Figure 3.5-5	Nodalization of Full Height 1/2 Scale ACC Test Section	3-40
Figure 3.5-6	Flow Damper Outlet Pressure Given at BREAK (Case 1).....	3-41
Figure 3.5-7 (1/3)	Comparison between Test and Analysis of Flow Rate (Full Height 1/2 Scale Test Case 1)	3-42
Figure 3.5-7 (2/3)	Comparison between Test and Analysis of Integrated Flow Rate (Full Height 1/2 Scale Test Case 1)	3-42
Figure 3.5-7 (3/3)	Comparison between Test and Analysis of Gas Pressure in Test Tank (Full Height 1/2 Scale Test Case 1)	3-43
Figure 3.5-8 (1/3)	Comparison between Test and Analysis of Flow Rate (Full Height 1/2 Scale Test Case 2)	3-43
Figure 3.5-8 (2/3)	Comparison between Test and Analysis of Integrated Flow Rate (Full Height 1/2 Scale Test Case 2)	3-44
Figure 3.5-8 (3/3)	Comparison between Test and Analysis of Gas Pressure in Test Tank (Full Height 1/2 Scale Test Case 2)	3-44
Figure 3.5-9 (1/3)	Comparison between Test and Analysis of Flow Rate (Full Height 1/2 Scale Test Case 3)	3-45
Figure 3.5-9 (2/3)	Comparison between Test and Analysis of Integrated Flow Rate (Full Height 1/2 Scale Test Case 3)	3-45
Figure 3.5-9 (3/3)	Comparison between Test and Analysis of Gas Pressure in Test Tank (Full Height 1/2 Scale Test Case 3)	3-46
Figure 3.5-10	Neutron Reflector Configuration of US-APWR.....	3-51
Figure 3.5-11	Flow Regimes and Heat Transfer Modes at Cooing Holes in Neutron Reflector during Reflooding Period.....	3-52
Figure 3.5-12	Normal Wall Flow Regimes	3-53
Figure 3.5-13	Hot Wall Flow Regimes	3-54
Figure 3.6-1	US-APWR Vessel Profile.....	3-72

Figure 3.6-2	US-APWR Vessel Noding for Hot Assembly Under Guide Tube (Vertical View)	3-73
Figure 3.6-3	US-APWR Vessel Sections 1 to 2 (Horizontal View)	3-74
Figure 3.6-4	US-APWR Vessel Sections 3 to 4 (Horizontal View)	3-75
Figure 3.6-5	US-APWR Vessel Sections 5 to 6 (Horizontal View)	3-76
Figure 3.6-6	US-APWR Vessel Sections 7 to 8 (Horizontal View)	3-77
Figure 3.6-7	US-APWR Vessel Sections 9 to 10 (Horizontal View)	3-78
Figure 3.6-8	US-APWR WCOBRA/TRAC(M1.0) Model Vessel/Loop Layout	3-79
Figure 3.6-9	US-APWR RCP Homologous Single-phase and Two-phase Pump Head Curve	3-80
Figure 3.6-10	US-APWR RCP Homologous Single-phase and Two-phase Pump Torque Curve	3-81
Figure 3.6-11	US-APWR RCP Two- Phase Head Multiplier	3-82
Figure 3.6-12	US-APWR RCP Two- Phase Torque Multiplier	3-83
Figure 3.6-13	Sample Power Shape for US-APWR Analysis	3-84
Figure 3.6-14	Peak Cladding Temperature of Hot Rod	3-85
Figure 3.6-15	Hot Assembly Channel Total Flow Rate	3-86
Figure 3.6-16	Core Pressure	3-87
Figure 3.6-17	Lower Plenum Liquid Level	3-88
Figure 3.6-18	Downcomer Liquid Level	3-89
Figure 3.6-19	Accumulator Flow Rate	3-90
Figure B-1	ACC Nodalization	B-7
Figure B-2	Flow Resistance Calculation Diagram in Subroutine ACCUM1	B-8

List of Acronyms

ACC	Accumulator
APWR	Advanced Pressurized-Water Reactor
ASTRUM	Automated Statistical Treatment of Uncertainty Method
BOL	Begin Of Life
CCFL	Countercurrent Flow Limitation
CD	Discharge Coefficient
CHF	Critical Heat Flux
CS	Containment Spray
CSS	Containment Spray System
CV	Containment Vessel
CVCS	Chemical and Volume Control System
CSAU	Code Scaling Applicability and Uncertainty
CE	Combustion Engineering
CWO	Core Wide Oxidation
DCD	Design Control Document
DECLG	Double Ended Cold Leg guillotine
DNB	Departure from Nucleate Boiling
DVI	Direct Vessel Injection
ECC	Emergency Core Cooling
ECCS	Emergency Core Cooling System
EPS	Emergency Power Source
ESF	Engineered Safety Feature
FA	Fuel Assembly
GT	Guide Tube
HA	Hot Assembly
HFP	Hot Full Power
HHSI	High Head Safety Injection
HTC	Heat Transfer Coefficient
ICIS	In-Core Instrumentation System
LBLOCA	Large Break Loss of Coolant Accident
LHSI	Low Head Safety Injection
LOCA	Loss of Coolant Accident
LP	Lower Plenum of reactor vessel
LMO	Local Maximum Oxidation
MHI	Mitsubishi Heavy Industries, Ltd.
MSLB	Main Steam Line Break
MTC	Moderator Temperature Coefficient
NPSH	Net Positive Suction Head
NR	Neutron Reflector
NRC	U.S. Nuclear Regulatory Commission
OLM	On Line Maintenance
OH	Open Hole
PCT	Peak Cladding Temperature
PIRT	Phenomena Identification Ranking Table
PLOW	LOW-Power region
PWR	Pressurized Water Reactor
PZR	Pressurizer

RCCA	Rod Cluster Control Assemblies
RCP	Reactor Coolant Pump
RCS	Reactor Coolant System
RHR	Residual Heat Removal
RV	Reactor Vessel
RVH	Reactor Vessel Head
RVI	Reactor Vessel Internal
RWSP	Refueling Water Storage Pit
SDV	Safety Depressurization Valve
SG	Steam Generator
SI	Safety Injection
SL	Surge Line
SRP	Standard Review Plan
SRV	Safety Relief Valve
Tinlet	Primary coolant temperature at reactor vessel inlet nozzle
TDF	Thermal Design Flow
TMIN	MINimum film boiling Temperature
UP	Upper Plenum of reactor vessel
UCP	Upper Core Plate
UPI	Upper Plenum Injection

1.0 INTRODUCTION

This report describes the acceptability of using of analysis codes and methodologies approved for conventional Pressurized Water Reactors (PWR) in their application to the US-APWR. The basic design of the US-APWR is almost the same as a conventional 4-loop PWR and the thermal hydraulic behavior of the US-APWR during a Large Break Loss of Coolant Accident (LBLOCA) is also almost the same as a conventional 4-loop PWR. Therefore, the LBLOCA analysis methodology for the US-APWR can be applied to the approved methodology for a conventional PWR with several modifications to reflect the US-APWR design features. The methodology is a statistical method with WCOBRA/TRAC.

Chapter 2 describes US-APWR plant design and features in comparison with a conventional 4-loop PWR plant. Major components of the US-APWR that is, the core, fuel assemblies, neutron reflector, reactor vessel, steam generator, reactor coolant pump, pressurizer, and engineered safety features, are described. The ECCS of the US-APWR consists of the accumulators and high head injection system. The US-APWR accumulator plays the role of both a conventional accumulator and a low head injection system by regulating injection flow rate with variable flow chamber resistance, which is dependent on the accumulator water level. The high head injection system consists of four (4) independent trains and injects from the RWSP to the reactor vessel downcomer. The RWSP is located in the lower part of the containment and enables recirculation without switching suction of the high head pumps.

The Chapter 3 describes the LBLOCA code and methodology for the US-APWR based on the US-APWR design and features identified in Chapter 2. The US-APWR uses an already approved statistical method with WCOBRA/TRAC, which is called ASTRUM (Automated Statistical Treatment of Uncertainty Method). First, the general behavior of LBLOCA transients in the US-APWR is described. Then, a Phenomena Identification and Ranking Table (PIRT) is developed and compared to that of a conventional PWR. Although minor differences from the conventional PWR due to the US-APWR design appear in the PIRT, almost all phenomena rankings are the same as the conventional PWR.

Modification and validation of WCOBRA/TRAC for modeling of the US-APWR accumulator are described. Applicability of WCOBRA/TRAC to Direct Vessel Injection (DVI) and the Neutron Reflector (NR) is also discussed.

Finally, a sample calculation model and corresponding results of the US-APWR with WCOBRA/TRAC are provided. The statistical method and treatment of uncertainty in the US-APWR analysis are also presented.

2.0 US-APWR PLANT DESIGN AND FEATURES

This section describes certain aspects of the US-APWR design in order to assist in the understanding the applicability of the approved methodologies for current PWRs to the US-APWR. The US-APWR features highly reliable preventative functions and well-established mitigation systems with active safety functions, and passive safety functions. The primary system design, loop configuration, and main components are similar to those of currently operating PWRs.

2.1 Main Specifications

The US-APWR is an advanced PWR of improved design to enhance reliability while retaining the basic features of conventional 4-loop PWRs. The main specifications of the US-APWR in comparison with current 4-loop PWRs in the U.S. are shown in Table 2-1.

2.2 Reactor and Core

2.2.1 General Features

The reactor configuration of the US-APWR is shown in Figure 2-1. A comparison of core parameters between the US-APWR and US current 4-loop PWRs are shown in Table 2-2.

The fuel assemblies, rod cluster control assemblies, reactor vessel internals and thermal hydraulic design are described below.

2.2.2 Fuel Assemblies

The fuel assembly consists of the 264 fuel rods arranged in a square 17x17 array, together with 24 control rod guide thimbles, an in-core instrumentation guide tube, 11 grid spacers, and top and bottom nozzles. This design maintains the same grid spacing (approximately 18 inches) as the 17x17 fuel assembly design in current plants. This relatively shorter grid spacing provides greater margin to grid fretting and improves DNB performance in comparison with the widely used standard design of about 14 ft heated length and 10 grid design. Fuel assembly characteristics are shown in Table 2-3.

2.2.3 Reactor Vessel Internals

The arrangement of the reactor vessel internals (RVI) of the US-APWR is shown in Figure 2-1. The increased fuel element length in the US-APWR is enabled by the integration of the lower core plate and lower core support plate.

The coolant flows from the RV inlet nozzles down the annulus between the core barrel and the RV and then into the plenum at the bottom of the RV. The flow then turns and passes through the lower core support plate and into the core. After passing through the core, the coolant enters the upper plenum and then flows radially to the core barrel outlet nozzles. A small amount of coolant flows into the vessel head plenum from the annulus to cool the

vessel head area.

A neutron reflector (NR) is used in the US-APWR to improve neutron utilization and thus the fuel cycle cost, to reduce neutron irradiation of the RV, and to increase structural reliability by eliminating bolts in the high neutron flux region. The NR assembly is shown in Figure 2-2.

The NR is located between the core barrel and core, and lines the core cavity. The NR consists of ten thick stainless steel blocks. These blocks are aligned by alignment pins and fixed to the lower core support plate by tie rods and bolts. The top and bottom are supported and aligned by alignment pins that are welded to the core barrel.

The NR is cooled by up-flow through cooling holes in the blocks. The flow is sufficient to avoid coolant boiling and prevent excessive stress and thermal deflections of the blocks due to gamma heating. The nominal value of total core bypass flow is approximately 7.5% of total reactor coolant system (RCS) flow rate. It is relatively larger than the flow rate at a conventional PWR plant so as to allow enough cooling for the NR and to keep the Reactor Vessel Head (RVH) coolant temperature at T_{inlet} . The total bypass flow is confirmed to be bounded by the design value of 9.0 percent, which includes the uncertainty. Thus, the 9.0% is used in the LBLOCA analysis.

2.3 Reactor Coolant System

2.3.1 General Features

The RCS consists of the RV, the steam generators (SGs), the reactor coolant pumps (RCPs), the pressurizer (PZR) and the reactor coolant pipes and valves. The flow schematic for the RCS is shown in Figure 2-3.

The reactor coolant flows through the hot leg pipes to the SGs and returns to the RV via the cold leg pipes and the RCPs. The PZR is connected to one hot leg via the surge line and to two cold legs via the spray lines.

The reactor coolant system, including connections to related auxiliary systems, constitutes the reactor coolant pressure boundary.

The reactor coolant system performs the following functions.

- Circulates the reactor coolant through the reactor core and transfers heat to the secondary system via the steam generators.
- Cools the core sufficiently to prevent core damage during reactor operation.
- Forms the reactor coolant pressure boundary, which functions as a barrier to prevent radioactive materials in the reactor coolant from being released to the environment.
- Functions as a neutron moderator and reflector and as a solvent for boron.
- Controls the reactor coolant pressure.

The RV, SGs, RCPs, and PZR are individually described below.

2.3.2 Reactor Vessel

The reactor vessel (RV), shown in Figure 2-4, is a vertical cylindrical vessel with hemispherical top and bottom heads. The top head is a removable flanged closure head connected to the RV upper shell flange by stud bolts. Pads on the RV nozzles support the vessel.

The RV has four inlet nozzles, four outlet nozzles and four Direct Vessel Injection (DVI) nozzles, which are located between the upper reactor vessel flange and the top of the core, so as to maintain coolant in the reactor vessel in the case of leakage in the reactor coolant loop.

2.3.3 Steam Generators

The SGs, shown in Figure 2-5, are vertical shell U-tube evaporators with integral moisture separating equipments.

The design of the SGs for the US-APWR has been improved to attain high efficiency and reliability by adopting 3/4 inch (19.05 mm) outer diameter tubes made of alloy 690 thermal treated, which are arranged triangularly in 1 inch (25.4mm) pitch.

The reactor coolant enters the tube inlet plenum via the hot side primary coolant nozzle, flows through the inverted U-tubes, transferring heat from the primary side to the secondary side, and leaves from the SG lower head via the cold side primary coolant nozzle. The lower head is divided into inlet and outlet chambers by a vertical partition plate extending from the apex of the lower head to the tube sheet.

Steam generated on the shell side (secondary side) flows upward and exits through the outlet nozzle at the top of the vessel. Feedwater enters the steam generator at an elevation above the top of the U-tubes through a feedwater nozzle. The feedwater enters a feeding and is distributed through nozzles attached to the top of the feeding.

2.3.4 Reactor Coolant Pumps

The reactor coolant pumps (RCPs) for the US-APWR are upsized versions of the Type 93A pumps used in conventional Westinghouse's design PWRs. Their design is similar to that of the Type 93A RCPs.

The RCPs of US-APWR, shown in Figure 2-6, are vertical, single-stage, centrifugal, shaft seal units, driven by three-phase induction motors. The shaft is vertical with the motor mounted above the pump. A flywheel on the shaft above the motor provides additional inertia to extend pump coastdown. The pump suction is at the bottom, and the discharge is located on the side.

The reactor coolant that enters from the bottom of the casing is accelerated by the impeller and causes a pressure increase across the diffuser. The diffuser is located at the center of the casing in order to attain high hydraulic efficiency.

The US-APWR reactor coolant pump has achieved larger capacity and higher efficiency than those of the Type 93A pump by improving of the impeller and diffuser configuration.

2.3.5 Pressurizer

The pressurizer (PZR), shown in Figure 2-7, is a vertical, cylindrical vessel with hemispherical top and bottom heads. The PZR is connected to one hot leg of the reactor coolant loops via the surge line and to two cold legs via the spray lines.

Electrical immersion heaters in the bottom head and the spray nozzle located in the top head control the primary system pressure.

The relief and safety valves at the top head provide overpressure protection of the RCS. The overpressure protection function of the US-APWR is performed as follows.

- Spring-loaded safety relief valves (SRVs) are installed on separate relief lines at the top of the pressurizer.
- An additional relief line has motor-operated relief valves for safety depressurization valves (SDVs). The valves are arranged in parallel and are driven by motor operators. A remotely controlled, motor-operated isolation valve is installed upstream of each the SDVs to allow isolation in the event of a leak.
- The relief lines discharge steam and water into the pressurizer relief tank inside the containment.
- Safety relief valves are installed in each residual heat removal system to provide overpressurization protection for unacceptable combinations of high reactor coolant system pressure and low reactor coolant system temperature.

2.4 Engineered Safety Features

2.4.1 General Features

The engineered safety features (ESFs) serve to mitigate the consequences of a design basis accident in which radioactive fission products are released from the reactor coolant system. The ESFs consist of the emergency core cooling system (ECCS), containment spray system (CSS), containment system, annulus air cleanup system and main control room heat, ventilation and air conditioning system.

The simplified configuration of the ECCS and CSS is shown in Figure 2-8.

The US-APWR employs the following advanced technologies for the ECCS and CSS to enhance its simplification.

a. Four-train, Direct Vessel Injection for High Head Injection System

The US-APWR employs a 4-train direct vessel injection (DVI) system. This system configuration increases redundancy and independence, and enhances safety and reliability. The capacity of each train is 50% of the capacity of a single train of a conventional two train system. Inter-connecting piping between each train is also eliminated.

The support system and the emergency AC power supply system also adopt a 4-train

configuration to enhance the reliability of the system.

b. Emergency Water Storage inside the Containment

The US-APWR eliminates potentially high risk operator actions to realign the suction in an emergency such as a Loss of Coolant Accident (LOCA) by installing the Refueling Water Storage Pit (RWSP) inside the containment. The RWSP is formed with a lined concrete structure and works as the emergency water source. This design significantly contributes to lowering the estimated core damage frequency.

c. Passive Low Head Injection

The safety system of the US-APWR consists of an optimized combination of active and passive components. The advanced accumulator is a passive component employed to enhance safety by improving flow injection characteristics and eliminating the need of the low head injection system. By adopting the vortex damper mechanism, the advanced accumulator supplies water with a large flow rate at the early stage of LOCA, and lower flow rate at the later stages.

The ECCS, CSS and containment system are described below.

2.4.2 Emergency Core Cooling System

The ECCS, shown in Figure 2-9, includes the accumulator system, high head injection system and emergency letdown system. The ECCS injects borated water into the reactor coolant system following a postulated accident and performs the following functions:

- Following a loss-of-coolant accident, the ECCS cools the reactor core, prevents serious damage to the fuel and fuel cladding, and limits the zirconium-water reaction in the fuel cladding to a very small amount.
- Following a main steam line break (MSLB), the ECCS provides negative reactivity to shut down the reactor.
- In the event that the normal CVCS letdown and boration capability are lost, the ECCS provides emergency letdown and boration of the RCS to systematically shutdown the reactor.

Compliance of the US-APWR ECCS with the 10 CFR 50.46 acceptance criteria is evaluated by ECCS Performance Analysis.

The ECCS is designed to perform the following major safety-related functions:

- Safety Injection
- Safe Shutdown
- Containment pH Control

These functions are provided by safety-related equipment with redundancy to deal with single failure, environmental qualification, and protection from external hazards.

• Safety Injection

The primary function of the ECCS is to remove stored and fission product decay heat from the reactor core following an accident. The ECCS meets the acceptance criteria of 10CFR50.46(b) for the following items:

- Peak cladding temperature
- Maximum calculated cladding oxidation
- Maximum hydrogen generation
- Coolable core geometry
- Long-term cooling

The ECCS automatically initiates with redundancy sufficient to ensure these functions are accomplished, even in the unlikely event of the most limiting single failure occurring coincident with, or during the event.

The Safety Injection System (SIS), in conjunction with the rapid insertion of the control rod cluster assemblies (reactor scram), provides protection in the following events:

- LOCA
- Ejection of a control rod cluster assembly
- Secondary steam system piping failure
- Inadvertent opening of main steam relief or safety valve
- SG tube rupture

- Safe Shutdown

The portions of the ECCS also operate in conjunction with the other systems of the cold shutdown design. The primary function of the ECCS during a safety grade cold shutdown is to ensure a means for feed and bleed for boration, and make up water for compensation of shrinkage.

- Containment pH Control

NaTB baskets are located in the containment and are capable of maintaining the desired post-accident pH conditions in the recirculation water. The pH adjustment is capable of maintaining containment water pH at least 7.0, to enhance the retention capacity in the containment and to avoid stress corrosion cracking of the austenitic stainless steel components.

2.4.2.1 Accumulator System

The accumulator system stores borated water under pressure and automatically injects it if the reactor coolant pressure decreases significantly. The accumulator system consists of four accumulators and the associated valves and piping, one for each RCS loop. The system is connected to the cold legs of the reactor coolant piping and injects borated water when the RCS pressure falls below the accumulator operating pressure. The system is passive. Pressurized nitrogen gas forces borated water from the tanks into the RCS.

As shown in Figure 2-10 accumulators incorporate internal passive flow dampers and a stand pipe which inject a large flow to refill the reactor vessel during the first stage of injection, and then reduce the flow as the water level in the accumulator drops. When the water level is above the top of the standpipe, water enters the flow damper through both inlets at the top of the standpipe and at the side of the flow damper such that water is injected at a large flow rate. When the water level drops below the top of the standpipe, water enters the flow damper only through the side inlet, so that accumulator injects water at a relatively low flow rate.

The accumulators provide large flow injection to refill the reactor vessel and continue with small flow injection during core reflooding in conjunction with the safety injection pumps.

The combined performance of the accumulator system and the high head injection system eliminates the need for a conventional low head injection system. The accumulator system's performance for the US-APWR is shown in Figure 2-10.

2.4.2.2 High Head Injection System

The direct vessel injection (DVI) is employed for the high head injection system. The high head injection system consists of four independent trains, each containing a safety injection pump and the associated valves and piping. The safety injection pumps start automatically upon receipt of the safety injection signal. One of four independent safety electrical buses is available to each safety injection pump.

The safety injection pumps are aligned to take suction from the refueling water storage pit and to deliver borated water to the DVI nozzles in the reactor vessel. Two safety injection trains are capable of meeting the design cooling function for a Large Break LOCA, assuming a single failure in one train and another train out of service for maintenance. In conventional PWRs, the requirement for a Large Break LOCA is met through a low head injection pump that generally serves also as an RHR pump. Therefore, the capacity of the US-APWR high head injection pump is larger than the conventional high head pump in order to provide sufficient flow during the large break LOCA.

The refueling water storage pit in the containment provides a continuous borated water source for the safety injection pumps, thus eliminating the need for realignment from the refueling water storage pit to the containment sump.

2.4.2.3 Emergency Letdown System

The emergency letdown system performs a "feed and bleed" (FAB) letdown boration to establish cold shutdown conditions if the normal chemical and volume control system (CVCS) is unavailable. The emergency letdown system directs the reactor coolant from two reactor vessel hot legs (B and D) to the refueling water storage pit, from which highly borated water can be returned to the reactor vessel using the safety injection pumps.

2.4.3 Containment Spray System

The containment spray system (CSS), shown in Figure 2-11, consists of four independent trains, each containing a containment spray/residual heat removal (CS/RHR) heat exchanger, a CS/RHR pump, spray nozzles, piping and valves. The CS/RHR heat exchangers and the CS/RHR pumps are used for both CSS and RHRs function. The CSS sprays borated water into the containment vessel in the event of a loss-of-coolant accident.

The containment spray system functions to maintain the containment vessel internal peak pressure below the design pressure and reduce it to approximately atmospheric pressure in the event of a loss of coolant accident or a main steam line break.

The CSS is designed based on the following.

- Its safety functions can be accomplished if there is a single failure of an active component for a short term following an accident with one train out of service for

maintenance, or a single failure of an active component or a single failure of a passive component for a long term following an accident with one train out of service for maintenance.

- The emergency power source can supply electrical power to the essential equipment of the CSS, so that safety functions can be maintained during a loss of offsite power.
- The CSS is automatically initiated by a containment spray signal.
- The CSS design permits periodic tests and inspections to verify integrity and operability.
- The CSS is capable of reducing the containment pressure to less than 50% of the peak calculated pressure for the design basis loss-of-coolant accident within 24 hours after the postulated accident.

The CSS is automatically actuated on receipt of a containment spray signal. When the signal is received, the CS/RHR heat exchanger outlet valves open and the CS/RHR pumps start. The CS/RHR pump motor is connected to a safety bus, so the emergency power source can supply electrical power in case of a loss of offsite power. The CS/RHR pumps take suction from the refueling water storage pit, and the stop valve on the inlet line is always open during reactor operation. The spray water is cooled by the CS/RHR heat exchangers and is delivered to the spray headers located at the top of the containment vessel.

The refueling water storage pit (RWSP) in the containment provides a continuous suction source for the CS/RHR pumps, thus eliminating the need for realignment from the refueling water storage pit to the containment sump.

The safety system pumps (CS/RHR pumps and safety injection pumps), which require sufficient net positive suction head (NPSH) to draw water from the recirculation sumps inside the containment, are located at the lowest level of the reactor building to secure the required NPSH. Also, they are located adjacent to the containment to minimize pipe lengths.

2.4.4 Containment System

The containment system includes the containment vessel, the annulus enclosing the containment penetration area, and the containment isolation function performed by the isolation valves, airlocks and equipment hatch.

The containment system provides an effective leak-tight barrier and environmental radiation protection under all postulated conditions, including a loss-of-coolant accident.

2.4.4.1 Containment Vessel

The containment vessel is designed to completely enclose the reactor and reactor coolant system and to ensure that essentially no leakage of radioactive materials to the environment would result even if a major failure of the reactor coolant system were to occur. The configuration of containment vessel is shown in Figure 2-12.

The containment vessel consists of a prestressed, post-tensioned concrete structure with a cylindrical wall, a hemispherical dome, and a flat reinforced concrete foundation slab. The

inside surface of the structure is lined with carbon steel.

The design pressure and temperature of the containment vessel are defined by the following postulated accidents.

- Loss- of-coolant accident (LOCA)
- Main steam line break (MSLB)

The containment vessel is designed to contain the energy and radioactive materials that result from a postulated loss-of-coolant accident, and for an 68 psig internal pressure to ensure a high degree of leak tightness during normal operation and under accident conditions.

An internal polar crane is supported by the containment vessel. A continuous crane girder transfers the polar crane loads to the containment vessel wall.

Hydrogen igniters are provided for protection against possible detonation following a core damage accident.

2.4.4.2 Refueling Water Storage Pit

The refueling water storage pit (RWSP) is located in the lowest part of the containment vessel. The RWSP provides a continuous suction source for both the safety injection pumps and the CS/RHR pumps. The wall and the floor of the RWSP are lined with stainless steel liner plates. The RWSP has four recirculation sumps on the floor; these sumps are provided with recirculation screens.

Table 2-1 Comparison of Principal Parameters⁽¹⁾⁽²⁾

Parameter	US-APWR	US Current 4-loop PWR	Ratio
Core Thermal Output (MWt)	4,451	3,565 (3853)	1.25
Operation Pressure (psia)	2,250	2,250 (2250)	-
Hot Leg Temperature (deg. F)	617	620 (626)	-
Cold Leg Temperature (deg. F)	551	557 (559)	-
Thermal Design Flow (gpm/loop)	112,000	93,600	1.20
Number of Fuel Assembly	257	193 (193)	1.33
Fuel Assembly Lattice	17x17	17x17	-
Effective Fuel Length (ft)	14	12 (14)	-
Number of Fuel Rods per FA	264	264	-
Average Linear Heat Rate (kW/ft)	4.6	5.7 (5.2)	0.8
Number of RCCAs	69	53 (57)	1.30
Number of Control Rods per RCCA	24	24 (24)	-
SG Heat Transfer Area (ft ²)	91,500	55,000	1.66
PZR Volume (ft ³)	2,900	1,800	1.6
PZR Volume to Thermal Power (ft ³ /MWt)	0.65	0.50	1.3
Containment Design Pressure (psig)	68	52 (56.5)	-

(1) Vogtle Unit #1 is used as the U.S. current 4-loop PWR design.

(2) Data in parentheses are specific to South Texas Project Unit 1 and 2, a current 4-loop PWR using 14-ft fuel. They were retrieved from the database of International Nuclear Safety Center and last updated on 01/97.

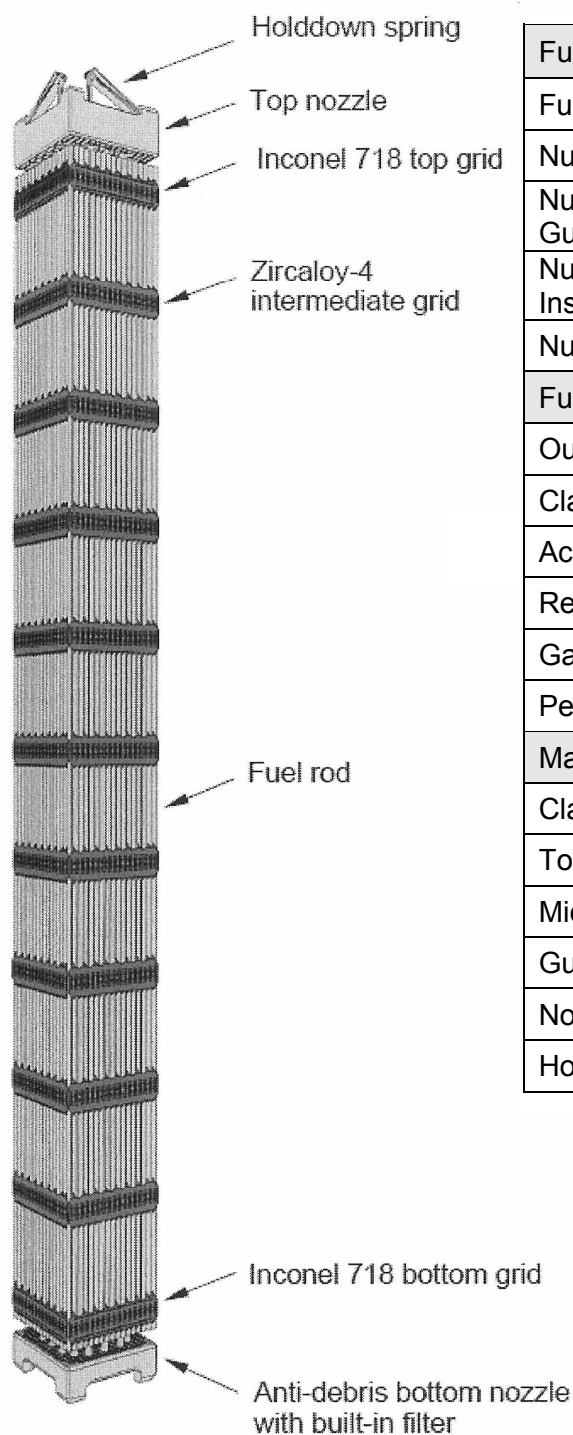
Table 2-2 Key Parameters of Core Design

Parameter	US-APWR	US Current 4-loop PWR
Core Thermal Output	4,451 MWt	3,565MWt
Heat Generated in Fuel	97.4 %	97.4 %
Number of Fuel Assemblies	257	193
Fuel Assembly Lattice	17x17	17x17
Effective Fuel Length	14 ft	12 ft
Average Linear Heat Rate	4.6 kW/ft	5.7 kW/ft
Primary System Pressure	2,250 psia	2,250 psia
Thermal Design Flow (TDF)	448,000 gpm	374,400 gpm
Coolant Temperature		
Hot Leg	617 °F*	620 °F*
RV Average	584 °F*	588 °F*
Cold Leg	551 °F*	557 °F*
Core Bypass Flow	7.5 %** 9.0%***	6.3 %

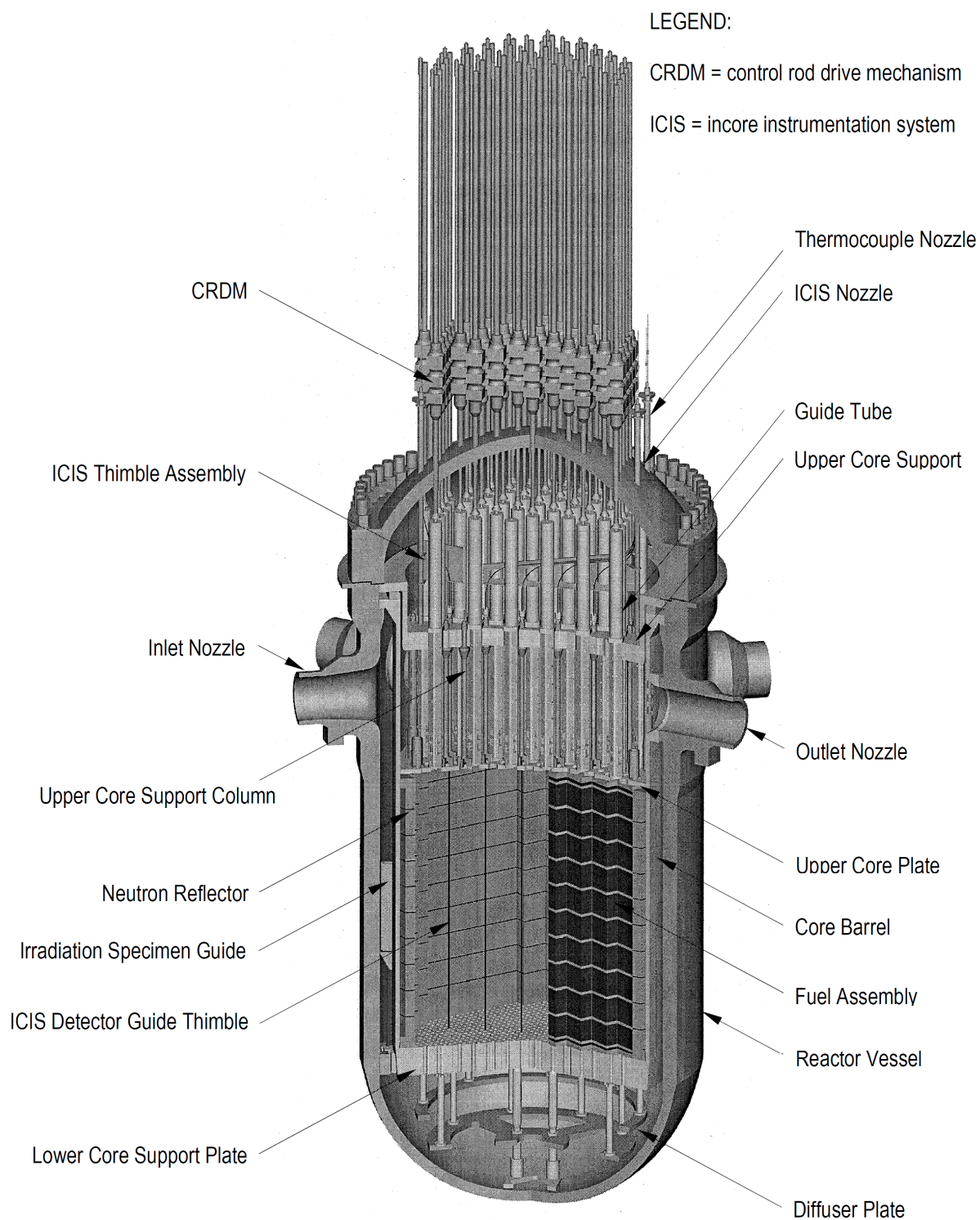
* Given as approximate figures

** Including margin

*** Including uncertainty for LOCA Analysis

Table 2-3 Fuel Assembly Specification

Fuel Assemblies	
Fuel Rods Array	17 x 17
Number of Fuel Rods	264
Number of Control Rod Guide Thimbles	24
Number of In-core Instrumentation Guide Tube	1
Number of Grid Spacers	11
Fuel Rods	
Outside Diameter	0.374 in. (9.50mm)
Cladding Thickness	0.022 in. (0.57mm)
Active Fuel Length	165.4 in. (4,200mm)
Reload Fuel Enrichment	Max. 5 wt%
Gadolinia Content	Max. 10 wt%
Pellet Density	97 %TD
Materials	
Cladding	ZIRLO™
Top & Bottom Grids	Inconel 718
Middle Grids	Zircaloy-4
Guide Thimbles	Zircaloy-4
Nozzles	Stainless Steel
Holddown Springs	Inconel 718

**Figure 2-1 Reactor General Assembly**

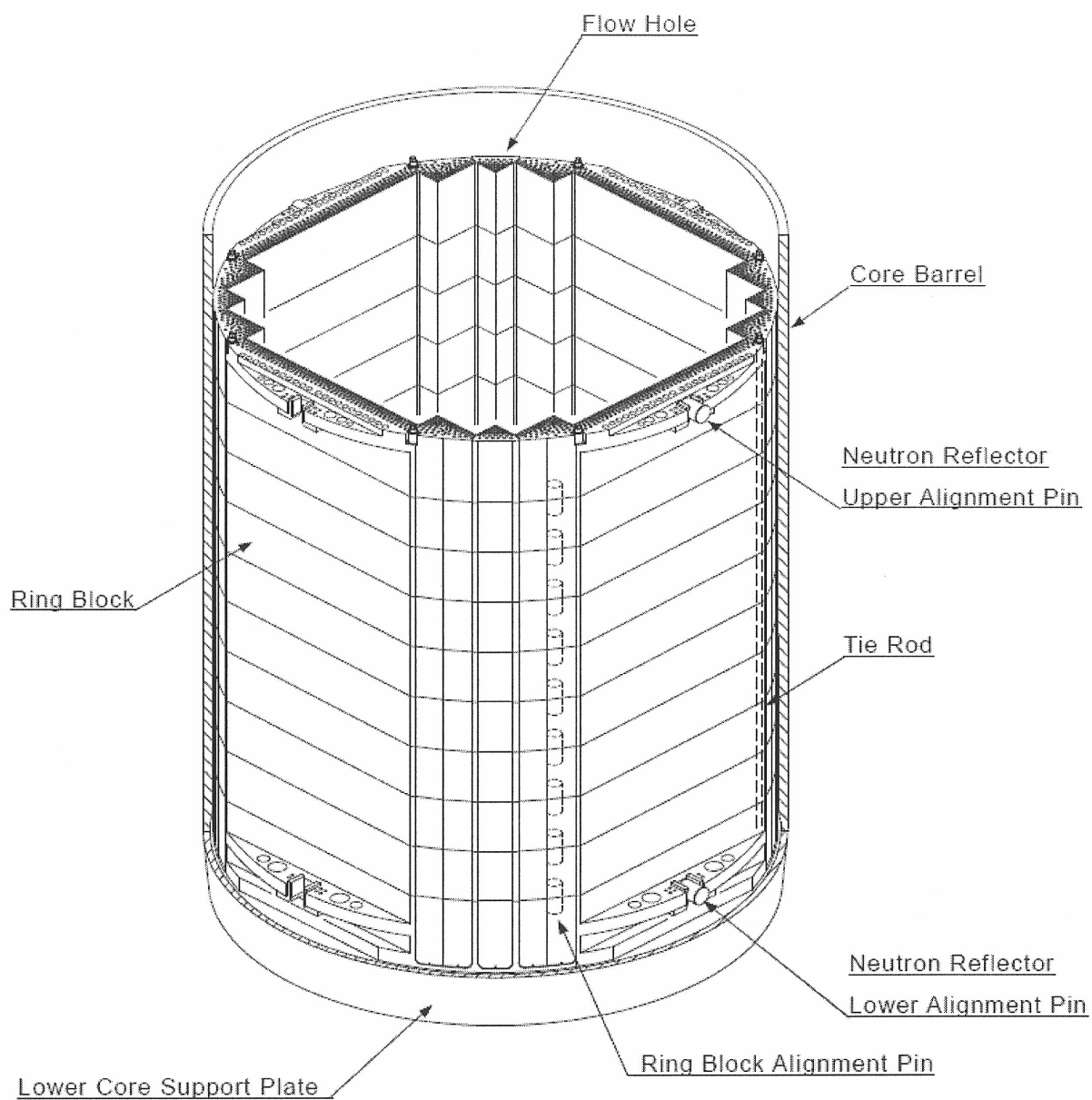


Figure 2-2 Neutron Reflector Assembly

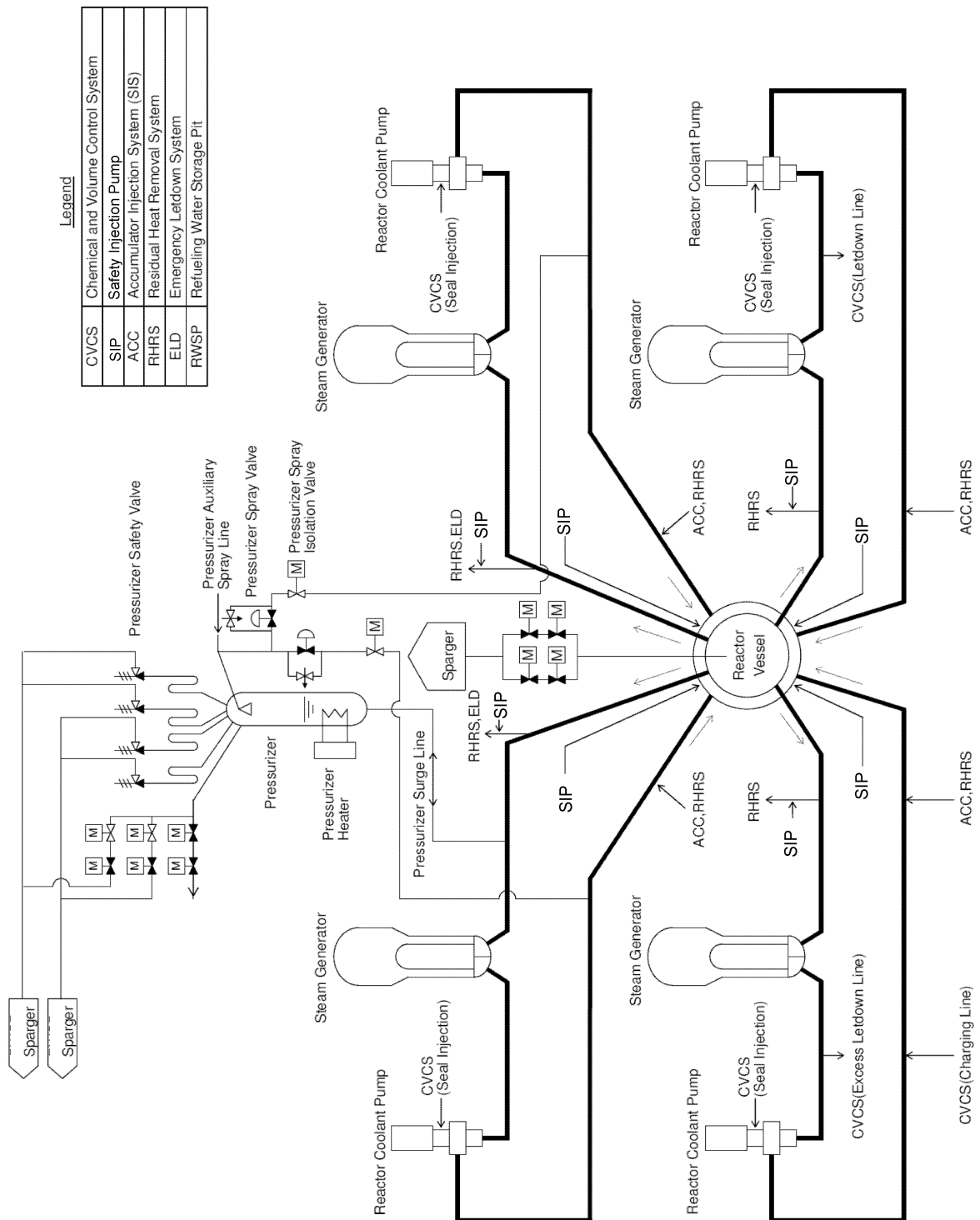


Figure 2-3 Reactor Coolant System

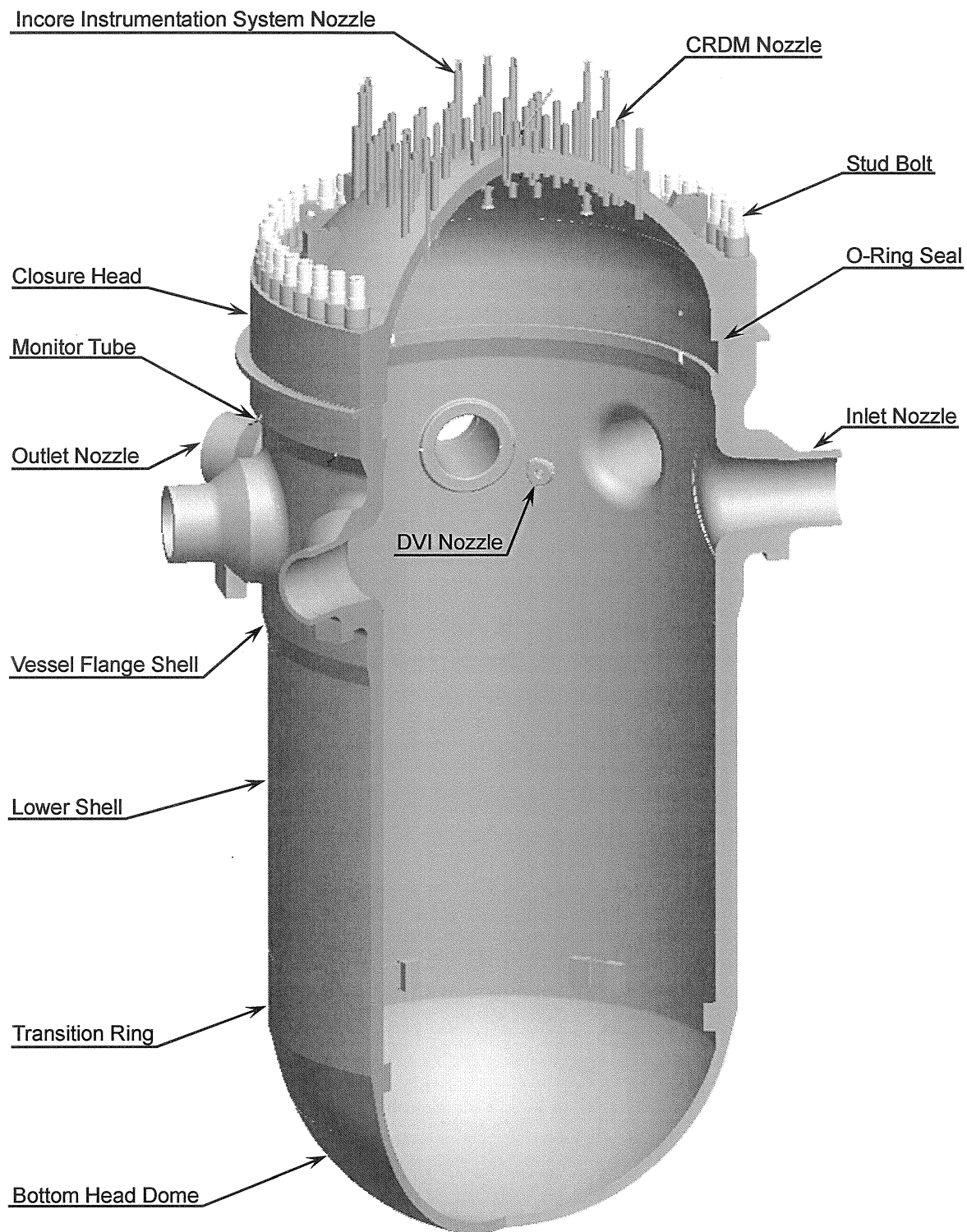


Figure 2-4 Reactor Vessel

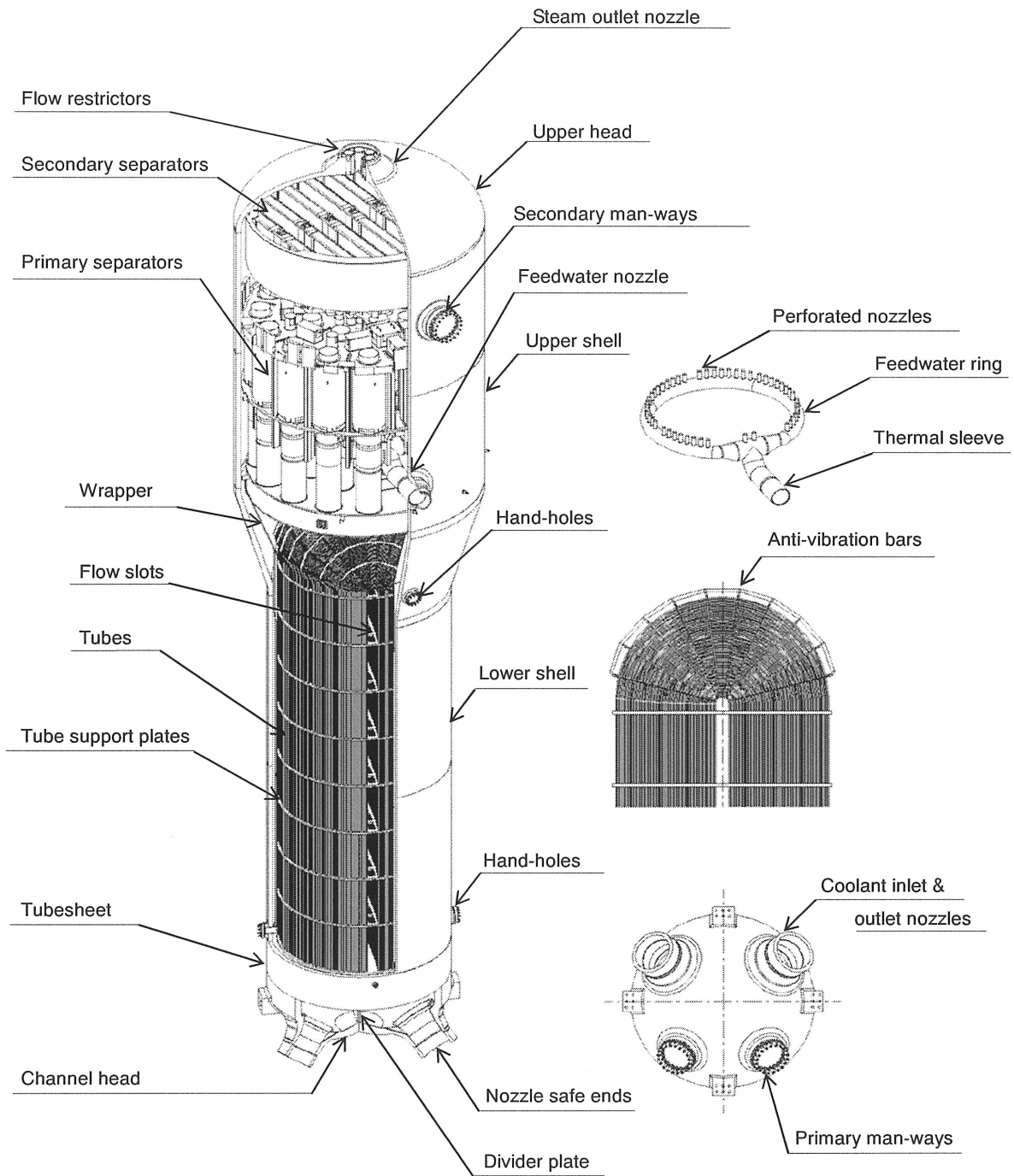


Figure 2-5 Steam Generator

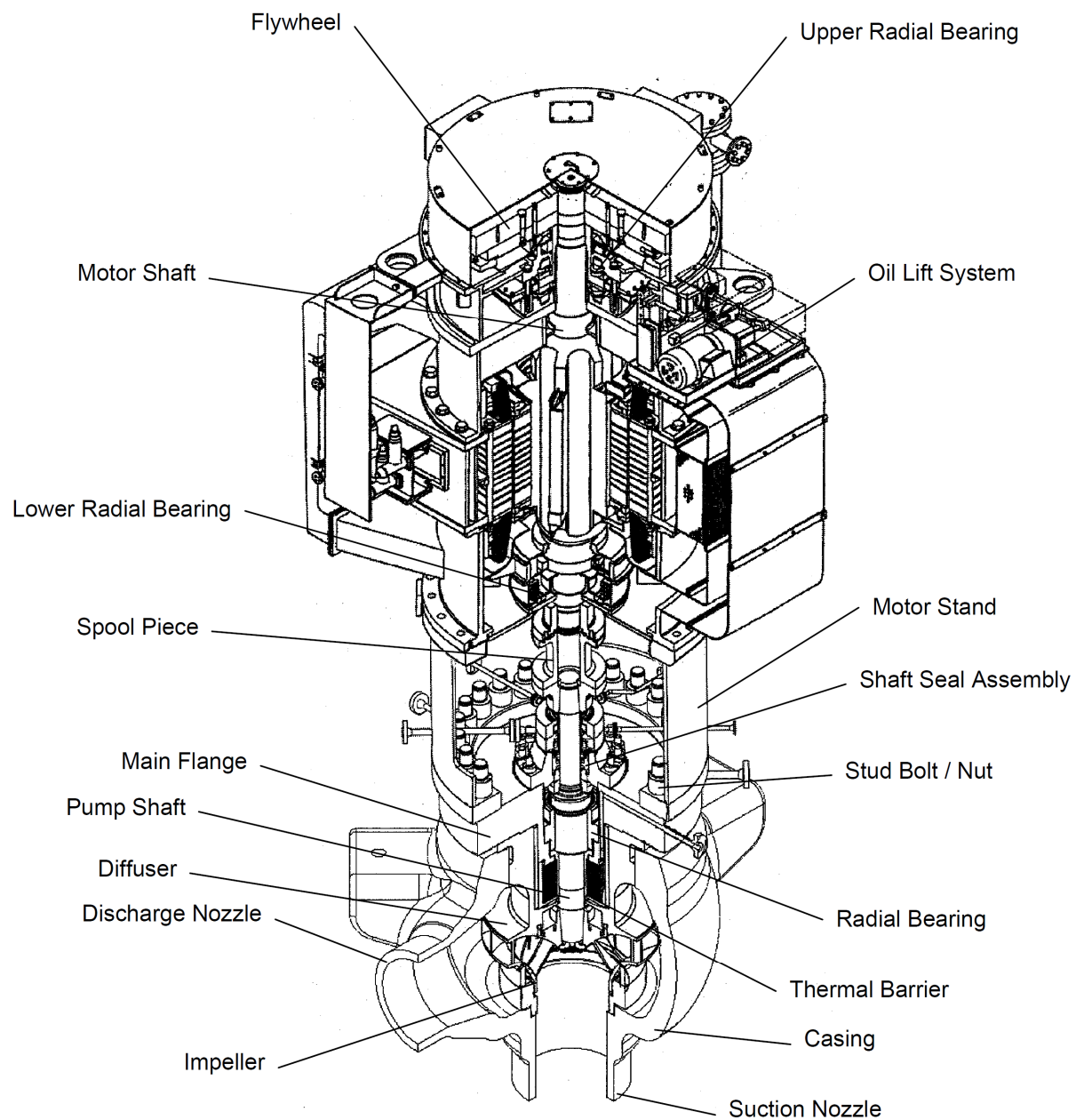
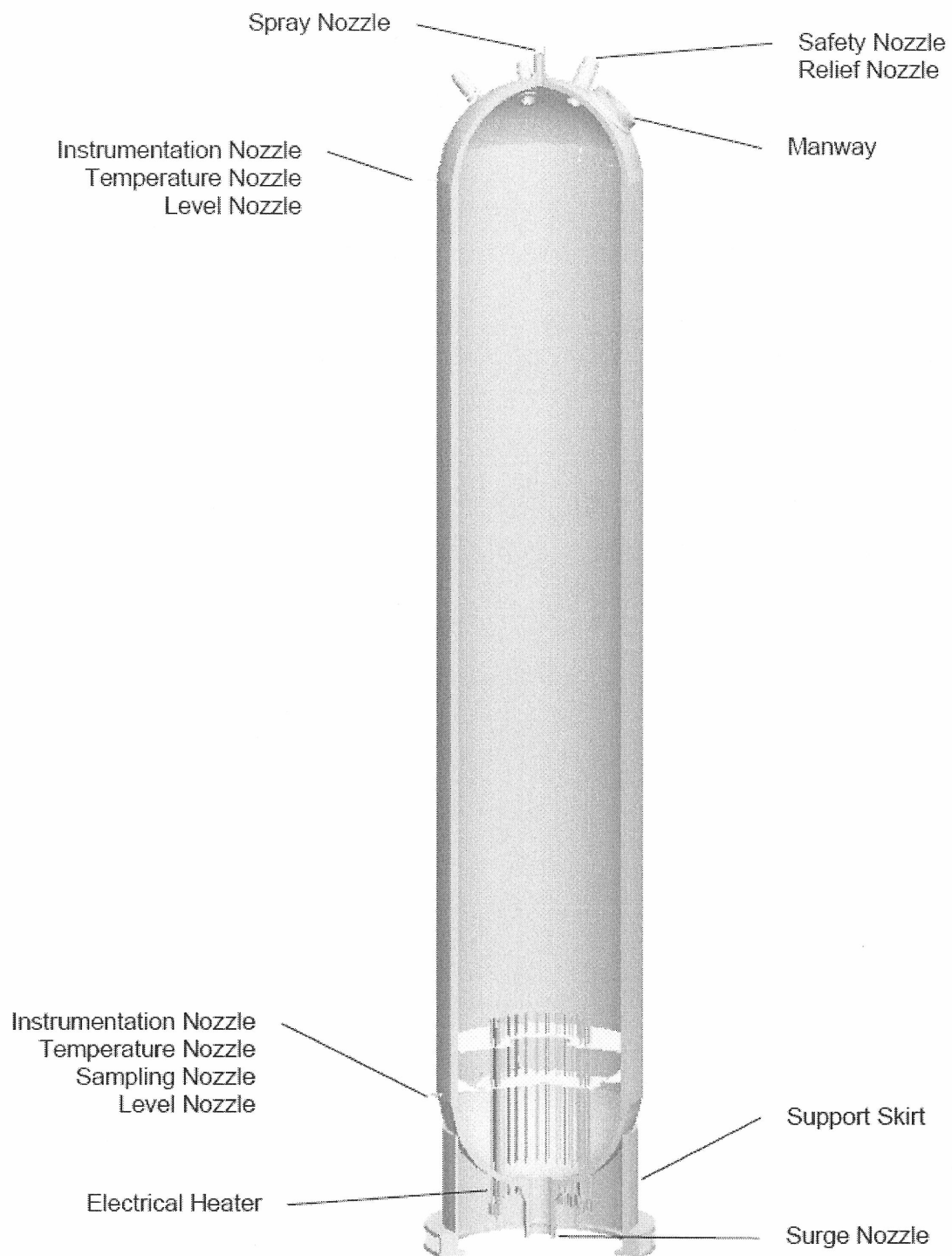


Figure 2-6 Reactor Coolant Pump

**Figure 2-7 Pressurizer**

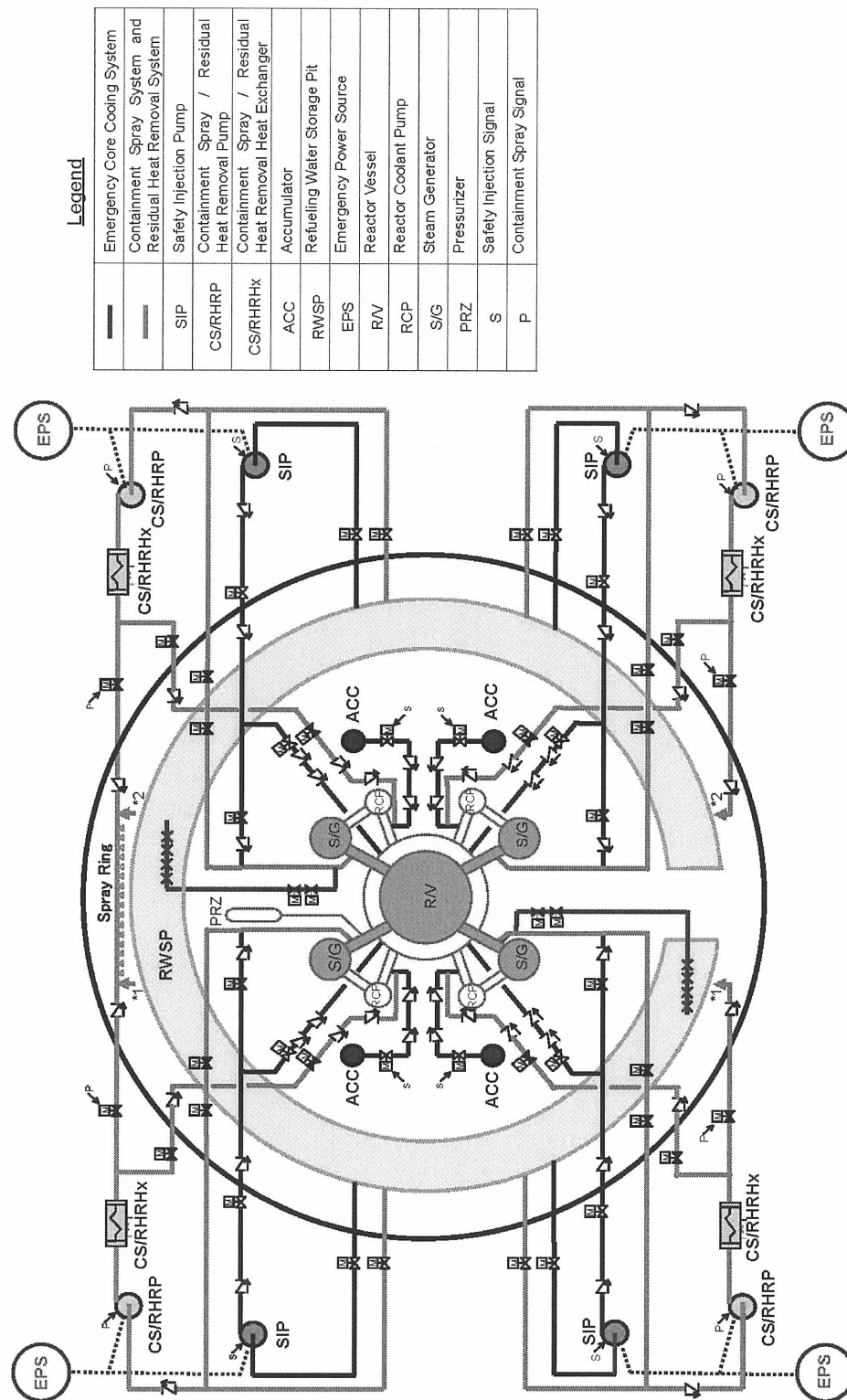


Figure 2-8 Simplified Configuration of ECCS and CSS

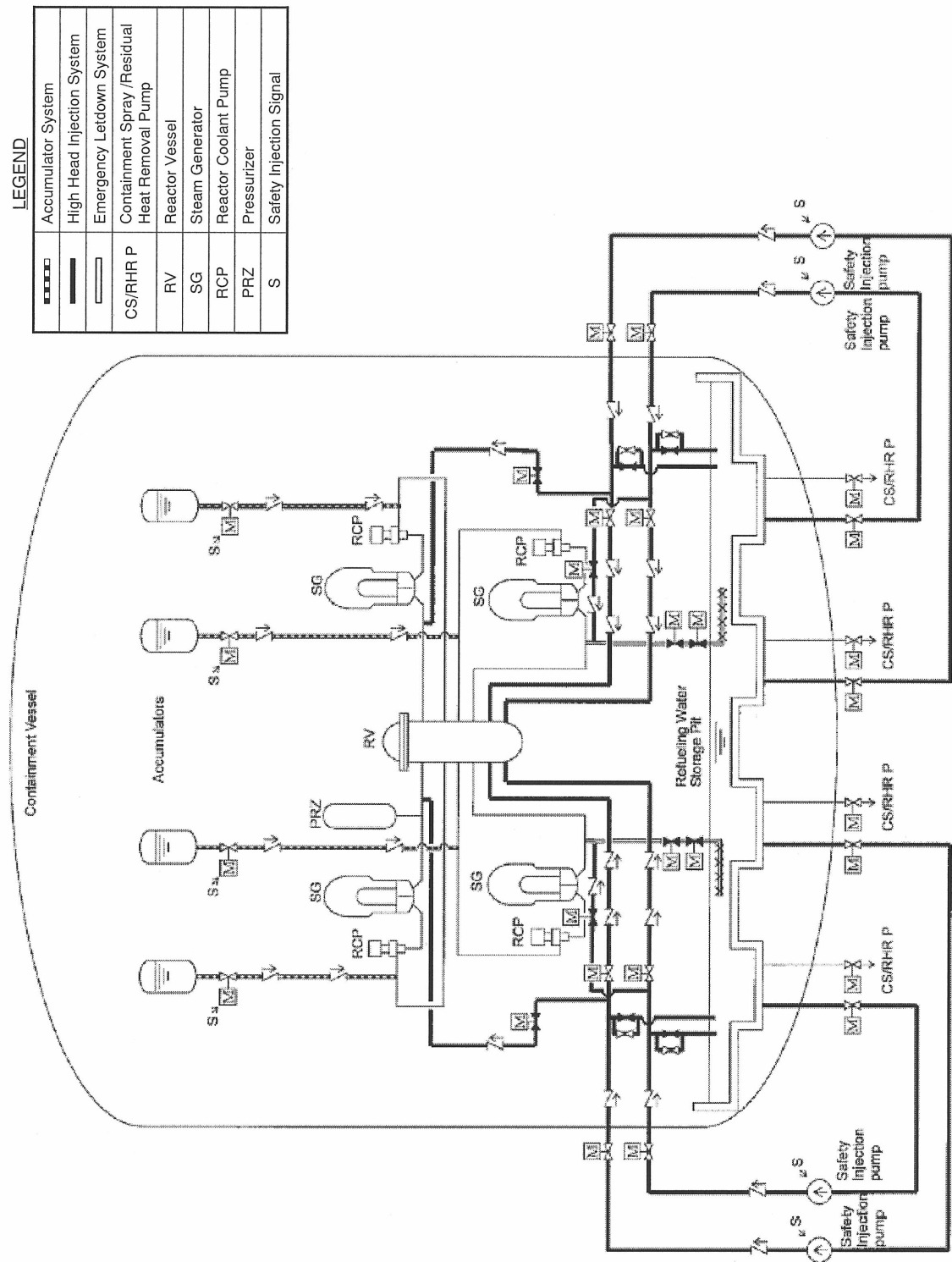


Figure 2-9 Emergency Core Cooling System

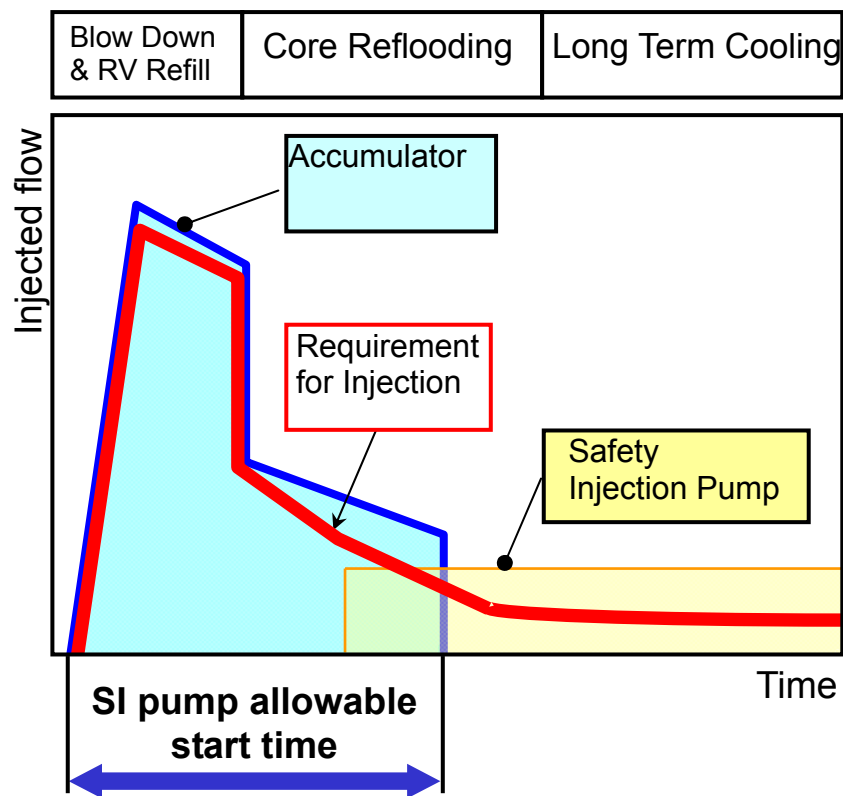
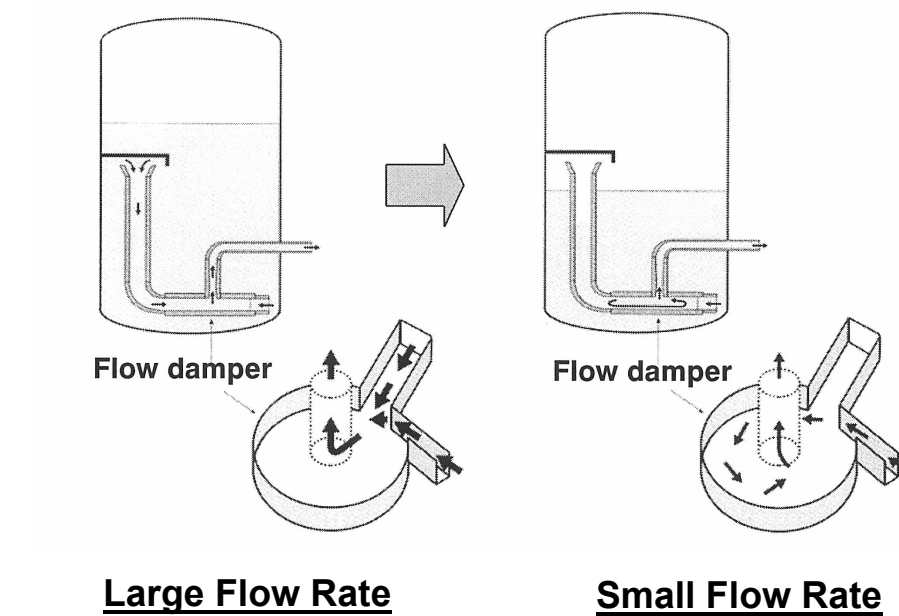


Figure 2-10 Safety System Performance for US-APWR

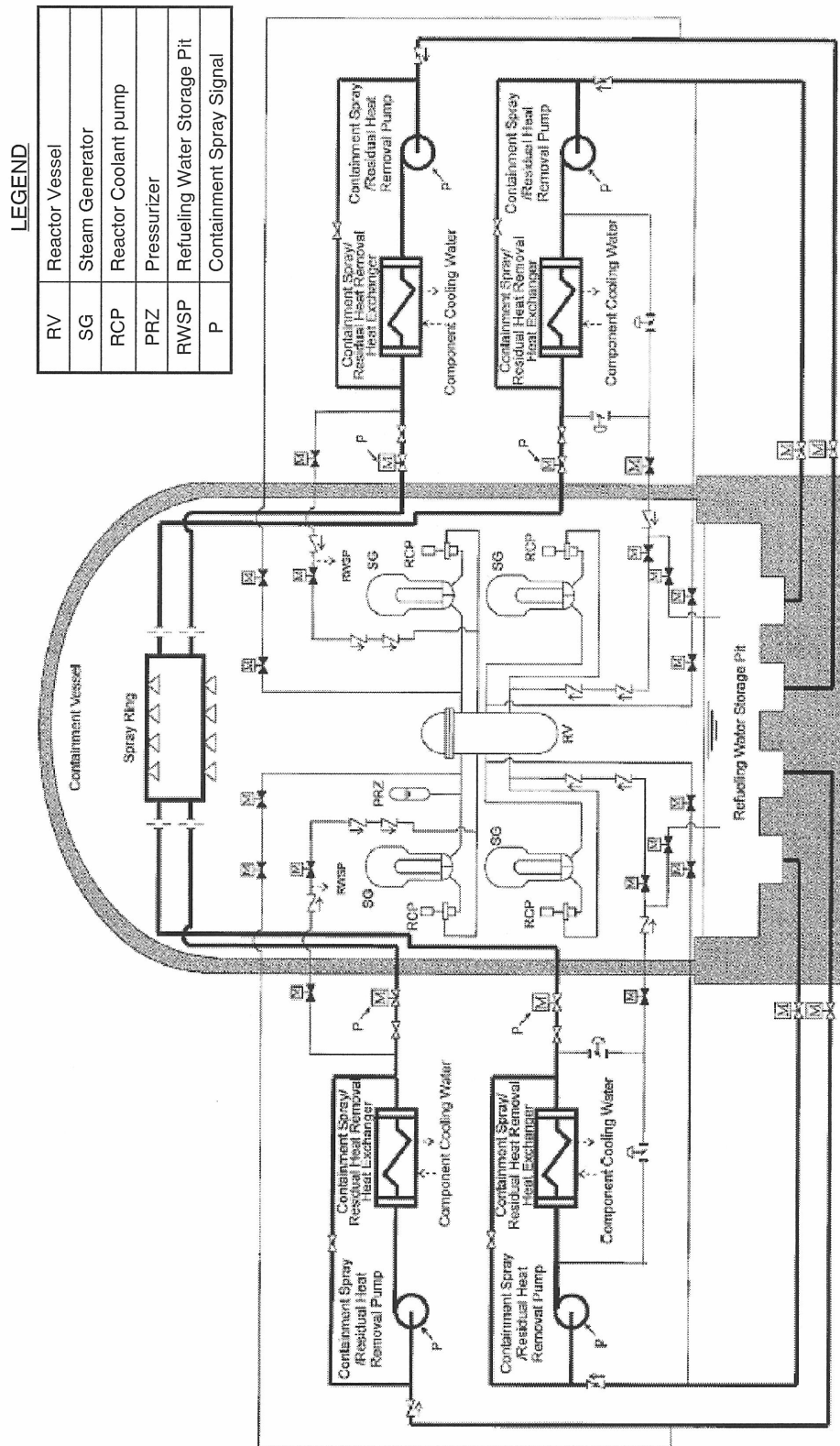


Figure 2-11 Containment Spray System

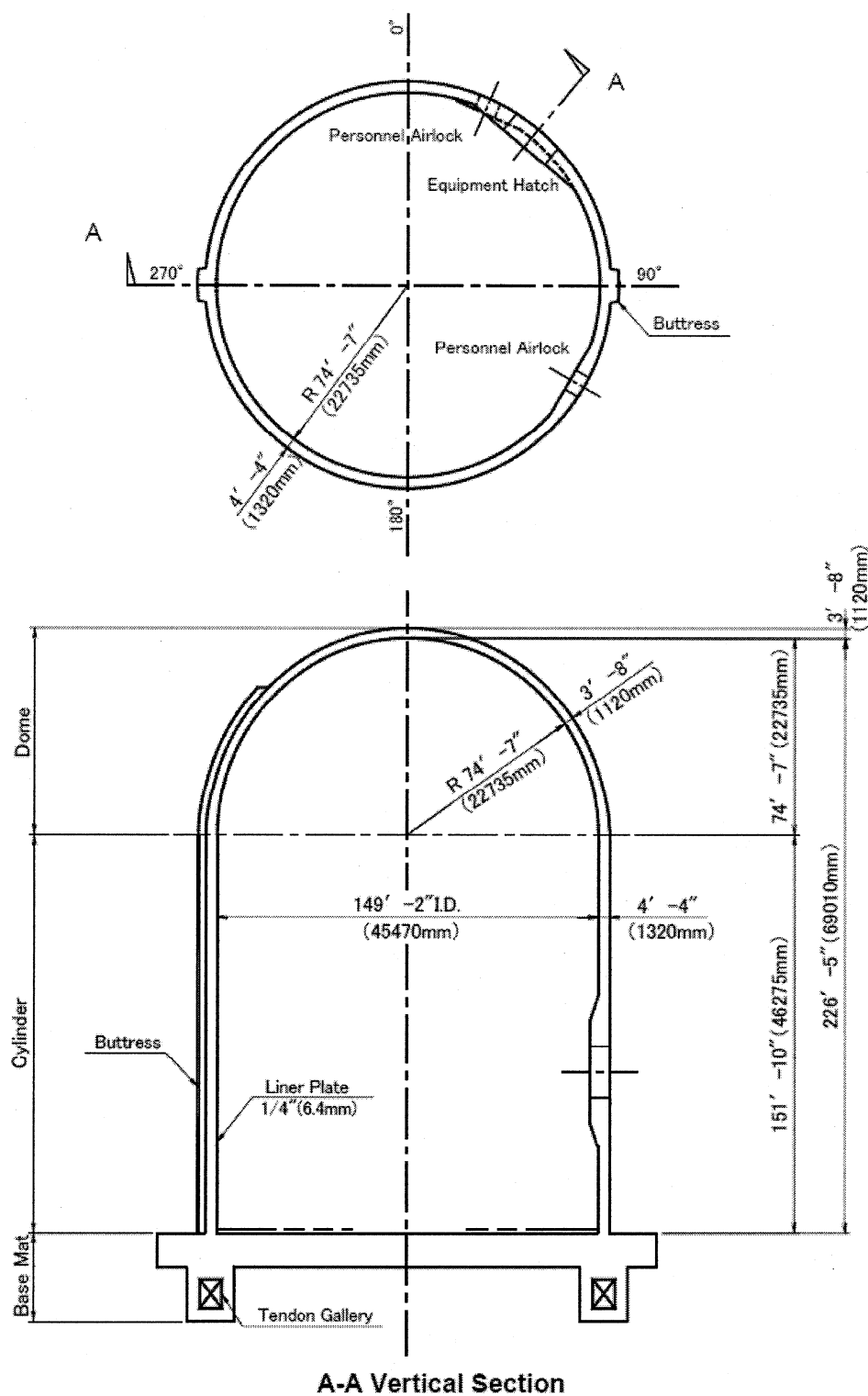


Figure 2-12 Configuration of Containment Vessel

3.0 LBLOCA CODE AND METHODOLOGY

3.1 Introduction

This chapter of the report identifies and discusses certain design features of the US-APWR, which have been approved by the NRC, in order to evaluate the applicability of the WCOBRA/TRAC code to the US-APWR. These evaluations confirm the applicability of WCOBRA/TRAC to MHI's new design, including its improved design features such as the advanced accumulator, the use of Direct Vessel Injection (DVI) for safety injection, and the Neutron Reflector's (NR) improved design.

To confirm the applicability of the WCOBRA/TRAC code to the US-APWR, the significant phenomena, especially in the components that are identified as US-APWR design features, are identified and ranked based on the existing PIRT of conventional PWRs. In particular, the applicability of the advanced accumulator (Ref.4) as a new design is confirmed by introducing a modified flow resistance model and performing model validation with a comparison between calculation results and test data.

As the results, the WCOBRA/TRAC code can be used for the purposes of performing best-estimate analyses for the US-APWR, taking into account some minor modifications. The basis for this conclusion is that for LBLOCA events, no new phenomena are identified for the US-APWR, when compared to conventional 3- and 4-loop plants, and the test database that supports validation of this code is applicable to the US-APWR.

In addition, the uncertainty evaluation method, "Realistic Large Break LOCA Evaluation Methodology Using Automated Statistical Treatment of Uncertainty Method (ASTRUM)", which has been approved, can be applied to the analysis because the manner of treatment for uncertainty is very similar to conventional plants, too.

3.2 US-APWR Features

The US-APWR is a 4-loop plant with a reactor core consisting of 257 fuel assemblies of the 17x17 design. It will generate 4466 MWt, of which 4451 MWt will be generated in the reactor. Several of the US-APWR design features such as the neutron reflector (NR), model US-APWR RCP, and direct vessel injection (DVI) are improvements over prior PWR designs.

With respect to NR and DVI, the applicability of WCOBRA/TRAC to these features has already been reviewed by the NRC and has been approved in the AP600 and AP1000 designs. The Model US-APWR RCP is just a larger version of the 93A RCP used for conventional Westinghouse design PWRs. Therefore, the WCOBRA/TRAC code can incorporate the model US-APWR RCP.

The advanced accumulator is adopted for the US-APWR as a new design. This design initially delivers a sufficiently high flow rate to fill the lower plenum and downcomer, and initiate reflooding. When the water level drops below the inlet of the stand pipe, the flow rate is reduced significantly. Because it is a new design, the development of a simulated model of advanced accumulator characteristics is necessary for WCOBRA/TRAC.

3.3 Description of US-APWR LBLOCA Transient

3.3.1 General Description

The LBLOCA has been identified as a double-ended guillotine break or a split break in the cold leg pipe. This hypothesized break is a design-based accident for PWRs and is expected to produce the maximum fuel rod cladding temperature. The LBLOCA transient is subdivided into three time periods. These time periods are identified as “blowdown”, “refilling” and “reflooding”.

The design of the US-APWR is based on that of the conventional Westinghouse- designed PWRs. The ECCS configuration of the US-APWR is similar to that of the existing conventional Westinghouse-designed PWRs in which the pumped safety injection and accumulator injection are provided.

In a conventional PWR, the functions of the ECCS during a LOCA are assigned to three subsystems: the accumulator system, the Low Head Safety Injection (LHSI) system and the High Head Safety Injection (HHSI) system.

In the US-APWR, the advanced accumulator (ACC) shifts its flow rate from large flow to small flow automatically. For the high flow period the ACC performs the function of the standard accumulator in the 4-loop PWR design. For the low flow periods the ACC performs the function of LHSI beyond the time period required to quench the core. Both the accumulator function and LHSI function are combined together in the ACC to simplify the system (Ref.4).

The system configuration for the ECCS of the US-APWR is shown in Figure 3.3-1. Four ACCs are installed and each is connected to a Reactor Coolant System (RCS) cold leg. Four HHSI systems are installed and inject directly into the reactor vessel downcomer following accumulator injection flow. The US-APWR safety injection representative flow during a LBLOCA is shown in Figure 3.3-2. Therefore, the function and performance of the US-APWR safety injection systems are the same as a conventional 4-loop PWR.

Time sequences for the US-APWR LOCA transient are shown in Table 3.3-1. They are the same as for a conventional 4-loop PWR.

Figure 3.3-3 schematically shows US-APWR LOCA sequences and injection behavior of the US-APWR ECCS systems. The figure indicates the US-APWR system function is the same as a conventional 4-loop PWR.

3.3.2 Blowdown Period

The US-APWR LBLOCA blowdown starts at the location of the large break in the cold leg pipe, as the large pressure difference between the RCS and the containment forces coolant water rapidly out the broken cold leg. The break flow rate is limited by critical flow. At first, subcooled water is expelled out if the RCS pressure is high enough. Then, when the RCS pressure falls down to the saturation pressure, a two-phase mixture or steam is expelled out due to coolant flashing. The intact loop coolant begins to flash, increasing the flow resistance. The performance of the reactor coolant pumps will degrade as the coolant flashes.

The break changes from subcooled to saturated critical flow, and the break mass flow rate decreases rapidly. The mass flow from the vessel side of the break is much larger than that from the pump side because of the large flow resistances of the pump and the steam

generator tubes.

As critical heat flux is reached in the core, heat transfer changes from the nucleate boiling to the film boiling regime, and the core dries out. The fuel rod cladding temperature rises rapidly due to the degraded rod-to-coolant heat transfer.

During all phases of the LBLOCA, decay heat from the fuel, reverse heat transfer from the steam generators, and latent heat from structures are heat sources to the core. The RCS pressure falls below the secondary system pressure and reverse heat transfer occurs. Then the primary coolant is heated and vaporized by the secondary system. On the other hand, fission power reduces automatically as the fission products and actinides decay.

The RCS pressure falls below that of the nitrogen gas in the ACCs, then the check valves that normally isolate the accumulators from the RCS open, and expanding nitrogen gas forces borated water into the vessel downcomer through the intact cold legs at a large flow rate.

The water injected from the ACC continues to bypass the lower plenum. As the countercurrent steam velocity decreases, the ACC water begins to penetrate the lower plenum and refilling begins.

During blowdown, some of the water in the lower plenum boils away or is swept out by high velocity steam flow moving down through the core and up the downcomer to the broken cold leg. The amount of water remaining in the lower plenum determines the duration of the next period (refilling) of the LBLOCA.

3.3.3 Refilling Period

During refilling, the ACC refills the lower plenum immediately by large flow injection following the blowdown period. The HHSI system, consisting of low flow capacity pumps, also actuates automatically and injects emergency coolant into the vessel downcomer via the DVI nozzles.

ECC water in the reactor vessel downcomer flows down by gravity or is swept out the break point by a pressure differential and upward-escaping steam flow that levitates the liquid. This levitation is referred to as the Countercurrent Flow Limitation (CCFL) phenomenon. The reactor vessel wall and internals are large metal structures at temperatures above saturation. When subcooled ECC fluid contacts the metal structures in the downcomer, steam is generated.

The refilling period ends when the water level in the lower plenum reaches the bottom of the fuel rods.

3.3.4 Reflooding Period

Reflooding begins when the lower plenum is completely filled with ECC water. The core begins to reflood with ECC water after the lower plenum is filled.

During the reflooding period, the ACC refills the downcomer immediately by large flow injection, and establishes the core reflooding condition by maintaining the downcomer water level. A small flow injection can maintain core cooling after refilling condition.

The primary source of ECC water for reflooding is the small flow of the ACCs injected into the

cold legs, and the secondary source is the HHSIs. The ACC flow rate switches from large flow to small flow automatically when the water level in the ACC tank reaches the inlet of the standpipe.

At the beginning of the reflooding period, the fuel rods are relatively hot because the rod-to-coolant heat transfer has not been very effective during most of the blowdown and all of the bypass/refilling period. Because of high fuel rod temperatures at the beginning of reflooding, the flow regimes in the core during reflooding should change the conditions, starting with single-phase liquid and progressing upward through the core with nucleate boiling, transition boiling, film boiling, churn two-phase flow, dispersed droplet flow, and single-phase steam flow. When water firstly covers the bottom of the fuel rods, the fuel cladding surface is not wetted because film boiling is the main heat transfer mechanism. Eventually, the fuel cladding temperature falls below the minimum film boiling temperature, and the liquid wets the fuel cladding surface and cools it. The fuel cladding temperature at that elevation drops down sharply to nearly the coolant saturation temperature, that is, the rods are quenched. Quenching progresses from the bottom to the top as the core is reflooded. Some top-quenching also occurs in addition to bottom-quenching at the same time, as explained below.

The quenching process releases a large amount of heat to the reflooding water and steam is generated. The generated steam carries water droplets upward as it rises between the fuel rods. These entrained droplets help to cool the rods at higher elevations. As the bottom quenching progresses upward through the core, more liquid is carried over to the upper plenum pool and the level of the two-phase mixture can reach the hot leg. At first, water from the pool cannot flow down to cool the rods because the generated steam is flowing upward through the holes in the upper core support plate. This phenomenon is similar to that occurring in the downcomer during bypass. At some point, however, water films penetrate the holes and begin to quench the fuel rods from the top. Top-down quenching by falling films takes place first at the core periphery where decay heat is the lowest.

If liquid carried through the hot legs reaches the steam generators, it will be vaporized by reverse heat transfer from the steam generator, causing a pressure increase in the upper plenum. The pressure increase reduces the reflooding rate, giving rise to a steam binding effect. The core vapor mass flow rate decreases alongside the decreasing quench velocity, and this reduces the amount of liquid entrained and carried over to the hot legs. The upper plenum pressure decreases, causing an increase in flooding rates. This cyclical process may be repeated, at a decreasing rate, until the entire core is reflooded.

Table 3.3-1 Typical Sequence of the LBLOCA of US-APWR

Period	Summary of LBLOCA Transient
Blowdown	<p>Cold leg break occurs</p> <p>The containment high pressure "S" signal generated</p> <p>Fuel cladding temperature reaches its peak (in the blowdown peak cladding temperature(PCT) case)</p> <p>Start of accumulator injection</p>
Refilling	<p>Start of core-reflooding</p>
Reflooding	<p>Accumulator injection flow rate switches to small</p> <p>Start of HHSI to vessel directly *</p> <p>(Fuel cladding temperature reaches its peak in the reflooding PCT case)</p> <p>Core temperatures are reduced to long-term steady state levels associated with dissipation of residual heat generation</p> <p>Continued operation of the HHSI supplies water during long-term cooling</p>

*Loss of offsite power is assumed.

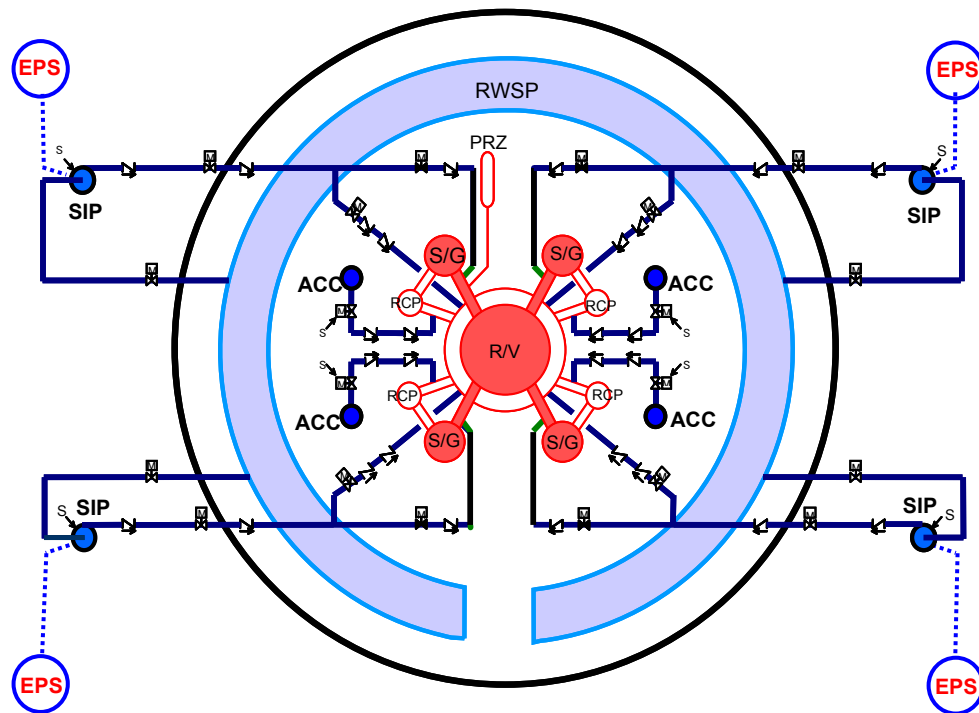


Figure 3.3-1 System Configuration of ECCS of US-APWR

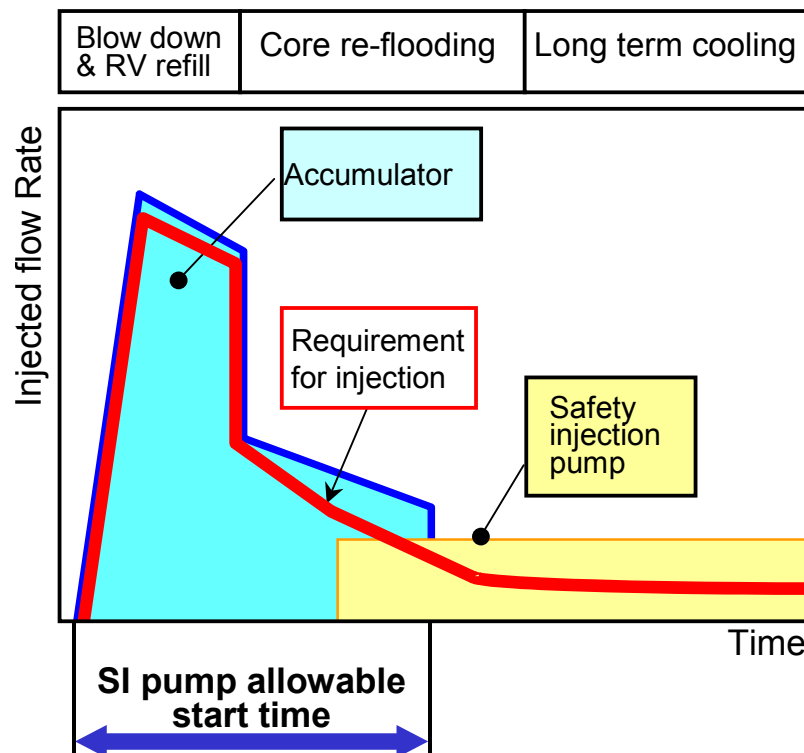
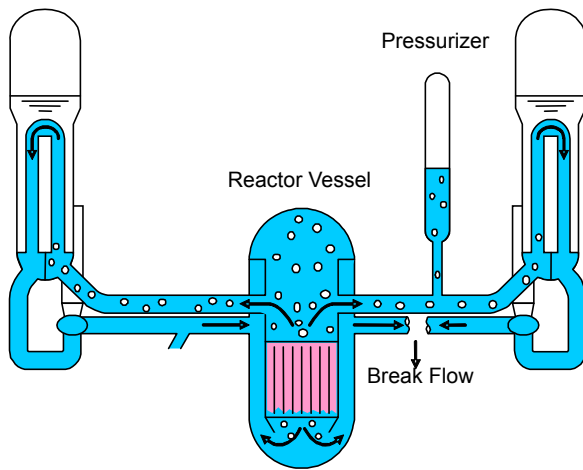
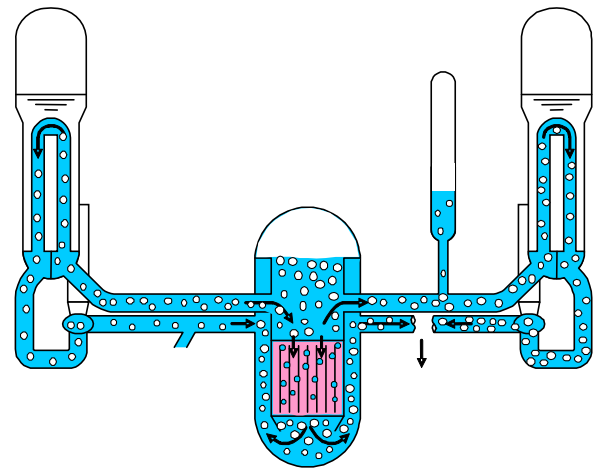


Figure 3.3-2 ECCS Flow Injection Performance during LBLOCA

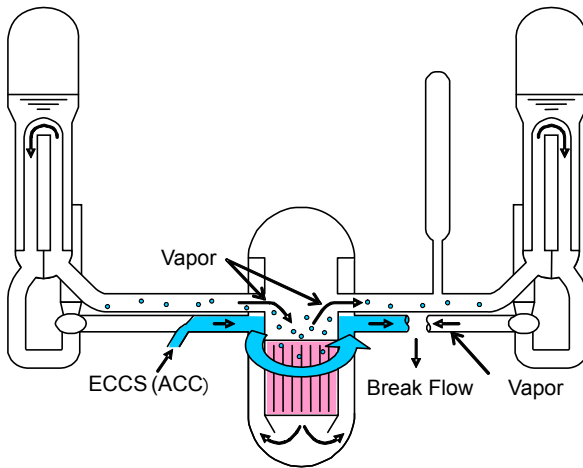
Steam Generator



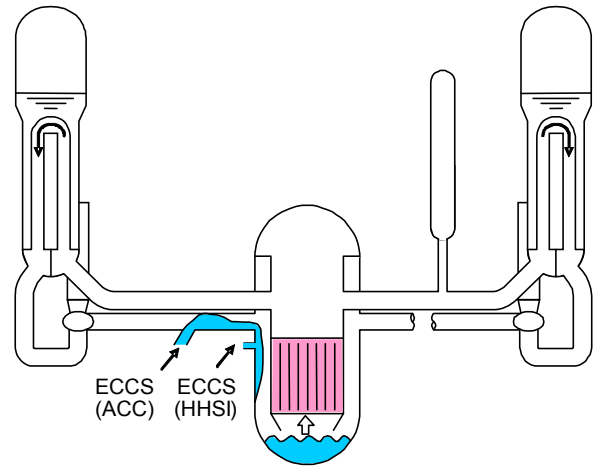
1. Blowdown (Initial Phase)



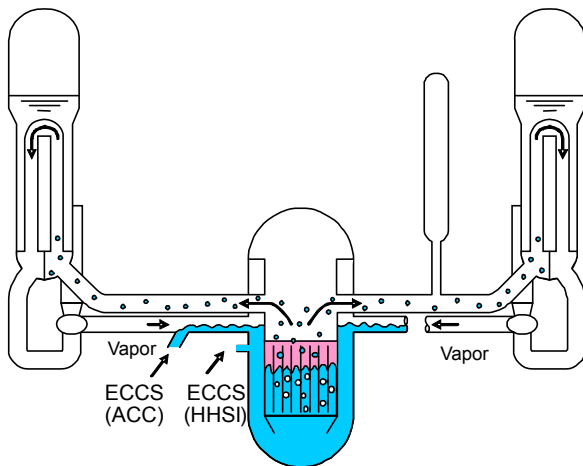
2. Blowdown (Flashing)



3. ECCS Bypass Phenomena



4. Refilling



5. Core reflooding

Figure 3.3-3 Transient of LBLOCA in US-APWR

3.4 Phenomena Identification and Ranking (PIRT)

3.4.1 LBLOCA PIRT

In this section, the modeling requirements for performing a LBLOCA best-estimate calculation for the US-AWR are identified and discussed. In developing the requirements, the individual phenomena and processes that must be modeled to achieve an accurate estimate of the Peak Cladding Temperature (PCT) are identified as well for a conventional 4-loop plant.

A Phenomena Identification and Ranking Table (PIRT) for the US-APWR is developed, using the same process that is described in the Westinghouse PIRT (Ref.5) for a conventional 4-loop plant. The following highly ranked models and phenomena are identified from the PIRT as well.

- a) Critical flow
- b) Broken loop resistance
- c) Fuel rod (fuel conductivity, gap conductivity, rod internal pressure, decay heat, cladding swelling and burst, ZIRLO™ -water reaction, and fuel relocation)
- d) Core heat transfer
- e) ECC bypass
- f) Entrainment/Steam binding
- g) Accumulator nitrogen
- h) Condensation

The PIRT for all operating conventional plant designs (3- and 4-loop plants with cold leg ECCS injection) (Ref.6) and the US-APWR is provided in Table 3.4-1. The development of the US-APWR PIRT was established based on the existing PIRT in which Westinghouse ranked and identified phenomena as a starting point, and included additional information relevant to the US-APWR specific features. In this table, the conventional 3- and 4-loop plants with cold leg injection are treated as a single group.

In the ranking of importance of the thermal hydraulic phenomena, Westinghouse did not rank any phenomena with a ranking less than "5". This ranking should not be interpreted to mean that those phenomena that were not ranked can be ignored or do not have to be simulated.

The existing PIRT and the US-APWR PIRT are presented using the same format from the Code Scaling, Applicability and Uncertainty (CSAU) evaluation, with the CSAU ranking as a comparison guide. Conventional PWR and MHI's US-APWR also retained the same definition of the LOCA periods as identified in the CSAU PIRT. The blowdown phase of the accident extends from the accident initiation to the initiation of the accumulator injection into the intact loops (approximately 600 psia in Westinghouse 3- and 4-loop plants). Refilling is assumed to begin when the lower plenum is refilled. Reflooding continues from the bottom of the core recovery and continues until the PCT has occurred and the cladding is cooling down. These definitions are different from the traditional definitions for the blowdown and refilling periods (refilling usually begins when ECC bypass ends).

Instead of "numerical values", three ranking levels are applied to each phenomenon in the US-APWR PIRT. The rankings are assigned using the following definitions (Ref.7).

H = The process is considered to have high importance. Accurate modeling of the

process is considered to be crucial to the correct prediction of the transient. Models used to predict the process must be validated. (Ranked 7-9) (More than [] sensitivity)

M = The process is considered to have medium importance. Modeling has to be done for appropriate process simulation, although the level of influence of the process on the entire transient is expected to be lower than that for those ranked high. (Ranked 5-6) (More than [] sensitivity)

L = The process is considered to have low importance. The phenomena need to be modeled in the code or explained in adequate detail in the methodology, although accuracy in modeling the process is not considered very influential on the whole transient.

N/A = The process is considered not to occur at all.

The rankings of the various processes in terms of importance were confirmed by five thermal-hydraulic analysts and engineers at MHI. A meeting was held in June 2007 to establish the PIRT for an LBLOCA in the US-APWR.

3.4.1.1 Fuel Rod

3.4.1.2 Core

3.4.1.3 Upper Plenum

3.4.1.4 Hot Leg

3.4.1.5 Pressurizer

3.4.1.6 Steam Generators

3.4.1.7 Pump

3.4.1.8 Cold Leg/Accumulator

3.4.1.9 Downcomer

3.4.1.10 Lower Plenum

3.4.1.11 Break

3.4.1.12 Loop

3.4.2 Effects of US-APWR Design on Westinghouse PIRT Conclusions

3.4.2.1 Advanced Accumulator

3.4.2.2 Direct Vessel Injection (DVI)

3.4.2.3 Neutron Reflector (NR)

Table 3.4-1 US-APWR PIRT (1/2)

Table 3.4-1 US-APWR PIRT (2/2)

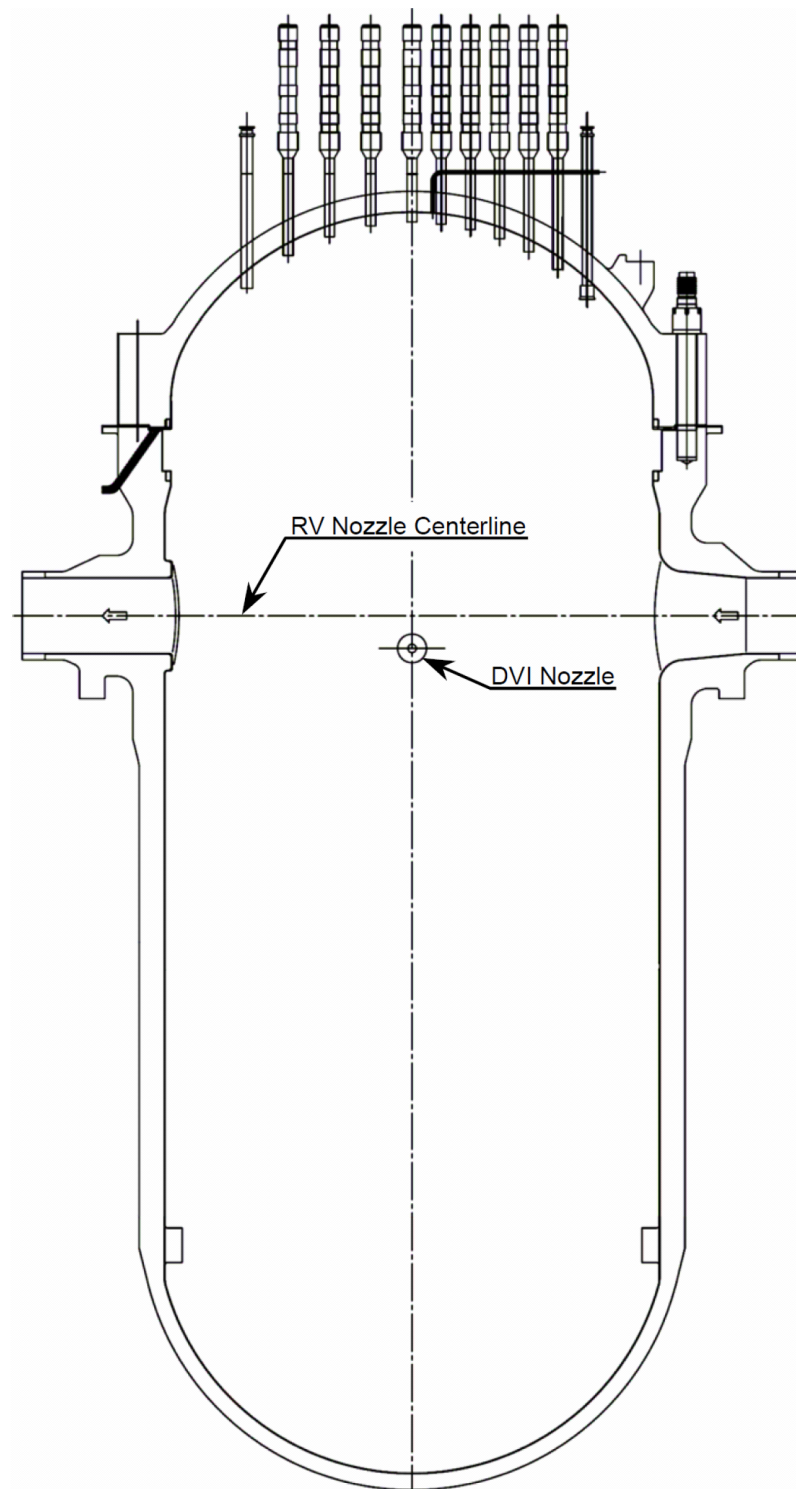


Figure 3.4-1 Location of Direct Vessel Injection Nozzle

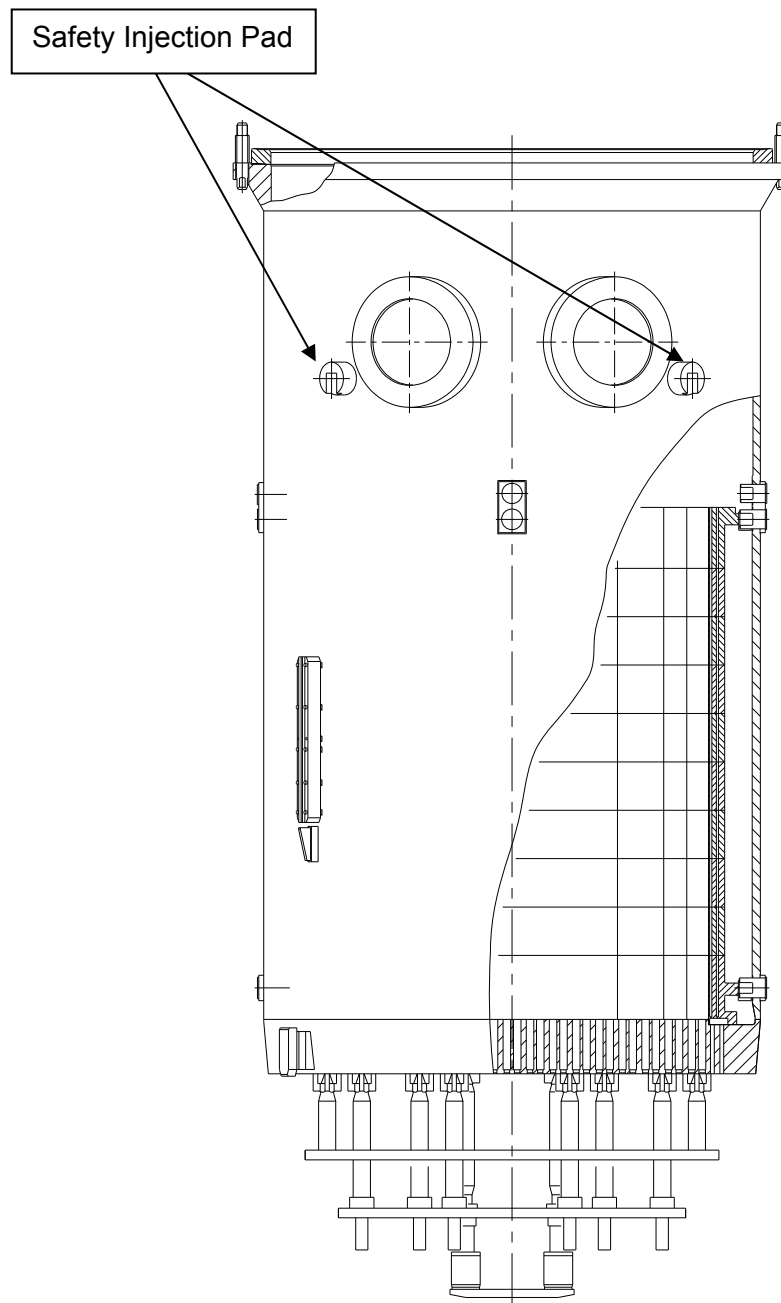


Figure 3.4-2 Safety Injection Pad of Direct Vessel Injection

3.5 WCOBRA/TRAC Code Applicability to US-APWR

3.5.1 Advanced Accumulator

3.5.1.1 Code Applicability

The ACC is a water storage tank with a flow damper in it that switches the flow rate of the cooling water injected into the reactor vessel from a large to a small flow rate. A simplified drawing of the ACC is shown in Figure 3.5-1.

There is a vortex chamber at the inlet of the injection pipe in the accumulator tank. The small flow rate pipe is tangentially attached to the vortex chamber. The large flow rate pipe is radially attached to the vortex chamber on one end and connected to the standpipe on the other end. The inlet port for the stand pipe is located on the level of the interface between the volume of water for the large flow rate injection and that for the small flow rate injection in the tank. The outlet port of the flow damper is connected to the injection pipe. The ACC is thus a simple device with no moving parts.

The accumulator is a pressure vessel partially filled with water and pressurized with nitrogen gas (N_2). The accumulator is isolated from the Reactor Coolant System (RCS) by two check valves. When a LOCA occurs and pressure in the reactor vessel decreases, the check valves in the injection pipe open to permit the injection of cooling water into the vessel. Since the water level in the accumulator tank is at first higher than the elevation of the inlet of the stand pipe, water flows through both the large and small flow rate pipes. The pressure at the throat is comparatively lower than that at the injection pipe during large flow rate. If the pressure at the throat drops below the critical pressure of cavitation inception, cavitation may occur. As a result of tests, a cavitation factor has been introduced to simulate the flow rate characteristics.

High flow continues until the water level in the accumulator tank comes down to the inlet level of the stand pipe. The flow in the large flow rate pipe almost comes to a stop then, and the flow from the small flow rate pipe forms a strong vortex in the vortex chamber. As a result of centripetal force, a large pressure drop occurs along the radius of the vortex chamber between the small flow rate pipe and the output port. Therefore, a small flow rate is achieved as a result of the vortex, rather than with moving parts. This flow continues until the accumulator is empty, after which the nitrogen cover gas is discharged.

Therefore, the injection flow characteristics in the ACC with regards to the following items should be simulated by WCOBRA/TRAC.

- Flow resistance change due to cavitation characteristics. A cavitation equation as an empirical correlation has been obtained by testing (Ref.4).
- Sudden switching from high flow rate to low flow rate due to the existence of a stand pipe.

Injection Flow Rate

WCOBRA/TRAC does not model flow resistance change due to cavitation factor and flow switching caused by the stand pipe because the conventional ACC does not control those flows. The existing flow resistance model of the code is only a constant value given by the input and friction correlation, and the model has no water level-dependent flow resistance. Therefore, flow resistance change and flow switching must be revised in the code by using empirical correlations (Ref.4), and any switching of the equation depends on water level or residual water volume in the ACC, respectively.

Discharge of N₂ Gas

WCOBRA/TRAC already has a model for the discharge of N₂ gas after the emptying of water as the discharge gas is simulated by subcooled vapor, which is approved by the NRC.

Consequently, the model that should be revised in WCOBRA/TRAC was clarified, and the empirical correlations are incorporated into the WCOBRA/TRAC code to model advanced accumulator characteristics.

3.5.1.2 Model Revisions

The revised WCOBRA/TRAC code with the advanced accumulator model is named WCOBRA/TRAC(M1.0).

The total resistance coefficient, K_{ACC} , is determined from the ACC flow rate coefficient, C_v , and the resistance coefficient from the injection piping. The flow rate coefficient is a function of the cavitation factor, σ_v , and the water level in the ACC. The total resistance coefficient is calculated each time step as follows.

(1) σ_v is calculated from the flow condition at flow damper

$$\sigma_v = \frac{P_D + P_{at} - P_v}{(P_A + \rho g H) - \left(P_D + \frac{\rho V_D^2}{2} + \rho g H' \right)} \quad (3.5.1-1)$$

- σ_v : Cavitation factor
- P_{at} : Atmospheric pressure (abs)
- P_D : Flow damper outlet pressure (gage)
- P_A : Gas pressure in accumulator (gage)
- P_v : Vapor pressure (abs)
- ρ : Density of water
- g : Acceleration of gravity
- H : Distance between ACC water level and vortex chamber
- H' : Distance between outlet pipe and vortex chamber
- V_D : Velocity of injection pipe

(2) The flow rate coefficient C_v is calculated using the following correlations obtained from test

data that covers the range of applicability for the US-APWR design (Ref.4). The empirical correlations of C_v are derived separately for large and small flow rate injections as a function of the cavitation factor of σ_v as shown in Figure 3.5-2.

$$\text{For large flow rate: } C_v = 0.7787 - 0.6889 \exp(-0.5238 \sigma_v) \quad (3.5.1-2)$$

$$\text{For small flow rate: } C_v = 0.07197 - 0.01904 \exp(-6.818 \sigma_v) \quad (3.5.1-3)$$

(3) C_v is converted to K_D

$$K_D = 1/C_v^2 \quad (3.5.1-4)$$

K_D : Flow resistance coefficient of flow damper

(4) Total resistance coefficient is calculated by;

$$K_{acc} = K_D + K_{pipe} \quad (3.5.1-5)$$

K_{acc} : Total resistance coefficient of flow damper and injection piping

K_{pipe} : Total resistance coefficient of injection piping

Since subroutines ACCUM1 and ACCM1X calculate flow resistance and residual water volume, respectively, these subroutines were revised to incorporate the correlations. The advanced accumulator model as coded is described in Appendix B.

3.5.1.3 Model Validation

Analyses for actual pressure and full height 1/2 scale tests were performed to validate the revised model. The purpose of the analyses was to confirm that the analytical results were in a good agreement with test data.

(1) Summary of test facility description



(2) Test cases and test conditions

The validation analysis was performed subject to full height 1/2 scale test (Ref.4), which includes the test cases to simulate the ECCS performance during a LBLOCA. Only the following three cases of all test cases simulate the range of initial tank pressure and RCS pressure conditions during a LBLOCA. The ACC tank gas pressure and the exhaust tank pressure corresponding to RCS pressure are shown in Table 3.5-2.

- Case 1: The initial test tank pressure was 586 psig (4.04 MPa (gage)) simulating the condition for ECCS performance during a LBLOCA.

- Case 2: The initial test tank pressure was 657 psig (4.53 MPa (gage)) to obtain data for high pressure design.
- Case 3: The initial tank pressure was 758 psig (5.23 MPa (gage)) to obtain data for large differential pressure design.
- The pressure in the exhaust tank was 14 psig (0.098 MPa (gage)) for Cases 1, 2, and 3. Since the pressure of the exhaust tank becomes the same as the pressure of the containment vessel (CV) after the blowdown phase during a LBLOCA, and ECCS performance analysis uses approximately 14 psig (0.098 MPa (gage)) and the backpressure was set at 14 psig (0.098 MPa (gage)).

(3) Analytical model and boundary conditions for test analyses

The analytical model of the advanced accumulator is shown in Figure 3.5-5. The model is based on the nodalization described in Appendix B including the standard nodalization schemes such as node length, flow area and volume.



(4) Analysis conditions

Analysis conditions for full height 1/2 scale test are shown in Table 3.5-3 based on test condition shown in Table 3.5-2.



The input data including the analytical model, boundary conditions and the analysis conditions are prepared in the same method as plant analysis.

(5) Analysis results and comparison with test data

Analysis results are shown in Figure 3.5-7 to Figure 3.5-9. Analysis results are in good agreement with test data, especially for integrated injection flow rate, which is the most important for reflooding PCT until there is enough time to validate the advanced accumulator modeling.

Consequently, it is confirmed that the ACC modeling by the revised code "WCOBRA/TRAC(M1.0)" is valid for the simulation of ACC injection flow rate in the US-APWR safety analysis.

3.5.1.4 Uncertainty

The advanced accumulator has two kinds of uncertainties: one is an empirical correlation of Equation 3.5.1-2 and 3.5.1-3, and the other relates to flow switching water level. These uncertainties are evaluated to determine how it is treated for the LOCA safety analysis.

(1) Uncertainty of the Characteristic Equations for Flow Rates

Instrument Uncertainties

Dispersion Deviation from Experimental Equations

Manufacturing Error

Total Uncertainty of Experimental Equation Applicable to US-APWR

The total uncertainty of empirical equations used for safety analysis of a LBLOCA on the US-APWR including the instrument uncertainties, the data dispersion and manufacturing error is treated as statistical parameter in ASTRUM.

(2) Uncertainties of Water Level for Switching Flow Rates for US-APWR**(3) Treatment of Dissolved Nitrogen Gas Effect****3.5.1.5 Summary**

The model that should be revised in WCOBRA/TRAC was clarified through the code applicability investigation, and the empirical correlations of the flow damper in the advanced ACC were incorporated into the WCOBRA/TRAC code to model ACC characteristics.

The methodology to calculate flow damper characteristics including empirical correlation was

described on a model basis and coded in WCOBRA/TRAC.

The WCOBRA/TRAC code, which is modified slightly, is called WCOBRA/TRAC(M1.0) in this report.

Analyses for full height 1/2 scale tests on actual pressure were performed to validate the model of WCOBRA/TRAC with the revised model concerning the flow damper. As a result of comparison with analysis and test data, it has been confirmed that the revised WCOBRA/TRAC code (WCOBRA/TRAC(M1.0)) is in good agreement with test data. In addition, it has already been confirmed that there is no scaling effect between ACC tests and the US-APWR (Ref.4). Therefore, the code is validated and has the capability of NPP simulation with water injection characteristics of the ACC.

The total uncertainty of flow damper flow resistance and flow switching used for safety analysis of a LBLOCA on the US-APWR is derived from the full height 1/2 scale test data.

The treatment for uncertainties of flow damper resistance and flow switching for the US-APWR safety analysis using the ASTRUM methodology are determined as statistical parameters.

Table 3.5-1 Phenomena/Model in WCOBRA/TRAC for ACC

Table 3.5-2 Test Conditions of Full Height 1/2 Scale Test

	Test Tank Pressure	Exhaust Tank Pressure	Objective
	psig (MPa gage)	psig (MPa gage)	
Case 1	586 (4.04)	14 (0.098)	Obtain flow characteristics for ECCS performance evaluation during a LBLOCA
Case 2	657 (4.53)	14 (0.098)	Obtain flow characteristics for high pressure design
Case 3	758 (5.23)	14 (0.098)	Obtain flow characteristics for large differential pressure

Table 3.5-3 Analysis Conditions

Table 3.5-4 Instrument Uncertainties (1/2) (Large Flow)**Table 3.5-4 Instrument Uncertainties (2/2) (Small Flow)****Table 3.5-5 Dispersion of Data from Experimental Equation**

Table 3.5-6 Total Uncertainty of Flow Rate Coefficient (Experimental Equations) for Safety Analysis of US-APWR

--

Table 3.5-7 Additional Bias to Flow Rate Coefficient (Experimental Equations)

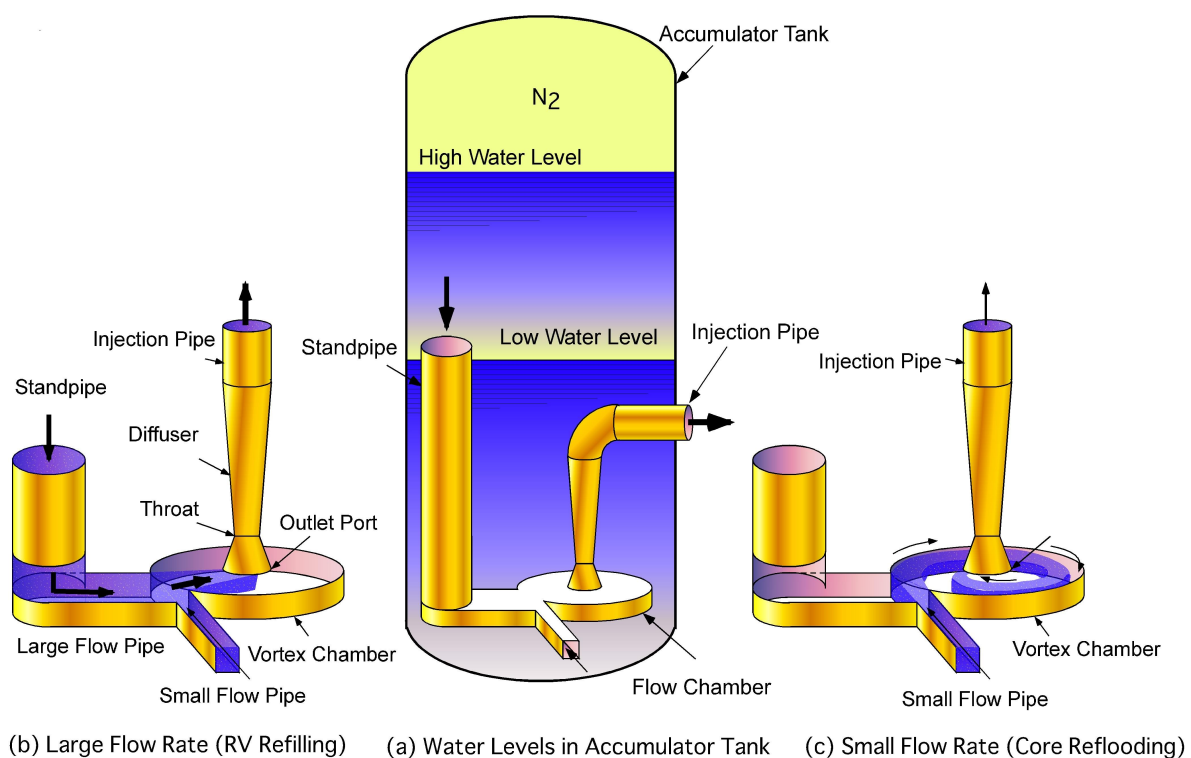


Figure 3.5-1 Principle of Advanced Accumulator



Figure 3.5-2 Flow Characteristics of Flow Damper

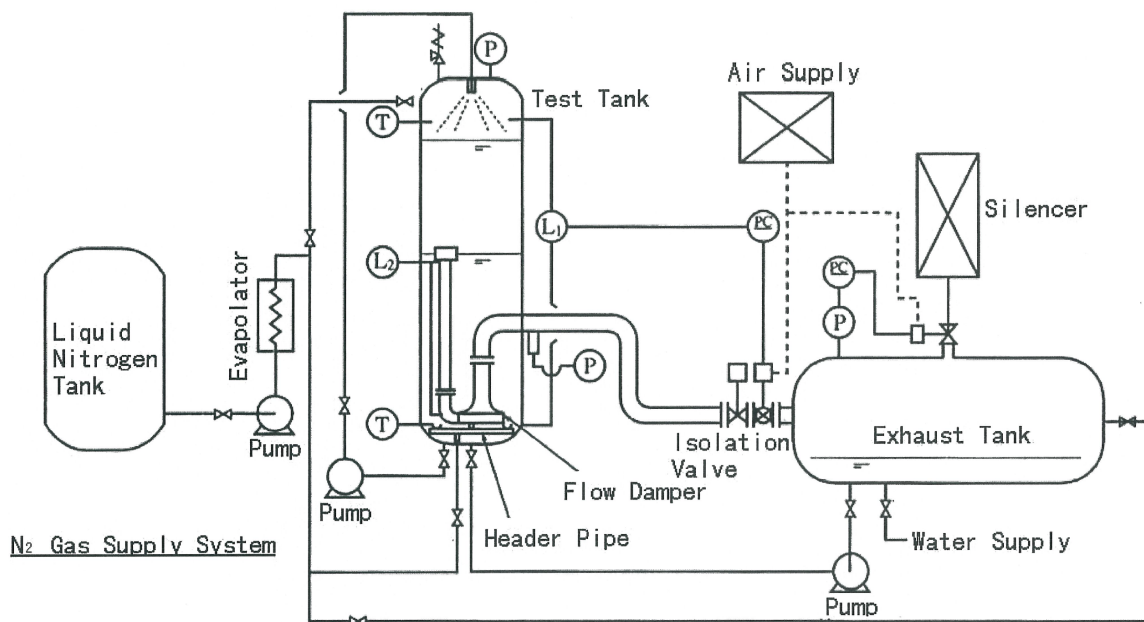


Figure 3.5-3 Schematic Drawing of Full Height 1/2 Scale Test Facility



Figure 3.5-4 Outline Drawing of Full Height 1/2 Scale Test Facility

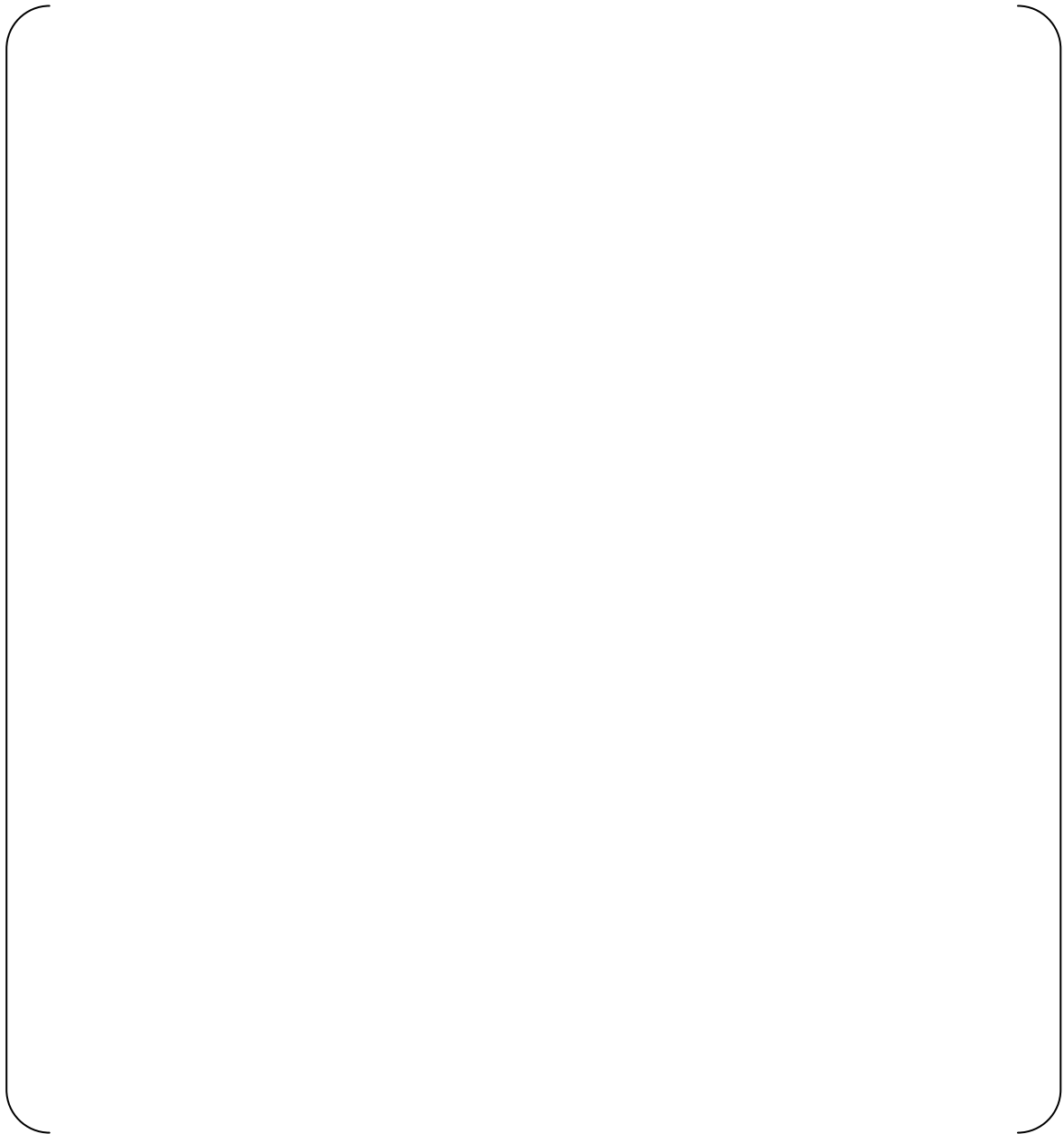


Figure 3.5-5 Nodalization of Full Height 1/2 Scale ACC Test Section



Figure 3.5-6 Flow Damper Outlet Pressure Given at BREAK (Case 1)



**Figure 3.5-7 (1/3) Comparison between Test and Analysis of Flow Rate
(Full Height 1/2 Scale Test Case 1)**



**Figure 3.5-7 (2/3) Comparison between Test and Analysis of Integrated Flow Rate
(Full Height 1/2 Scale Test Case 1)**



Figure 3.5-7 (3/3) Comparison between Test and Analysis of Gas Pressure in Test Tank (Full Height 1/2 Scale Test Case 1)



Figure 3.5-8 (1/3) Comparison between Test and Analysis of Flow Rate (Full Height 1/2 Scale Test Case 2)



**Figure 3.5-8 (2/3) Comparison between Test and Analysis of Integrated Flow Rate
(Full Height 1/2 Scale Test Case 2)**



**Figure 3.5-8 (3/3) Comparison between Test and Analysis of Gas Pressure in Test
Tank (Full Height 1/2 Scale Test Case 2)**



**Figure 3.5-9 (1/3) Comparison between Test and Analysis of Flow Rate
(Full Height 1/2 Scale Test Case 3)**



**Figure 3.5-9 (2/3) Comparison between Test and Analysis of Integrated Flow Rate
(Full Height 1/2 Scale Test Case 3)**



Figure 3.5-9 (3/3) Comparison between Test and Analysis of Gas Pressure in Test Tank (Full Height 1/2 Scale Test Case 3)

3.5.2 Direct Vessel Injection (DVI)

The applicability of WCOBRA/TRAC to DVI was reviewed and approved by the NRC for the AP600 (Ref.2) and AP1000 (Ref.3) designs.

Therefore, no modifications to treat the uncertainty of the DVI model are unnecessary for the US-APWR.

3.5.3 Neutron Reflector

As discussed in section 3.4.2.2, it is concluded that the PIRT ranking of the thermal hydraulic phenomenon in the NR of the US-APWR is “Medium” during reflooding period.

The NR weighs more than [] lbm and adds mass adjacent to the core region. The steam generation and entrainment from its cooling holes may potentially have an impact on the reflooding heat transfer in the core and the ultimate peak cladding temperature.

Liquid flow into the NR would result in additional steam generation, which may retard the quench front and progress in the core in the same manner as the steam binding effect from the vapor generation in the steam generators. At the same time, since the flow path of the NR and the core channels form parallel paths between the lower plenum and the CCFL region below the upper core plate, the liquid flow into the NR may divert the core flow for cooling.

3.5.3.1 Thermal Hydraulic Behavior in NR Cooling Hole

Reflooding begins when the lower plenum of the reactor vessel is completely filled with water. The core and NR which surrounds the circumference of the core (see Figure 3.5-10), begin to reflood with ECC water after the lower plenum is filled. At this stage, the temperature of the NR is lower than the core temperature and is higher than the reflood water temperature. Figure 3.5-11 shows the flow regimes and heat transfer modes anticipated in the NR region.

In the upper region of this column, liquid droplets and liquid lumps are generated, as shown in Figure 3.5-11. Heat transfer modes under these flow regimes are classified as follows.

Consequently, the NR wall is cooled down by steam, liquid droplets, the water column and other mechanisms generated under the water level. It is a characteristic of the thermal hydraulics at the reflooding stage of the NR that the mechanisms of heat transfer and flow regimes like these rise to the upper region of the NR as the reflooding event progresses.

3.5.3.2 Applicability of WCOBRA/TRAC

3.5.3.3 Flow Regime in WCOBRA/TRAC

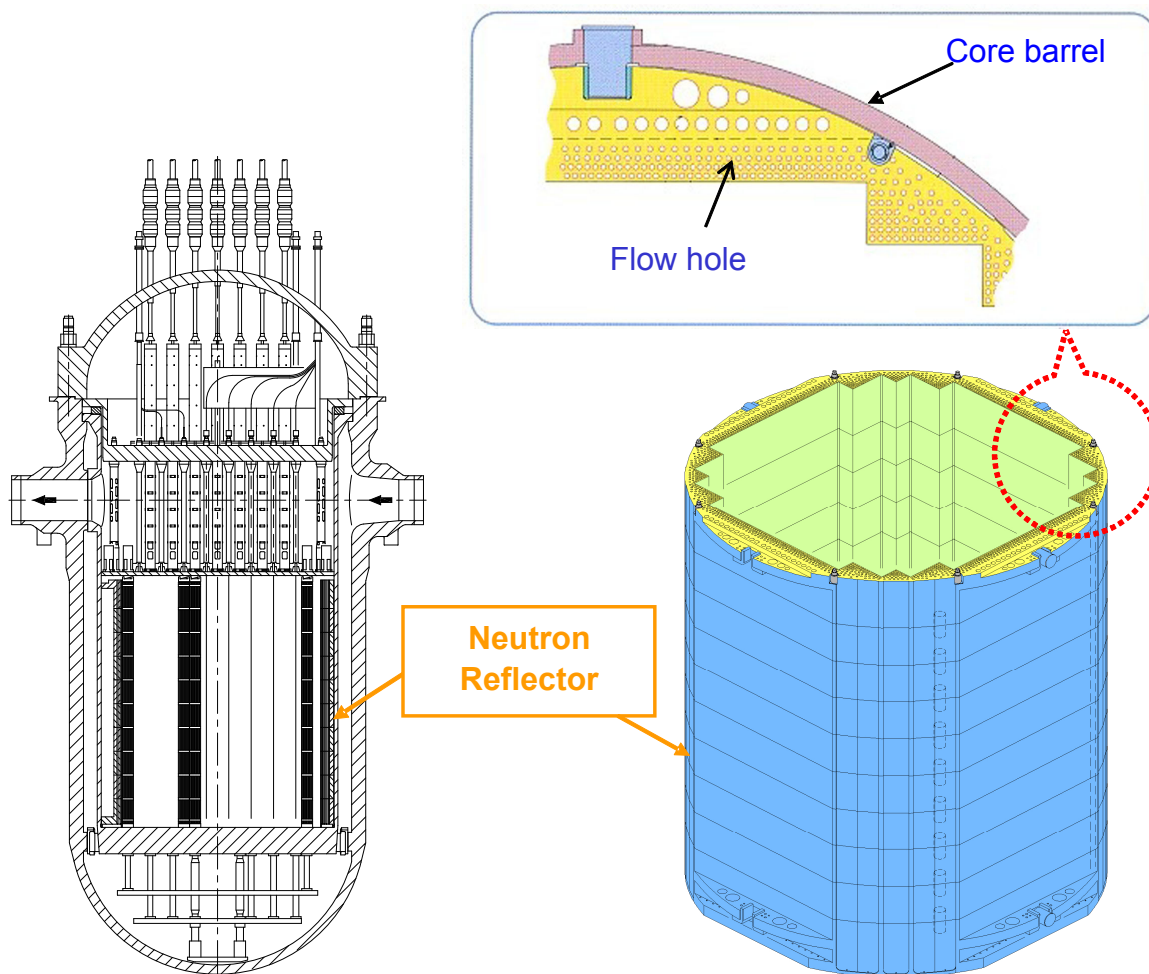


Figure 3.5-10 Neutron Reflector Configuration of US-APWR



Figure 3.5-11 Flow Regimes and Heat Transfer Modes at Cooling Holes in Neutron Reflector during Reflooding Period

Figure 3.5-12 Normal Wall Flow Regimes

Figure 3.5-13 Hot Wall Flow Regimes

3.6 Sample Plant Analysis

3.6.1 Nodalization of Plant Analysis

Nodalization for the US-APWR is established based on the same scheme used for the Westinghouse conventional 3- and 4-loop PWRs, as discussed in the WCOBRA/TRAC Code Qualification Document (Ref.6).

3.6.1.1 Vessel Model

3.6.1.2 Core Model

3.6.1.3 Loop Model

3.6.2 Calculation Process

3.6.2.1 Steady-State Calculation

The PWR LOCA calculation by WCOBRA/TRAC(M1.0) is initialized from a state in which the flow, the temperature, the power, and the pressure can be roughly considered to be stationary. WCOBRA/TRAC(M1.0) steady-state calculations are performed before the transient calculations to ensure that the desired steady-state PWR conditions are achieved.

Steady-state acceptance criteria are based on design information. [

]

3.6.2.2 Transient Calculation

The transient calculation is performed continuously if the obtained steady-state calculation results satisfy the acceptance criteria.

For the transient calculation, a postulated double-ended guillotine break or a split break are assumed to occur in one of the cold legs. The broken cold leg 1-D component arrangements are the same as shown in section 11-2 of Ref.5.

[

] The

GOTHIC code (Ref.13,14,15) is used for containment backpressure analysis.

3.6.3 Models for Sample Plant Analysis

3.6.3.1 NR Hot Wall Model

3.6.3.2 Homologous Pump Curves for the US-APWR RCP

The RCP of the US-APWR is just a larger version of the 93A RCP used for the conventional Westinghouse design PWR. The US-APWR RCP is a centrifugal type RCP and the same type as 93A RCP.

The WCOBRA/TRAC code has a pump model that is designed to model any centrifugal pump and which can include two-phase effects (Ref.6).

The pump model in the WCOBRA/TRAC code is an empirical model based on single- and two-phase flow data from scaled pumps (Ref.6).

The pump head and torque during two-phase flow are assumed to vary as a function of void fraction from the single-phase value to a “fully degraded” or minimum value that occurs at intermediate void fractions (Ref.6).

For the pump head:

$$H = H_1 + M(\alpha) \cdot (H_2 - H_1) \quad (3.6.3-1)$$

where:

- H = Pump head
- H_1 = Single-phase pump head
- H_2 = Fully degraded pump head
- $M(\alpha)$ = Two-phase head multiplier

For the pump torque:

$$T = T_1 + N(\alpha) \cdot (T_2 - T_1) \quad (3.6.3-2)$$

where:

- T = Pump torque
- T_1 = Single-phase pump torque
- T_2 = Fully degraded pump torque
- $N(\alpha)$ = Two-phase torque multiplier

Two-phase performance (fully degraded homologous curves and the two-phase multiplier) of the 93A RCP model was established by using 1/3-scale model air/water test data of a 93A pump carried out at Purdue University (Ref.16).

Generally, the specific speed is a function of the similarity between pumps. The specific

speed, N_s , is defined by;

$$N_s = \frac{\omega_R \sqrt{Q_R}}{(H_R)^{3/4}} \quad (3.6.3-3)$$

where:

ω_R = Rated pump speed (rpm)
 Q_R = Rated volumetric flow rate (gpm)
 H_R = Rated head (ft)

Table 3.6-3 shows pump rated characteristics of a 1/3-scale model of the 93A RCP model (Ref.6), the full scale 93A RCP model (Ref.17) and the US-APWR RCP model.

As shown in Table 3.6-4, the specific speed of the US-APWR RCP model is very similar to those of the 1/3-scale model of the 93A model and the 93A model. Therefore, two-phase performance [] of the US-APWR RCP can be obtained by using data from 1/3 scale model of the 93A air/water test (Ref.16).

[

] The results are shown in Figure 3.6-9 and Figure 3.6-10.

The fully degraded homologous curves of the US-APWR RCP model are similar to those of the 93A model (Ref.6).

As shown in Figure 3.6-11 and Figure 3.6-12, [

] Therefore, []

Ultimately, [

]

The effect of scaling is minimized in the US-APWR RCP model by using data from the Westinghouse 1/3 scale model, which is very similar in specific speed to the US-APWR RCP. Therefore, []

3.6.3.3 Containment Pressure Calculation Model

The GOTHIC code is used for minimum containment pressure analysis. Containment pressure by GOTHIC is used as the boundary conditions of the break in WCOBRA/TRAC(M1.0). Minimum containment pressure analysis is performed according to SRP6.2.1.5 (Ref.18) requirements.

3.6.4 Analysis Conditions

Major LOCA parameters for WCOBRA/TRAC are divided into the following three categories as in Ref.5.

Plant Physical Description
Plant Initial Operating Conditions
Accident Boundary Conditions

The US-APWR sample plant analysis conditions and the assumptions in major LOCA parameters for WCOBRA/TRAC(M1.0) are listed in Table 3.6-5.

3.6.5 Analysis Results

The transient is initiated from the end of the steady-state run with the break model inserted in the broken loop. The sequence of events for the transient shown in Table 3.6-6 represents the forced events (e.g., trips, etc) and those observed in the calculation (e.g., end of blowdown, etc).

3.6.5.1 Blowdown Phase

During the first few seconds of the transient, the flow is split, DNB occurs and the cladding temperature rises promptly as the core power is reduced. Figure 3.6-14 shows the peak cladding temperature of the hot rod.

Figure 3.6-15 shows hot channel core flow rate. In the early blowdown phase, the core flow direction is upward and core heat transfer takes place as a two-phase mixture that is pushed into the core. The end of this phase occurs when the lower plenum mass is depleted, flow in the loops becomes two-phase, and the pump head is degraded.

Figure 3.6-16 shows core pressure. The RCS depressurization has progressed, and the break flow begins to dominate and pulls flow downward away from the core. As the system pressure continues to decrease, the break flow and the core flow are reduced consequentially.

3.6.5.2 Refilling Phase

In this phase, core heat-up continues when the lower plenum is filled with advanced accumulator injection water. Figure 3.6-17 shows the lower plenum collapsed liquid level. When the advanced accumulator injection water fills the lower plenum and begins to enter the core, the refill phase ends.

3.6.5.3 Reflooding Phase

In the sample analysis, the reflooding phase starts about 36 seconds from the beginning of the break. In this phase, coolant enters the core from the bottom and entrainment begins. As a result, core heat transfer increases. Figure 3.6-19 shows accumulator flow rate. The flow rate of the advanced accumulators switches from high flow to low flow at about 56 seconds, and after about 2 seconds, the reflooding PCT is reached. After reaching the PCT, core reflooding progresses and cladding temperature decreases. The reactor core is quenched in about 220 seconds, and this phase ends.

3.6.6 Sample Plant Analysis Summary

The phenomena observed in the sample analyses of the US-APWR are very similar to those occurring in a Westinghouse 4-loop PWR. WCOBRA/TRAC(M1.0) with the minor modifications for the improved features of the US-APWR can adequately model the US-APWR LBLOCA performance.

Table 3.6-1 Channel Descriptions for US-APWR Vessel Model (1/3)

Table 3.6-1 Channel Descriptions for US-APWR Vessel Model (2/3)

Table 3.6-1 Channel Descriptions for US-APWR Vessel Model (3/3)

Table 3.6-2 Gap Connections for US-APWR Vessel Model (1/3)

Table 3.6-2 Gap Connections for US-APWR Vessel Model (3/3)

Table 3.6-3 Comparison of Rated Characteristics of Various Pumps**Table 3.6-4 Comparison of Specific Speed of Various Pumps**

Table 3.6-5 Analysis Conditions for US-APWR

Parameter	Values
Plant Physical Description	
a) Dimensions	
b) Flow Resistance	
c) Pressurizer Location	
d) Hot Assembly Location	
e) Hot Assembly Type	
f) SG Plugging Level	
Plant Initial Operating Conditions (Reactor Power)	
a) Core Power	
b) Peak Relative Linear Heat Rate	
c) Hot Rod Relative Average Power	
d) Hot Assembly Rel. Average Heat Rate	
e) Hot Assembly Rel. Peak Linear Heat Rate	
f) Axial Power Distribution	
g) Low-power Region Rel. Power	
Plant Initial Operating Conditions (Fluid Conditions)	
a) Tavg	
b) Pressurizer Pressure	
c) Loop Flow	
d) Upper Head Temperature	
e) Pressurizer Level	
f) Accumulator Temperature	
g) Accumulator Pressure	
h) Accumulator Water Volume except dead water volume	
i) Accumulator Line Flow Resistance	
j) Accumulator Boron Concentration	
Accident Boundary Conditions	
a) Break Location	
b) Break Type	
c) Break Size	
d) Offsite Power	
e) Safety Injection Flow	
f) Safety Injection Temperature	
g) Safety Injection Delay	
h) Containment Pressure	
i) Single Failure	
j) Control Rod Drop Time	

Table 3.6-6 Sequence of Events for US-APWR Sample Transient Analysis

Time	Event after DECLG Break
0 sec	DECLG break occurs
6 sec	SI signal issued
- 10 sec	Upwards Flow Phase
11 sec	Blowdown PCT 1563 °F (851°C) at about 10.8 ft (no ECC contribution)
13 sec	Accumulator injection started
36 sec	Refill ended
56 sec	Accumulator injection switched from high flow to low flow
58 sec	Reflooding PCT 1669 °F (909°C) at 10.3 ft
124 sec	SI injection started
- 220 sec	Core quenched

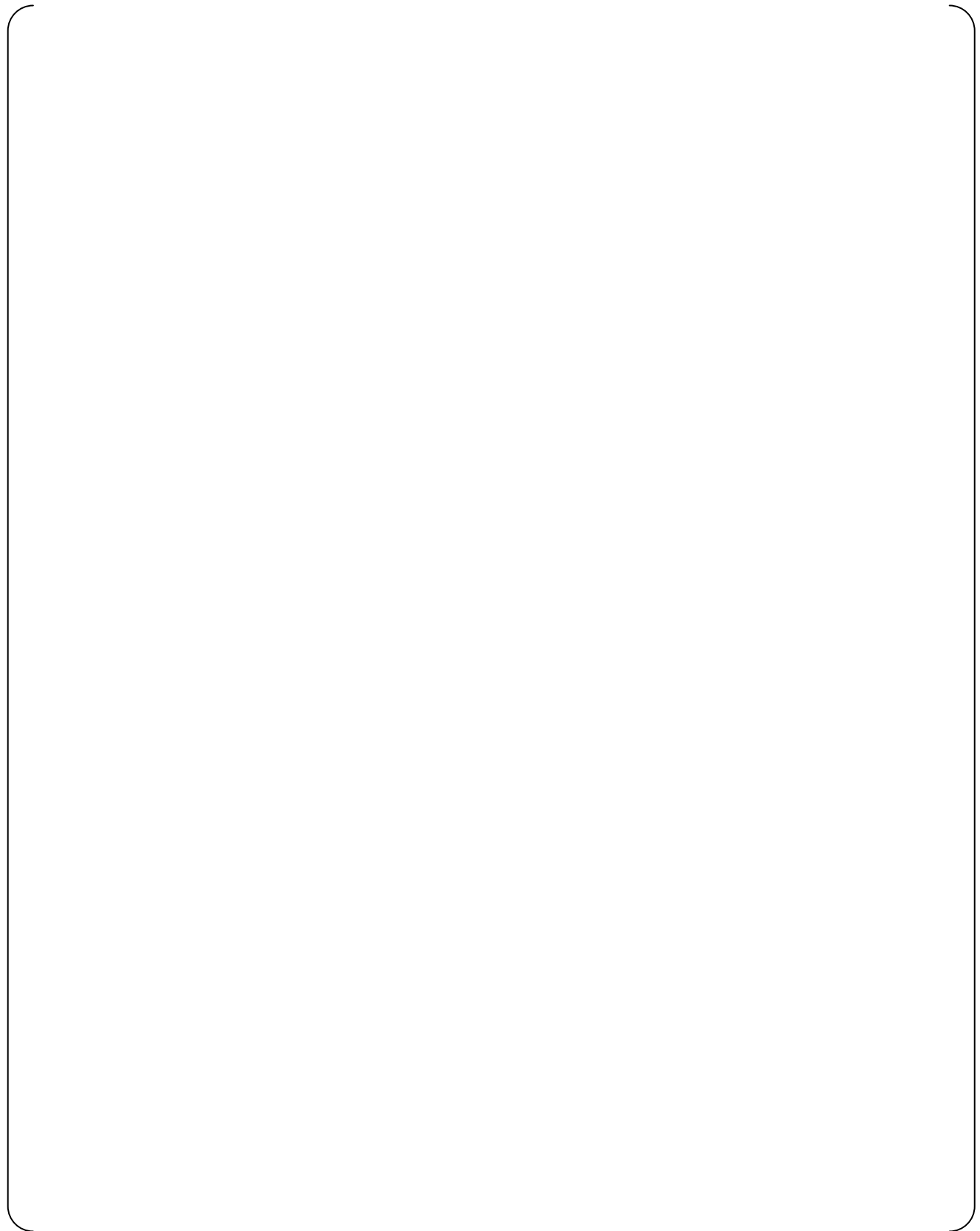


Figure 3.6-1 US-APWR Vessel Profile

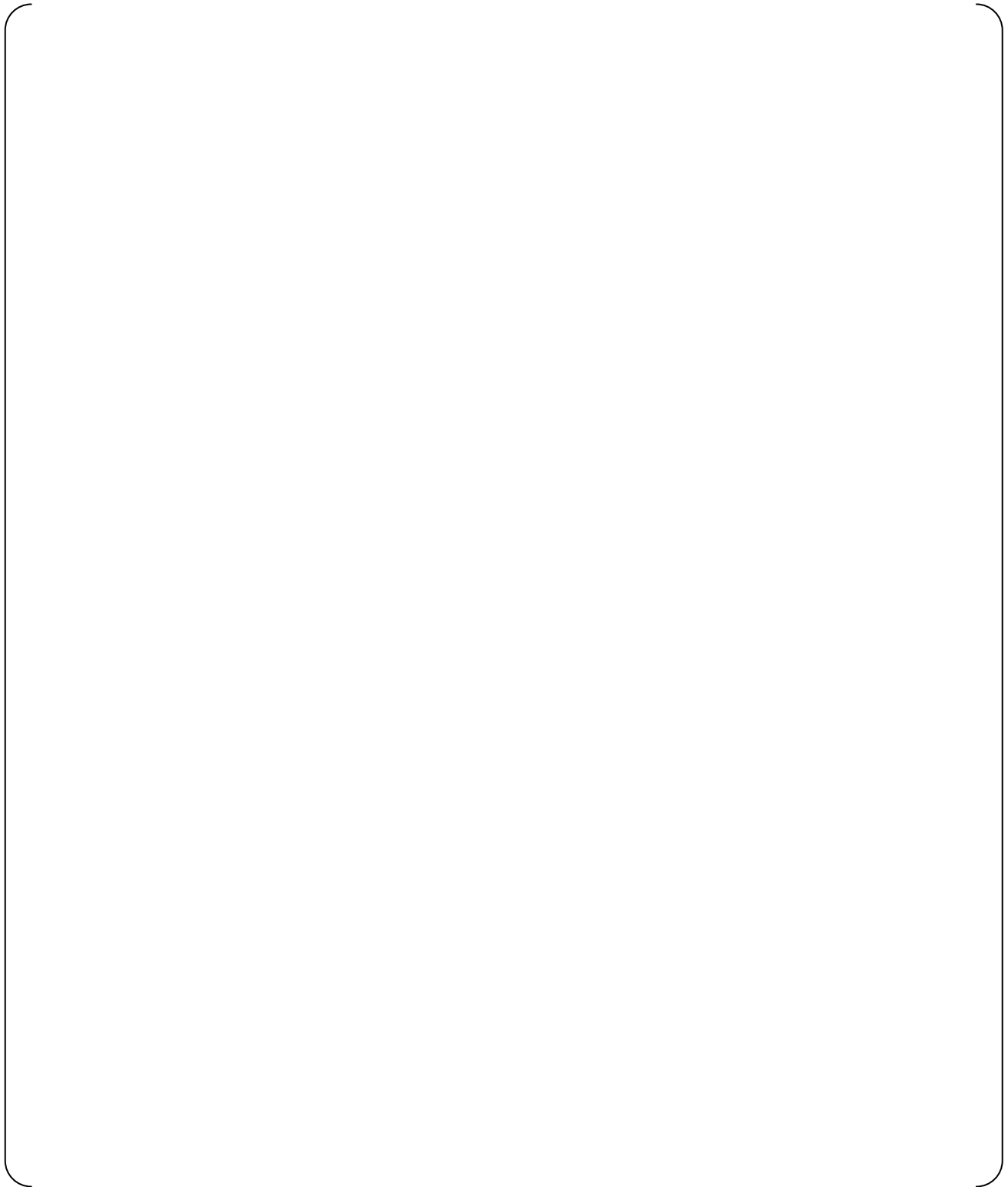


Figure 3.6-2 US-APWR Vessel Noding for Hot Assembly Under either Support Column or Open Hole (Vertical View)

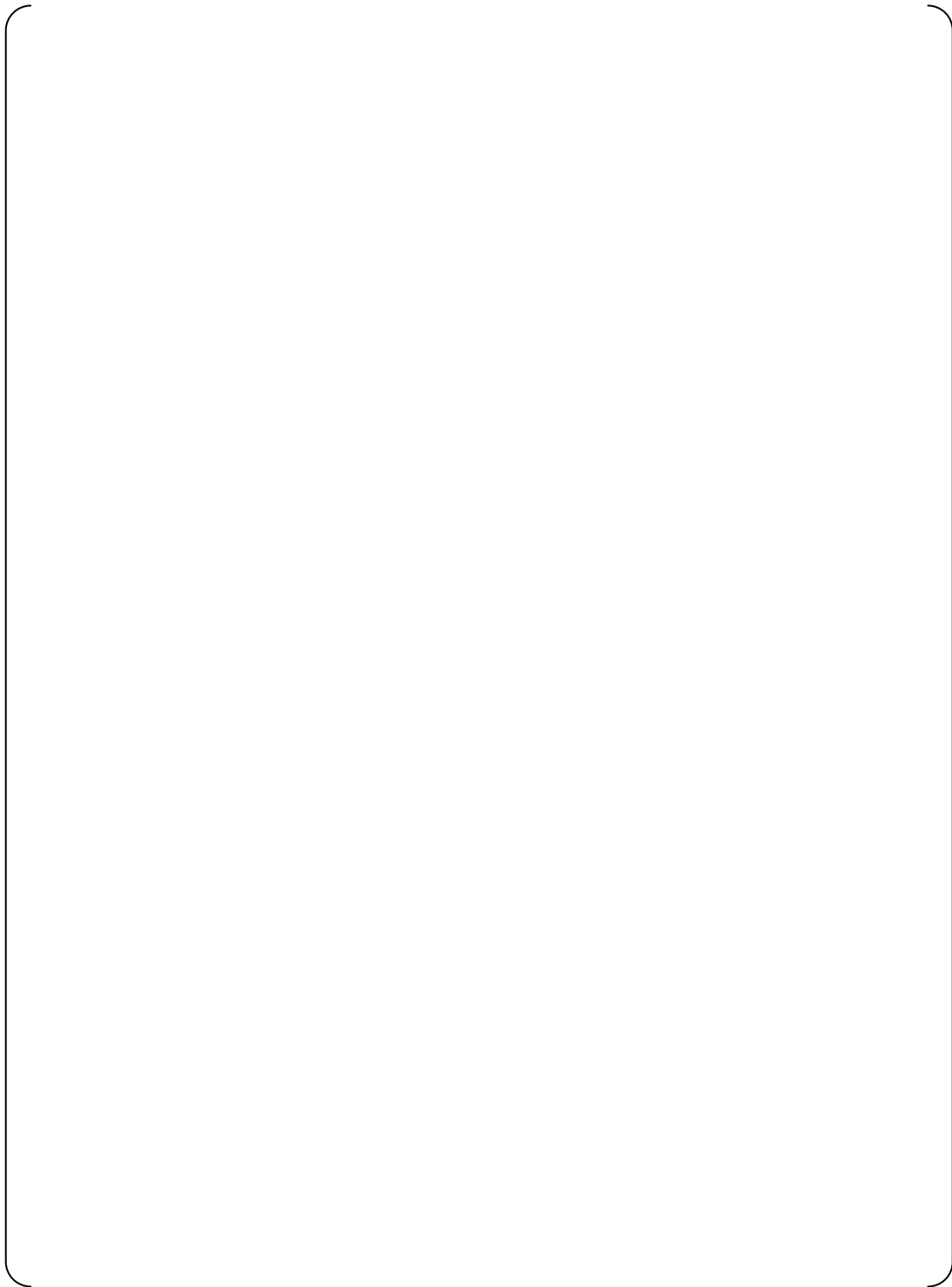


Figure 3.6-3 US-APWR Vessel Sections 1 to 2 (Horizontal View)

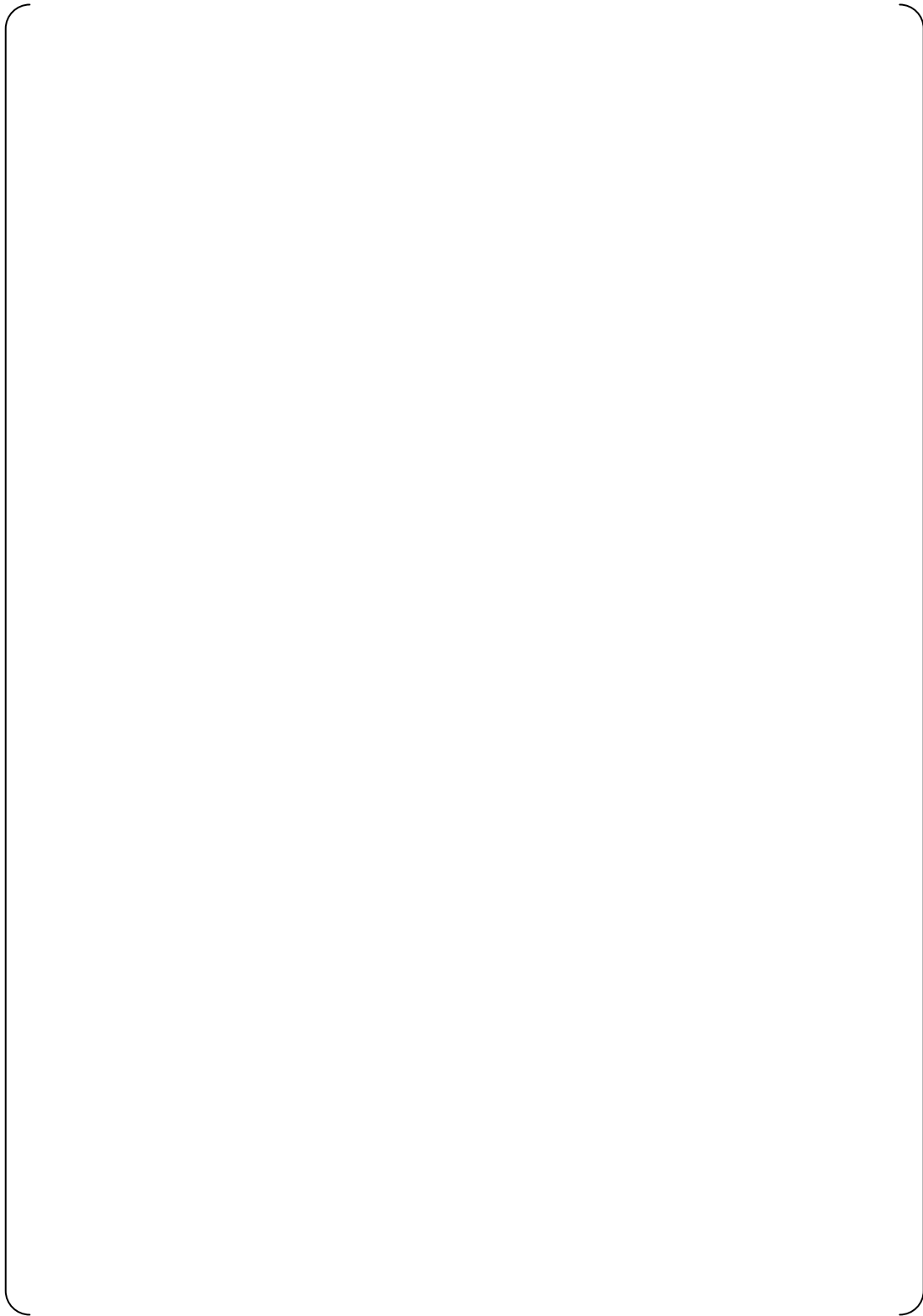


Figure 3.6-4 US-APWR Vessel Sections 3 to 4 (Horizontal View)

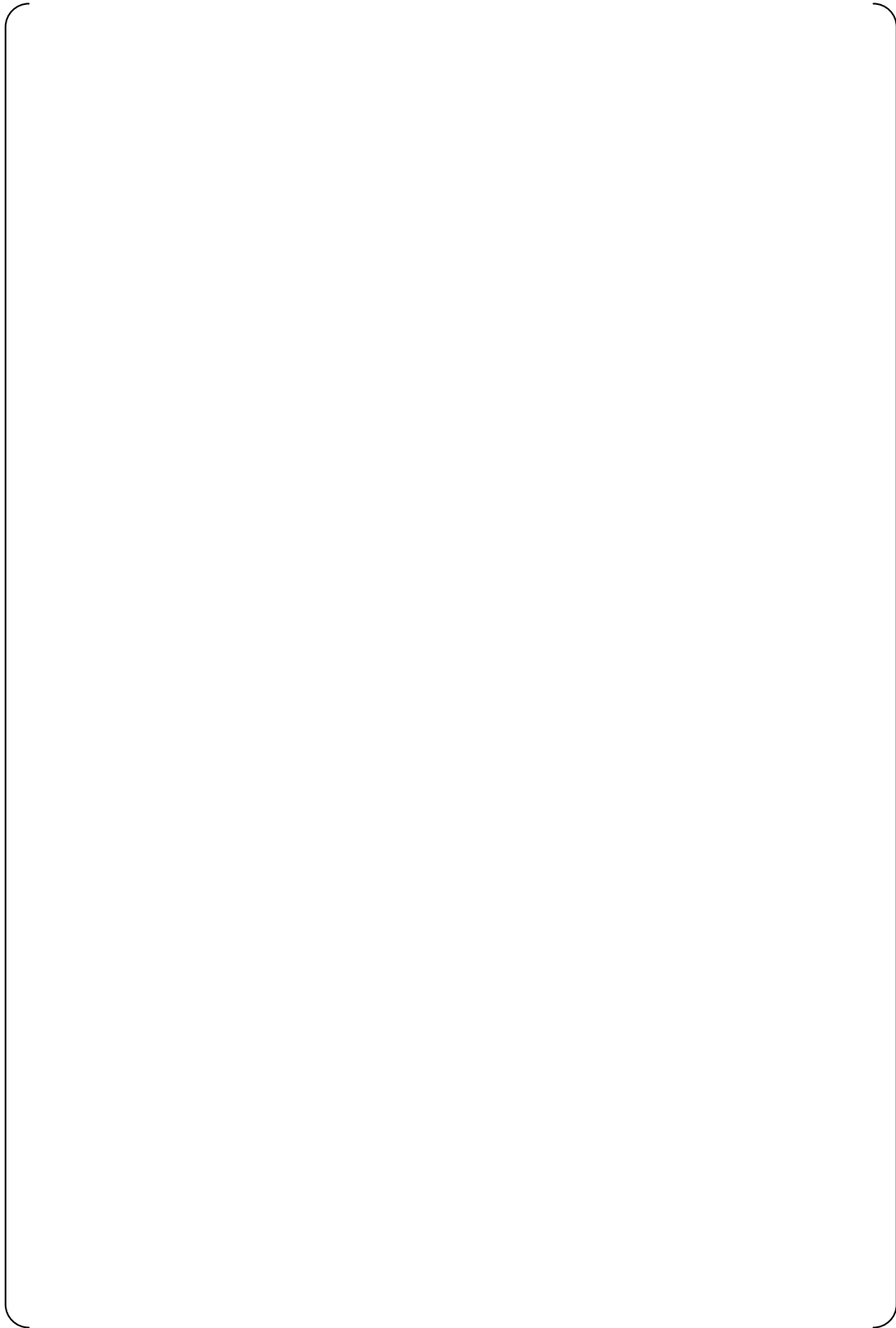


Figure 3.6-5 US-APWR Vessel Sections 5 to 6 (Horizontal View)

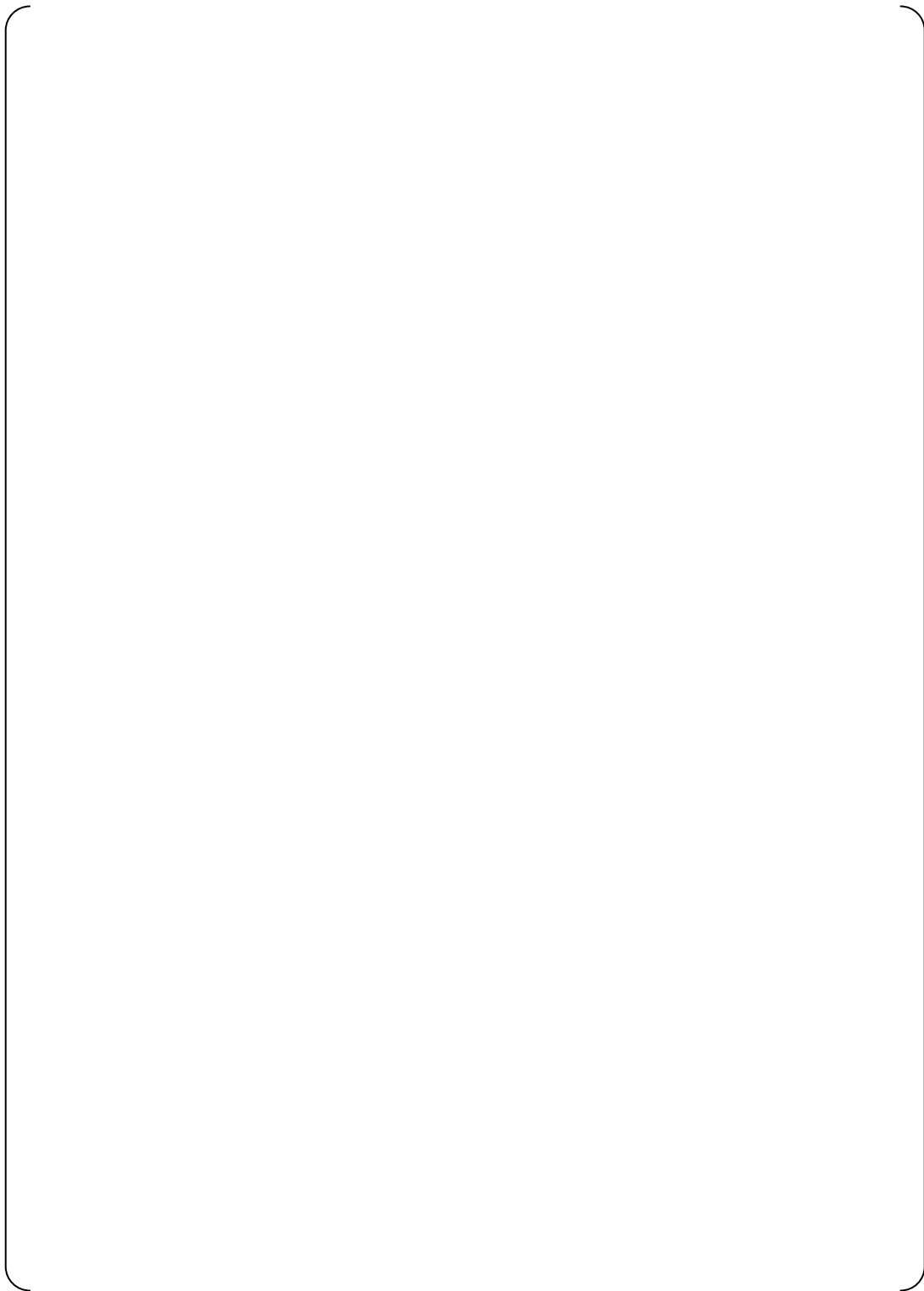


Figure 3.6-6 US-APWR Vessel Sections 7 to 8 (Horizontal View)

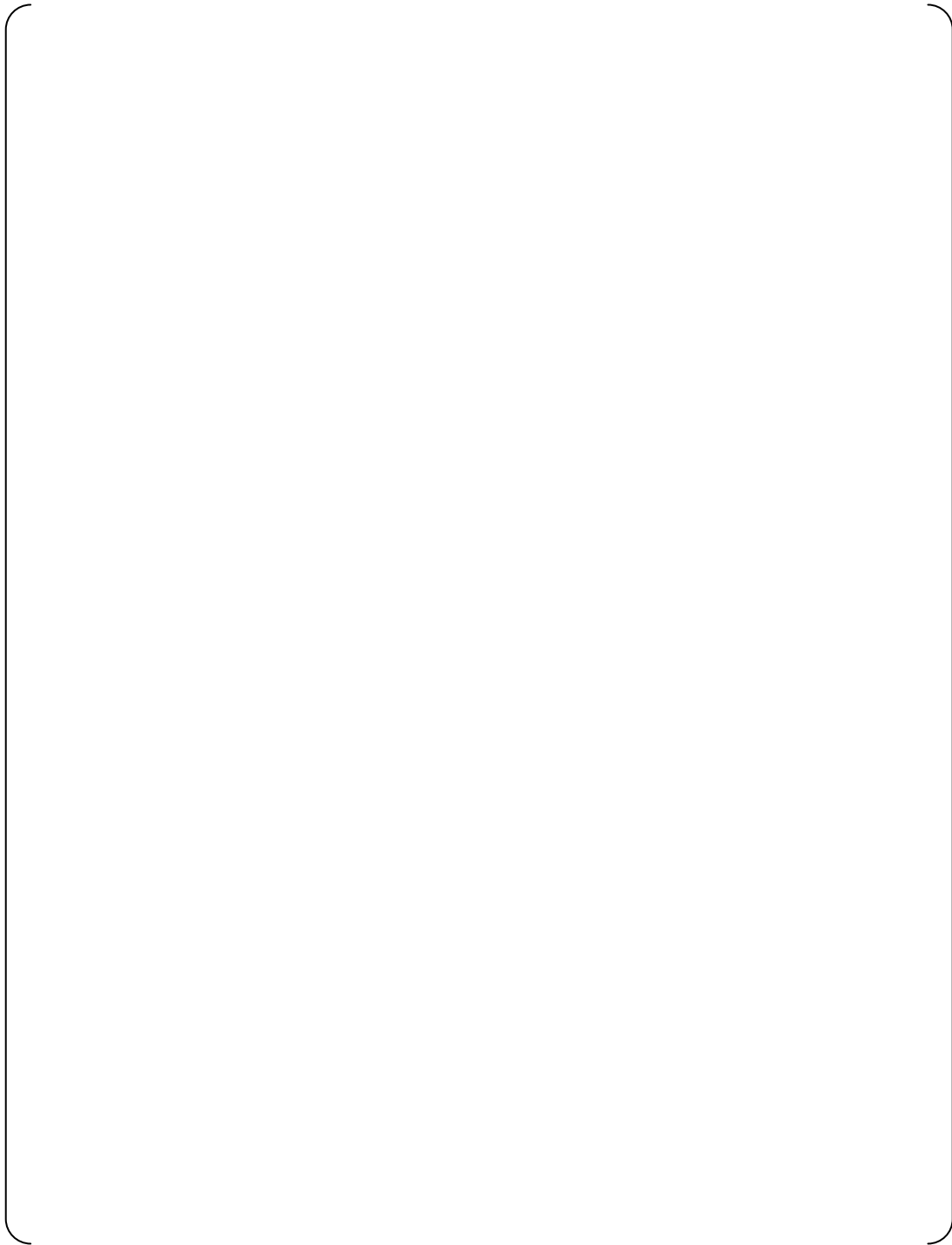


Figure 3.6-7 US-APWR Vessel Sections 9 to 10 (Horizontal View)

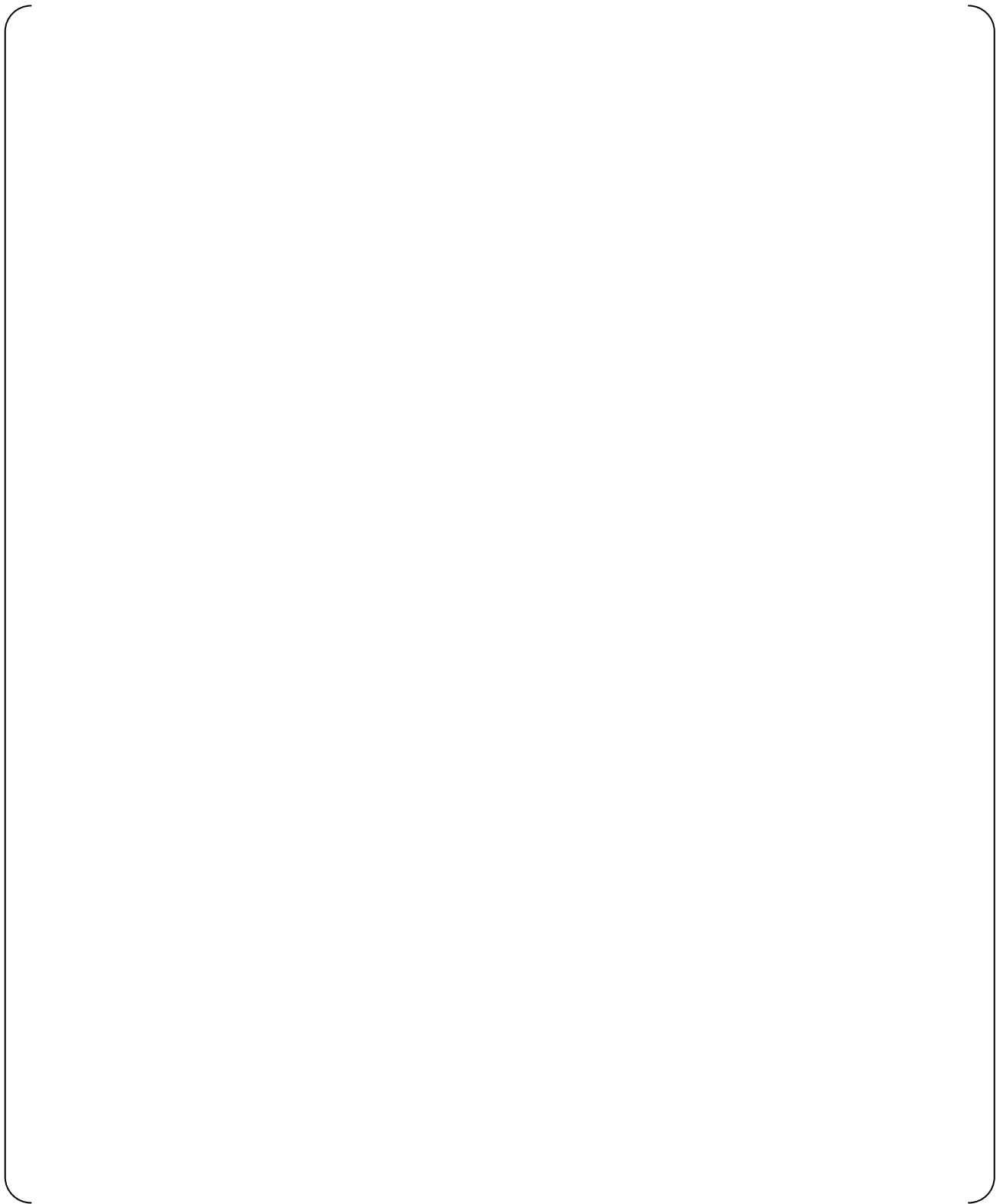


Figure 3.6-8 US-APWR WCOBRA/TRAC(M1.0) Model Vessel/Loop Layout



Figure 3.6-9 US-APWR RCP Homologous Single-phase and Two-phase Pump Head Curve



Figure 3.6-10 US-APWR RCP Homologous Single-phase and Two-phase Pump Torque Curve



Figure 3.6-11 US-APWR RCP Two- Phase Head Multiplier



Figure 3.6-12 US-APWR RCP Two- Phase Torque Multiplier



Figure 3.6-13 Sample Power Shape for US-APWR Analysis

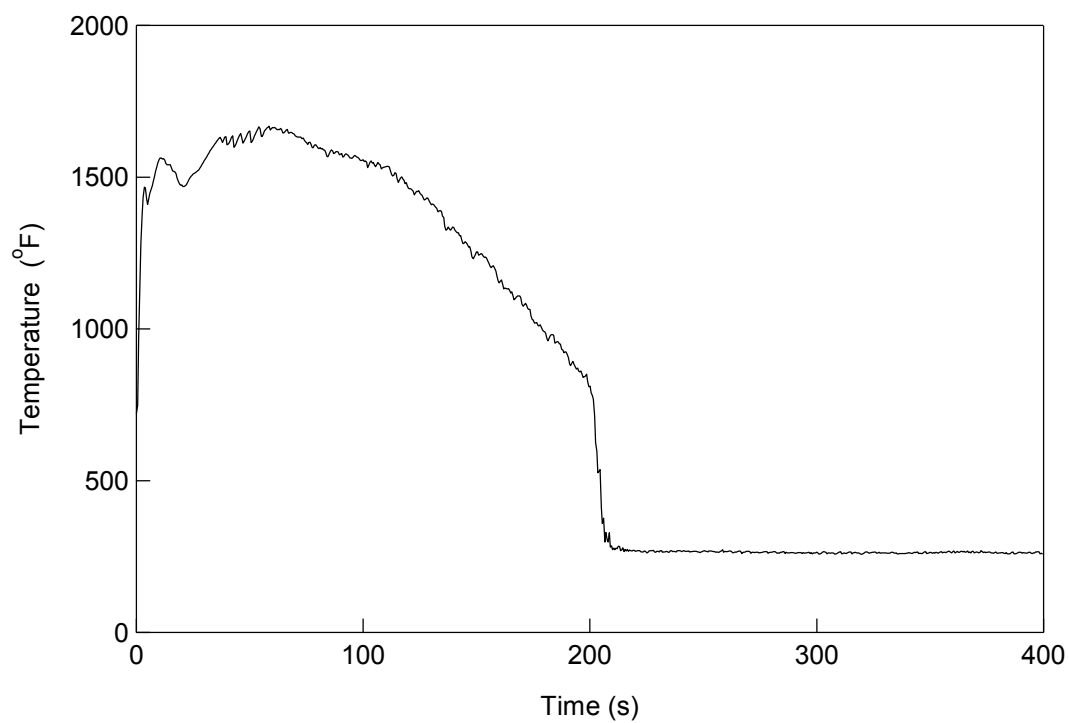


Figure 3.6-14 Peak Cladding Temperature of Hot Rod

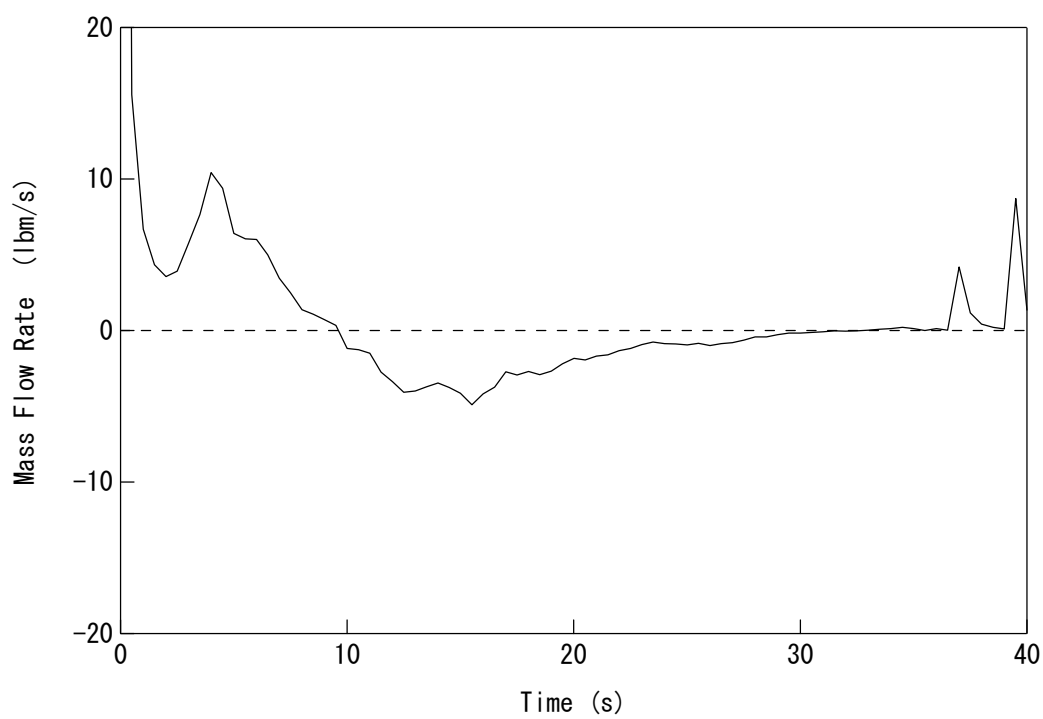


Figure 3.6-15 Hot Assembly Channel Total Flow Rate

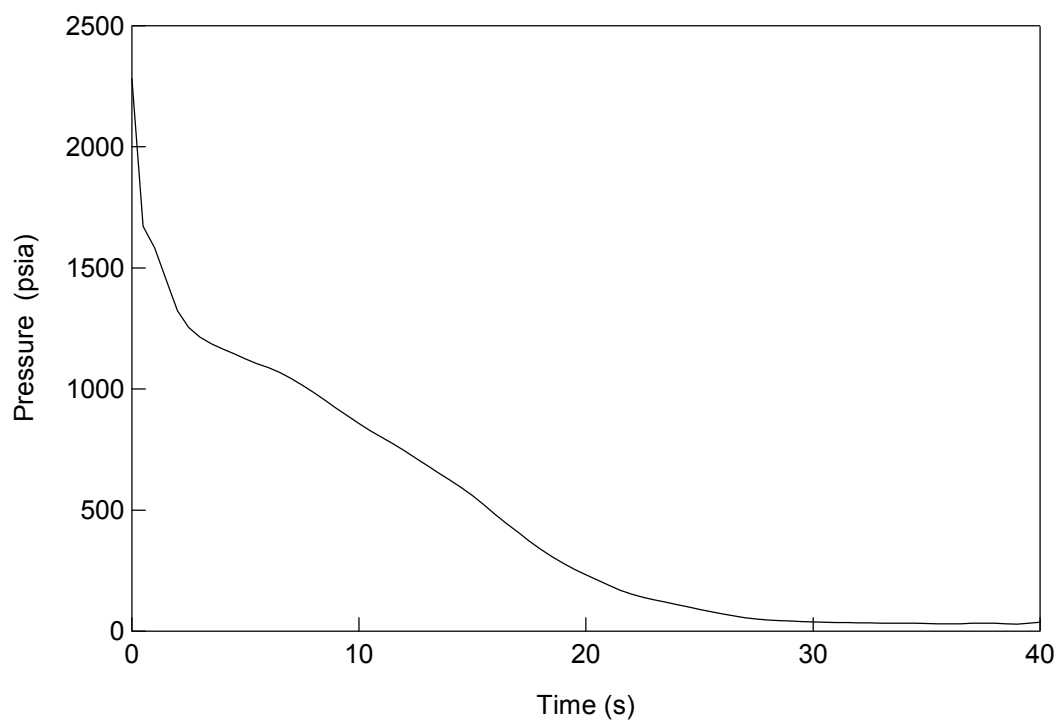
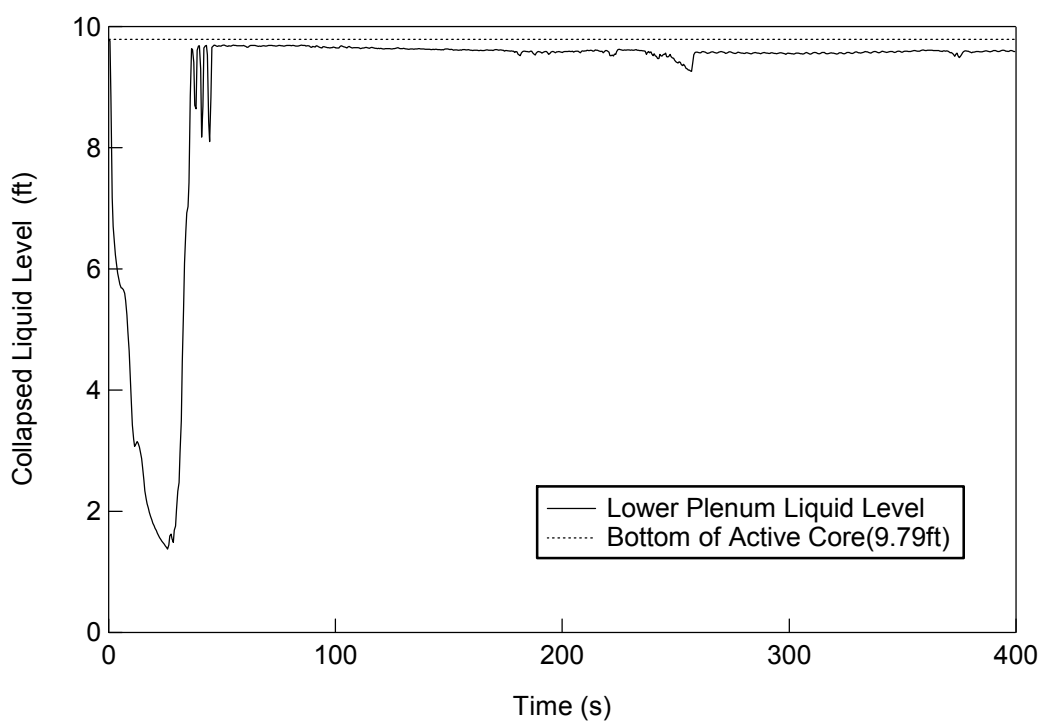


Figure 3.6-16 Core Pressure



Collapsed Liquid Level: Section 1 and 2

Figure 3.6-17 Lower Plenum Liquid Level

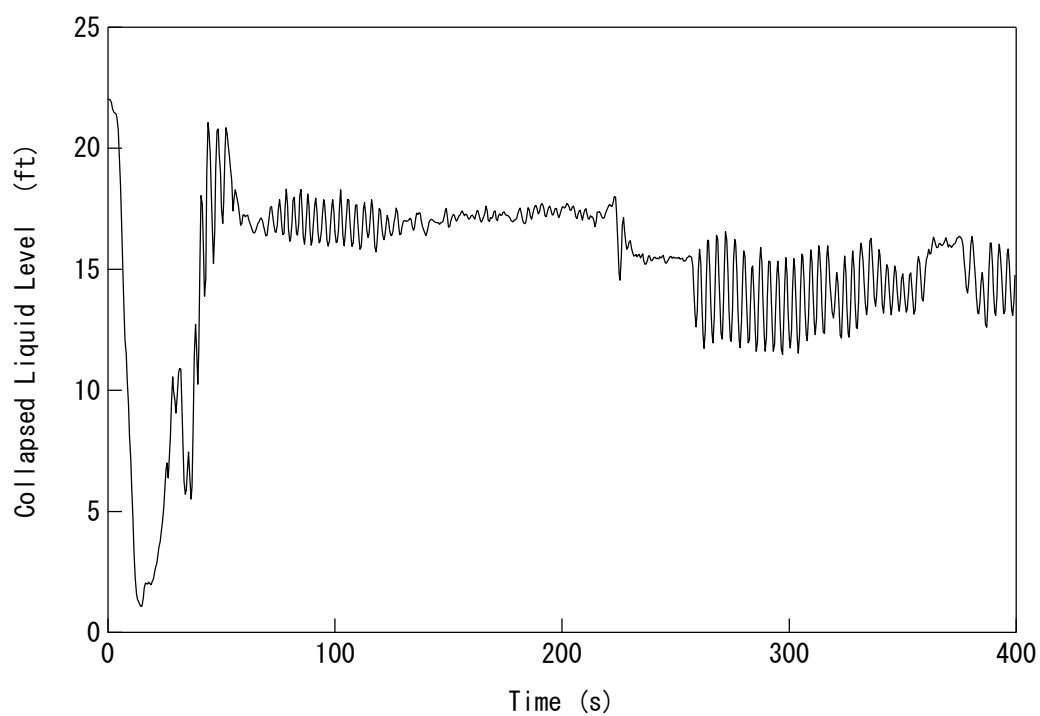


Figure 3.6-18 Downcomer Liquid Level

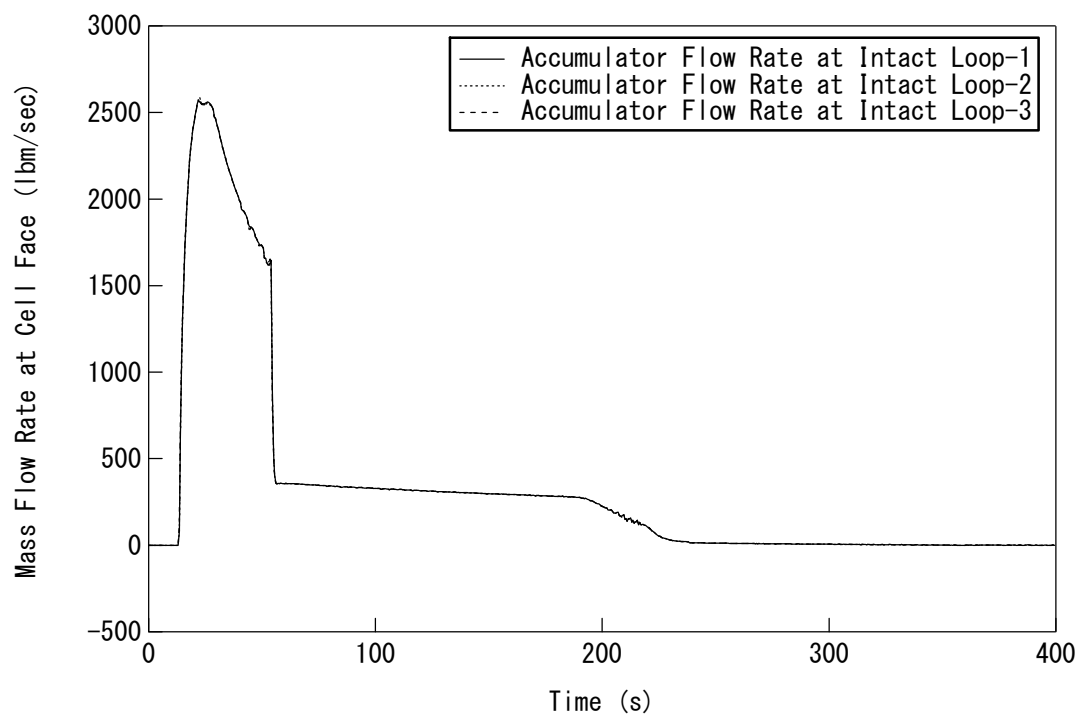


Figure 3.6-19 Accumulator Flow Rate

3.7 ASTRUM Methodology Applied to US-APWR

3.7.1 Statistical Methodology of ASTRUM

The ASTRUM methodology was approved by the NRC for the Westinghouse 2-,3- and 4-loop PWRs and the CE design PWR as WCAP-16009-P-A Rev.0 (Ref.5).

The ASTRUM methodology of using Monte Carlo sampling of the inputs for 124 runs of WCOBRA/TRAC demonstrates the conformance of the computed numerical values of peak cladding temperature, maximum local oxidation and core-wide oxidation to the acceptance criteria of 10 CFR 50.46 at the 95/95 tolerance level and, therefore, is acceptable.

The methodology for the consideration of non-parametric tolerance limits was presented by Wilks (Ref.19). The sampling is achieved by executing several calculations in which all uncertainty parameters are simultaneously ranged within their distributions. The results of the calculations are ranked based on the value assumed by the parameters in question (e.g., PCT, etc.) for each of the calculations. The maximum value is expected to bound a certain fraction of the population of the parameter with a given confidence level.

The sample size determines the cumulative probability and the confidence level. There is one parameter that should be evaluated: the sample size, N=59, is derived from the following Wilks' formula in order to obtain a 95/95 value.

$$1 - \alpha^N > \beta \quad (3.7-1)$$

α : Probability = 0.95
 β : Confidence level = 0.95
N : Sample size

The 10 CFR 50.46 rule requires that the following acceptance criteria be met in order to confirm adequate ECCS performance under LOCA transient.

- The calculated maximum fuel element cladding temperature shall not exceed 2200°F.
- The calculated total oxidation of the cladding shall nowhere exceed 0.17 times the total cladding thickness before oxidation.
- The calculated total amount of hydrogen generated from the chemical reaction of the cladding with water or steam shall not exceed 0.01 times the hypothetical amount that would be generated if all of the metal in the cladding cylinders surrounding the fuel, excluding the cladding surrounding the plenum volume, were to react.

It is therefore necessary to evaluate these three parameters. The enhancement of the order statistics was provided by Guba, et al. (Ref.20). In Guba, the sample size N required to bound a fraction b of the population for a number of outcomes, with a probability α is determined by the following formula.

$$\beta = \sum_{k=0}^{N-p} \frac{N!}{(N-k)!k!} \alpha^k (1-\alpha)^{N-k} \quad (3.7-2)$$

α : Probability
 β : Confidence level
 N : Sample size

If the evaluation parameters are written as a matrix formula arranged by sampling size N , it becomes a matrix with N rows and 3 columns as below. The rows indicate each evaluation parameter. In the following matrix, the first row, y_1 , means peak cladding temperature (PCT), the second row, y_2 , means local maximum oxidation (LMO) and the third row, y_3 , means core-wide oxidation (CWO). The rows show each sampling case N .

$$\begin{pmatrix} y_{11} & \cdot & \cdot & \cdot & y_{1N} \\ y_{21} & \cdot & \cdot & \cdot & y_{2N} \\ y_{31} & \cdot & \cdot & \cdot & y_{3N} \end{pmatrix}$$

If y_1 is arranged in ascending order, it becomes as follows. The evaluation value is assumed $y_{1\max}=U_1$. The column U_1 is a result of the case where y_1 is the highest value ($y_{1\max}$) among cases 1 to N . Neither y_2 nor y_3 are listed at these highest values.

$$\begin{pmatrix} y_{11} & \cdot & \cdot & \cdot & y_{1N} & y_{1\max} \\ y_{21} & \cdot & \cdot & \cdot & y_{2N} & y_{2N} \\ y_{31} & \cdot & \cdot & \cdot & y_{3N} & y_{3N} \end{pmatrix} \quad U_1$$

The matrix is rearranged about y_2 in ascending order excluding the y_2 corresponding to $y_1=U_1$, and it is assumed that $y_{2\max}=U_2$. There is no correlation between variables. If this procedure can be performed repeatedly, it becomes the following.

$$\begin{pmatrix} y_{11} & \cdot & \cdot & \cdot & \cdot & y_{1\max} \\ y_{21} & \cdot & \cdot & \cdot & \cdot & y_{2\max} \\ y_{31} & \cdot & \cdot & \cdot & \cdot & y_{3\max} \end{pmatrix} \quad U_3 \quad U_2 \quad U_1$$

In this case, the number of cases in which the screen line is divided is three (U_1 , U_2 and U_3).

$$\beta < 1 - \sum_{k=0}^2 N C_k \alpha^{N-k} (1-\alpha)^k = 1 - \alpha^N - N \alpha^{N-1} (1-\alpha) - \frac{N(N-1)}{2} \alpha^{N-2} (1-\alpha)^2 \quad (3.7-3)$$

From Formula 3.7-3, $N=124$ can be obtained for a probability at $\alpha=0.95$ and confidence level of $\beta=0.95$. Therefore, 124 cases are calculated, and each result of three evaluation parameters (PCT, LMO and CWO) of a maximum value will satisfy 95/95. Also, the three evaluation parameters (PCT, LMO and CWO) are independent, therefore PCT, LMO and CWO have been evaluated as conservative estimates.

3.7.2 ASTRUM Methodology Applicability to US-APWR

As discussed in 3.2, the US-APWR and conventional PWRs have very similar designs. And the only minor modifications to the ASTRUM methodology are required to reflect the improved feature of the US-APWR.

Table 3.7-1 through Table 3.7-3 show the uncertainty treatment of ASTRUM methodology for the US-APWR. In the ASTRUM methodology, the treatment of the uncertainty is divided into parameters that affect the thermal hydraulic response of RCS and a local model. The effects of parameters that affect the thermal hydraulic response of RCS are used in the WCOBRA/TRAC (M1.0) code. Local models are used in the HOTSPOT code.

As discussed in 3.6.1, flow resistances of flow damper and accumulator line are treated as uncertainties. For most of parameters, the treatment of uncertainty is the same as for the Westinghouse 3- and 4-loop plants. As a result, the same methodology of uncertainty can be used for the US-APWR.

The best-estimate methodology establishes a sampling of the distribution of PCT that could occur due to changes in plant or model variables. The input values falls under three categories:

- Plant physical description,
- Plant initial operating conditions
- Accident boundary conditions

The uncertainty treatments of local model and global model for the US-APWR are shown in Table 3.7-2 and Table 3.7-3, respectively. The uncertainty treatments of local model and global model are the same as for conventional 4-loop plant (Ref.6).

The following paragraphs describe the assumptions in the key LOCA parameters for US-APWR. The sample case input values as well as the plant operating range. For most of the parameters used in the sample plant analysis, the nominal value was assumed. For others, a bounding or conservative value was assumed.

The uncertainty associated with these parameters is taken into account for the uncertainty analysis.

3.7.2.1 Plant Physical Description

3.7.2.2 Plant Initial Operating Conditions: Reactor Power

3.7.2.3 Plant Initial Operating Conditions: Fluid Conditions

3.7.2.4 Accident Boundary Conditions

Table 3.7-1 Uncertainty Treatment for US-APWR (2/2)

Table 3.7-2 Local Model Uncertainty Treatment for US-APWR

[illegible]

Table 3.7-3 Global Model Uncertainty Treatment for US-APWR

4.0 CONCLUSIONS

This report provides an assessment of the WCOBRA/TRAC code that was approved by the NRC for the Westinghouse-design 2-,3- and 4- Loop PWRs (Ref.1, 6) , and the CE-design PWR, the AP600 (Ref.2) , and the AP1000 (Ref.3) Design Certifications with the purpose to determine the applicability and appropriateness of its use for Design Certifications of the US-APWR.

The US-APWR design features that need to be separately evaluated have been identified, as the advanced accumulator DVI and NR improved design. It can be confirmed that the WCOBRA/TRAC code has applicability to the analysis US-APWR LBLOCA transient with minor modifications for the improved features of the US-APWR. The applicability of the WCOBRA/TRAC(M1.0) code for the US-APWR was evaluated successfully based on the CSAU approach using the PIRT.

The sample calculation of the LBLOCA transient by the WCOBRA/TRAC(M1.0) code using typical input data of the US-APWR was performed to demonstrate the capability of the WCOBRA/TRAC(M1.0) code for the transient of the US-APWR.

This report also described that the ASTRUM methodology, which includes this WCOBRA/TRAC(M1.0), has the same applicability to the US-APWR because the treatment of the uncertainty in the analysis of the LBLOCA transient in the US-APWR is almost the same as conventional 4 loop PWR plants.

In conclusion, the WCOBRA/TRAC(M1.0) code and the ASTRUM methodology are acceptable to provide analysis results for the US-APWR Design Control Documents (DCD). In addition, the nodding model of the WCOBRA/TRAC(M1.0) code for the US-APWR plant is acceptable for the LOCA safety analysis calculation.

5.0 REFERENCES

- 1 Dederer, S. I., et al., 1999, "Application of Best Estimate Large Break LOCA Methodology to Westinghouse PWRs with Upper Plenum Injection," WCAP-14449-P-A, Revision 1, and WCAP-14450-NP-A, Revision 1 (Non-Proprietary).
- 2 Final Safety Evaluation Report Related to Certification of the AP600 Standard Design, NUREG-1512, August 1998.
- 3 Final Safety Evaluation Report (FSER) for the Westinghouse AP1000 Advanced Reactor Design, September 20, 2004.
- 4 T. Ogino, et al. "The Advanced Accumulator", MUAP-07001-P (R5), Mitsubishi Heavy Industries, June 2013
- 5 M.E., Nissley, et al., "Realistic Large Break LOCA Evaluation Methodology Using Automated Statistical Treatment of Uncertainty Method (ASTRUM)", WCAP-16009-P-A, January 2005
- 6 Bajorek, S. M., et al., 1998, "Code Qualification Document for Best Estimate LOCA Analysis," WCAP-12945-P-A, Volume 1, Revision 2, and Volumes 2 through 5, Revision 1, and WCAP-14747 (Non-Proprietary).
- 7 Wilson & Boyack, 1998 G.E. Wilson and B.E. Boyack, "The Role of the PIRT Process in Experiments, Code Development and Code Applications Associated with Reactor Safety Analysis," Nucl. Eng. Des. 186 (November 1998), pp. 23–37
- 8 Boyack, B., et al., "Quantifying Reactor Safety Margins: Application of Code Scaling Applicability, and Uncertainty (CSAU) Evaluation Methodology to a Large Break, Loss of Coolant Accident," NUREG/CR-5249, 1989
- 9 "Compendium of ECCS Research for Realistic LOCA Analysis," 1987, NUREG-1230.
- 10 "Measurement Uncertainty", ANSI/ASME PTC 19.1, 1985.
- 11 Bjomard, T. A. & Griffith, P., 1977, "PWR Blowdown Heat Transfer," Thermal and Hydraulic Aspects of Nuclear Reactor Safety, ASME, New York, Vol. 1, pp. 17-41.
- 12 N. MURAKAMI, et al., "Mitsubishi Fuel Design Criteria and Methodology", MUAP-07008-P-A(R2), Mitsubishi Heavy Industries, 2013
- 13 "GOTHIC Containment Analysis Package User Manual, Version 7.2a(QA)," NAI 8907-02 Rev 17, January 2006.
- 14 "GOTHIC Containment Analysis Package Technical Manual, Version 7.2a(QA)," NAI 8907-06 Rev 16, January 2006.
- 15 "GOTHIC Containment Analysis Package Qualification Report, Version 7.2a(QA)," NAI 8907-09 Rev 9, January 2006.
- 16 Westinghouse Research Report 75-7E9-CORL-R1, "Air/Water Mixed Flow Testing of The WEMD 93A Model Reactor Coolant Pump," February 1975.
- 17 Bordelon, F. M., et al., 1974, "SATAN VI Program: Comprehensive Space-Time Dependent Analysis of Loss-of-Coolant", WCAP-8302.
- 18 STANDARD REVIEW PLAN, NUREG-0800, "6.2.1.5 MINIMUM CONTAINMENT PRESSURE ANALYSIS FOR EMERGENCY CORE COOLING SYSTEM PERFORMANCE CAPABILITY STUDIES"
- 19 Wilks, S. S., 1941, "Determination of Sample Sizes for Setting Tolerance Limits," The Annals of Mathematical Statistics, Vol.12, pp. 91-96.
- 20 Guba, A., Makai, M., Lenard, P., 2003, "Statistical Aspects of Best Estimate Method-I," Reliability Engineering and System Safety, Vol. 80, 217-232.
- 21 Nagai, et al. "CFD Analysis for Advanced Accumulator," MUAP-09025(R3), Mitsubishi Heavy Industries, June 2013
- 22 United States – Advanced Pressurized Water Reactor Advanced Topical Report Safety Evaluation for Topical Report MUAP-07001-P, Revision 5, "The Advanced Accumulator", 2013.

Appendix A Thermal Properties of Nuclear Fuel Rods

A-1 Fuel Thermal Conductivity

The US-APWR fuel type (UO₂ pellet, 17x17 array, ZIRLO™ cladding) is the same as that used for conventional Westinghouse PWRs. Therefore, the fuel rod modeling of WCOBRA/TRAC(M1.0) for the US-APWR in the Large Break LOCA transient is identical to that used by Westinghouse for 17x17 fuel assemblies with ZIRLO™ cladding which has been reviewed and approved by the NRC (Ref. A-1).

The WCOBRA/TRAC code already incorporates the thermal properties of nuclear fuel. The fuel initial temperature and uncertainty are calculated by the fuel design code. Since the stored energy of high burn-up fuel is affected when taking into account the thermal conductivity degradation with burn-up, it is preferable to use a model that has the thermal conductivity degradation with burn-up. Therefore, fuel thermal conductivity is incorporated using the same model as in Mitsubishi's FINE fuel design code (Ref. A-2), which is shown below.

Uncertainty of the fuel thermal conductivity has already been partially considered in the stored energy uncertainty in ASTRUM. The same treatment of the stored energy uncertainty in the ASTRUM methodology can be applied to the US-APWR fuel.

The thermal conductivity of 95% TD UO₂ fuel is determined by the following expression, which is derived from Mitsubishi's fuel design code. It takes into consideration the degradation effect with burn-up (Ref. A-3).

$$k_{UO_2 95} = \frac{1}{A + \beta \cdot BU + B \cdot T} + C \cdot T^3$$

$k_{UO_2 95}$: Thermal conductivity for 95% TD fuel (W/cm-K)
BU	: Burn-up (MWd/kgUO ₂)
T	: Temperature (°C)
A	=11.8
B	=0.0238
C	=8.775x10 ⁻¹³
β	=0.35

Correction for density is based on Bakker's equation (Ref. A-4).

$$k_{UO_2} = k_{UO_2 95} \left(\frac{f_{TD}}{0.95} \right)^{1.7}$$

k_{UO_2}	: Thermal conductivity (W/cm-K)
f_{TD}	: Fraction to theoretical density

These functions are coded into WCOBRA/TRAC as a new routine, TCONF. The thermal conductivity is calculated in subroutine SSTEMP and TEMP. Subroutine TCONF is called from there.

A-2 References

- A-1. Davidson, S. L. and Nuhfer, D.L., "VANTAGE+ Fuel Assembly Reference Core Report", WCAP-12610, June 1990 (PROPRIETARY)
- A-2 N. MURAKAMI, et al., "Mitsubishi Fuel Design Criteria and Methodology", MUAP-07008-P-A Rev.2, Mitsubishi Heavy Industries, 2013
- A-3. Wiesenack, W., "Assessment of UO₂ Conductivity Degradation Based on In-Pile Temperature Data", ANS 1997 International Topical Meeting on LWR Fuel Performance, March 1997, Portland, Oregon
- A-4. Bakker, K. et al., "Determination of a Porosity Correction Factor for the Thermal Conductivity of Irradiated UO₂ Fuel by Means of the Finite Element Method", Journal of Nuclear Materials, 226, 1995, pp.128-143

Appendix B Advanced Accumulator Model Built into WCOBRA/TRAC

B-1 Advanced Accumulator Model

B-2 References

- B-1 Bajorek, S. M., et al., 1998, "Code Qualification Document for Best Estimate LOCA Analysis," WCAP-12945-P-A, Volume 1, Revision 2.
- B-2 "COBRA/TRAC - A Thermal-Hydraulics Code for Transient Analysis of Nuclear Reactor Vessels and Primary Coolant Systems, Programmers' Manual", NUREG/CR-3046, PNL-4385, vol.5 R4, Mar. (1983).
- B-3 T. Ogino, et al. "The Advanced Accumulator", MUAP-07001-P (R5), Mitsubishi Heavy Industries, June 2013



Figure B-1 ACC Nodalization

Figure B-2 Flow Resistance Calculation Diagram in Subroutine ACCUM1

Appendix C Resolution of Requests for Additional Information

INTRODUCTION

Many Requests for Additional Information (RAI) were generated during the USNRC review of MUAP-07011-P. The majority of the RAIs were issued formally, as letters from the USNRC to MHI. Late in the licensing process, additional RAI were provided on a more informal basis at an audit to MUAP-07011-P.

First set of RAIs through third set of RAIs were issued for both public and non-public use. Forth through seventh set of RAIs were for non public use only.

Tables C-1 through C-3 guide to the location where all RAIs were resolved.

Table C-1 First Set of Requests for Additional Information ^(Ref.RAI-1)

Question	Topic	Reference	Note
1	Software Quality Assurance	Ref.1	
2.1	Plant Design and Features	Ref.1	
2.2	Plant Design and Features	Ref.1	
3.1	General Description	Ref.1	Followed by Q1.1 in 2 nd RAIs
3.2	PIRT	Ref.1	
3.3	PIRT	Ref.1	Followed by Q1.2 in 2 nd RAIs
3.4	PIRT	Ref.1	
3.5	PIRT	Ref.1	
3.6	PIRT	Ref.1	Followed by Q1.3 in 2 nd RAIs
3.7	PIRT	Ref.1	Followed by Q1.4 in 2 nd RAIs
3.8	PIRT	Ref.1	
3.9	PIRT	Ref.1	
3.10	PIRT	Ref.2	Followed by Q1.5 in 2 nd RAIs
3.11	PIRT	Ref.2	
3.12.1	Advanced Accumulator	Ref.1	
3.12.2	Advanced Accumulator	Ref.1	
3.12.3	Advanced Accumulator	Ref.1	Followed by Q1.6 in 2 nd RAIs
3.12.4	Advanced Accumulator	Ref.1	
3.12.5	Advanced Accumulator	Ref.1	
3.12.6	Advanced Accumulator	Ref.1	Followed by Q1.7 in 2 nd RAIs
3.12.7	Advanced Accumulator	Ref.1	
3.12.8	Advanced Accumulator	Ref.1	
3.12.9	Advanced Accumulator	Ref.1	Followed by Q1.8 in 2 nd RAIs
3.12.10	Advanced Accumulator	Ref.1	Followed by Q1.9 in 2 nd RAIs
3.12.11	Advanced Accumulator	Ref.1	
3.12.12	Advanced Accumulator	Ref.1	
3.12.13	Advanced Accumulator	Ref.1	
3.12.14	Advanced Accumulator	Ref.1	
3.12.15	Advanced Accumulator	Ref.1	
3.12.16	Advanced Accumulator	Ref.2	
3.12.17	Advanced Accumulator	Ref.1	
3.13.1	Neutron Reflector	Ref.1	
3.13.2	Neutron Reflector	Ref.2	Followed by Q1.10 in 2 nd RAIs
3.13.3	Neutron Reflector	Ref.1	
3.13.4	Neutron Reflector	Ref.2	
3.14.1	Sample Plant Analysis.	Ref.1	
3.14.2	Sample Plant Analysis.	Ref.1	
3.14.3	Sample Plant Analysis.	Ref.1	
3.14.4	Sample Plant Analysis.	Ref.1	
3.14.5	Sample Plant Analysis.	Ref.2	
3.15.1	Sample Plant Analysis.	Ref.1	Followed by Q1.2 and Q1.11 in 2 nd RAIs
3.15.2	Sample Plant Analysis.	Ref.1	
3.16.1	Uncertainty Treatment	Ref.1	
3.16.2	Uncertainty Treatment	Ref.1	

3.16.3	Uncertainty Treatment	Ref.1	
3.16.4	Uncertainty Treatment	Ref.1	Followed by Q1.12 in 2 nd RAIs

Table C-2 Second Set of Requests for Additional Information (Ref.RAI-2)

Question	Topic	Reference	Note
1.1	PIRT	Ref.3	Follow-Up To Q 3.1 in 1 st RAIs
1.2	PIRT , Sample Plant Analysis	Ref.3	Follow-Up To Q 3.3 and Q 3.15.1 in 1 st RAIs
1.3	PIRT	Ref.3	Follow-Up To Q 3.6 in 1 st RAIs
1.4	PIRT	Ref.3	Follow-Up To Q 3.7 in 1 st RAIs
1.5	PIRT	Ref.3	Follow-Up To Q 3.10 in 1 st RAIs
1.6	Advanced Accumulator	Ref.3	Follow-Up To Q 3.12.3 in 1 st RAIs
1.7	Advanced Accumulator	Ref.3	Follow-Up To Q 3.12.6 in 1 st RAIs
1.8	Advanced Accumulator	Ref.3	Follow-Up To Q 3.12.9 in 1 st RAIs
1.9	Advanced Accumulator	Ref.3	Follow-Up To Q 3.12.10 in 1 st RAIs
1.10	Neutron Reflector	Ref.3	Follow-Up To Q 3.13.2 in 1 st RAIs
1.11	Sample Plant Analysis	Ref.3	Follow-Up To Q 3.15.1 in 1 st RAIs
1.12	Uncertainty Treatment	Ref.3	Follow-Up To Q 3.16.4 in 1 st RAIs
1	Neutron Reflector	Ref.3	
2	Neutron Reflector	Ref.3	
3	Neutron Reflector	Ref.3	
4	Neutron Reflector	Ref.3	
5	Neutron Reflector	Ref.3	
6	Neutron Reflector	Ref.3	
7	Neutron Reflector	Ref.3	
8	Neutron Reflector	Ref.3	
9	Advanced Accumulator	Ref.3	
10	Advanced Accumulator	Ref.3	
11	Advanced Accumulator	Ref.3	
12	Advanced Accumulator	Ref.3	
13	Advanced Accumulator	Ref.3	
14	Advanced Accumulator	Ref.3	
15	Advanced Accumulator	Ref.3	
16	Advanced Accumulator	Ref.3	
17	Advanced Accumulator	Ref.3	
18	Advanced Accumulator	Ref.3	
19	Safety Injection	Ref.3	
20	Direct Vessel Injection	Ref.3	
21	Direct Vessel Injection	Ref.3	
22	General Description	Ref.3	
23	General Description	Ref.3	
24	General Description	Ref.3	

25	PIRT	Ref.3	
26	Sample Plant Analysis	Ref.3	
27	Sample Plant Analysis	Ref.3	
28	Sample Plant Analysis	Ref.3	
29	Sample Plant Analysis	Ref.3	
30	Uncertainty Treatment	Ref.3	
31	Uncertainty Treatment	Ref.3	
32	General Description	Ref.3	
33	Nodalization	Ref.3	
34	Fuel Model	Ref.3	
35	PIRT	Deleted	Revised by Ref.5 after an audit
36	Uncertainty Treatment	Ref.3	
37	Documentation for Frozen Code	Ref.3	Response was supported by electric materials
38	Noding Sensitivity	Ref.3	
39	Scaling	Ref.3	
40	Uncertainty Treatment	Ref.3	
41	Sample Plant Analysis	Ref.3	Followed by RAI-4 in 4 th RAIs
42	Scaling	Ref.3	
43	Fuel Model	Ref.3	
44	Fuel Model	Ref.3	
45	ASTRUM Running Process	Ref.3	Followed by RAI-2 in 4 th RAIs Response was supported by electric materials
46	Loop Flow Closure	Deleted	The response was withdrawn, and revised in the response to 4 th set of RAIs
47	Random Sampling	Ref.3	

Table C-3 Third Set of Requests for Additional Information (Ref.RAI-3)

Question	Topic	Reference	Note
1	Explanation and Data for Blowdown PCT	Ref.4	Response was supported by electric materials

References for Table C-1 through C-3

1. Letter, Yoshiki Ogata (MHI) to Document Control Desk (USNRC), “ MHI’s Partial Responses to the NRC’s Requests for Additional Information on Topical Report MUAP-07011-P (R0) “Large Break LOCA Code Applicability Report for US-APWR” ”, UAP-HF-09173, April 24, 2009.
2. Letter, Yoshiki Ogata (MHI) to Document Control Desk (USNRC), “ MHI’s 2nd Part Responses to the NRC’s Requests for Additional Information on Topical Report MUAP-07011-P (R0) “Large Break LOCA Code Applicability Report for US-APWR” ”, UAP-HF-09252, May 21, 2009.
3. Letter, Atsushi Kumaki for Yoshiki Ogata (MHI) to Document Control Desk (USNRC), “ MHI’s Responses to the NRC’s Requests for 2nd Set Additional Information on US-APWR Topical Report “LARGE BREAK LOCA CODE APPLICABILITY REPORT, MUAP- 07011-P (R0)” ”, UAP-HF-10130, May 24, 2010.
4. Letter, Yoshiki Ogata (MHI) to Document Control Desk (USNRC), “ MHI’s Response to the NRC’s Request for 3rd Set of Additional Information on US-APWR Topical Report “LARGE BREAK LOCA CODE APPLICABILITY REPORT, MUAP- 07011-P (R0)” ”, UAP-HF-10228, August 6, 2010.
5. Letter, Yoshiki Ogata (MHI) to Document Control Desk (USNRC), “ Transmittal of Revised Responses to Three(3) Questions in 2nd set RAIs and 4th set RAIs on US-APWR Topical Report “LARGE BREAK LOCA CODE APPLICABILITY REPORT, MUAP- 07011-P (R0)” ”, UAP-HF-11128, April 28, 2011

Generated RAI for LARGE BREAK LOCA CODE APPLICABILITY REPORT FOR US-APWR, MUAP-07011**RAI-1. 1st set of RAIs (NONPUBLIC PROP., PUBLIC PROP.)**

"REQUEST FOR ADDITIONAL INFORMATION MUAP-07011 REV2", US-APWR TOPICAL REPORT Large Break LOCA Code Applicability MUAP-07011-P(R0), dated March 25, 2009.

RAI-2. 2nd set of RAIs (NONPUBLIC PROP., PUBLIC PROP.)

"REQUEST FOR ADDITIONAL INFORMATION US-APWR TOPICAL REPORT: LARGE BREAK LOCA CODE APPLICABILITY REPORT, MUAP- 07011-P (R0), dated March 15, 2010.

RAI-3. 3rd set of RAIs (NONPUBLIC PROP., PUBLIC PROP.)

"REQUEST FOR ADDITIONAL INFORMATION US-APWR Topical Report: LARGE BREAK LOCA Code Applicability, MUAP- 07011-P (R0), dated June 17, 2010.

RAI-4. 4th set of RAIs (NONPUBLIC PROP.)

"REQUEST FOR ADDITIONAL INFORMATION US-APWR Topical Report: LARGE BREAK LOCA Code Applicability, MUAP- 07011-P (R0), dated August 8, 2010.

RAI-5. 5th set of RAIs (NONPUBLIC PROP.)

REQUEST FOR ADDITIONAL INFORMATION US-APWR Topical Report: LARGE BREAK LOCA Code Applicability, MUAP- 07011-P (R0), dated November 17, 2010.

RAI-6. 6th set of RAIs (NONPUBLIC PROP.)

REQUEST FOR ADDITIONAL INFORMATION US-APWR Topical Report: LARGE BREAK LOCA Code Applicability, MUAP- 07011-P (R0), dated April 15, 2011.

RAI-7. Audit Item to MUAP-07011-P (NONPUBLIC PROP.)

AUDIT PLAN FOR THE UNITED STATES - ADVANCED PRESSURIZED WATER REACTOR DESIGN CERTIFICATION LBLOCA Topical Report MUAP-07011-P (Rev. 0) April 5 - 6, 2011

RAI-8. 7th set of RAIs (NONPUBLIC PROP.)

"REQUEST FOR ADDITIONAL INFORMATION US-APWR Topical Report: LARGE BREAK LOCA Code Applicability, MUAP- 07011-P (R0), dated October 31, 2011.

RESPONSES
to
THE FIRST SET OF REQUESTS FOR ADDITIONAL INFORMATION
for
LARGE BREAK LOCA CODE APPLICABILITY REPORT FOR US-APWR
MUAP-07011-P

(Submitted by UAP-HF-09173, UAP-HF-09252)

(Submitted by UAP-HF-09173)

INTRODUCTION

This document presents MHI's partial responses to the NRC's requests for additional information (RAI) on Topical Report MUAP-07011-P (R0) "Large Break LOCA Code Applicability Report for US-APWR" dated March 25, 2009.

This document provides the 40 items requested in this RAI. The remaining responses will be transmitted to the NRC by separate correspondence, no later than May 23, 2009.

REQUEST 1

CSAU-Step-4 clearly required identification of frozen code and where it is derived from. CSAU-Step-5 requires proper documentation with model described with references, and assessment of their range of applicability to US-APWR. There should be a clearly defined version of COBRA-TRAC that was approved by USNRC and is the basis of COBRA-TRAC (M1.0). A list of the changes, made from the last approved version, should be provided. How have these changes been validated?

RESPONSE

The code version that the WCOBRA/TRAC (M1.0) code is based on is WCOBRA/TRAC MOD7A Revision 6. The WCOBRA/TRAC MOD7A Revision 6 code has been approved by NRC for Westinghouse design 2/3/4 Loop PWRs and CE design PWR (Ref.1-1).

The following changes from the approved version of WCOBRA/TRAC.

1. Advanced accumulator model

The empirical correlations are incorporated into the WCOBRA/TRAC code to simulate advanced accumulator characteristics.

The empirical correlations are validated in advanced accumulator topical report (Ref.1-2). Therefore, only verification of model implementation was performed using full height 1/2-scaled test data.

3. Fuel thermal conductivity

Fuel thermal conductivity is incorporated using the same model as in Mitsubishi's FINE fuel design code (Ref.1-4).

It is incorporation of the fuel thermal properties, therefore, only verification of model implementation was performed.

Reference

1-1 M.E., Nissley, et al., "Realistic Large Break LOCA Evaluation Methodology Using Automated Statistical Treatment of Uncertainty Method (ASTRUM)", WCAP-16009-P-A, January 2005

1-2 T. Ogino, et al. "The Advanced Accumulator", MUAP-07001-P (R1), Mitsubishi Heavy Industries, 2007

1-3 Yeon-Jong Yoo et al., "Neutron Reflector Reflooding Confirmatory Test", MUAP-08008-P, Mitsubishi Heavy Industries, 2008

1-4 Shimomura, T., et al., "Fuel System Design Criteria and Methodology", MUAP-07008-P,
Mitsubishi Heavy Industries, 2007

REQUEST 2

Chapter 2.0 describes plant design and features. Here are questions for this section.

REQUEST 2.1

Report indicates (Section 2.4.2) three ECCS systems: Advance Accumulator, High Head Injection System and Emergency Letdown System. However, there is no description of Emergency Letdown System. This needs explanation.

RESPONSE

The following explanations are added regarding emergency letdown system.

The emergency letdown system performs a "feed and bleed" (FAB) letdown boration to establish cold shutdown conditions if the normal chemical and volume control system (CVCS) is unavailable. The emergency letdown system directs the reactor coolant from two reactor vessel hot legs (B and D) to the refueling water storage pit, from which highly borated water can be returned to the reactor vessel using the safety injection pumps.

REQUEST 2.2

Section 2.4.2 indicates role of ECCS in cooling the reactor for various events but the large break LOCA is not included. Please explain.

RESPONSE

Control rods are assumed not to insert during the large break LOCA. Therefore, the explanation since the third paragraph of 2-5 page of TR is corrected as follows.

The ECCS is designed to perform the following major safety-related functions:

- Safety Injection
- Safe Shutdown
- Containment pH Control

These functions are provided by safety-related equipment with redundancy to deal with single failure, environmental qualification, and protection from external hazards.

- Safety Injection

The primary function of the ECCS is to remove stored and fission product decay heat from the reactor core following an accident. The ECCS meets the acceptance criteria of 10CFR50.46(b) for the following items:

- Peak cladding temperature
- Maximum calculated cladding oxidation
- Maximum hydrogen generation
- Coolable core geometry
- Long-term cooling

The ECCS automatically initiates with redundancy sufficient to ensure these functions are accomplished, even in the unlikely event of the most limiting single failure occurring coincident with, or during the event.

The Safety Injection System (SIS), in conjunction with the rapid insertion of the control rod cluster assemblies (reactor scram), provides protection in the following events:

- LOCA
- Ejection of a control rod cluster assembly
- Secondary steam system piping failure
- Inadvertent opening of main steam relief or safety valve
- SG tube rupture

- Safe Shutdown

The portions of the ECCS also operate in conjunction with the other systems of the cold shutdown design. The primary function of the ECCS during a safety grade cold shutdown is to ensure a means for feed and bleed for boration, and make up water for compensation of shrinkage.

.

- Containment pH Control

NaTB baskets are located in the containment and are capable of maintaining the desired post-accident pH conditions in the recirculation water. The pH adjustment is capable of maintaining containment water pH at least 7.0, to enhance the retention capacity in the

containment and to avoid stress corrosion cracking of the austenitic stainless steel components.

REQUEST 3

Section 3.0 briefly describes LBLOCA code and methodology. Based on the review of this section, request for additional information is formulated in the questions listed below.

REQUEST 3.1

LBLOCA has been divided into three phases (Table 3.3-1) but is not clear what defines the boundaries of these phases. Refilling generally starts when accumulator flow comes in and ends when lower plenum is full. Provide a detail explanation of Table 3.3-1.

RESPONSE

The boundaries between each of the three phases of the LBLOCA for US-APWR are defined in the same way as described in the CSAU (Code Scaling, Applicability, and Uncertainty) evaluation methodology (Ref. 3.1-1). The boundaries of each phase of the LBLOCA are described in Ref. 3.1-1 as follows:

Blowdown Phase

The PWR LBLOCA blowdown starts at the time the break opens and ends when intact loop accumulator injection is initiated.

Refill Phase

The Refill period begins at the time accumulator injection flow is initiated and ends when the mixture level in the lower plenum reaches the core inlet.

Reflood Phase

Reflood begins at the time the lower plenum is completely filled with water. The core begins to reflood with ECC water after the lower plenum is filled.

References

- 3.1-1 Boyack, B., *et al.*, "Quantifying Reactor Safety Margins: Application of Code Scaling, Applicability, and Uncertainty (CSAU) Evaluation Methodology to a Large Break, Loss of Coolant Accident," NUREG/CR-5249 (1989).

REQUEST 3.2

RESPONSE

REQUEST 3.3

[]

RESPONSE

In general, the rewetting condition is that the fuel rod surface temperature decreases under the minimum film boiling temperature and the heat transfer regime changes from "Film Boiling" to "Transition Boiling."

[]

REQUEST 3.4

RESPONSE

REQUEST 3.5

[]

RESPONSE

[]

REQUEST 3.6

[]

RESPONSE

[]

REQUEST 3.7

RESPONSE

REQUEST 3.8

[]

RESPONSE

[]

REQUEST 3.9

[]

RESPONSE

[]

REQUEST 3.10

[Empty response box]

RESPONSE

A response to this question will be provided by May 23, 2009.

REQUEST 3.11

General comment. The stored energy release should be important as it affects coolant conditions. How does total heat release from the reactor system (excluding fuel rods) structures compare to the decay heat? Why is the reactor system stored energy not considered in the PIRT?

RESPONSE

A response to this question will be provided by May 23, 2009.

REQUEST 3.12

Subsection 3.5.1, Advanced Accumulator, and Appendix B, Advanced Accumulator Model Built into WCOBRA/TRAC, describes the advanced accumulator. The advanced accumulator is a new component in the APWR and it requires implementation and review of new correlation in COBRA-TRAC (M1.0). Based on the review, the questions listed below were developed for the advanced accumulator.

REQUEST 3.12.1

Will there be any nitrogen flow into the cold leg of the primary section either through ingress in the stand pipe or from the dissolved nitrogen?

RESPONSE

By design, the nitrogen gas will not be released from the advanced accumulator tank until the peak cladding temperature has occurred, as described in Subsection 3.4.2.1 of the Topical Report.

The test has confirmed that there is no possibility of nitrogen-gas ingress into the stand pipe during the switching from the high- to low-flow-rate mode (Ref. 3.12.1-1).

As for the flow with dissolved nitrogen into the primary cooling system, the amount is insignificant to cause adverse performance to core cooling. Please refer to the response to Question 5 in Reference 3.12.1-2.

References

- 3.12.1-1 Ogino, T., et al., "The Advanced Accumulator," MUAP-07001-P(R1), Mitsubishi Heavy Industries (2007).
- 3.12.1-2 MHI's Responses to NRC's Requests for Additional Information on Advanced Accumulator for US-APWR Topical Report MUAP-07001-P, Revision 1, UAP-HF-08174-P(R0) (September 2008).

REQUEST 3.12.2

Model validation uses same data that was used to develop the correlation (Tests 1, 2, 3, 4, and 6, Page 5-1, MUAP 07001-P (R1)). This could be a check on implementation but not a validation. Please indicate how this correlation applies to smaller scale tests and how it will apply to plant (full scale) that will have different size vortex chamber?

RESPONSE

In Subsection 3.5.1, it is reported that a verification study on the model implementation was performed using the full-height $\frac{1}{2}$ -scaled test data. In Reference 3.12.2-1, it is clarified that the flow characteristics of the flow damper are independent of scale. Therefore the correlation is considered to be applicable to both smaller scale tests and full-scale actual plant.

References

- 3.12.2-1 Ogino, T., et al., "The Advanced Accumulator," MUAP-07001-P(R1), Mitsubishi Heavy Industries (2007).

REQUEST 3.12.3

RESPONSE

REQUEST 3.12.4

Explain the statement that the test was divided based on C_{vmi} and C_{fmi} .

RESPONSE

REQUEST 3.12.5

RESPONSE

Effect of the manufacturing error associated with the flow rate coefficient is considered for both the large and small flow rate injection modes. For the detailed basis for the selection of the manufacturing uncertainty in each mode, please refer to the response to Question 18 in Reference 3.12.5-1.

References

- 3.12.5-1 Response to NRC's Questions for Topical Report MUAP-07001-P(R1), The Advance Accumulator, UAP-HF-07086-P(R0) (July 2007).

REQUEST 3.12.6

[]

RESPONSE

[]

REQUEST 3.12.7

On page 3-27, correct the reference to instrument uncertainties from Table 3.5-5 to Table 3.5-4.

RESPONSE

The reviewer is correct. The table number will be changed accordingly.

REQUEST 3.12.8

Are the values in Tables 3.5-4, 3.5-5 and 3.5-6 percentages?

RESPONSE

The reviewer is correct. All the values in Tables 3.5-4, 3.5-5 and 3.5-6 are in percentage.

REQUEST 3.12.9

On page 3-28, it is stated that the total uncertainty is treated as statistical parameter in ASTRUM. This statement needs to be expanded. How is this implemented in ASTRUM? Is the sampling done on both sides of the best estimate value? Does the range of parameters include 95% of values? How is bias in flow rate coefficient accounted for in the analysis?

RESPONSE

The total uncertainty of the empirical equations used in the LBLOCA analysis for the US-APWR, which includes the instrument uncertainties, data dispersion and manufacturing error, is treated as a statistical parameter in ASTRUM.

REQUEST 3.12.10

How is switching level uncertainty implemented in ASTRUM?

RESPONSE

The uncertainty in the water level to enable the flow switching is considered conservatively in the evaluation of the fuel cladding temperature. In the PCT evaluation, the required function of the advanced accumulator is to fill-up the lower plenum promptly during the refill period, then simultaneously raise the water level in the downcomer. Therefore, it is a conservative treatment qualitatively to shorten the duration of the large flow rate mode of the advanced accumulator. In ASTRUM, the maximum uncertainty in the switching level is assumed to result in the shortest duration of the large flow rate mode.

REQUEST 3.12.11

Do same uncertainties apply to plant? Is there a scale effect? Section 4.3 (Ref MUAP 07001) only mentions Reynolds number as scaling parameter.

RESPONSE

In Reference 3.12.11-1, it is discussed that the flow characteristics of the flow damper are independent of scale. Therefore, MHI considers applying the same uncertainties to the plant. Please refer to the response to Question 9 in Reference 3.12.11-2.

References

- 3.12.11-1 Ogino, T., et al., "The Advanced Accumulator," MUAP-07001-P(R1), Mitsubishi Heavy Industries (2007).
- 3.12.11-2 MHI's Responses to NRC's Requests for Additional Information on Advanced Accumulator for US-APWR Topical Report MUAP-07001-P, Revision 1, UAP-HF-08174-P(R0) (September 2008).

REQUEST 3.12.12

In Appendix B, page B-1; equation B-1 implies that the flow damper outlet pressure will always be greater than the vapor pressure. Provide a reference or documentation that supports this assumption.

RESPONSE

In Reference 3.12.12-1, it is shown that the outlet pressure of the flow damper is always larger than the vapor pressure in the full-height 1/2-scaled results (Fig. 4.2.4-5(2/2), Fig. 4.2.4-6(2/2), Fig. 4.2.4-7(2/2), Fig. 4.2.4-8(2/2), Fig. 4.2.4-9(2/2), Fig. 4.2.4-10(2/2) and Fig. 4.2.4-11(2/2) in Reference 3.12.12-1).

References

- 3.12.12-1 Ogino, T., et al., "The Advanced Accumulator," MUAP-07001-P(R1), Mitsubishi Heavy Industries (2007).

REQUEST 3.12.13

[]

RESPONSE

[]

REQUEST 3.12.14

[]

RESPONSE

[]

REQUEST 3.12.15

Explain the basis of Eqs. B-9 and B-10. There is a factor of two differences when it is derived using expressions from COBRA-TRAC manual (Eq. 4-197 and 4-256). Is there is difference in definitions?

RESPONSE

One-dimensional friction factor in WCOBRA/TRAC is defined in Equation (4-197) of Ref. 3.12.15-1 as:

$$f = \frac{\left(\frac{dP}{dx} \right)_f D_h}{2\rho_m U_m |U_m|}.$$

Rearranging Equation (4-197) yields:

$$\left(\frac{dp}{dx} \right)_f = f \frac{2\rho_m U_m |U_m|}{D_h}, \quad (1)$$

where $(dp/dx)_f$ is the pressure gradient associated with frictional losses, ρ_m is mixture density, D_h is hydraulic diameter and U_m is mixture velocity.

The form loss in a one-dimensional component is defined on Page 29 of Ref. 3.12.15-2 as:

$$\Delta P = \frac{k \rho U_m^2}{2},$$

where k is a form loss coefficient. Integrating Equation (1) over the length of a momentum cell and including the form loss provides the total pressure loss:

$$\Delta P_{Total} = f \frac{\Delta x}{D_h} 2\rho_m U_m^2 + k \frac{\rho U_m^2}{2} = \left(2f + \frac{kD_h}{2\Delta x} \right) \frac{\Delta x}{D_h} \rho U_m^2,$$

where $2f$ is a value calculated by the code, or an input to be provided as "FRIC," and $(kD_h/2\Delta x)$ is an input to be provided as "FRIC." "FRIC" is an input value for one-dimensional components as additive loss coefficients.

The momentum cell length Δx is defined as follows:

$$\Delta x = \frac{DX_{i-1} + DX_i}{2},$$

where DX is cell length. Finally, FRIC is defined as

$$\left(\right)$$

References

- 3.12.15-1 Nissley, M. E., et al., "Realistic Large Break LOCA Evaluation Methodology Using Automated Statistical Treatment of Uncertainty Method (ASTRUM)," WCAP-16009-P-A (January 2005).
- 3.12.15-2 Liles, D. R., et al., "TRAC-PD2: An advanced Best-Estimate Computer Program for Pressurized Water Reactor Loss-of-Coolant Accident Analysis," NUREG/CR-2054 (1981).

REQUEST 3.12.16



RESPONSE

The response to this question will be provided by May 23, 2009.

REQUEST 3.12.17

Page B-5, how are QLTMIN and VDMIN estimated for input?

RESPONSE

- QLFTMIN

[]

- VDMIN

[]

REQUEST 3.13

In Section 3.5.3, Neutron Reflector, the report describes modeling of a new component of APWR.

REQUEST 3.13.1

There is no description of cooling holes and stored energy in the neutron reflector. Provide a reference or description of the cooling holes including the number and size of these holes.

RESPONSE

The Neutron Reflector (NR) is a thick stainless steel structure located between the core and the core barrel. The NR is cooled by the core bypass flow through () flow holes. There are several flow paths in and around the NR region which can provide cooling during reflood. The NR is cooled by flow at the outer boundary of the core, the flow through the holes which penetrate through the length of the NR, and the fluid in the back of the NR.

The NR is modeled in WCOBRA/TRAC US-APWR model as an unheated structure with through-holes as the only cooling surface. Its interface to the core and to the back side of the NR are considered adiabatic, which maximizes the steam generation within the NR. The flow holes through the NR have a diameter of () in. In WCOBRA/TRAC US-APWR model, [

]

REQUEST 3.13.2

COBRA-TRAC (M1.0) has been modified to model the flow field in the unheated flow channel, hot wall flow regime, for the flow channels in NR. Provide a reference or explanation for the following questions. Are the flow regimes described for hot wall and normal flow regimes applicable to flow channels in the neutron reflector? Does the model switch to normal wall flow regime when wall cools below T_{CHF} ? Is the limit used for T_{CHF} valid for channel flow of neutron reflector, if so why?

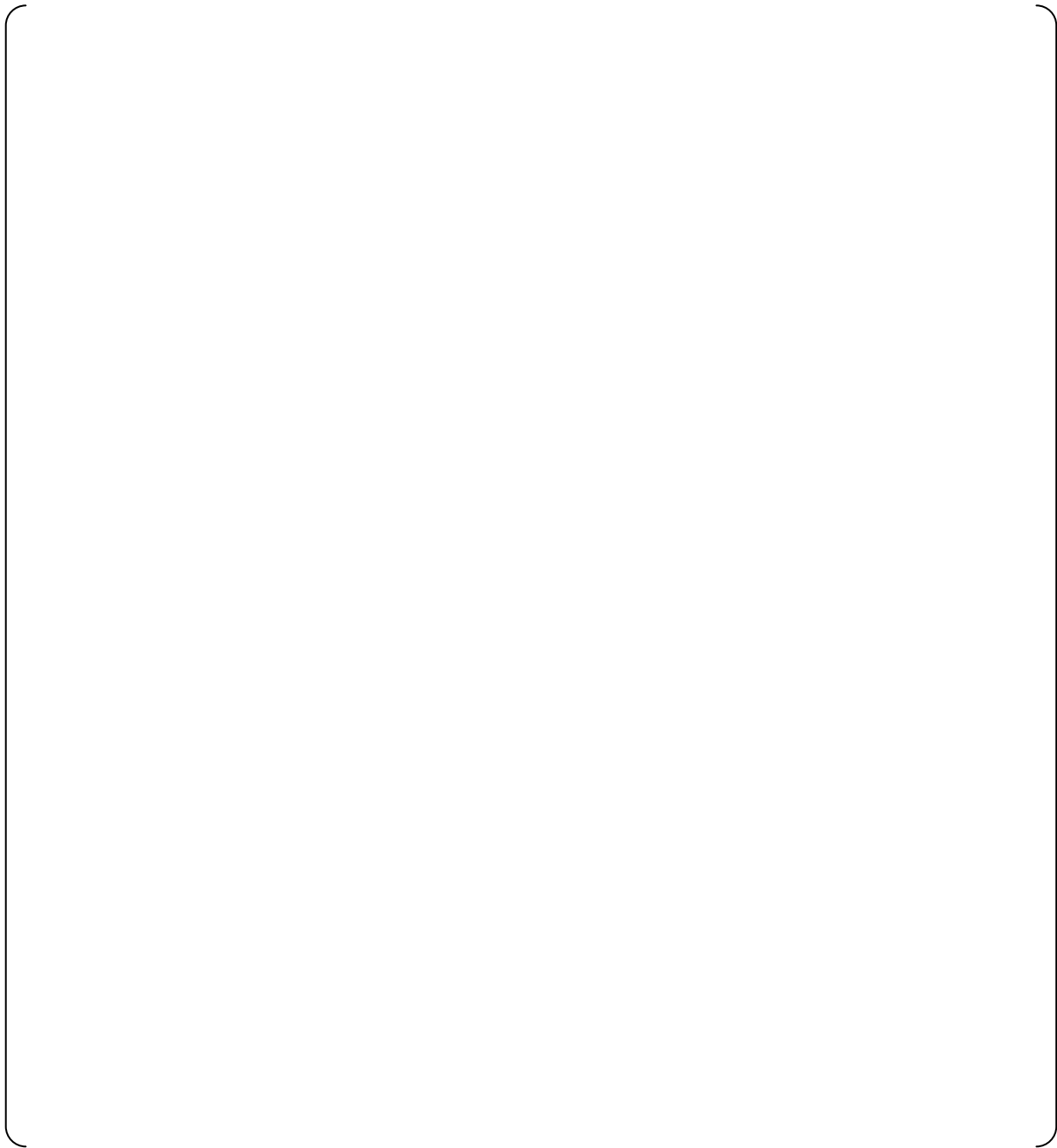
RESPONSE

The response to this question will be provided by May 23, 2009.

REQUEST 3.13.3

The expression for α_{critical} for flow regime is described in COBRA-TRAC manual, Equation 3-39, but no reference provided. The section states that it is derived in Chapter 4 but it is not shown in that chapter in the version of the manual provided. Provide a reference or explanation to resolve the above issue.

RESPONSE



REQUEST 3.13.4

Provide a reference or explanation to the following questions. How much stored energy is in NR and how does the heat transfer to fluid compare to decay heat?

RESPONSE

The response to this question will be provided by May 23, 2009.

REQUEST 3.14

The plant model is described in Section 3.6, Sample Plant Analysis.

REQUEST 3.14.1

Nodes communicate with other nodes in the radial, azimuthal and axial directions. Provide a reference or explanation on how the friction terms (wall, turbulent, etc.) are specified or computed through the gaps (interface between nodes)?

RESPONSE

For the friction terms in the lateral and axial directions, wall-to-fluid drag for each phase and the vapor-to-liquid drag are modeled in the code, as shown in the section 4 of Reference 3.14.1-1.

The wall drag and the interfacial shear are defined in each cell applied momentum equation, the wall drag is constituted with the wall shear and form loss. As for the boundary between the nodes, only the form loss coefficient defined with velocity head loss is directly input into the code for both axial and lateral flows. The value of the loss form coefficient depends on the geometry of the flow path.

On the other hand, the wall shear and the interfacial shear are evaluated by the co-relations that depend on the flow regime model in the code.

Reference

- 3.14.1-1 Bajorek, S. M., et al., 1998, "Code Qualification Document for Best Estimate LOCA Analysis," WCAP-12945-P-A, Volume 1, Revision 2.

REQUEST 3.14.2

Provide a reference or explanation for the following questions. How are the fuel rods nodalized for conduction calculation? How does this nodalization compare to the previously approved 4-loop Westinghouse PWR representation?

RESPONSE

[Empty response box]

REQUEST 3.14.3

In Subsection 3.6.1.3, Loop Model, DVI injects coolant through downward pointing nozzle in the vessel. Provide a reference or description on how it is specified in COBRA part of the code?

RESPONSE

[]

REQUEST 3.14.4

RESPONSE

Table RAI 3.14.4-1 shows the steady-state acceptance criteria for US-APWR. [

]

References

- 3.14.4-1 M. E. Nissley *et al.*, "Realistic Large Break LOCA Evaluation Methodology Using Automated Statistical Treatment of Uncertainty Method (ASTRUM)," WCAP-16009-P-A, January 2005.
- 3.14.4-2 S. M. Bajorek *et al.*, "Code Qualification Document for Best Estimate LOCA Analysis," WCAP-12945-P-A, Volume 1, Revision 2, and Volumes 2 through 5, Revision 1, and WCAP-14747 (Non-Proprietary), 1998.

Table RAI 3.14.4-1 Steady-State Acceptance Criteria

--

REQUEST 3.14.5

In Subsection 3.6.3.2, Homologous Pump Curves for the US-APWR RCP, the report describes the pump model. Figures 3.6-11 and 3.6-12 are shown as for US-APWR. Specific speed indicates similarity of pump performance in single phase flow. However, in case of two phase flow there are other length scales (bubble size) that are independent of pump size. It has been found that smaller pump degrades more than larger pumps with same pump specific speed (NUREG/CR-5249, App L). Provide a reference or discussion to why the 1/3 scale data will represent US-APWR for two phase degradation?

RESPONSE

The response to this question will be provided by May 23, 2009.

REQUEST 3.15

Section 3.6.5, Analysis Results, discusses the results from the analyses.

REQUEST 3.15.1

In Subsection 3.6.5.1, the blowdown phase shows hot channel flow rate in Figure 3.61-5. Provide a reference or discussion on why does flow increase around 5 seconds?

RESPONSE

Hot channel flow rate is shown in Figure 3.6-15. (not in Figure 3.61-5)

During the first few seconds of the transient, the subcooled water is discharged through the break at a rate that exceeds the capacity of the RCPs in the coast down mode and the core water inventory decreases rapidly.

At around 5 seconds, the RCPs in the intact loops are still delivering the single-phase water to the core. As the result, the core flow will increase temporarily.

After that, as the coolant in the loops become two-phase, the RCP performance is degraded; the RCP-driven flow decreases; the break flow begins to dominate; and then the core flow decreases again.

REQUEST 3.15.2

The description of refill phase indicates that this phase ends when the downcomer is full. Figure 3.6-18 indicates that the downcomer level is less than the level at the beginning of the transient when the downcomer is filled with liquid. Provide a reference or explanation of the ending of refill phase.

RESPONSE

As described in Subsection 3.3.3, the refill phase ends when the water level in the lower plenum reaches the bottom of the fuel rods.

Therefore, the description should be modified as follows;

"In this phase, the core heat-up continues when the lower plenum is filled with the advanced accumulator injection water. Figure 3.6-17 shows the lower plenum collapsed liquid level. When the advanced accumulator injection water fills the lower plenum and begins to enter the core, the refill phase ends."

REQUEST 3.16

In Section 3.7, ASTRUM Methodology Applied to US-APWR, the report describes ASTRUM methodology as related to the US-APWR design. It is based on non-parametric approach described by Wilks and later on by Guba et al. This step is consistent with CSAU step 13 but differs from CSAU demonstration where response surface method was used. In non parametric approach, the plant and model parameters are randomly sampled and a set of 124 calculations are performed to achieve 95%/95% values of the three parameters of the acceptance criteria.

REQUEST 3.16.1

How is it assured that the values of any parameter obtained by random sampling of the distribution, is obtained from the full range of the distribution and is not selected from only one part of the distribution?

RESPONSE

REQUEST 3.16.2

The description of matrix, first paragraph on page 3-90, below Equation 3.7-2, states that it has N rows and 3 columns which are incorrect. Correct it by changing N rows and 3 columns to 3 rows and N columns.

RESPONSE

What is pointed out is right. MHI will change the sentence to "N columns 3 rows".

REQUEST 3.16.3

In Subsection 3.7.2, the report describes the parameters used for uncertainty analyses. There is no mention of uncertainty in global phenomena such as pump, condensation/flashing etc. as were identified in the PIRT. What are the important global parameters and how are they accounted for in the uncertainty analyses?

REQUEST 3.16.4

Tables 3.7-1 and 3.7-2 do not provide any information on type of distribution, range and basis of this information. Provide the reference or document that has this information for the US-APWR?

RESPONSE

The treatments of the global/local models and other parameters used in the uncertainty analyses for US-APWR are basically the same as those used in the approved ASTRUM methodology. The information on the types of the distribution, range, and basis for each of these models and parameters is also the same.

In performing the uncertainty analyses, the parameters that have uncertainty distributions in Tables 3.7-1 and 3.7-2 in the Topical Report are the same as those used in the approved ASTRUM methodology shown in Tables 1-8 through 1-11 of WCAP-16009-P-A (Reference 3.16.4-1).

Although the Topical Report does not describe the global models in Subsection 3.7.2, Table 1-7 of WCAP-16009-P-A (Reference 3.16.4-1) shows that [

]

Reference

- 3.16.4-1 M.E., Nissley, et al., "Realistic Large Break LOCA Evaluation Methodology Using Automated Statistical Treatment of Uncertainty Method (ASTRUM)", WCAP-16009-P-A, January 2005
- 3.16.4-2 FirstEnergy Nuclear Operating Company, "Beaver Valley Power Station, Unit No.1 and No.2 BV-1 Docket No.50-334, License No.DPR-66 BV-2 Docket No.50-412, License No.NPF-73 10 CFR 50.46 Report of Changes or Errors in ECCS Evaluation Models" L-05-168, December 22, 2006

Table 1 Uncertainty Distributions for Global Models

Table 2 Uncertainty Distributions for Local Models

Table 3 Power-Related Parameters Considered in Uncertainty Methodology

--

Table 4 Initial and Boundary Conditions Considered in Uncertainty Methodology

--



Figure 1 Blowdown Heatup HTC Multiplier Distribution

(Submitted by UAP-HF-09252)

INTRODUCTION

This document presents MHI's 2nd part responses to the NRC's requests for additional information (RAI) on Topical Report MUAP-07011-P (R0) "Large Break LOCA Code Applicability Report for US-APWR" dated March 25, 2009.

This document provides the remaining 6 (six) out of 46 (forty-six) items requested in this RAI. The first part of responses to the RAI were already transmitted to the NRC by preceding correspondence, on April 24, 2009 (30 days after the issuance of the formal RAI), as mutually agreed by NRC and MHI.

REQUEST 3.10

RESPONSE

REQUEST 3.11

General comment. The stored energy release should be important as it affects coolant conditions. How does total heat release from the reactor system (excluding fuel rods) structures compare to the decay heat? Why is the reactor system stored energy not considered in the PIRT?

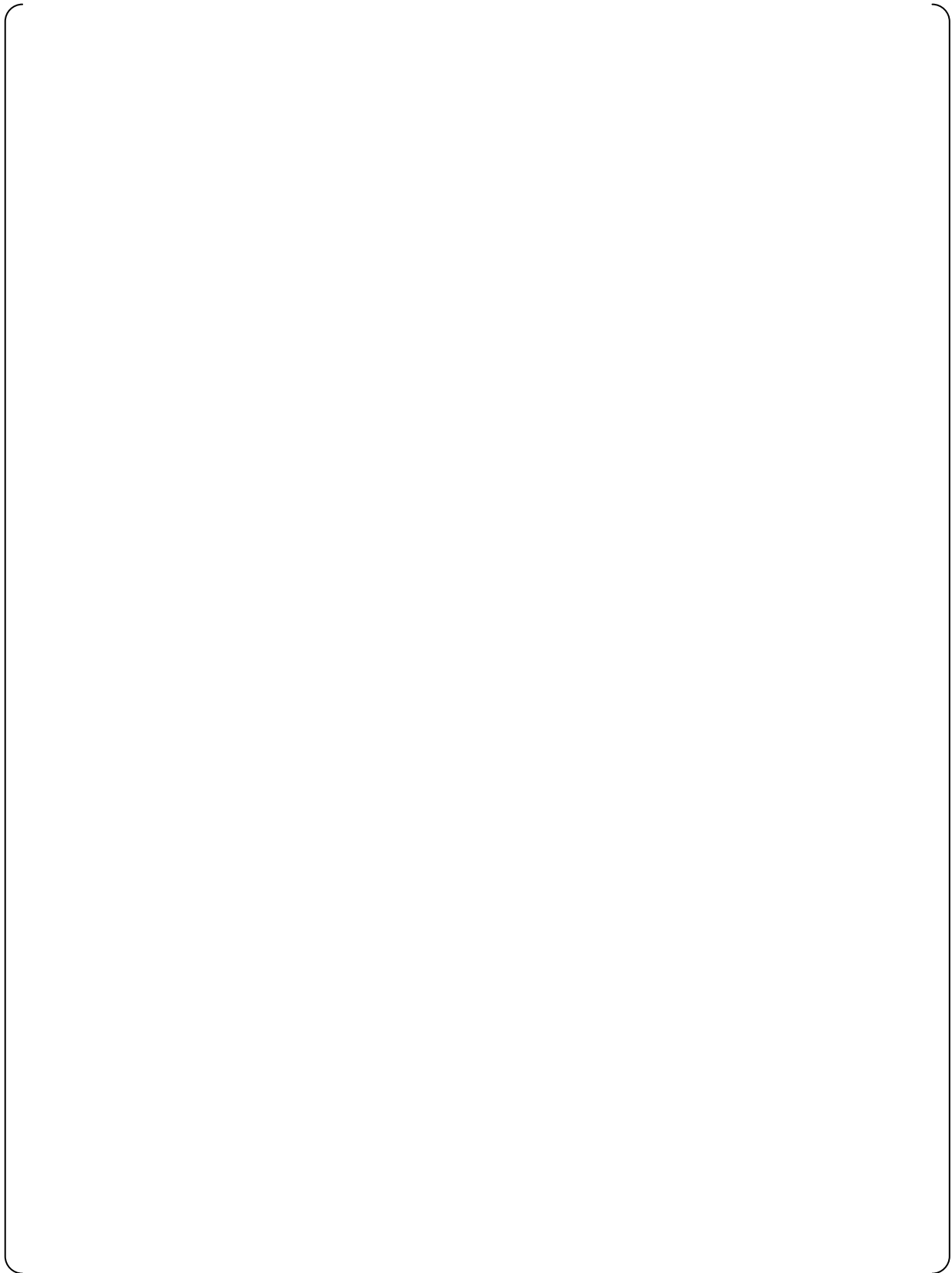
RESPONSE



REQUEST 3.12.16

RESPONSE





REQUEST 3.13.2

COBRA-TRAC (M1.0) has been modified to model the flow field in the unheated flow channel, hot wall flow regime, for the flow channels in NR. Provide a reference or explanation for the following questions. Are the flow regimes described for hot wall and normal flow regimes applicable to flow channels in the neutron reflector? Does the model switch to normal wall flow regime when wall cools below T_{CHF} ? Is the limit used for T_{CHF} valid for channel flow of neutron reflector, if so why?

RESPONSE

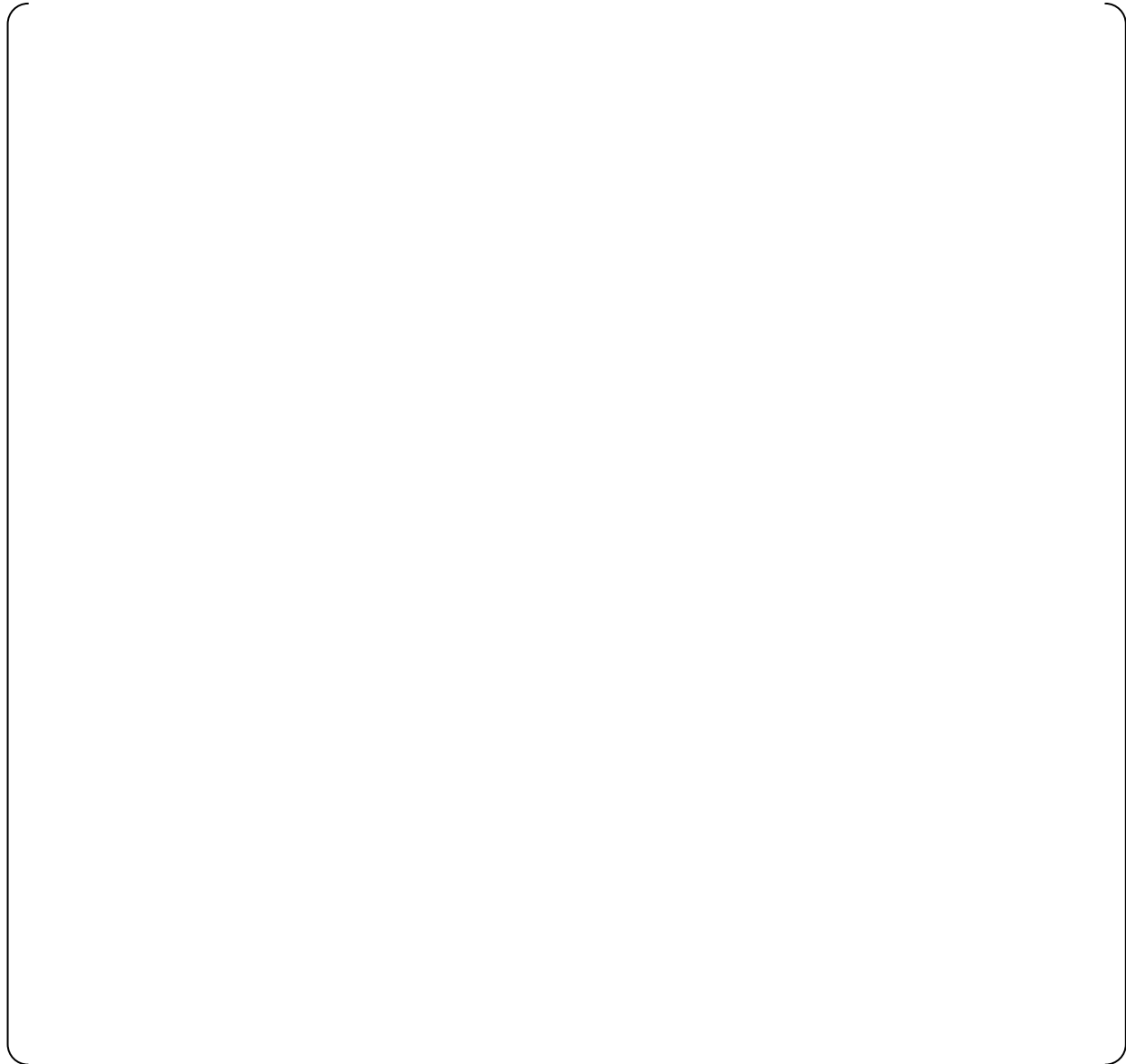
Reference 3.13-2-1 Neutron Reflector Reflooding Confirmatory Test, MUAP-08008-P(R0) (2008).

REQUEST 3.13.4

Provide a reference or explanation to the following questions. How much stored energy is in NR and how does the heat transfer to fluid compare to decay heat?

RESPONSE

Figure RAI-3.13.4-1 compares the amount of heat release from NR with total decay heat of fuel rod in the US-APWR reference calculation of Reference 3.13.4-1.



REQUEST 3.14.5

In Subsection 3.6.3.2, Homologous Pump Curves for the US-APWR RCP, the report describes the pump model. Figures 3.6-11 and 3.6-12 are shown as for US-APWR. Specific speed indicates similarity of pump performance in single phase flow. However, in case of two phase flow there are other length scales (bubble size) that are independent of pump size. It has been found that smaller pump degrades more than larger pumps with same pump specific speed (NUREG/CR-5249, App L). Provide a reference or discussion to why the 1/3 scale data will represent US-APWR for two phase degradation?

RESPONSE

The MHI shows two references as to why the 1/3 scale two-phase data is able to be used for the US-APWR RCP.

The first reference (Ref. 3.14.5-1) revealed that "scaling down the size of the pump while maintaining the same design specific speed produces very similar performance characteristics both in single and two-phase flows. Effects due to size and operating speed were not discernible within the range of test conditions and within experimental uncertainties."

Also, similar results were observed in the two-phase pump experiments using the different geometrically scaled pumps (scale 1:5 and 1:4) conducted by KWU (Ref. 3.14.5-2).

[]

References

- 3.14.5-1 Kamath, P. S. and Swift, W. L., "Two-Phase Performance of Scale Models of a Primary Coolant Pump," EPRI NP-2578, Final Report, 1982
- 3.14.5-2 Kastner, W. and Seeberger, G. J., "Pump Behavior and Its Impact on a Loss of Coolant Accident in a Pressurized Water Reactor," Nuclear Technology, Vol. 60, 1983

RESPONSES
to
THE SECOND SET OF REQUESTS FOR ADDITIONAL INFORMATION
for
LARGE BREAK LOCA CODE APPLICABILITY REPORT FOR US-APWR
MUAP-07011-P

(Submitted by UAP-HF-10130)

Question 1.1 (Follow-Up To Question 3.1)

The response to Question 3.1 clarifies the definitions of the three phases during a large break LOCA transient consistent with the CSAU methodology defined in NUREG/CR-5249. Accordingly, correct the description of LBLOCA phases provided in MUAP-07011-P (R0) "Large Break LOCA Code Applicability Report for US-APWR" Section 3.4.1 "LBLOCA PIRT."

Confirm the applicability of the defined phases (blowdown and refilling) as utilized in the Phenomena Identification and Ranking Table (PIRT) presented in MUAP-07011-P Table 3.4-1 "US-APWR PIRT" or adjust the PIRT accordingly. Review all MHI documents that describe phases of large break LOCA and provide a consistent definition of end of blowdown phase.

RESPONSE

In the same way with the approved methodology, the description of US-APWR LBLOCA transient in the topical report is according to the traditional definitions. After the large break occurs, the RCS pressure decreases because of the coolant inventory decreasing in the RCS and the blowdown phase starts. The pressure level of the RCS decreases until the containment atmosphere pressure and the blowdown phase ends in the topical report. This definition for blowdown period is also the same as that described in the DCD rev.2 (Ref.1.1-1). This definition is difference from the definition of the blowdown phase ending described in the CSAU methodology report (Ref.1.1-2).

On the other hand, the same definition for the LBLOCA periods as that of CSAU PIRT is used for the US-APWR PIRT. The blowdown phase during the LBLOCA is from accident initiation to the initiation of the accumulator injection into the intact loops. The refill phase is defined to start with accumulator injection start and continue until the lower plenum is refilled. The reflood phase is defined to start from the bottom of the core recovery and continues until the peak cladding temperature has occurred and the cladding is cooling down. These definitions are different from the transitional definitions for the blowdown and refill phases. However, to remain consistent with the CSAU PIRT, the US-APWR PIRT is adjusted accordingly in the same way as the existing 4-loop PWR PIRT that has been approved. The PIRT is used to specify the important phenomenon during LBLOCA, the definitions of the three phases in PIRT do not always need to be completely the same as that of the transient periods. The PIRT for US-APWR in the topical report was established according to the scenario specification.

Therefore it is not necessary to correct the definition of each phase for establishment the PIRT described in the Topical report.

Reference

- 1.1-1 MUAP-DC001 Revision 2 "Design Control Document for the US-APWR"
- 1.1-2 NUREG/CR-5249 "Quantifying Reactor Safety Margins ; Application of Code Scaling, Applicability, and Uncertainty Evaluation Methodology to a Large-Break, Loss-of Coolant Accident"

Question 1.2 (Follow-Up To Question 3.3 and Question 3.15.1)

The response to Question 3.3 describes the occurrence of PCT during the blowdown period and refers to the response to Question 3.15.1 for additional discussion.

The responses to Question 3.3 and Question 3.15.1 do not appear consistent. Also, explain the cause of the blowdown peak, including whether it is due to flooding from the top or from the bottom of the core and identify the cause for the corresponding quench process.

RESPONSE

The occurrence of PCT during the blowdown phase is caused by the downward flow in the core from the HA upper-ports shown in Figure 1.2-1.

The upward flow remains at the hottest point in the core because of superior flow rate from the three intact loops up until the downward flow occurs. As degradation of RCP performance due to two-phase grows, the core flow reverses to downward flow. Because of the downward flow, PCT occurs and the cladding temperature decreases for a moment. It could be identified that the downward flow, or flooding, is caused from the top as shown in Figures 1.2-1 and 1.2-2.

Figure 1.2-3 shows cladding temperature at PCT location. In addition, the cladding at PCT location does not experience the quench process, which means the nucleate boiling condition, during blowdown phase.

The response to Question 1.11 provides the additional explanation for PCT during the blowdown phase.



Figure 1.2-1 Mass flow rate in HA channel at the top of core



Figure 1.2-2 Mass flow rate in HA channel at the PCT location



Figure 1.2-3 Cladding temperature at PCT location

Question 1.3 (Follow-Up To Question 3.6)

The response to Question 3.6 states that the safety injection signal delay is set with conservative margin and therefore pressurizer pressure as a control parameter is not identified as a significant phenomenon in the PIRT.

Describe the relationship between the pressurizer model uncertainty and the actuation of safety injection. In addition, specify the delay in initiation of safety injection and explain how it is determined.

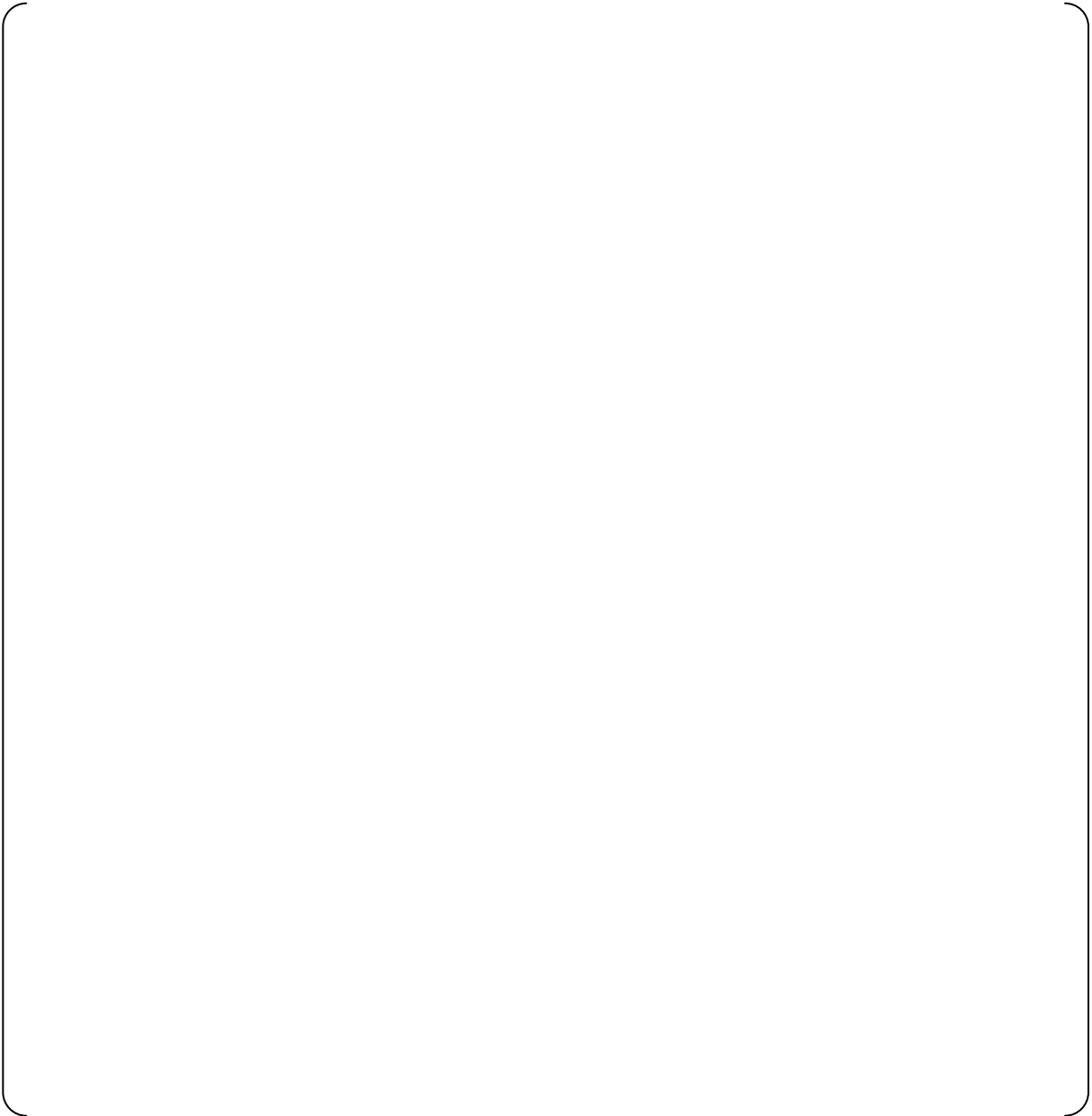
RESPONSE

Question 1.4 (Follow-Up To Question 3.7)

RESPONSE







Question 1.5 (Follow-Up To Question 3.10)

The response to Question 3.10 addresses DVI condensation in the downcomer and its ranking in provided in MUAP-07011-P (R0) "Large Break LOCA Code Applicability Report for US-APWR" Table 3.4-1 "US-APWR PIRT."

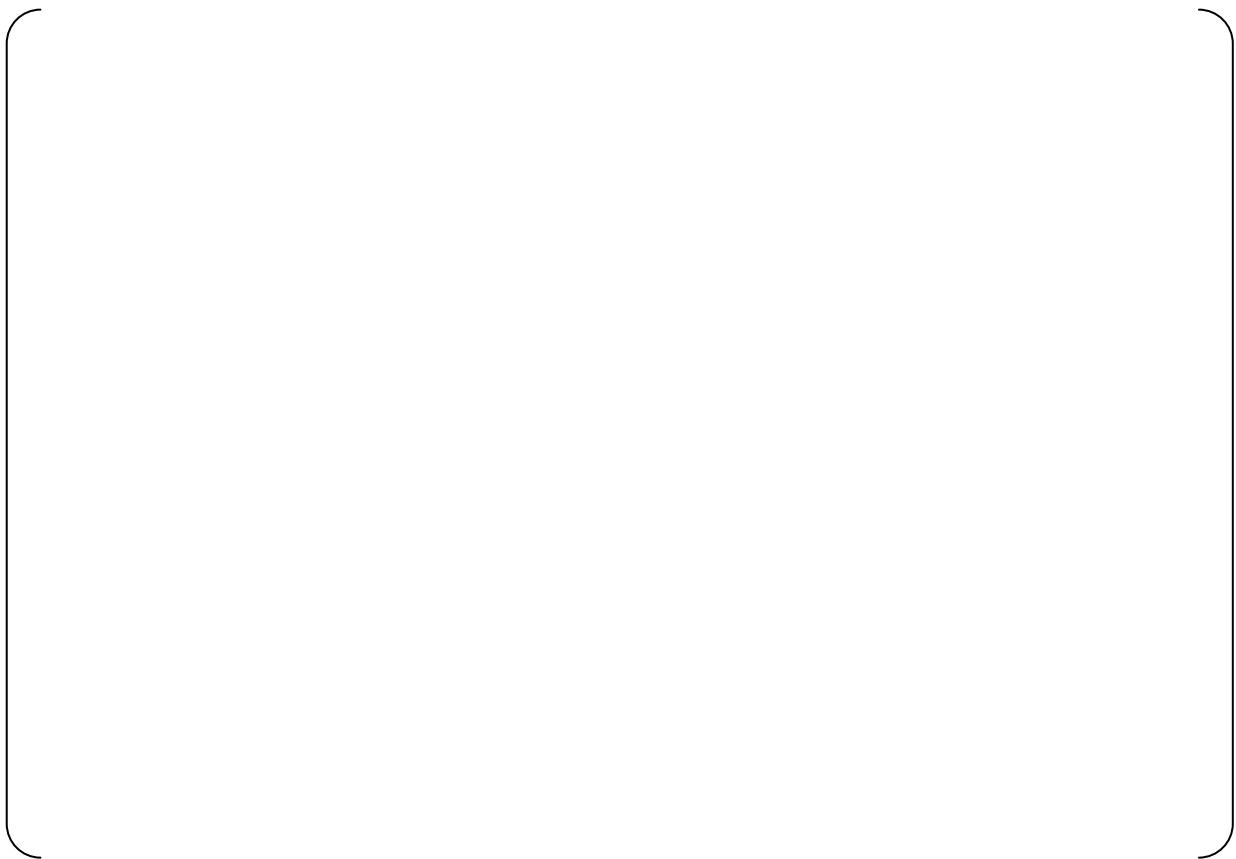
Explain the source of oscillations in downcomer level between 40 seconds and 125 seconds and its impact on PCT. In addition, explain how the uncertainty in the prediction of these oscillations is accounted for in the uncertainty estimation of PCT.

RESPONSE

Downcomer oscillation between 40 seconds and 125 seconds is generated by difference of downcomer water head and core water head and upper plenum pressure variation due to variation of vapor generation caused by change of core water level and flow rate accompanied by variation of core heat transfer.



Figure 1.5-1 Downcomer collapsed water level



Question 1.6 (Follow-Up To Question 3.12.3)

The response to Question 3.12.3 discusses the effect of advanced accumulator test device instrument uncertainty on flow coefficient with variation in cavitation factor. Provide additional information to explain why cavitation factor increases when the system is depressurizing. In addition, explain why there is a larger instrument uncertainty for a larger cavitation factor.

RESPONSE

Cavitation factor is simply described as follows:

$$\sigma = (P_d - P_v) / \Delta P$$

where,

σ : Cavitation factor

P_d : Pressure of flow damper outlet piping

P_v : Vapor pressure of water

ΔP : Differential pressure of flow damper

When the tank is depressurizing, discharge flow rate decreases. This means ΔP decreases with depressurization of the tank. Therefore, this is the reason that cavitation factor increase when the tank is depressurizing.

As shown in the equation, larger cavitation factor means smaller ΔP . Instrument error (E) depends on its range. Instrument uncertainty ($E/\Delta P$) is relatively larger when ΔP is smaller. Therefore, when there is a larger instrument uncertainty for a larger cavitation factor.

Question 1.7 (Follow-Up To Question 3.12.6)

RESPONSE



Question 1.8 (Follow-Up To Question 3.12.9)

The response to Question 13.12.9 discusses the treatment of the total uncertainty associated with the empirical equations of the advanced accumulator model. Provide additional information explaining whether there a bias in the flow rate correlation and how it is handled.

As per response to Question 3.12.4, the data distribution is not symmetrical on both sides of the line representing the correlation. Describe how this asymmetry is handled in sampling or "S".

RESPONSE

As described in the section 5.1 of the advanced accumulator Topical Report (Ref.1.8-1), the fitting curves of the flow rate correlation C_v for the large flow mode and small flow mode (equations 5-2, 5-3) were derived using the least-squares method from the data of the full height 1/2 scale tests. There is no bias in the equations. The experimental flow rate correlations of C_v (equations 3.5.1-2 and 3.5.1-3) are used in the LBLOCA analysis as they are. As for the asymmetric distribution to the flow rate correlation, a larger range of []% is applied to the dispersion deviation of σ_D for both the positive and negative sides in the ASTRUM analysis. The same as for the σ_D in the large flow mode, the larger dispersion deviation of []% is applied to σ_D in the small flow mode.

Following the above approach, the maximum total uncertainties of []% for large flow mode and []% for small flow mode are used in the LBLOCA analysis as shown in Table 3.5-6 of the Large Break LOCA Topical Report .

Reference

- 1.8-1 Ogino, T., et al., "The Advanced Accumulator," MUAP-07001-P(R1), Mitsubishi Heavy Industries (2007).

Question 1.9 (Follow-Up To Question 3.12.10)

The response to Question 3.12.10 states that the uncertainty in advanced accumulator switching is conservatively accomplished by shortening the duration of the large injection rate, but implementation in ASTRUM is not described.

Provide a description of how switching level uncertainty is implemented in ASTRUM, including quantification of the uncertainty and its basis.

RESPONSE

The switching level uncertainty range is [], calculated from the measurement error and the 1/2 scale test results as given in Table 4.2.4-2 of MUAP-07001-P(R1) "THE ADVANCED ACCUMULATOR".

In the last sentence of the response to question 3.12.10, "In ASTRUM, the maximum uncertainty in the switching level is assumed to result in the shortest duration of the large flow rate mode." It implies that for the shortest duration of the large flow rate mode, the fixed value of the highest switching level from the maximum uncertainty of [] is used in all runs in the ASTRUM analysis and the switching level uncertainty is not randomly sampled as a statistical parameter. As the indicator for the flow mode switching, accumulator water volume at the highest switching level is input in the ASTRUM analysis. By applying this approach, the advanced accumulator switching is considered conservatively enough in the LBLOCA analysis.

Question 1.10 (Follow-Up To Question 3.13.2)

The response to Question 3.13.2 describes the applicability of the WCOBRA/TRAC(M1.0) flow regimes in modeling the neutron reflector flow channels.

Explain the sudden drop in the measured surface temperatures seen in Figure 3.13-2-2 provided in the response to Question 3.13.2 at approximately 5 s into the transient. Identify the reasons for and the consequences from the code's inability to capture the observed temperature drop in temperatures.

RESPONSE

Question 1.11 (Follow-Up To Question 3.15.1)

The response to Question 3.15.1 explains the core flow response during the blowdown period. Provide additional information, which includes plots for pump inlet void fraction, pump flow rates, and break flow rates. In addition, explain the relationship of hot rod PCT (peaks and valleys) and hot assembly channel flow rate.

RESPONSE

Figure 1.11-1 and 1.11-2 provide the pump inlet void fractions of the broken and intact loop. Figure 1.11-3 and 1.11-4 provide the pump flow rates of the broken and intact loop. And Figure 1.11-5 and 1.11-6 provide the break flow rates of the RCP side and the RV side.





Figure1.11-1 Void fraction at pump inlet in the broken loop



Figure1.11-2 Void fraction at pump inlet in the intact loop



Figure1.11-3 Mass flow rate at pump in the broken loop



Figure1.11-4 Mass flow rate at pump in the intact loop

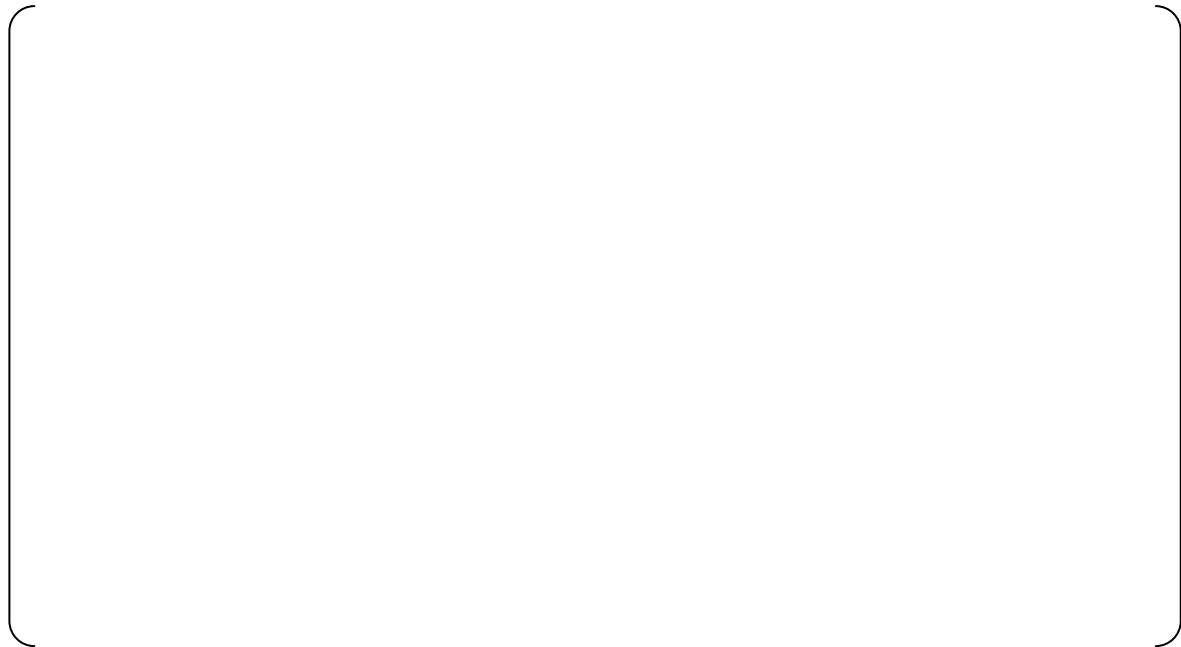


Figure1.11-5 Break mass flow rate at RCP side



Figure1.11-6 Break mass flow rate at RV side



Figure1.11-7 Cladding temperature at the PCT location



Figure1.11-8 Mass flow rate in HA channel at the PCT location

Question 1.12 (Follow-Up To Question 3.16.4)

The responses to Question 3.16.3 and 3.16.4, pertaining to the parameters used in the uncertainty analyses, are provided by the applicant in a single response. Provide additional information to include a comparative table that lists geometric and operational differences between Westinghouse 4-loop plant and the US-APWR design. Justify the use of the range and distribution of all the uncertainty parameters from the Westinghouse 4-loop plant to US-APWR application in ASTRUM. Explain how the medium and high rank phenomena are covered through parameters considered for uncertainty analyses. In particular, justify the applicability of WCOBRA/TRAC(M1.0) to a taller core and a lower average heat generation rate and evaluate the impact of these changes on the uncertainty ranges of the associated parameters.

RESPONSE

The comparison results of the important geometrical information between a WH 4 loops plant and US-APWR are provided in table 2.1 and 2.2 of topical report in order to consider the applicability of the WCOBRA/TRAC(M1.0) code to the LBLOCA analysis for the US-APWR plant.

The comparison results about the parameters related to the Scaling effect is described in the response of question 39. The geometry information that is not included in table 2.1 and 2.2 of topical report could not affect to change the PIRT described in the topical report. Because the fundamental system geometries are not different between conventional 4-loop PWR and US-APWR from the view point of coolant behavior in the core during LBLOCA as severe postulated accident. In addition, there are not significant differences from conventional PWR plant on operational procedure which affects LBLOCA analysis.

WCOBRA/TRAC (M1.0) is a modified version of the approved WCOBRA/TRAC, and both codes are basically the same. Important phenomenon during the LBLOCA is indicated in the PIRT, the models to evaluate the important phenomenon contained in WCOBRA/TRAC code have been validated based on the appropriate experimental analyses. Therefore, most of the models in MCOBRA/TRAC and statistical methodology can be applied to US-APWR LBLOCA analysis by MCOBRA/TRAC(M1.0), unless having significant differences of plant system geometries and the operation ranges from that of the conventional PWR plant.

For the applicability to US-APWR LBLOCA analysis, considerations regarding the design differences between US-APWR and conventional PWR are given below.

In the ECCS performance analysis during LBLOCA with the WCOBRA/TRAC code, the uncertainties about the physical calculation models and the plant operation conditions are treated as the ASTRUM calculation data or conditions. It has been already identified that the most important phenomena related the plant geometry are the ECCS bypass and the Steam binding in order to evaluate the ECCS performance during LBLOCA in the conventional 4- loop PWR. Since these phenomena give enough effects on the reflooding behavior for the reflooding start time and the reflooding rate. The scaling effect about the core height difference between the conventional 4-loop PWR and US-APWR is needed to be considered. The effect on these important phenomena is examined as follows.

It has been confirmed that these phenomena model contained in the WCOBRA/TRAC have the conservative biases for the LBLOCA analysis based on the several test validation results. Therefore, it has been proved that the WCOBRA/TRAC code provides

the conservative results on the PCT evaluation for LBLOCA of the conventional 4-Loop plant. As described in the response to Question 39, it has been confirmed that the applicability of the scale up capability for the important phenomena such as the ECCS bypass and the Steam binding to the US-APWR, that includes the different core height. Therefore, the WCOBRA/TRAC(M1.0) code can be applied to the LBLOCA analysis in US-APWR without the additional biases of these phenomena model.

In addition, other important models that are treated as the uncertainty distributions for the statistical analysis are the heat transfer coefficient model of cladding wall at the hot spot and the critical flow model at the loop break point. The uncertainty distributions of the heat transfer coefficient model and the critical flow model have been evaluated according to the comparison between the test data and the calculation results. The lower linear heat rate relates to the heat transfer model so that the plant feature of the lower linear heat rate of US-APWR affects the cladding temperature directly. Although having said that, the effect of the different plant geometry does not affect the applicability of the heat transfer coefficient model since the scaling effect on the flow regime map model that determine the appropriate heat transfer coefficient model has just a small dependency. The effect of this difference does not affect the applicability of the critical flow model and the uncertainty, because the test conditions that have been used for the V&V envelope the US-APWR geometry.

The uncertainties of the operational condition are treated as input data to perform the statistical analysis (ASTRUM). Even under the situation that the operation condition is slightly different compared to the US-APWR, the models and the statistical analysis methodology are still applicable. Table 1.12-1 shows the comparison of some operating ranges of typical parameters used in the ASTRUM analysis for the WH 4-Loop PWR and US-APWR. As shown in Table 1.12-1, there is slight difference on the values of the operation condition for US-APWR, however, the operation range doesn't deviate from the application range of the all models included in the WCOBRA/TRAC(M1.0) code.

Consequently, the uncertainties of models and operation conditions for the LBLOCA analysis of US-APWR are treated appropriately by the WCOBRA/TRAC(M1.0) code as described in the topical report.

Table 1.12-1 Operating range information used in ASTRUM analysis

Question 1

RESPONSE

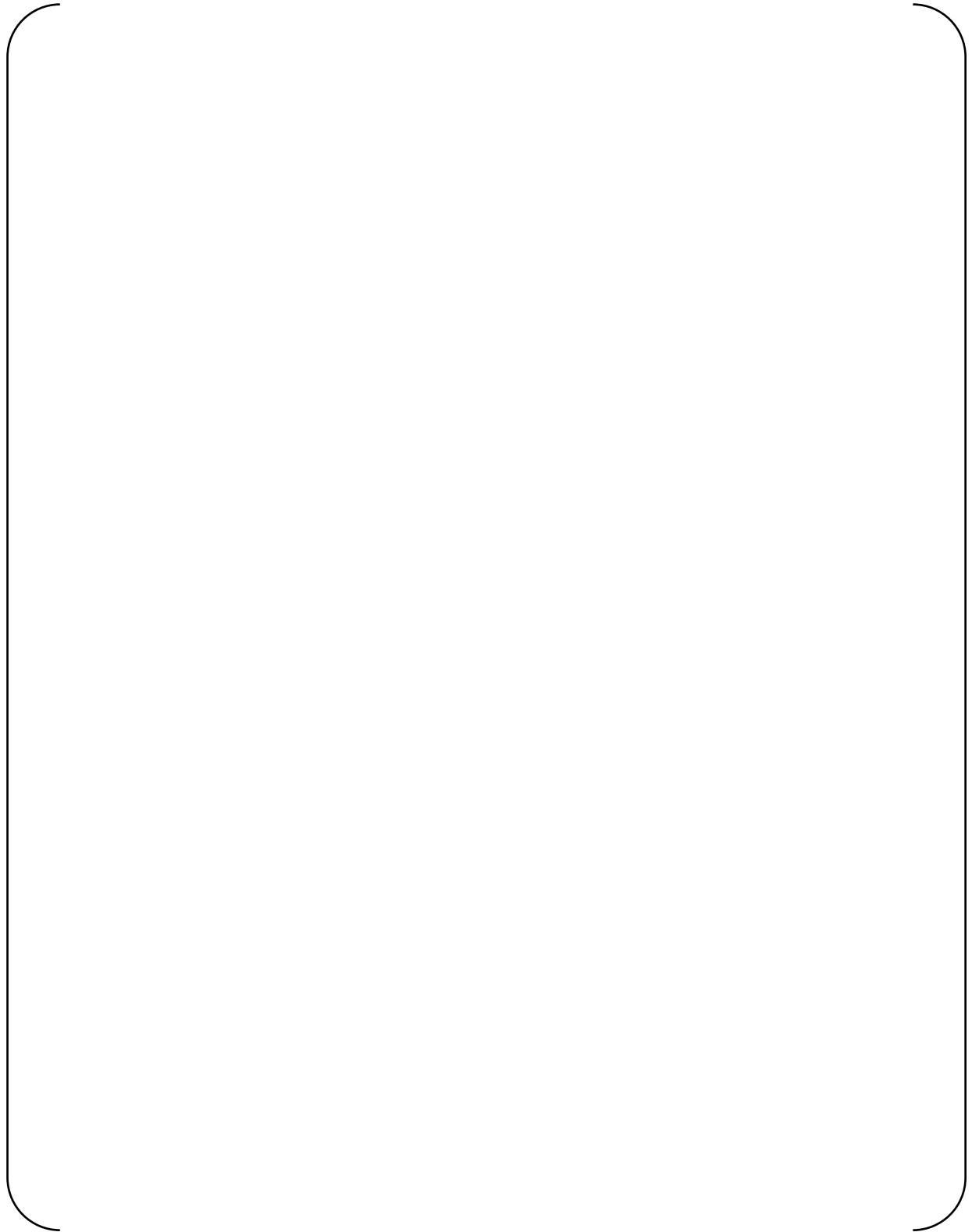




Question 2

RESPONSE





Question 3



RESPONSE







Question 4

As the US-APWR neutron reflector structure surrounds immediately the core periphery, the reflector ring blocks are subjected to high fluence dose rates that cause heat generation in the reflector metal from the irradiation exposure. The coolant flow through the neutron reflector holes cools the reflector ring blocks to minimize void swelling from irradiation of the reflector metal structure under normal operating conditions. As a result of heat deposition and cooling, a certain quasi steady-state temperature field is established within the neutron reflector metal wall volume at normal operating conditions.

As the amount of thermal energy, stored in the neutron reflector metal structure and available for release during a large break LOCA, is determined by this initial steady-state temperature field across the reflector wall, describe the applied approach in calculating the initial temperature field in the reflector metal structure. Provide the obtained results for the initial steady-state temperature field in the neutron reflector metal structure at nominal operating conditions and describe the initialization for the temperature field in the unheated conductors simulating the neutron reflector metal wall in the US-APWR WCOBRA/TRAC(M1.0) model.

Identify possible factors, if any, which can influence the prediction for the initial temperature field in the neutron reflector metal wall. For factors that can lead to higher initial temperature predictions, provide an assessment of the associated temperature effect.

RESPONSE

The neutron reflector (NR) metal temperature field was simulated using the ABAQUS code, which is a general purpose Finite Element Analysis computer program. In this analysis, the NR metal temperature distribution was calculated by using conservative values for the following inputs:

- Coolant flow rate through the NR holes
- Heat generation rate due to gamma irradiation

As stated in Question 4, the NR metal temperature is determined by the balance of the heat deposition (gamma irradiation) and the heat removal (coolant flow). Therefore, conditions that would cause high heat deposition and low heat removal were assumed for the analysis.

[

Question 5

RESPONSE

Question 6

Provide description of the nodalization scheme implemented in the input for the unheated conductors representing the neutron reflector metal ring blocks in the US-APWR WCOBRA/TRAC(M1.0) neutron reflector model. Substantiate the applicability of the nodding approach to adequately capture the release of thermal energy from the reflector metal wall governed by thermal conductivity within the structure metal wall and convection heat transfer to the surrounding fluid. In addition, provide the thermal properties data for the neutron reflector material and explain their implementation in the input model. Discuss possible effects of irradiation on the neutron reflector material thermal properties.

RESPONSE

(a) Description of nodalization scheme

The neutron reflector (NR) is located between the core and core barrel, and consists of thick stainless steel blocks. The NR is cooled by the coolant flow through [] flow holes in the blocks.

(b) Applicability of nodding approach

(c) Thermal properties data for NR material used in WCOBRA/TRAC(M1.0)

(d) Effects of irradiation on NR material thermal properties



Question 7

RESPONSE





Question 8

RESPONSE

Question 9

Table 6.3-5 "Safety Injection System Design Parameters (Sheet 2 of 3)" in MUAP-DC001 Revision 2 "Design Control Document for the US-APWR" describes the advanced accumulator as a vertical cylindrical vessel made of carbon steel with stainless steel cladding. During accumulator discharge and nitrogen gas expansion, heat, initially stored in the accumulator metal wall, is released to the contained gas volume due to heat transfer between the nitrogen gas and the tank wall driven by the gas temperature departure from the initial equilibrium temperature level. In turn, reduction in the tank wall temperature field, upon its propagation to the outer wall surface, will trigger heat transfer between accumulator wall and the ambient containment atmosphere. Heat transfer to the nitrogen volume inside the accumulator affects the gas pressure that drives the accumulator discharge.

The above described effects are compounded by the presence of a flow damper device that retards the advanced accumulator emptying and protracts the time period during which heat transfer between the tank wall and the nitrogen gas takes place. Quantify the effect of heat transfer from the accumulator wall to the nitrogen gas and demonstrate the WCOBRA/TRAC (M1.0) capability to account adequately for this effect in predicting the accumulator discharge performance.

RESPONSE

During the large flow rate phase, the effect of the heat transfer from the accumulator metal wall to the gas is not significant, due to the small heat transfer surface area per accumulator tank wall unit volume. However, during the small flow rate phase, the pressurization and depressurization inside the accumulator tank caused by heat transfer affect the gas pressure that drives the accumulator discharge.

During an LBLOCA transient, the containment temperature and pressure are raised due to the break flow from the primary system and the heat is transferred from the containment atmosphere to the tank wall. The heat conduction in the tank wall from the outer to the inner surface pressurizes the gas in the tank.

Therefore, to calculate the heat transfer between accumulator wall and the ambient containment atmosphere and between the nitrogen gas and the tank wall that helps the accumulator emptying, the condition between containment atmosphere and the tank outer wall and between the tank wall and tank inner gas are assumed to be adiabatic in the LBLOCA analysis.

Question 10

Upon reduction in pressure during the accumulator injection, nitrogen gas, initially dissolved in the accumulator liquid, will be released out of the liquid phase. Describe the effects of nitrogen gas release from the accumulator water and how these effects are modeled in WCOBRA/TRAC (M1.0) including validation and treatment of associated uncertainties. In particular, evaluate the effects of out-of-solution nitrogen gas on the performance characteristics of the advanced accumulator flow damper device.

RESPONSE

As stated in the response to RAI 4 (Ref. 10-1) to the advanced accumulator topical report (Ref. 10-2), if some of the tiny bubbles, which are released out of the liquid phase due to the reduction in pressure, are entrained in the flow coming into the vortex damper, they can reduce the apparent density of the water and cause a reduction in the flow rate coefficients for the flow damper.

However, since the diffusion coefficient of nitrogen is very small as discussed in the last paragraph of the response to RAI 5-b (Ref. 10-1), the bubbles cannot increase significantly in a very short time (less than 1 sec) during which the bubbles go through the flow damper.

The released nitrogen gas was not modeled in the WCOBRA/TRAC (M1.0), because its effect to the flow damper device is negligible. The resistance of the discharged flow rate from the accumulator due to the nitrogen-gas is accounted in the uncertainty of the accumulator flow line resistance.

References

- 10-1: UAP-HF-08174-P (R0) "MHI' Responses to NRC's RAI on Advanced Accumulator for US-APWR Topical Report MUAP-0701-P (R1)" September 2008
- 10-2: MUAP-07001-P (R1) "The Advanced Accumulator," 2007

negligible. For small flow injection, σ_v hardly affects C_v , and the influence of the difference of the pressure, P_D , to the injection characteristic can be negligible, even if there was some difference on cavitation inception.

Question 12

[]

RESPONSE

[]

Question 13

RESPONSE

Question 14

RESPONSE

Question 15

RESPONSE

Question 16

RESPONSE

Question 17

RESPONSE

Question 18

RESPONSE

Question 19

RESPONSE



Question 20

RESPONSE



Question 21

Following reactor vessel refill and partial recovery of downcomer coolant inventory accumulator discharge, direct vessel injection provides safety flow during the core reflood phase and long term cooling.

Describe the WCOBRA/TRAC direct vessel injection modeling approach for the US-APWR, including its validation for the specific direct vessel injection configuration and downcomer characteristics of the US-APWR design. Demonstrate the code capabilities in predicting the effects of direct vessel injection on downcomer liquid inventory. In particular, address effects related to injection flow distribution, downcomer liquid temperature response, as well as potential for void development in the downcomer region and associated liquid spillover through the break.

RESPONSE

Question 22

It is stated in Section 3.3.3 "Refilling Period" of MUAP-07011-P (R0) "Large Break LOCA Code Applicability Report for US-APWR" that the High Head Safety Injection (HHSI) system turns on automatically and injects emergency coolant into the vessel downcomer during the refill period of a large break LOCA. This description of HHSI injection into the vessel during the refill period does not appear consistent with information found in Table 3.3-1 and in Figure 3.3-2, both of which indicate HHSI occurs during the core reflood period. In addition, MUAP-DC001 Revision 2 "Design Control Document for the US-APWR" Section 15.6.5.3.3.1 "Large Break LOCA Analysis Results" states that HHSI begins coolant injection into the vessel during the reflood period.

Explain the sequence of HHSI system operation following a large break LOCA, including delay time between ECCS actuation signal generation and start of vessel injection. In the case of the reference large break LOCA transient calculation, presented in MUAP-DC001 Revision 2 "Design Control Document for the US-APWR" Section 15.6.5.3.3.1 "Large Break LOCA Analysis Results," ECCS actuation signal is generated at 6 s and start of vessel injection occurs at 124 s, 90 s after the end of the blowdown phase predicted 34 s transient time. Clarify or correct the apparent inconsistency between the information provided in MUAP-07011-P R(0) Section 3.3.3 "Refilling Period" and that found in Table 3.3-1 "Typical Sequence of the LBLOCA of US-APWR" and in Figure 3.3-2 "ECCS Flow Injection Performance during LBLOCA" of the same report as well as in MUAP-DC001 Revision 2 "Design Control Document for the US-APWR" Section 15.6.5.3.3.1 1 "Large Break LOCA Analysis Results".

RESPONSE

In the plant analysis described in the topical report, SI signal actuated by the low pressure in the pressurizer's vapor space during a LBLOCA transient. The assumed delay time to start the HHSI injection is [

]. The most severe condition for the core and the PCT occurrence time in the US-APWR LBLOCA transient tend to occur until about [] after the break, therefore, the assumption for delay time is conservative enough for US-APWR LBLOCA analysis. The same delay time is used in the LBLOCA analysis of DCD Revision 2 (Ref. 22-1).

The description in Section 3.3.3 of the topical report "Refilling Period" about the coolant injection through the DVI is not consistent with Table 3.3-1 "Typical Sequence of the LBLOCA of US-APWR" and that illustrated in Figure 3.3-2 "ECCS Flow Injection Performance during LBLOCA". The statement of HHSI in Section 3.3.3 "Refilling Period" should be eliminated, instead should be added to be a part of "Reflooding Period".

The description in Table 3.3-1 about "start of core-reflooding" during the refilling period is not consistent with the description in Section 3.3.3. This part of table 3.3-1 should be corrected as "start of core-reflooding" is the start of "Reflooding" period.

The information of Figure 3.3-2 is consistent with the description in Section 3.3.3.

Reference

22-1 MUAP-DC001 Revision 2 "Design Control Document for the US-APWR"

Question 23

MUAP-07011-P R(0) "Large Break LOCA Code Applicability Report for US-APWR" Table 3.3-1 "Typical Sequence of the LBLOCA of US-APWR" states that the ECCS actuation signal, or "S" signal, is generated by a containment high pressure condition during the blowdown period. MUAP-DC001 Revision 2 "Design Control Document for the US-APWR" Section 15.6.5.3.3.1 "Large Break LOCA Analysis Results" states that the ECCS signal is generated due to low pressurizer pressure signal in the reference large break LOCA transient calculation.

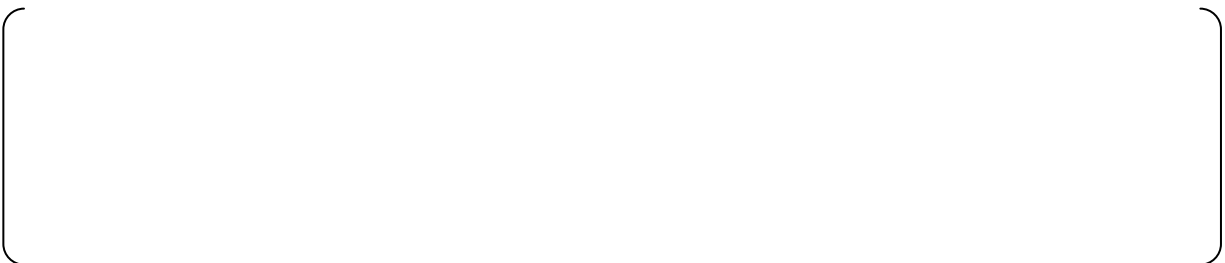
Present all parameters and related conditions that can lead to S signal actuation following a large break LOCA in the US-APWR design. For each parameter, give the corresponding set point for signal generation along with pertinent causes for delay times and variation ranges, as applicable. Identify any assumptions made with regard to the implementation of the safety actuation signal logic in the US-APWR large break LOCA analysis methodology using WCOBRA/TRAC(M1.0). Include a summary table listing all numerical data for each of the parameters identified. Explain how the information provided in this table relates to the data provided in MUAP-DC001 Revision 2 "Design Control Document for the US-APWR" Table 15.0-4 "Reactor Trip and ESF Actuation Analytical Limits and Time Delays Assumed for Transient Analyses."

RESPONSE

As described below, there are two kinds of parameters and related conditions that can lead to the ECCS signal actuation following a large break LOCA in the US-APWR design.

- Low pressurizer pressure
- High containment pressure

For these two ECCS actuation signals, the requested information (set point, pertinent causes for delay times and variation ranges) is described in Subsection 7.3.1.5.1 and Table 7.3-4 of the DCD Revision 2, and then a summary included in all numerical data is shown in Table 23-1.



The difference between the analytical limit in Table 15.0-4 of the DCD Revision 2 and the setpoint in Table 23-1 accounts for instrumentation channel error and setpoint error.

Table 23-1 Summary Table



Question 24

Describe the logic for reactor trip, main reactor coolant pump trip, and main steam line isolation following a large break LOCA in the US-APWR design. For each parameter, give the corresponding set point for signal generation along with pertinent causes for delay times and variation ranges, as applicable. Identify any assumptions made with regard to the implementation of the safety actuation signal logic in the US-APWR large break LOCA analysis methodology using WCOBRA/TRAC(M1.0). Identify and substantiate any assumptions with regard to the main coolant pump response following pump trip signal actuation for coolant pumps in both affected and intact loops.

RESPONSE

(a) Logic for reactor trip and requested information

As described below, there are three kinds of parameters and related conditions that can lead to reactor trip signal following a large break LOCA in the US-APWR design.

- Low pressurizer pressure
- Low reactor coolant flow
- Over temperature ΔT

The logic for these three reactor trip signals is described in Subsection 7.2.1.4.3.5, Subsection 7.2.1.4.3.3, Subsection 7.2.1.4.3.1 and Figure 7.2-2 (Sheet 5 of 21) of the DCD Revision 2. And the requested information (set point, pertinent causes for delay times and variation ranges) is described in Table 7.2-3 of the DCD Revision 2.

(b) Logic for main reactor coolant pump trip and requested information

The logic for main reactor coolant pump trip following a large break LOCA in the US-APWR design is described in Subsection 7.3.1.5.1 and Figure 7.2-2 (Sheet 11 of 21) of the DCD Revision 2. And the requested information (set point, pertinent causes for delay times and variation ranges) is described in Subsection 7.3.1.5.1 of the DCD Revision 2.

(c) Logic for main steam line isolation and requested information

As described below, there is one type of parameter and related condition that can lead to main steam line isolation following a large break LOCA in the US-APWR design.

- High-high containment pressure

The logic for this main steam line isolation signal is described in Subsection 7.3.1.5.2 and Figure 7.2-2 (Sheet 9 of 21). And the requested information (set point, pertinent causes for delay times and variation ranges) is described in Table 7.3-4 of the DCD Revision 2.

(d) Assumptions in the US-APWR LBLOCA analysis methodology

ECCS action signal

The treatment of the ECCS actuation signal in the US-APWR LBLOCA analysis

methodology using WCOBRA/TRAC(M1.0) is answered in the RAI response of Question 23.

Reactor trip

--

Main reactor coolant pump trip

--

Main steam line isolation

--

Question 25

A comparison between the list of highly ranked models and phenomena provided in Section 3.4.1 "LBLOCA PIRT" and the information contained in Table 3.4-1 "US-APWR PIRT" of MUAP-07011-P R(0) "Large Break LOCA Code Applicability Report for US-APWR" reveals that not all the highly ranked models and phenomena given in Table 3.4-1 were included in the section text. In particular, not all of the H-ranked items identified in the Phenomena Identification and Ranking Table (PIRT) were included in the Section 3.4.1 "LBLOCA PIRT" list.

Explain how the list of highly ranked models and phenomena provided in MUAP-07011-P R(0) Section 3.4.1 "LBLOCA PIRT" correspond to the ranking in the US-APWR PIRT as documented in Table 3.4-1 "US-APWR PIRT" and substantiate any discrepancies.

RESPONSE

The description in Section 3.4.1 in the topical report does not yet cover all the high ranked phenomena. The following description is provided to complement the lack of information/description for the high ranked phenomena.

Fuel rod	
Core	
Pump	
Downcomer	

In conclusion, the description given in Section 3.4.1 is now consistent with that given in the table 3.4-1.

Question 26

MUAP-07011-P R(0) "Large Break LOCA Code Applicability Report for US-APWR" Section 3.6.3.3 "Containment Pressure Calculation Model" explains that the containment pressure used as a boundary condition for WCOBRA/TRAC(M1.0) large break LOCA analyses is calculated with the GOTHIC code in accordance with SRP 6.2.1.5 requirements. Furthermore, MUAP-DC001 Revision 2 "Design Control Document for the US-APWR" Section 6.2.1.5 "Minimum Containment Pressure Analysis for Performance Capability Studies of the Emergency Core Cooling System" describes the GOTHIC analytical model.

SRP 6.2.1.5 refers to RG 1.157 and BTP 6-2 for guidance on an acceptable minimum containment pressure model for ECCS performance evaluation. Prove that the applied single-volume US-APWR GOTHIC containment model yields containment pressure responses that are conservatively low for LOCA analyses across the entire spectrum of ASTRUM run conditions for best-estimate large break LOCA analyses with WCOBRA/TRAC(M1.0). Identify all assumptions and conservative margins used in the representation of the containment volume, associated heat structures, and RWSP water volume initial conditions as well as governing modeling assumptions such as multipliers for heat transfer coefficients for steam condensation on pool water. Quantify the margin of conservatism in the predicted containment pressure responses. If the containment pressure history presented in MUAP-DC001 Revision 2 "Design Control Document for the US-APWR" Figure 6.2.1-80 was applied to all best-estimate large break LOCA analyses, justify that it was conservative assumption for all cases analyzed.

RESPONSE

Single node modeling for containment volumes doesn't provide biased results in one direction for the US-APWR containment pressure evaluation. Whether the calculated pressure transient during LOCA is overestimated or underestimated depends on various assumptions regarding free volume, component and heat and mass transfer phenomena. Conservatisms obtained by assuming single node modeling are identified as follows:

Considering the described conservative assumptions in the DCD methodology for calculating minimum containment pressure following a LOCA event, the demonstrated conservatism relative to the BE model, and the relative insensitivity of the PCT to the containment pressure, the DCD methodology will give conservatively low containment pressure for all the ASTRUM cases.

Table 26-1 Biased Assumption for Minimum Containment Pressure Evaluation

Item	Assumption in DCD	Best Estimate (Some Parts Tend to be Conservatively Biased)	Regulatory Requirement by SRP6.2.1.5[1], SRP BTP 6.2[2] and RG 1.117[3]
Free Volume	Maximum		Maximum
Purge	Equivalent volume for depressurization is considered in margin for initial containment volume		System lines should be assumed
Containment Volume Modeling	Single node		N/A
Initial RWSP Liquid Volume	Maximum value in operation		N/A
Passive Heat Sinks	-Overestimated -Surface heat resistances by coatings are ignored		- Passive heat sinks should be considered - No resistance should be considered
Fluid Initial Condition	Pressure: Lowest value in operation, 14.396psia Temperature: Lowest value in operation, 70degF Humidity: 100%		Pressure: Lowest Temperature: Lowest Humidity: Maximum
Condensation Heat Transfer Coefficient with Passive Heat Sinks	4×Tagami for peak HTC and interpolated 1.2×Uchida subsequent to peak		4×Tagami for Peak HTC and Interpolated 1.2×Uchida subsequently
Other Heat Transfer Mode with Passive Heat Sinks	-Natural and forced convection -Radiation with containment atmosphere		N/A
Heat and Mass Transfer with RWSP Liquid Phase	Initial surface area with no multiplier on GOTHIC internal model as described in the text		N/A
Heat Transfer with Ambient	Considered with lowest outer temperature, -40 degF		A reasonably low ambient temperature
Containment Spray Initiation	At 0 sec		All containment spray trains operating at maximum flow conditions
Containment Spray Operation	All trains (4/4) operating with maximum flowrate		All containment spray trains operating at maximum flow conditions
Heat Removal by Containment Spray (CS)/ Component Cooling Water (CCW) System	Spray fluid temperature is fixed to be 32 degF		Maximum heat removal capacity
Containment Steam Mixing with Spilled ECCS Water	Treated as drops with diameter small enough achieve thermal equilibrium with the containment atmosphere		Steam-water mixing should be considered

Table 26-2 Pool Interfacial Heat and Mass Transfer Correlations

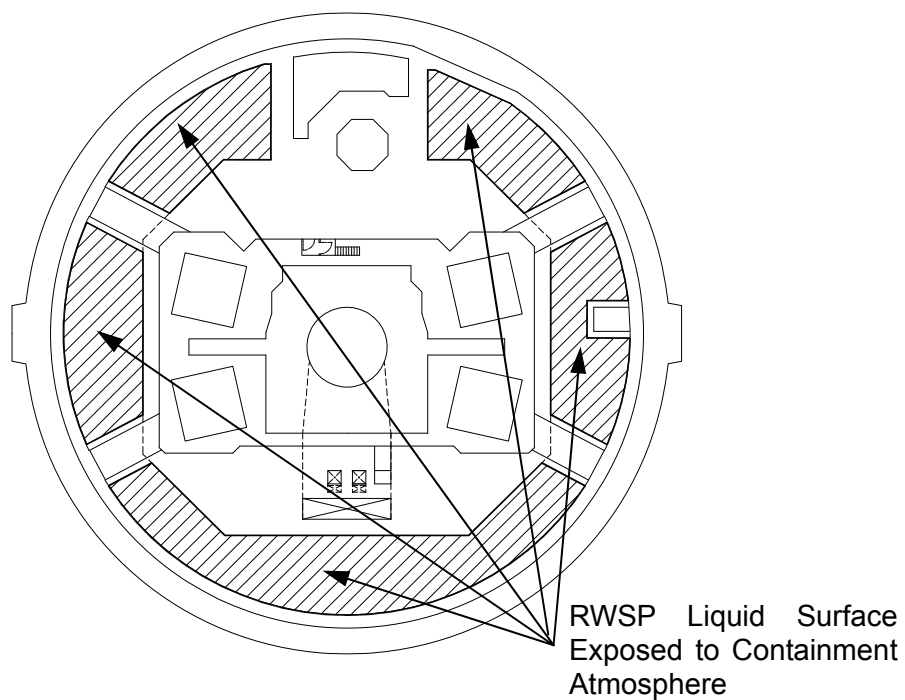



Figure 26-1 RWSP Surface Area



Security-Related Information – Withheld Under 10 CFR 2.390

Figure 26-2 RWSP Location

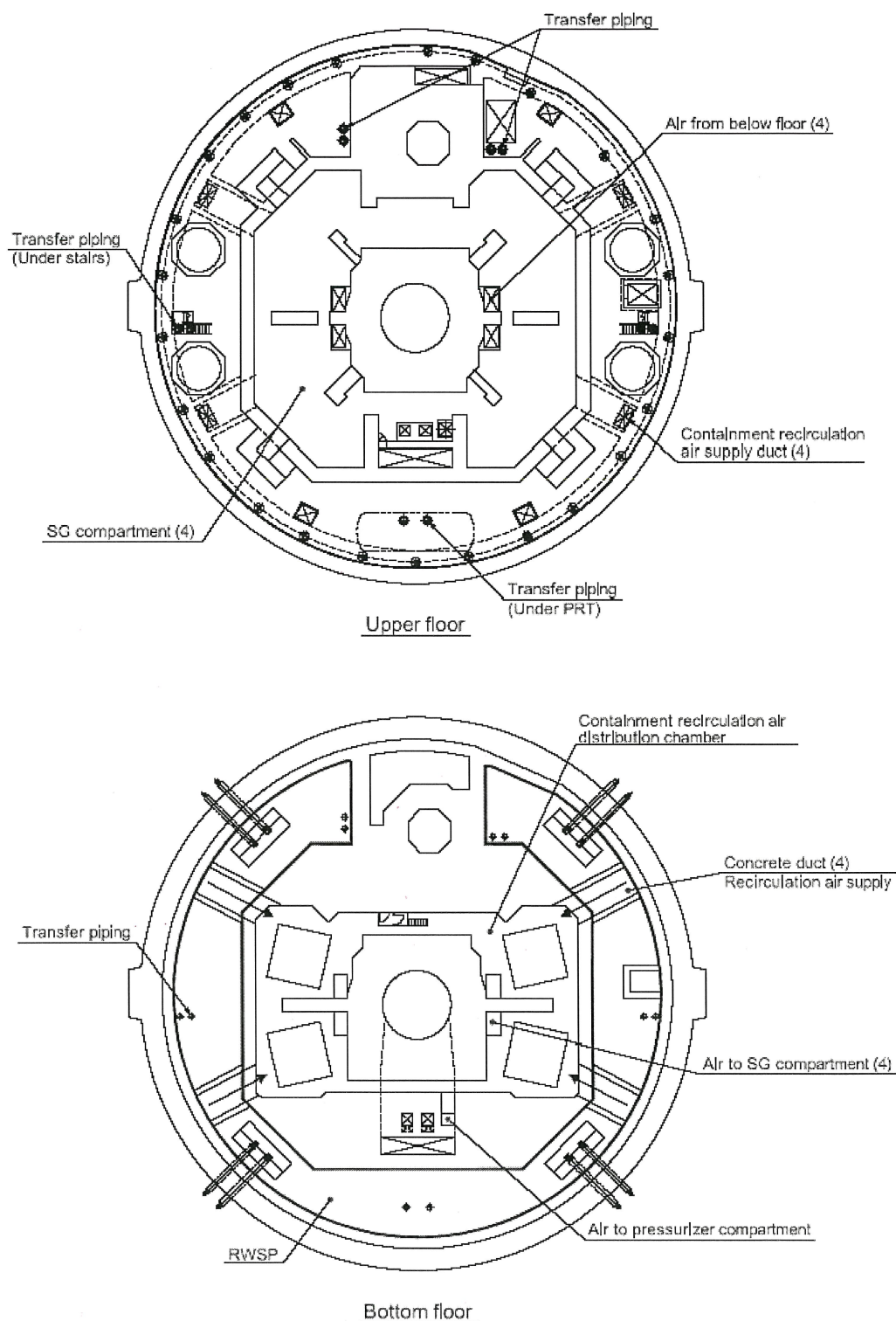


Figure 26-3 RWSP and Containment Connecting Paths (1/2)

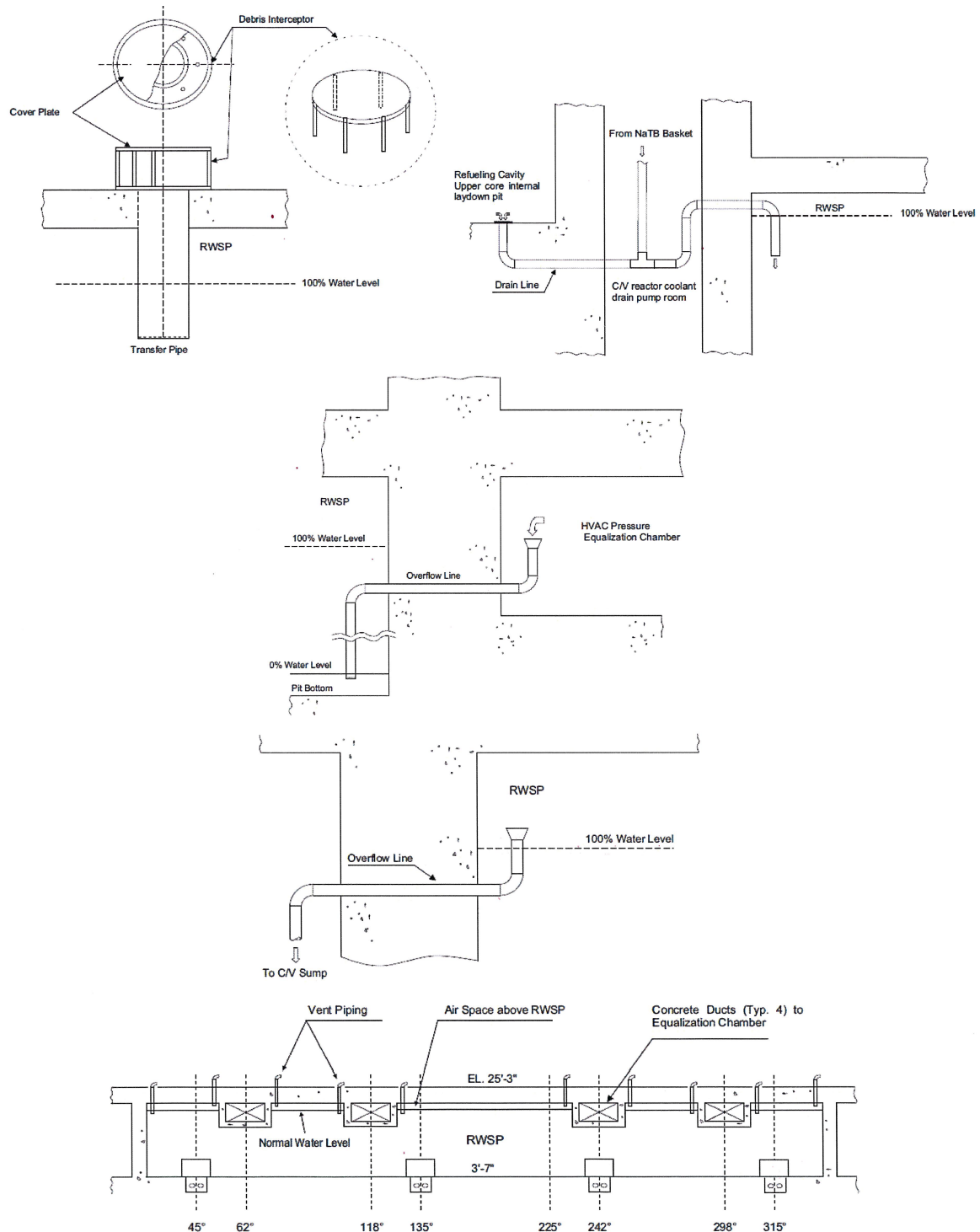


Figure 26-3 RWSP and Containment Connecting Paths (2/2)

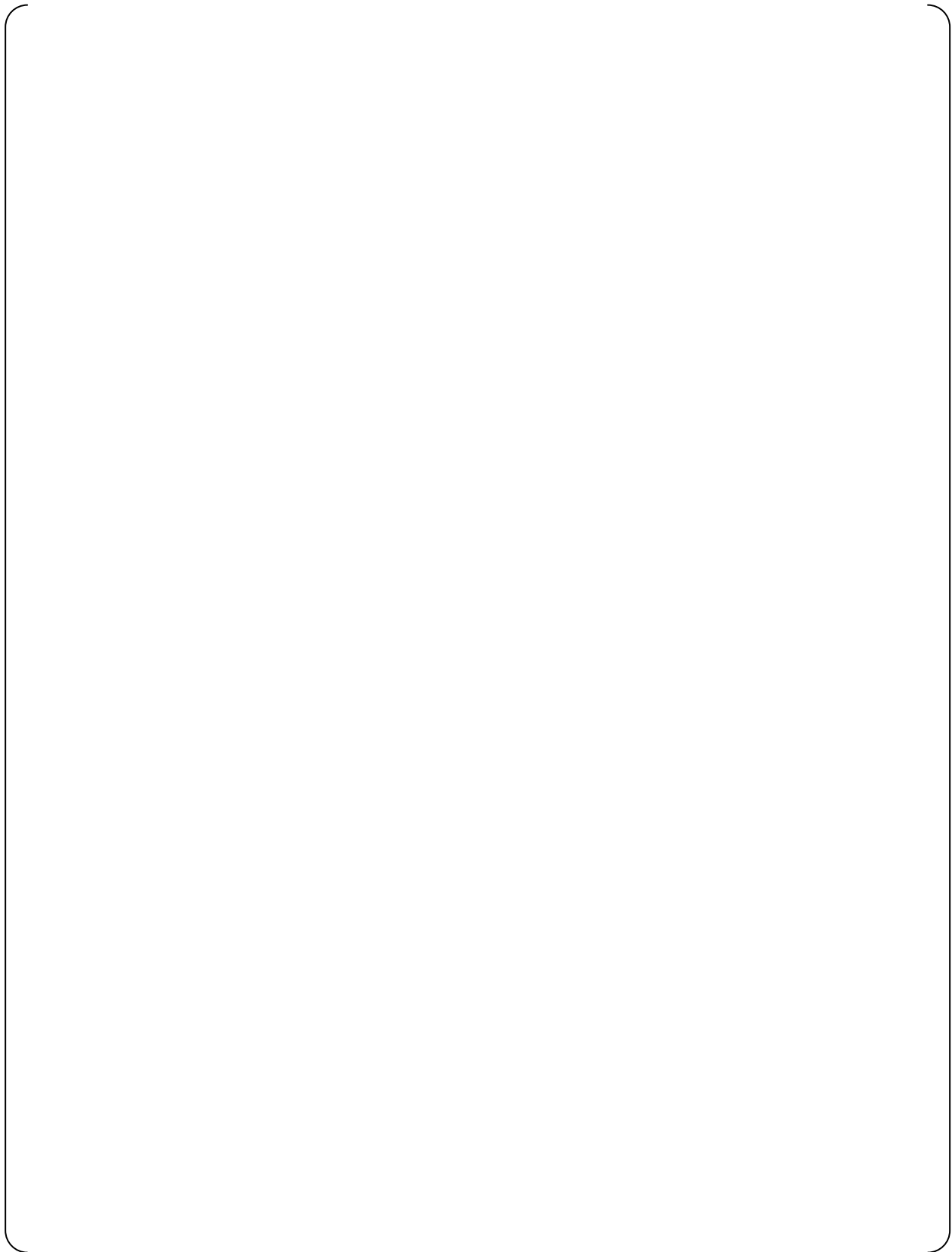
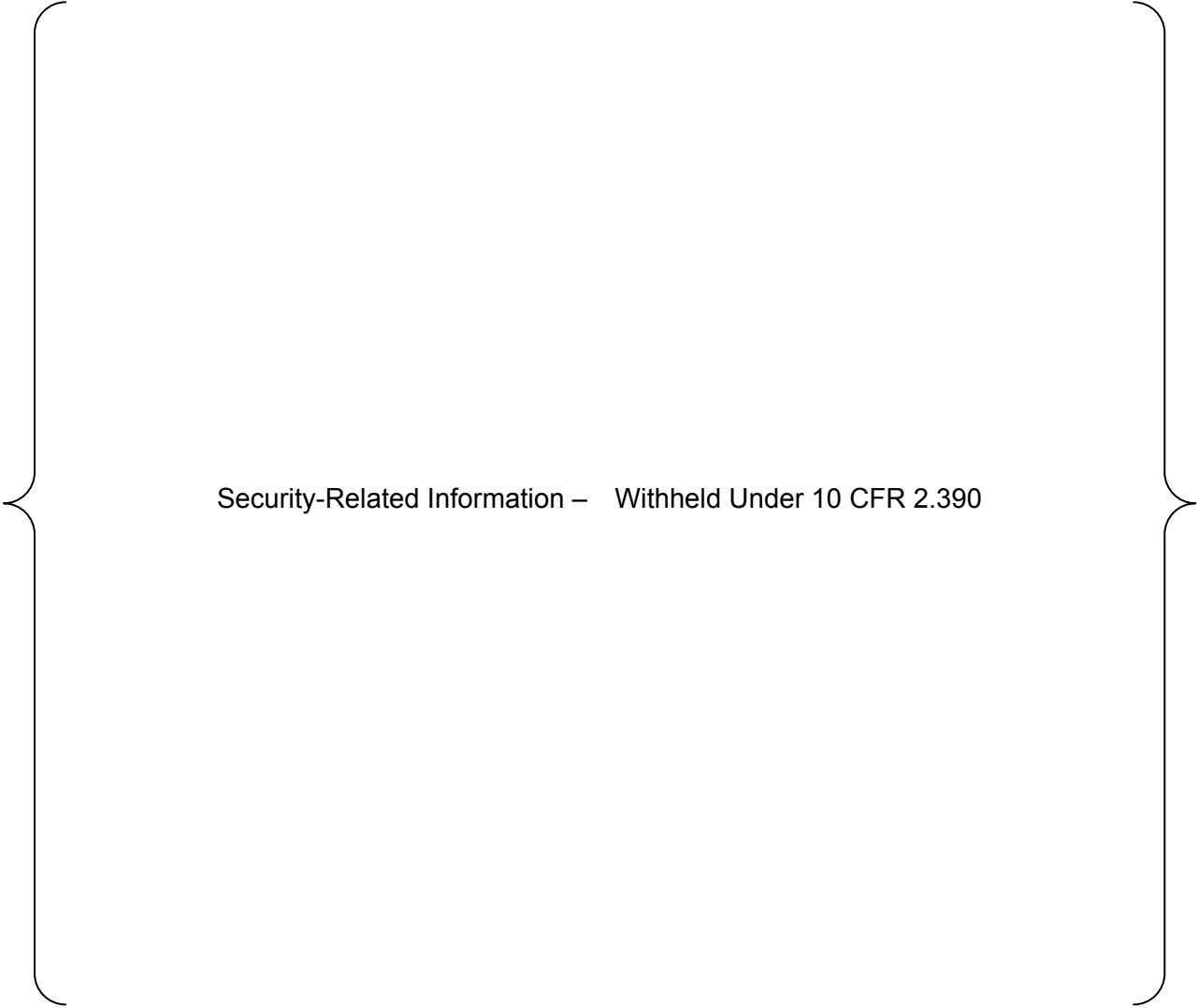


Figure 26-4 Analytical Assumption for Steam Condensation at Surface of RWSP Liquid



Security-Related Information – Withheld Under 10 CFR 2.390

Figure 26-5 Containment Spray Covering Region



Figure 26-6 Interface Heat and Mass Transfer in GOTHIC



Figure 26-7 Containment Pressure



Figure 26-8 Hot Rod PCT for Sensitivity Case and Base Case

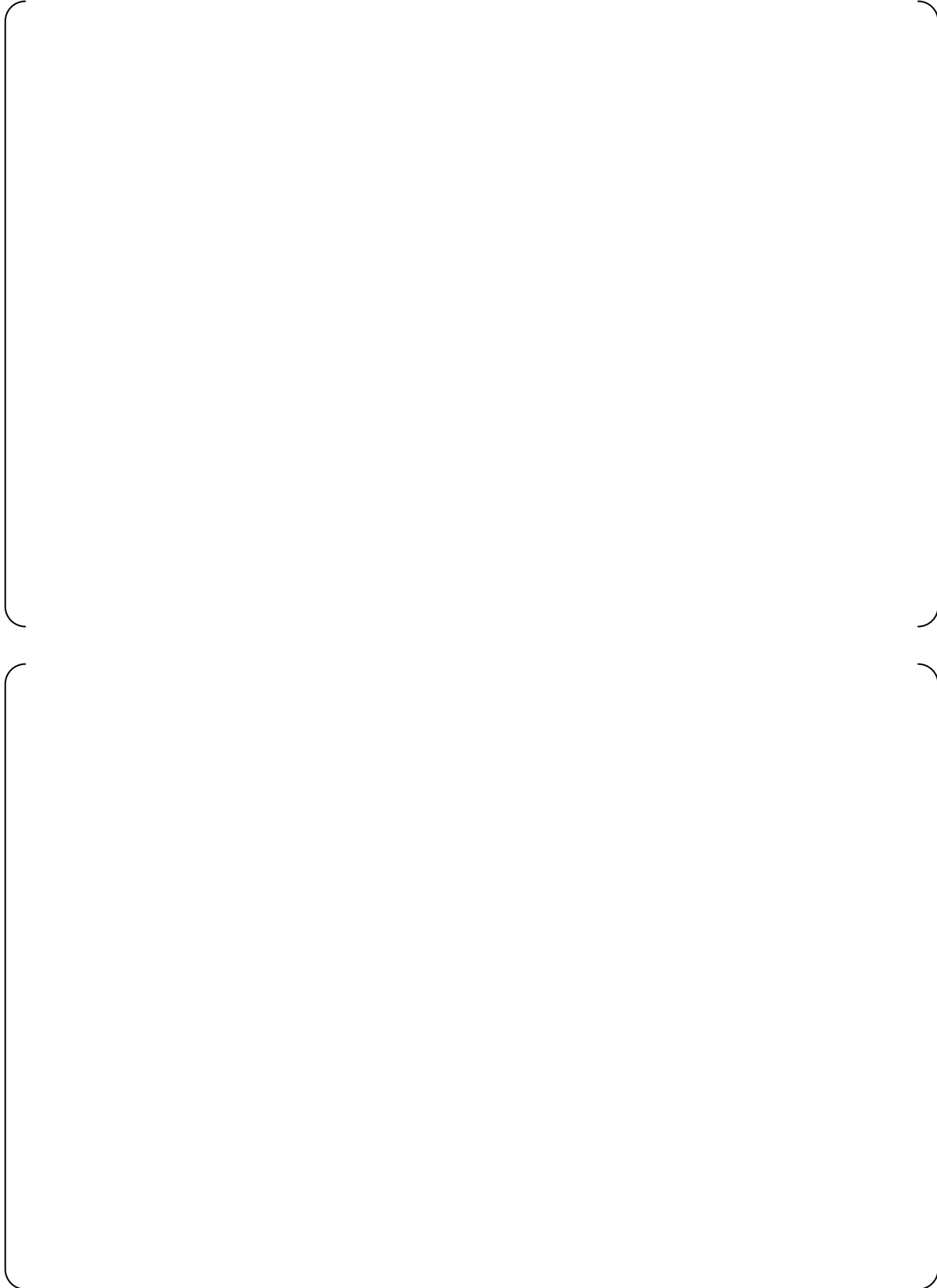
References:

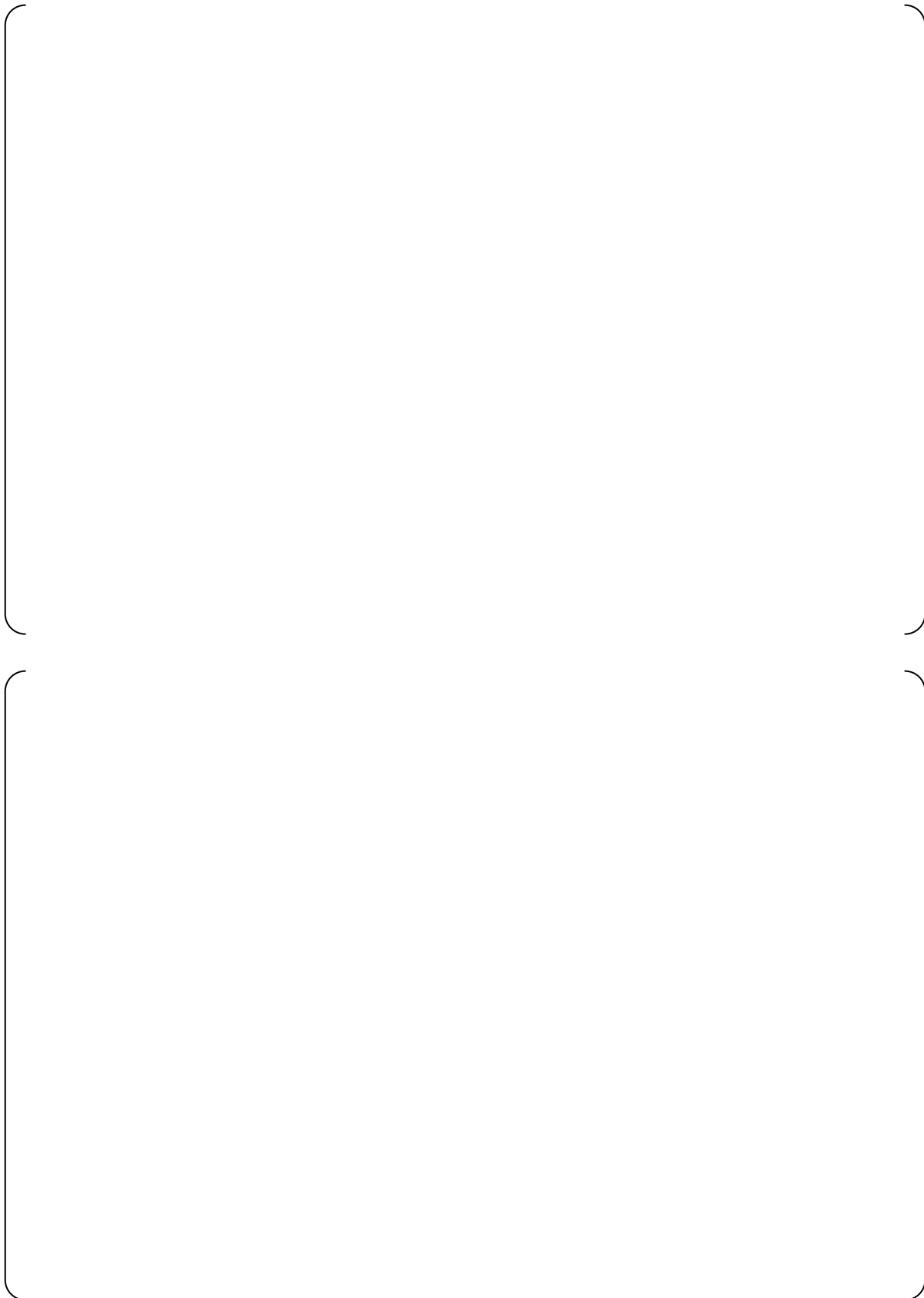
1. NUREG-800 Standard Review Plan 6.2.1.5, "Minimum Containment Pressure Analysis for Emergency Core Cooling System Performance Capability Studies", Revision 3
2. NUREG-800 Standard Review Plan Branch Technical Position 6-2, "Minimum Containment Pressure Model for PWR ECCS Performance Evaluation", Revision 3
3. Regulatory Guide 1.157, "Best-Estimate Calculations of Emergency Core Cooling System Performance"
4. Validation Report AI-6.1-171, "Heat and Mass Transfer at Conductor Surfaces in GOTHIC", Revision 0
5. NAI 8907-06 Revision 16, "GOTHIC Containment Analysis Package Technical Manual Version 7.2a (QA)"
6. Bird, Stewart and Lightfoot, "Transport Phenomena", Second Edition

Question 27

RESPONSE







Question 28

RESPONSE

Question 29

MUAP-07011-P R(0) "Large Break LOCA Code Applicability Report for US-APWR" Table 3.6-5 states the control rod drop time as "no drop". US-APWR DCD application FSAR Section 15.6.5.2.1 "Description of Large Break LOCA" credits reactor trip for core power reduction.

Clarify whether control rods are assumed to insert in the US-APWR best-estimate large break LOCA analyses. Identify the reactivity mechanisms that accomplish reactor shutdown following a large break LOCA. In addition, provide and substantiate the reactivity insertion and feedback coefficients applied in predicting the core power.

RESPONSE

For the US-APWR'S LBLOCA analysis, the "no drop" of control rods is assumed in order to maintain conservative margin. This assumption is commonly adopted when analyzing LBLOCA behavior for the ECCS performance analysis.

A large amount of negative reactivity is inserted in the reactor without control rods insertion because enough mass of the coolant released from the reactor vessel keep the void fraction in the core high. The core turns sub-critical instantly and shutdown after the large break occurs because of the insertion of large negative void reactivity. (Figure29-1 and Figure29-2)

In spite of the coolant being released from the reactor vessel, the borated-coolant is injected from the accumulators and the HHSI pumps to maintain sub-criticality during refill and reflood phases.

In addition, "the reactor trip" described in section 15.6.5.of DCD r2 (Ref. 29-1) means only trip signal actuation. This term does not mean "reactor shutdown".

Reference

29-1 MUAP-DC001 Revision 2 "Design Control Document for the US-APWR"

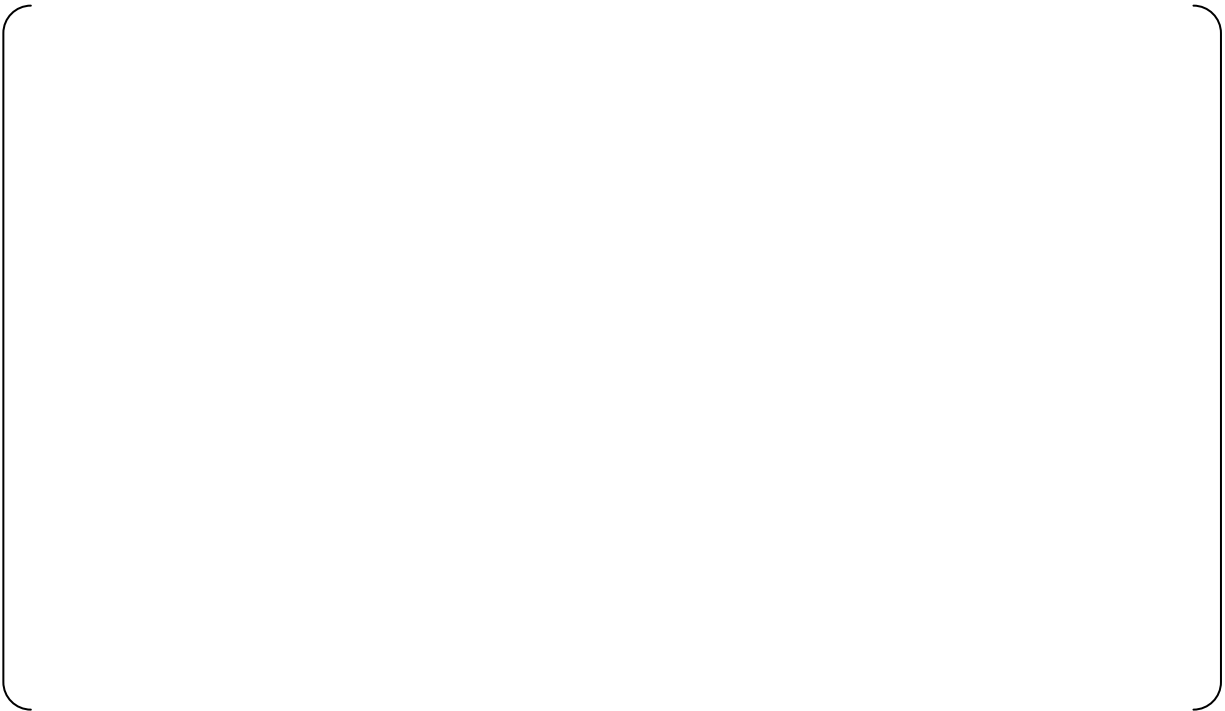


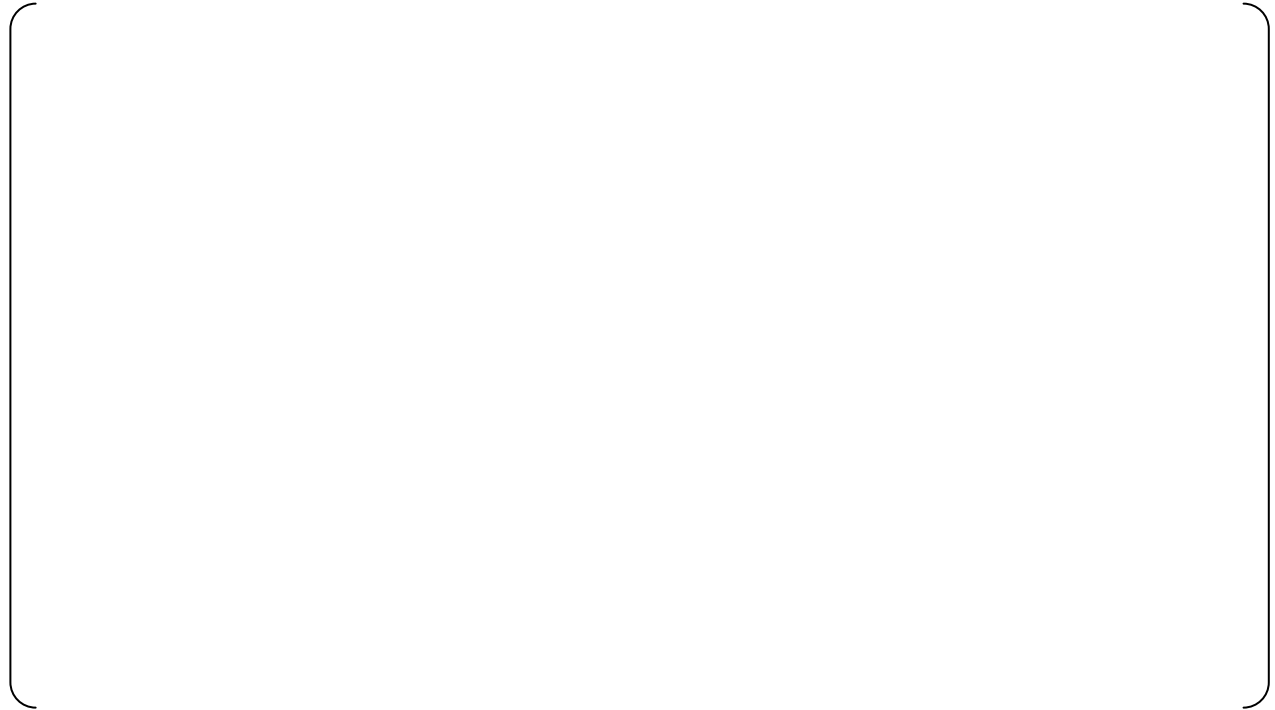
Figure 29-1 Reactivity inserted during LBLOCA



Figure 29-2 Core power during LBLOCA

Question 30

RESPONSE







Question 31

Table 3.7-1 "Uncertainty Treatment for US-APWR" of MUAP-07011-P R(0) "Large Break LOCA Code Applicability Report for US-APWR" identifies "Core Power" for uncertainty treatment. Describe how reactor core power level is treated in the ASTRUM uncertainty analysis for performing US-APWR best-estimate large break LOCA predictions. Explain treatment of instrument calibration and measurement uncertainty in determining initial power operating conditions.

RESPONSE

In determining initial power operating conditions for the US-APWR, the uncertainty of the core power level is within $\pm 2\%$ based on the calorimetric measurement uncertainty. Therefore, the initial core power in the ASTRUM uncertainty analysis is treated as shown in Table 31-1.

Table 31-1 Treatment of Core Power in the ASTRUM Uncertainty Analysis

--

Question 32

Some of the references cited in the first paragraph of MUAP-07011-P R(0) "Large Break LOCA Code Applicability Report for US-APWR" Section 4.0 "Conclusions" appear to be inconsistent with corresponding titles identified in Section 5.0 "References." In particular, references to the AP600 design and the AP1000 design appear incorrect. Verify all references in MUAP-07011-P R(0) Section 4.0 "Conclusions" and correct the list of references in Section 5.0 "References" as found appropriate.

RESPONSE

MHI has corrected and verified the references cited in the first paragraph of MUAP-07011-P R(0) "Large Break LOCA Code Applicability Report for US-APWR" Section 4.0 "Conclusions" to be as follows:

Original Paragraph

This report provides an assessment of the WCOBRA/TRAC code that was approved by the NRC for the Westinghouse-design 2-,3- and 4- Loop PWRs (Ref.1, 6) , and the CE-design PWR, the AP600 (Ref.3) , and the AP1000 (Ref.4) Design Certifications to determine the applicability and appropriateness of use for Design Certifications of the US-APWR.

Corrected Paragraph

This report provides an assessment of the WCOBRA/TRAC code that was approved by the NRC for the Westinghouse-design 2-,3- and 4- Loop PWRs (Ref.1, 6), the C E-design PWR, the AP600 (Ref.2), and the AP1000 (Ref.3) Design Certifications with the purpose to determine the applicability and appropriateness of its use for the Design Certification of the US-APWR.

Question 33

Section 3.6.1 "Nodalization of Plant Analysis" of MUAP-07011-P R(0) "Large Break LOCA Code Applicability Report for US-APWR" describes the nodalization scheme used for the WCOBRA/TRAC(M1.0) plant model. In addition to the plant nodalization analysis, provide description of the time step controls and numerical convergence criteria used in the WCOBRA/TRAC(M1.0) analyses. Include the results from any sensitivity studies performed to evaluate the effects of time step control and their applicability to the US-APWR design large break LOCA analyses.

RESPONSE

Table.33-1 Conditions for Sensitivity Analysis

--

Table.33-2 Result of Sensitivity analysis

--



Figure.33-1 Time Step Size



Figure.33-2 PCT Comparison

Question 34

RESPONSE

Question 36

Table 3.7-2 "Local Model Uncertainty Treatment for US-APWR" of MUAP-07011-P R(0) "Large Break LOCA Code Applicability Report for US-APWR" provides the fuel local parameters that are explicitly treated in the ASTRUM uncertainty analysis. Explain the treatment of fuel manufacturing tolerances in the ASTRUM uncertainty analysis.

RESPONSE



Question 37

MUAP-07011-P R(0) "Large Break LOCA Code Applicability Report for US-APWR" does not explicitly address NUREG/CR-5249 CSAU Step 5. Conformance with NUREG/CR-5249 CSAU Step 5 requires that adequate documentation of the frozen code identified in CSAU Step 4 be provided, including, at minimum, a user manual, user guide, developmental assessments reports, and the models and correlations quality evaluation report.

Provide the above-mentioned developmental assessments reports, and the models and correlations quality evaluation report for the frozen version of WCOBRA/TRAC (M1) code.

RESPONSE



Question 38

Section 3.6.1 "Nodalization of Plant Analysis" of MUAP-07011-P R(0) "Large Break LOCA Code Applicability Report for US-APWR" describes that the US-APWR nodalization scheme is identical to the one used for the Westinghouse conventional 3- and 4-loop PWR plants as discussed in the WCOBRA/TRAC Code Qualification Document WCAP-12945-P-A.

Identify and justify any differences in the WCOBRA/TRAC (M1.0) US-APWR plant and vessel model noding from that used in the referenced WCAP-12945-P-A report. In addition, describe the noding sensitivity studies performed for the cold leg piping in the vicinity of the break or justify the applicability of the studies performed previously for the conventional 4-loop PWR plants, considering system design and size differences from the US-APWR.

As new safety features in the US-APWR design, describe and present the results from noding sensitivity studies performed for the new advanced accumulator model as well as for the ECC direct vessel injection ports.

RESPONSE

As shown in MUAP-07011(R0) section 3.6.1, nodalization for the US-APWR is established based on the same scheme used for the conventional 3 and 4 loop plant (Ref.38-1).

Noding sensitivity studies of WCOBRA/TRAC(M1.0), which is related to the new or improved features of the US-APWR as mentioned above, have been performed. The contents of the studies are given below.

(1) Noding sensitivity study of the break point

(2) Noding sensitivity study of ACC injection point



Figure 38-1 Broken Loop Cold Leg Nodalization (Base Case)



Figure 38-2 Broken Loop Cold Leg Nodalization for Steady State Calculation
(Sensitivity Study)



Figure.38-3 RCP Side Cold Leg Break Flow (Break Point Node sensitivity)



Figure.38-4 RV Side Cold Leg Break Flow (Break Point Node sensitivity)



Figure.38-5 Core Pressure (Break Point Node sensitivity)



Figure.38-6 PCT (Break Point Node sensitivity)



Figure 38-7 Intact Loop Cold Leg Nodalization (Base Case)



Figure 38-8 Intact Loop Cold Leg Nodalization for Steady State Calculation
(Sensitivity Study)



Figure.38-9 Accumulator Flow Rate (ACC Injected Point Node sensitivity)



Figure.38-10 Lower Plenum Collapsed Liquid Level
(ACC Injected Point Node sensitivity)



Figure.38-11 Downcomer Average Collapsed Liquid Level
(ACC Injected Point Node sensitivity)



Figure.38-12 PCT (ACC Injected Point Node sensitivity)

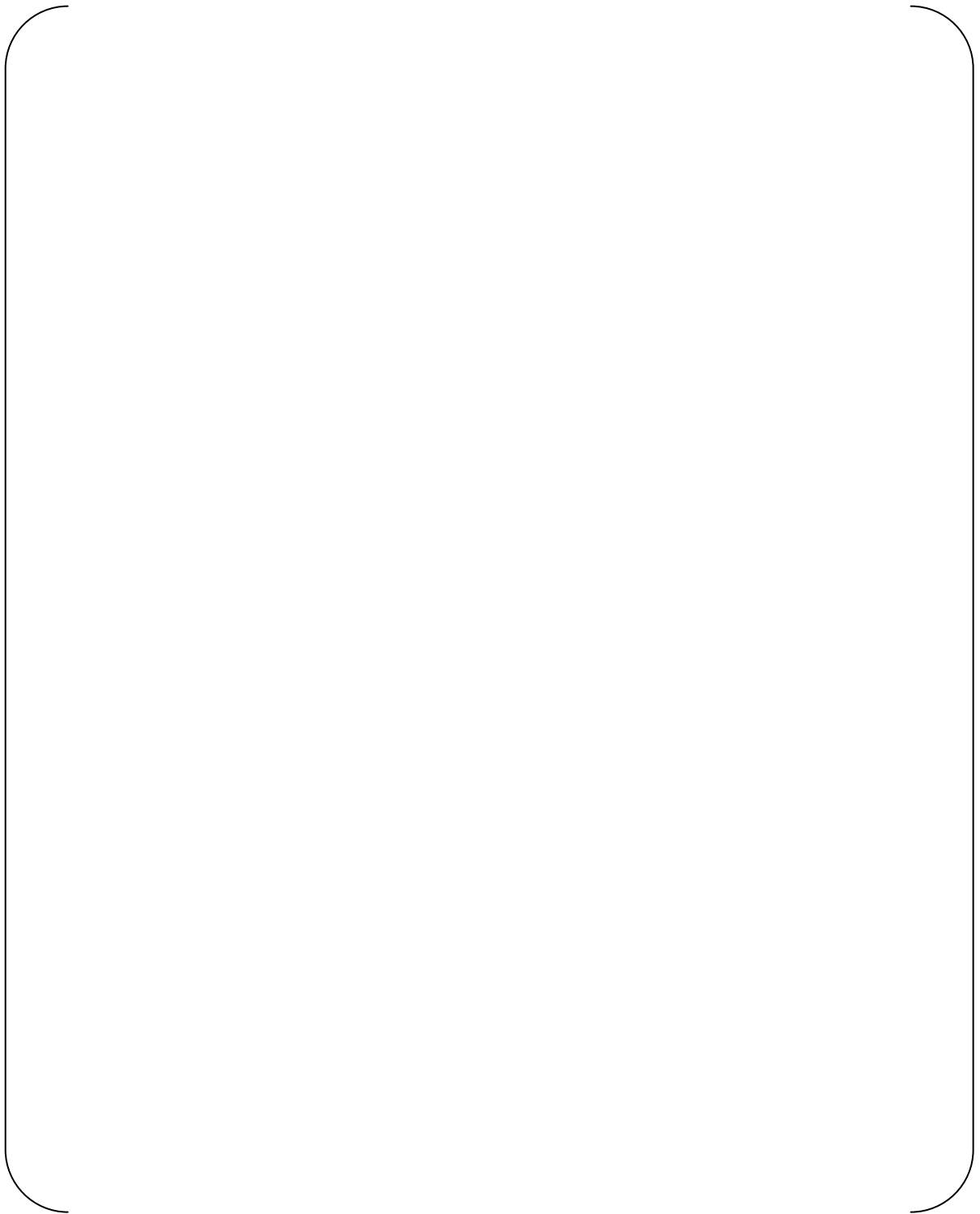


Figure.38-13 US-APWR Vessel 8 split DC Noding for Hot Assembly Under an Open Hole
(Vertical View)

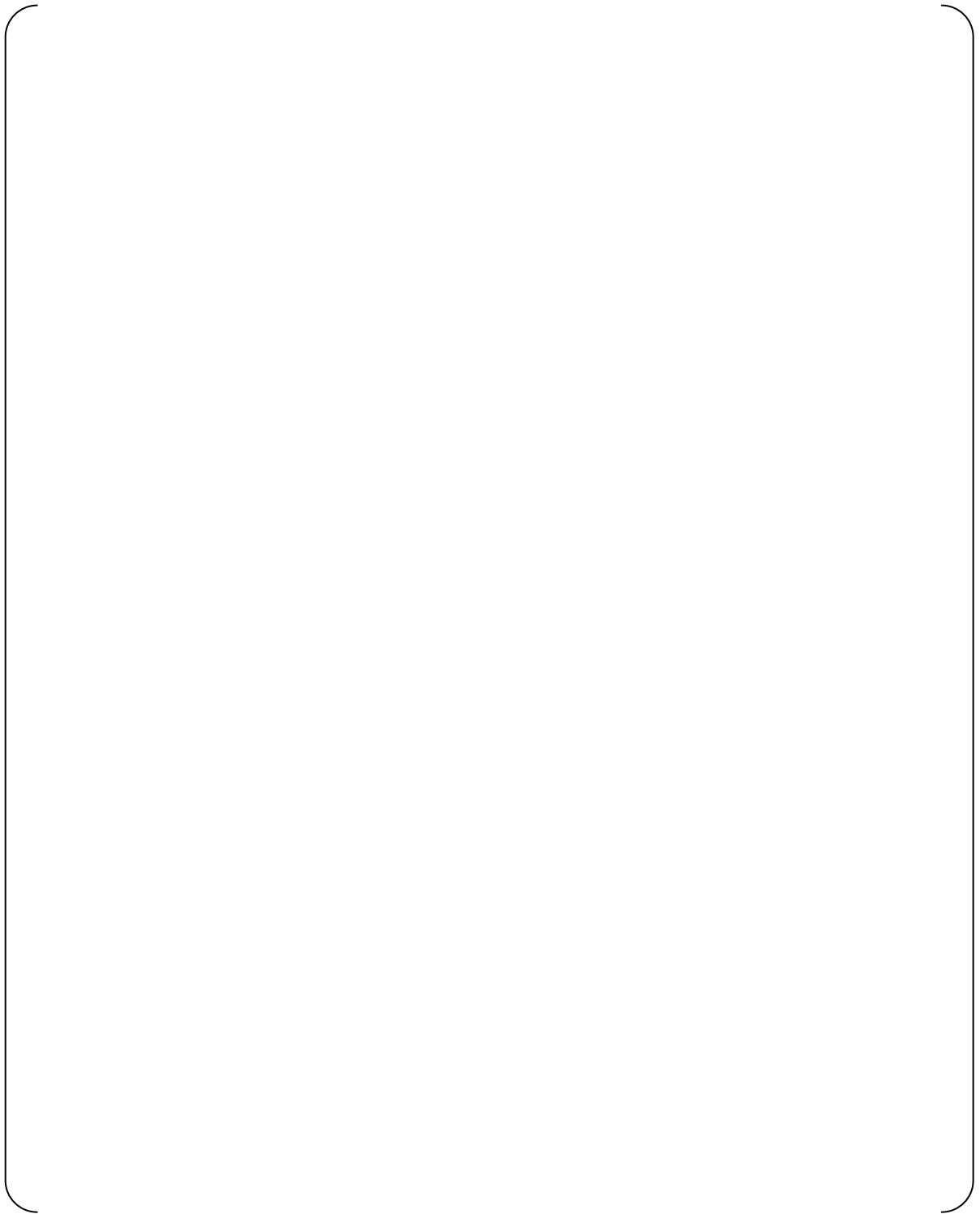


Figure.38-14 US-APWR Vessel Sections 1 to 2 (Horizontal View) 8 split DC

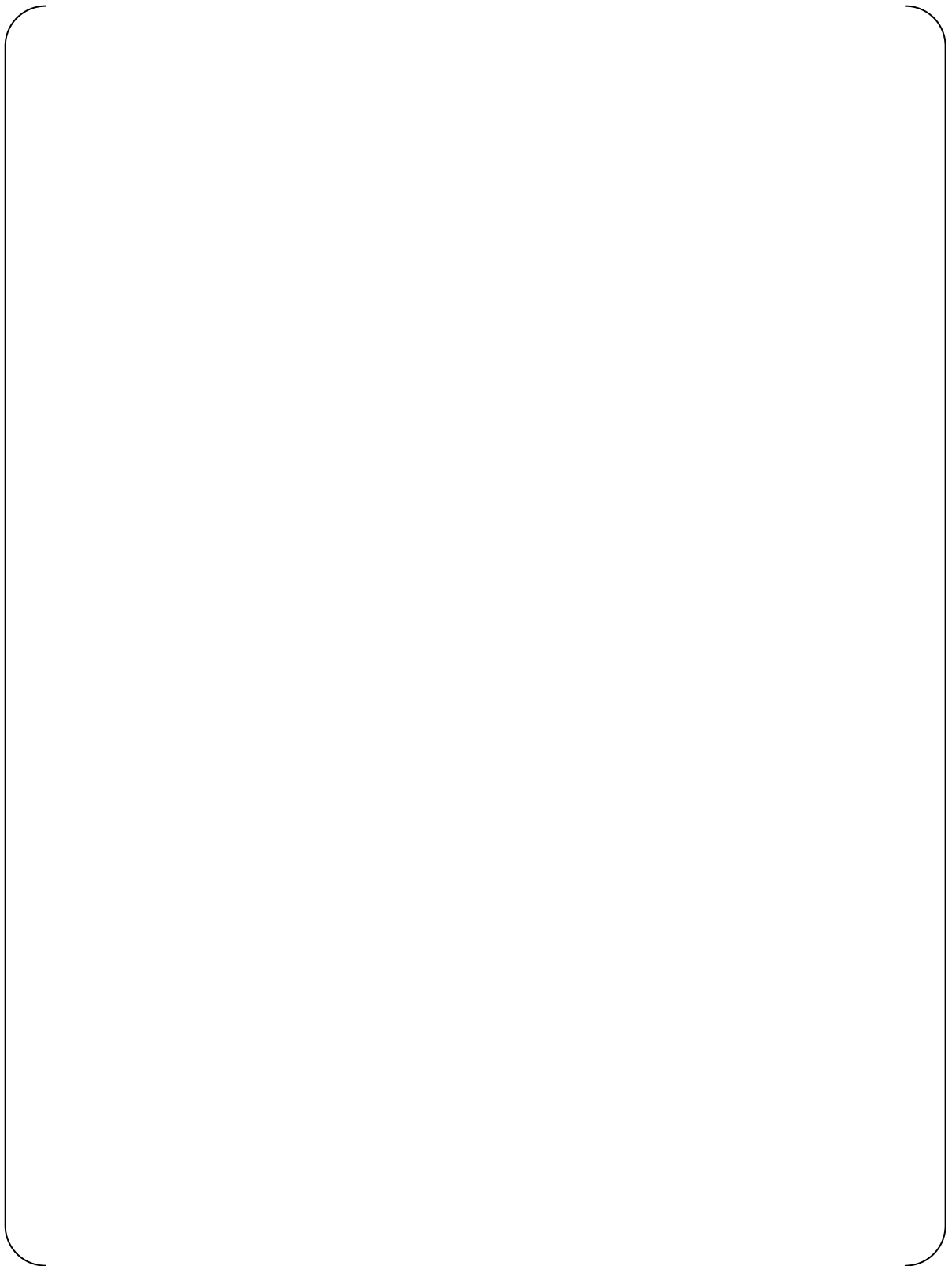


Figure.38-15 US-APWR Vessel Sections 3 to 4 (Horizontal View) 8 split DC

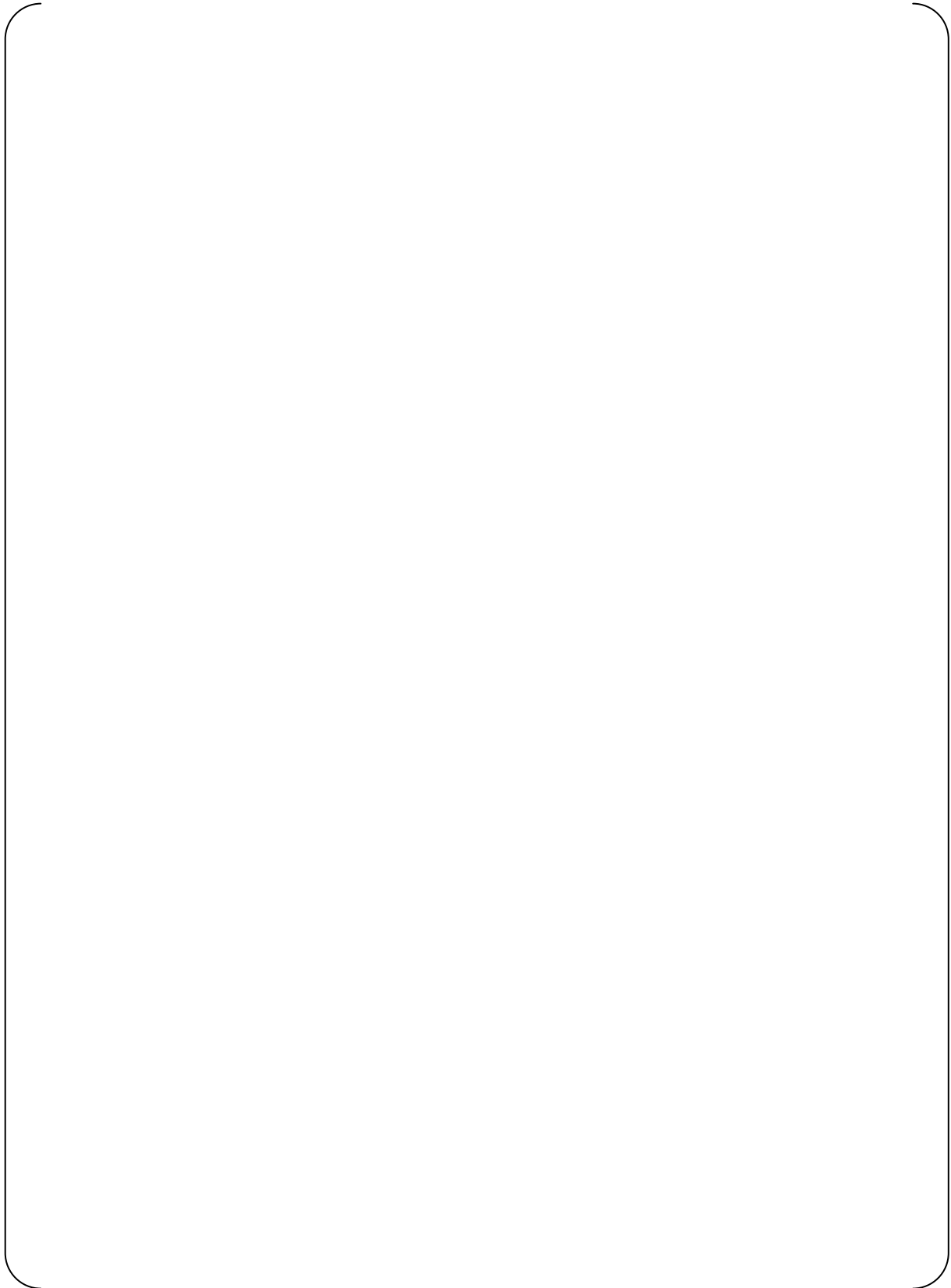


Figure.38-16 US-APWR Vessel Sections 5 to 6 (Horizontal View) 8 split DC

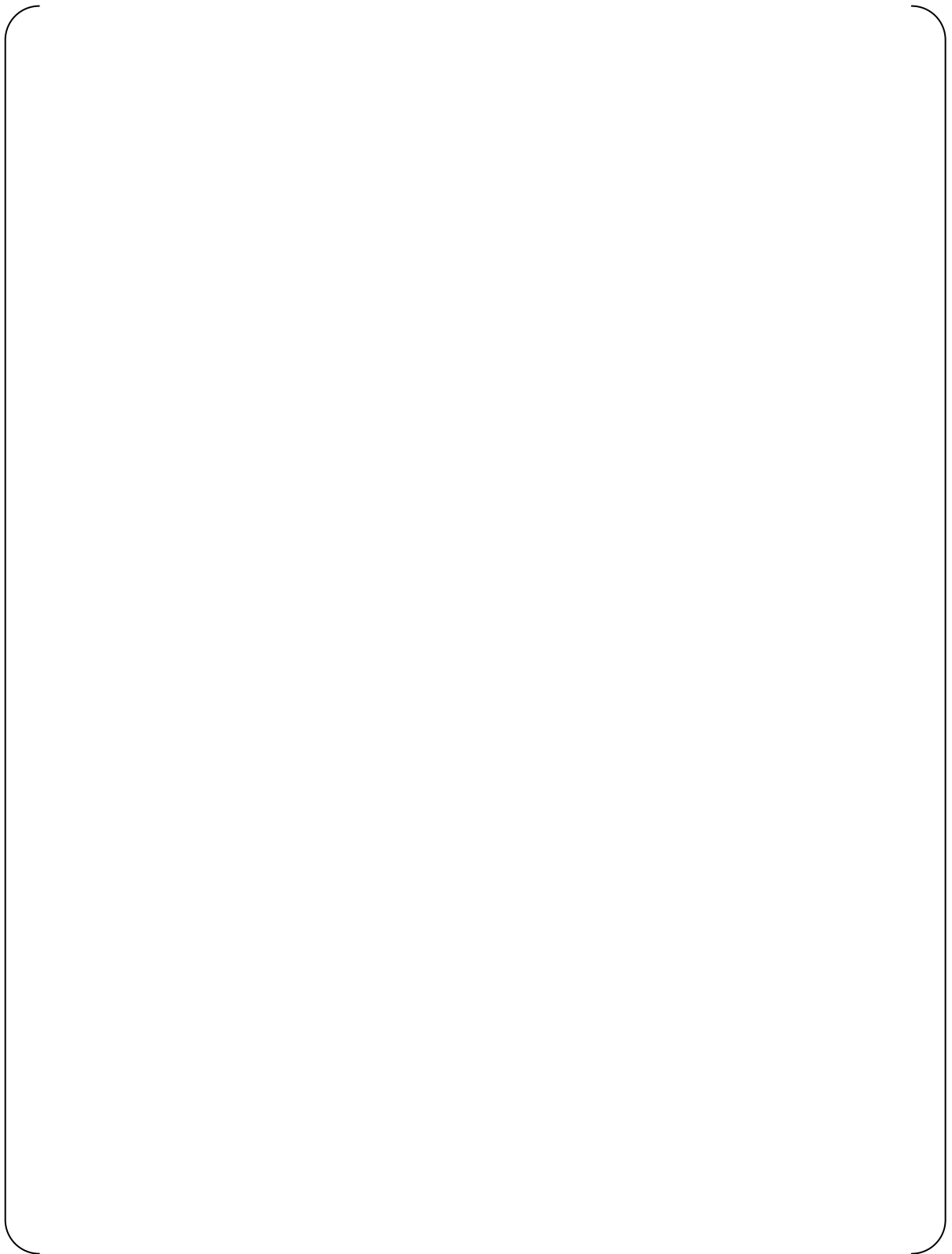


Figure.38-17 US-APWR Vessel Sections 7 to 8 (Horizontal View) 8 split DC

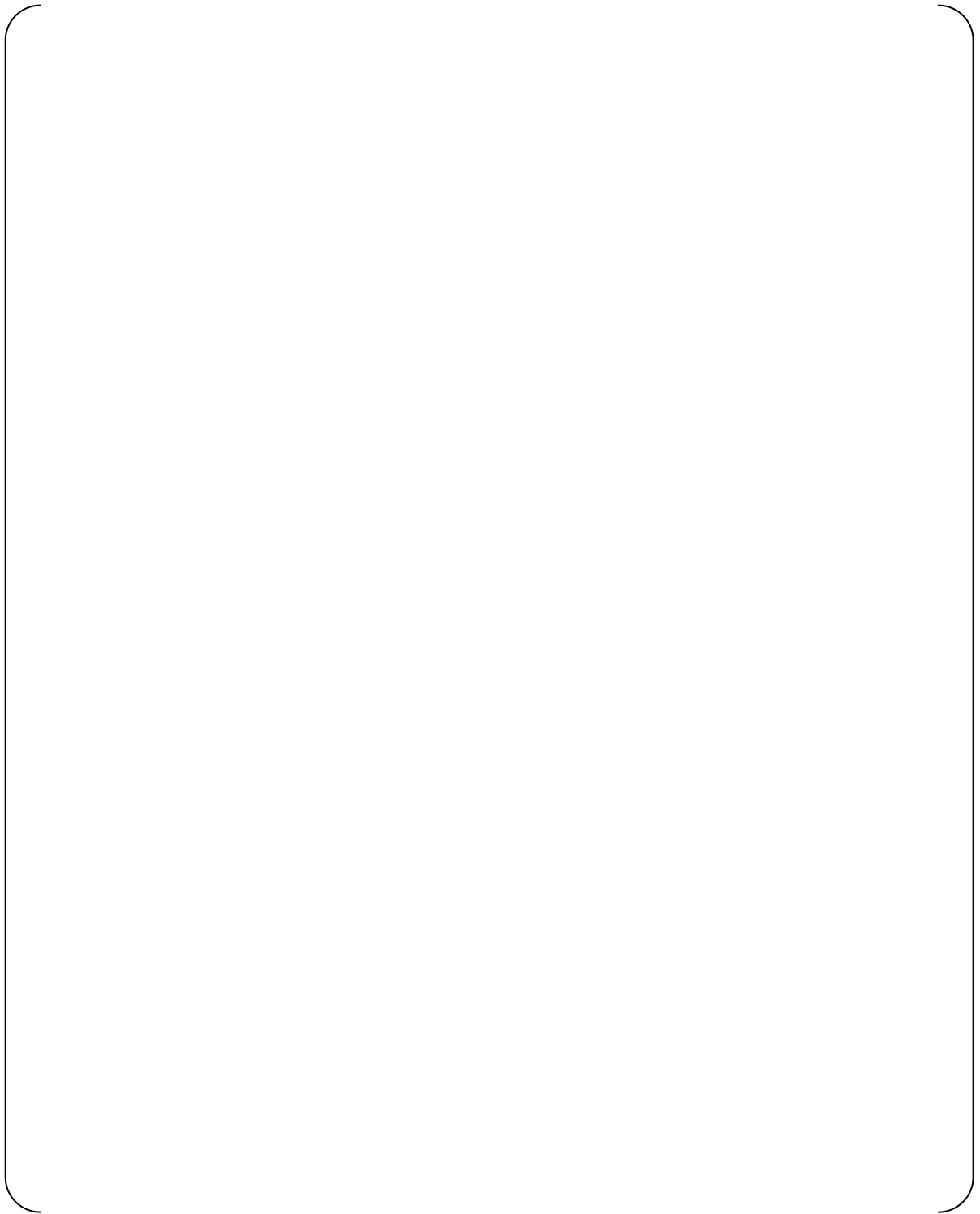


Figure.38-18 US-APWR Vessel Sections 9 to 10 (Horizontal View) 8 split DC



Figure.38-19 Accumulator Flow Rate (Noding sensitivity related to DVI)



Figure.38-20 PCT (Noding sensitivity related to DVI)



Figure.38-21 Broken Loop RV Side Break Flow (Noding sensitivity related to DVI)



Figure.38-22 Downcomer Average Collapsed Liquid Level
(Noding sensitivity related to DVI)

Question 39

Conformance with NUREG/CR-5249 CSAU Step 10 requires that the ability of a best-estimate code to scale-up the phenomena and processes observed from a test facility be evaluated on a case-by-case basis. The effects of scaling are not addressed in MUAP-07011-P R(0) "Large Break LOCA Code Applicability Report for US-APWR."

Considering that the power-to-volume ratio for the US-APWR may differ from the conventional 4-loop PWR as evaluated in either WCAP-12945-P-A or WCAP-16009-P-A, describe the assessment results for the scale-up capability of WCOBRA/TRAC(M1.0) as applicable to the US-APWR. In particular, address scaling and any associated distortion effects with regard to ECC bypass, liquid entrainment, and steam binding in the SG.

Evaluate scaling and dominant distortion effects for in-vessel phenomena resulting from the inclusion of the neutron reflector component in the US-APWR design.

RESPONSE

CASU Step 10 requires evaluating scaleup capabilities of a code up to a nuclear power plant and assessing the effect of test facility scale distortions on the capability of a code if exist (Ref. 39-1).

It is concluded that the full-length and power-to-volume scaling method is appropriate to simulate important LBLOCA behaviors in scaled experiments. With idealized power-to-volume scaling criterion, the time scale and fluid mass and energy distributions are preserved the same in the test facility as in the prototypical plant. Thus, one can expect similar thermal-hydraulic phenomena to occur in the experiment and the prototypical plant in the same time scale. Therefore, many correlations or models in WCOBRA/TRAC which is original version of WCOBRA/TRAC(M1.0) were developed and assessed based on the scale-down experiments which simulate the conventional PWR with the power-to-volume scaling criterion.

It was investigated if the scale effects exists in the WCOBRA/TRAC prediction of PCT during blowdown and reflood for different scaled test facilities. It was confirmed that there is no apparent scale trend as a function of facility scale and WCOBRA/TRAC can be applied to the conventional PWR without any bias (Ref. 39-2).

On the other hand, scale effects were observed for the ECC-bypass in the downcomer and the liquid de-entrainment in the upper plenum. Distortions of the downcomer and the upper plenum in the scale test facilities affect ECC-bypass and steam binding behavior. The full-scale Upper Plenum Test Facility (UPTF) has provided the necessary data for the code assessment related to these phenomena. It was found from the comparisons between the UPTF experiments and the scaled experiments that WCOBRA/TRAC conservatively underpredicts the ECC water delivered to the core during refill for a prototype plant and that WCOBRA/TRAC conservatively underpredicts the de-entrainment in the upper plenum and overestimates the entrainment into the hot legs and steam generators during reflood for a prototype plant. It was confirmed that WCOBRA/TRAC can be applied to the conventional PWR without any bias based on these comparisons (Ref. 39-2).

Considering the above assessments for the applicability of WCOBRA/TRAC to the conventional PWR, the scale-up capability of WCOBRA/TRAC(M1.0) to the US-APWR can be confirmed when the followings are examined.

- Examine that similar thermal-hydraulic phenomenon during LBLOCA transients occur in the US-APWR as in the conventional PWR base on the power-to-volume scaling criterion or other considerations. Confirm from these examinations that the experiments for the conventional PWR can be applied to the US-APWR and WCOBRA/TRAC(M1.0) which scaleup capability to the conventional PWR was assessed based on these experiments can be also applied to the US-APWR.
- Confirm that WCOBRA/TRAC(M1.0) can also be conservatively applied to the US-APWR for phenomena in which prediction the scale trend were observed.
- Confirm that effects of the neutron reflector on the LBLOCA behavior are sufficiently small and the thermal hydraulic behavior can be adequately evaluated by WCOBRA/TRAC(M1.0).

(1) Similarity of LBLOCA phenomena between the US-APWR and the conventional PWR
As the US-APWR component design and operating conditions are very similar to those of the conventional PWR, it is expected that the plant responses and important phenomena during a LBLOCA transient are identical with those in the conventional PWR. Actually, there are no differences in the PIRT tables between the conventional PWR and the US-APWR except the phenomena related to the advanced accumulator and the neutron reflector which are the US-APWR specific design features. Comparisons of plant main parameters and volume and flow area of each component are shown in Table 39-1 and Table 39-2 respectively.

Initial RCS pressure and coolant temperature distribution in the RCS for the US-APWR are same or almost same as for the conventional PWR. The ratio of RCS liquid volume between the US-APWR and the conventional four-loop PWR is () as shown in table 39-2. This value is nearly equal to the core power ratio of () between them. Then, the power-to-volume scaling criterion is almost satisfied between the US-APWR and the conventional four-loop PWR for RCS. Therefore, it is expected that phenomena and processes during LBLOCA transients in the US-APWR are generally similar to those in the conventional PWR.

But, individual component does not exactly satisfy the power-to-volume scaling criterion. Effects of these distortions from the scaling criterion on the LBLOCA behaviors are discussed as follows.

The core volume of the US-APWR is larger in comparison with the power ratio as the core height of the US-APWR is 14 feet. However, a dominant parameter for LBLOCA behavior is the absolute core power and stored energy as heat source rather than the core volume. Then, the distortion of the core from the scaling criterion hardly affects the LBLOCA behavior. WCOBRA/TRAC(M1.0) was validated against the blowdown, refill and reflood core heat transfer experiments of the G-2 loop facility. 17X17 14 feet fuel assembly was simulated in the G-2 loop facility which is identical with the US-APWR fuel assembly. Therefore, the applicability of WCOBRA/TRAC(M1.0) to the US-APWR fuel assembly has

been confirmed.

The downcomer volume of the US-APWR is larger, and the lower plenum volume of the US-APWR is smaller in comparison with the power ratio, while the sum of them nearly satisfies the power-to-volume scaling criterion. It is expected that coolant in the both components behaves together during blowdown. Therefore, phenomena in these region during blowdown is almost similar to that for the conventional PWR. Smaller lower plenum volume of the US-APWR decreases refilling time, and larger downcomer volume or longer downcomer axial length of the US-APWR increases the core inlet velocity during reflood. Then, the distortion of these components from the scaling criterion will affect the LBLOCA behavior during refill and reflood. However, changes of the initial condition of reflood and the core inlet velocity due to the scale distortions for these components are small and these parameters are expected to be in the range that WCOBRA/TRAC(M1.0) has been assessed against the reflood heat transfer experiments. Therefore, WCOBRA/TRAC(M1.0) can still be applied to the US-APWR.

The crossover leg, reactor coolant pump and cold leg don't satisfy the power-to-volume scaling criterion. However, as the volume of these components is small compared with other components and the sum of them nearly satisfies the power-to-volume scaling criterion, the scale distortions for these components hardly affect the similarity of LBLOCA behavior between the US-APWR and the conventional PWR.

The pressurizer total volume of the US-APWR is larger in comparison with the power ratio, while the pressurizer initial liquid plenum volume of the US-APWR is smaller in comparison with the power ratio. These distortions may affect the RCS pressure transient during subcooled blowdown and out-surge flowrate transient from the pressurizer which may affect the core flow during the core reverse flow period. However, the effect on the RCS pressure is limited to a short period of early blowdown and the effect on the core flow is not significant. Therefore, it is considered that the scale distortion of the pressurizer hardly affects the similarity of LBLOCA overall behavior.

The steam generator tubes don't satisfy the power-to volume scaling criterion. However, a dominant parameter is the flow resistances through the tubes related to the steam binding effect during reflood rather than the volume of the tube for LBLOCA behaviors. The steam generator tube diameter of the US-APWR is small compared with that of the conventional PWR and gives higher flow resistance. The tube number and flow area of the steam generator for the US-APWR is increased to compensate the tube diameter effect on the pressure drop. As the pressure drop through the steam generator tubes is almost same between the US-APWR and the conventional PWR, similar LBLOCA behaviors related to the steam generator is expected.

The US-APWR employs the advanced technologies for the ECCS. One is the advanced accumulator and the other is the direct vessel injection for high head injection system. Active low head injection system is eliminated as the advanced accumulator supplies water with low flow rate at later injection stage. However, the injection flowrate for the US-APWR is determined to satisfy the required injection flowrate for the core cooling

during LBLOCA transients the same as for the conventional PWR. Therefore, the new ECCS of the US-APWR hardly affects the similarity of LBLOCA behavior.

Initial RCS pressure and coolant temperature distribution in the RCS of the US-APWR are same or almost same as the conventional PWR. The RCS volume is nearly scaled by the power-to-volume scaling criterion between the US-APWR and the conventional four-loop PWR. The scale distortion of individual component hardly affects the LBLOCA behavior. Then, similar behaviors to the conventional PWR are expected in the US-APWR LBLOCA transients. Therefore, the experiments which simulate the LBLOCA behavior of the conventional PWR are also applicable to the US-APWR, and WCOBRA/TRAC which is assessed against these experiments can be applied to the US-APWR without any bias.

(2) WCOBRA/TRAC(M1.0) applicability to the area where scale effects are observed

(a)ECC-bypass in downcomer

ECC water injected from the accumulator flows down into the downcomer through the cold legs, and vapor generated in the core flows up in the downcomer and exits from the break. Then, an interaction between ECC water and vapor occurs in the downcomer, and the ECC delivery into the core is affected by the downcomer geometry like gap width and circumferential length which govern the two-phase flow interaction and then multi-dimensional two-phase flow behavior in the downcomer. In a scaled facility designed according to the power-to-volume scaling criterion with full-length, multi-dimensional behavior is weakened because radius is reduced. Consequently, the downcomer where the multi-dimensional two-phase behavior is dominant might be distorted in the scaled test facility. Two-phase flow distribution is evaluated in WCOBRA/TRAC(M1.0) by the intercell drag model in which counter current flow limiting situations are calculated. This model is applied where there is liquid flowing downward against vapor up flow and there is a significant void fraction gradient between the channels. WCOBRA/TRAC(M1.0) underpredicts the ECC delivered to the core for the full-scale UPTF experiments (Ref. 39-2). Therefore, WCOBRA/TRAC(M1.0) gives more conservative prediction for a plant in which multi-dimensional behavior is more dominant.

Comparison of the geometry parameters of the downcomer between the US-APWR and the conventional PWR is shown in Table 39-3. The ratio of reactor vessel inner diameter and core barrel outer diameter between the US-APWR and the conventional PWR are $\left(\frac{1}{2}\right)$ and $\left(\frac{1}{2}\right)$ respectively, while the ratio of the downcomer gap width between them is only $\left(\frac{1}{2}\right)$. The multi-dimensional behavior in the downcomer is expected to be pronounced for the US-APWR. Therefore, WCOBRA/TRAC(M1.0) gives more conservative prediction of ECC delivery into the core for the US-APWR, and it can be applied without any bias.

(b)Liquid de-entrainment in upper plenum

There are a lot of structures like guide tube and core support column in the upper plenum. Part of entrained liquid generated in the core and transferred to the upper plenum is de-entrained on the surface of these structures and is accumulated in the upper plenum. The de-entrainment in the upper plenum will affect liquid entrainment into the hot legs and steam generators and the steam binding effects.

The geometry of the structure in the upper plenum will affect amount of liquid

de-entrainment in the upper plenum. WCOBRA/TRAC(M1.0) was compared to the UPTF, the CCTF and the SCTF upper plenum de-entrainment test data as a function of scale. As the scale increase, the WCOBRA/TRAC(M1.0) more conservatively predicts mass inventory in the upper plenum. As the fraction of structure in the upper plenum is almost same among the tests, the diameter of the upper plenum would affect the prediction of the de-entrainment and more conservative prediction would be obtained when the upper plenum diameter or the distance to the hot legs is larger.

Comparison of the geometries of the upper plenum between the US-APWR and the conventional PWR is shown in Table 39-4. The fraction of structure in the upper plenum is almost same between them, while the core barrel inner diameter related to the distance to the hot legs is larger for the US-APWR. Therefore, WCOBRA/TRAC(M1.0) would give more conservative prediction of the de-entrainment in the upper plenum for the US-APWR, and it can be applied without any bias.

(3) WCOBRA/TRAC(M1.0) applicability considering Neutron Reflector

Applicability of WCOBRA/TRAC(M1.0) to the US-APWR with the neutron reflector is discussed in the response to Question 1.

(4) Conclusion

Similar LBLOCA behaviors to the conventional PWR are expected to occur in the US-APWR because the RCS of the US-APWR satisfies the power-to-volume scaling criterion with the conventional PWR and the effects of the distortions of individual component from the power-to-volume scaling criterion on the LBLOCA behavior are small. WCOBRA/TRAC(M1.0) is expected to give more conservative predictions of the ECC delivery and the de-entrainment in the upper plenum in which the scale trends are observed for the US-APWR. The effects of the neutron reflector is small and the thermal hydraulic behavior in the neutron reflector is adequately evaluated by WCOBRA/TRAC(M1.0). Therefore, WCOBRA/TRAC(M1.0) is applicable to the US-APWR as the conventional PWR.

References

- 39-1 Boyack B., et al., Quantifying Reactor Safety Margins, Application of Code, Scaling, Applicability, and Uncertainty Evaluation Methodology to a Large Break Loss-of-Coolant Accident, NUREG/CR-5249 R4, December 1989.
- 39-2 Bajorek, S. M., Young, M. Y., and Takeuchi, K., Code Qualification Document for Best Estimate LOCA Analysis, WCAP-12945-P-A, Revision 2, Westinghouse Electric Company, March 1998.
- 39-3 The ROSA-IV Group, ROSA-IV Large Scale Test Facility (LSTF) System Description, JAERI-M 84-237, December 1984.

Table 39-1 Comparison of Main Parameter

Parameter	Conventional PWR	US-APWR
Core Power (MWt)	3411	4451 (1.30)
RCS Pressure (MPa)	15.5	15.5
Fluid Temp. at Hot Leg (K)	598	601
Fluid Temp. at Cold Leg (K)	562	564
Core Inlet Flow (ton/s)	16.7	21.2 (1.27)

Table 39-2 Comparison of RCS Component Volume and Flow Area

Component	Conventional PWR*		US-APWR	
	Volume (m ³)	Flow Area (m ²)	Volume (m ³)	Flow Area (m ²)
Downcomer	20.4	3.38		
Lower Plenum	29.6			
Core	17.5	4.75		
Core Reflector	11.2			
Upper Plenum	28.4			
Upper Head	24.6			
Hot Leg (1/4)	2.98	0.427		
SG Plenum (1/4)	8.36			
SG Tube (1/4)	21.8	1.02		
Crossover Leg (1/4)	4.06	0.486		
RCP (1/4)	2.40			
Cold Leg (1/4)	2.78	0.384		
Pressurizer	51.0			
Pressurizer (liquid)	32.0			
PZR Surge Line	1.29			
Total Water Volume	335			
Total Volume	354			

* Values for conventional PWR are referred to JAERI-M84-237 (Ref. 39-3)

Table 39-3 Geometrical Parameters related to ECC Penetration into Downcomer

Parameter	Conventional PWR*	US-APWR
Downcomer Flow Area (m ²)	3.38	
Downcomer Gap Width (m)	0.26	
Reactor Vessel Inner Diameter (m)	4.394	
Core Barrel Outer Diameter (m)	3.874	
Cold Leg Inner Diameter (m)	0.699	

* Values for conventional PWR are referred to JAERI-M84-237 (Ref. 39-3)

Table 39-4 Geometrical Parameters related to De-entrain in Upper Plenum

Parameter	Conventional PWR*	US-APWR
Core Barrel Inner Diameter (m)	3.759	
Inside Cross Section Area of Core Barrel (m ²)	11.10	
Number of RCCA Guide Tube	57	
Number of Upper Support Column w/o Flow Hole	50	
Number of Upper Support Column with Flow Hole	0	
Total Number of Upper Support Column	50	
Total Cross Section of RCC Guide Tubes and Upper Support Columns (m ²)		

* Values for conventional PWR are referred to JAERI-M84-237 (Ref. 39-3)

Question 40

Section 3.7 "ASTRUM Methodology Applied to US-APWR" of MUAP-07011-P R(0) "Large Break LOCA Code Applicability Report for US-APWR" does not address the treatment of decay heat.

Describe the ASTRUM uncertainty analysis in the treatment of decay heat modeling in WCOBRA/TRAC (M1.0). In particular, present derivation of any applicable uncertainty ranges, sampling range bounds, type of uncertainty distribution, and any uncertainty dependencies, including such on burnup level.

RESPONSE

Reference

- 40-1 "American National Standard for Decay Heat Power in Light Water Reactors", ANSI/ANS-5.1-1979
- 40-2 "CSRL-V : PROCESSED RNDF/B-V 227-Neutron-Group and Pointwise Cross-Section Libraries for Criticality Safety, Reactor and Shielding Studies". NUREG/CR-2306, W.E. Ford, et al. ,1982.

Question 41

Figure 3.6-18 "Downcomer Liquid Level" in MUAP-07011-P R(0) "Large Break LOCA Code Applicability Report for US-APWR" shows oscillations in the predicted downcomer liquid level during a time period when the reflood PCT occurs at 77 s.

Provide an explanation of the oscillations and their effect on PCT. Include detail plots of downcomer liquid level, core liquid level, core flow, heat transfer coefficient at PCT location, and calculated PCT. Present an evaluation of the effects of the liquid level oscillations on hot spot heat transfer and resultant PCT to ensure that oscillations do not unduly enhance core heat transfer.

RESPONSE





Figure 41-1 Downcomer collapsed water level



Figure 41-2 Core collapsed water level in hot assembly channel



Figure 41-3 Total mass flow rate at PCT location in hot assembly



Figure 41-4 Liquid heat transfer coefficient at PCT location



Figure 41-5 Vapor heat transfer coefficient at PCT location



Figure 41-6 Heat transfer coefficient, heat flux/(Tw-Tsat) at PCT location



Figure 41-7 Clad and pellet average temperatures at PCT location



Figure 41-8 Core inlet liquid velocity (Sensitivity analysis)



Figure 41-9 Downcomer collapsed water level (Sensitivity analysis)



Figure 41-10 PCT (Sensitivity analysis)

Question 42

Comparing the US-APWR design against a conventional 12-ft core 4-loop PWR plant, the ratio of the core thermal power results in value of about 1.30 whereas the ratio of the hot leg area amounts to 1.14. Identify any detrimental effects on the US-APWR core thermal hydraulic response during a large break LOCA that result from this relative deviation in the US-APWR hot leg flow area. In addition, demonstrate that any such effects associated with processes occurring in the reactor hot legs have been properly accounted for in performing US-APWR best-estimate large break LOCA analyses using WCOBRA/TRAC(M1.0).

RESPONSE

The hot leg for one loop contains less than 1% of the total RCS, and the pressure drop in the hot leg is small compared with that in the core or the steam generators. Therefore, the phenomena or process in the hot leg is not significant for the LBLOCA transient. There is no high ranked phenomenon in the hot leg for US-APWR LBLOCA PIRT (Ref. 42-1).

Scaling approach can be effectively used to investigate similarity of LBLOCA transients between different nuclear steam supply systems. Two scaling approaches are considered here for the hot leg: power-to-volume scaling and modified power-to-volume scaling including Froude number scaling. Comparison of the hot leg characteristics between the conventional PWR and the US-APWR and the result of the scaling approaches are shown in Table 42-1.

The hot leg volume ratio between the conventional PWR and US-APWR excellently agrees with the power ratio. Therefore, the hot leg geometries of the conventional PWR and the US-APWR satisfy the power-to-volume scaling criterion which is the most important for LBLOCA transients (Ref. 42-2). When the power-to-volume scaling is satisfied, the time scale is preserved and same relative amount of fluid is available for energy and mass exchange. Thus, one can expect similar thermal-hydraulic phenomena to occur in the systems in the same time scale.

When not only the power-to-volume scaling but also the length is simultaneously preserved, the flow area ratio and the fluid velocity can be preserved. But, as the hot leg length of US-APWR is longer than that of the conventional PWR, the velocity is not preserved. However, the preservation of the flow area ratio in the hot leg is not essential for the similarity of LBLOCA behavior. For example, the pressure drop in the hot leg is not determined only by the velocity.

A scaling parameter introduced from the modified power-to-volume scaling including Froude number scaling is $L/D^{0.5}$ (Ref. 42-3). This scaling is important for two-phase flow regime similarity. This scaling parameter is not satisfied between the conventional PWR and the US-APWR as shown in Table 42-1. However, the horizontal stratification in the hot leg hardly occurs because the mixture level in the reactor vessel stays below the hot leg elevation and two-phase flow behavior in the hot leg can be evaluated with the homogeneous flow model during reflood when PCT is concerned. Any liquid that is swept into the hot leg will be entrained into the steam generators without de-entrain in the hot leg.

Thus, the flow regime similarity is not important in LBLOCA transients, and the disagreement with the Froude number scaling hardly affects the similarity of the LBLOCA transients between the conventional PWR and the US-APWR.

As the hot leg geometries of the conventional PWR and the US-APWR satisfy the important power-to-volume scaling criterion, similar thermal-hydraulic phenomena can be expected to occur in the hot legs. As the applicability of WCOBRA/TRAC(M1.0) to the conventional PWR has been confirmed, WCOBRA/TRAC(M1.0) can be also applied to US-APWR.

References

- 42-1 Mitsubishi Heavy Industries, Ltd., Large Break LOCA Code Applicability Report for US-APWR, MUAP-07011-P (R0), July 2007.
- 42-2 N. Zuber, et al., Evaluation of Scale-Up Capabilities of Best-Estimate Codes, Appendix C to Quantifying Reactor Safety Margins, NUREG/CR-5249 R4, December 1989.
- 42-3 N. Zuber, A Hierarchical, Two-Tiered Scaling Analysis, Appendix D to An Integrated Structure and Scaling Methodology for Severe Accident Technical Issue Resolution, NUREG/CR-5809, EGG-25659, November 1991.
- 42-4 The ROSA-IV Group, ROSA-IV Large Scale Test Facility (LSTF) System Description, JAERI-M 84-237, December 1984.

Table 42-1 Comparison of Hot Leg Geometries

Parameter X_i	Conventional PWR*	US-APWR	$[X_i]_{US-APWR}/[X_i]_{PWR}$
Core Power (MWt)	3411	4451	1.30
Inner Diameter (m)	0.737		
Flow Area (m ²)	0.427		
Length (m)	6.99		
Volume per loop (m ³)	2.98		
Power/Volume (MWt/ m ³)	1145		
L/D ^{0.5} (m ^{1/2})	8.14		

* Values for conventional PWR are referred to JAERI-M84-237 (Ref. 42-4)

Question 43

Appendix A "Thermal Properties of Nuclear Fuel Rods" in MUAP-07011-P R(0) "Large Break LOCA Code Applicability Report for US-APWR" describes the model for computing fuel thermal conductivity. To account for conductivity degradation with fuel burnup, the model uses a correlation by Wiesenack published in 1997, which is based on in-pile temperature data. Furthermore, MUAP-07011-P R(0) explains that the model is identical to the one used in the applicant's FINE fuel design code. A new routine, TCONF, has been implemented in WCOBRA/TRAC(M1.0) to compute the fuel conductivity at 95% of the theoretical density along with a correction factor accounting for the deviation of the actual fuel density from the theoretical value. The thermal conductivity is calculated in subroutines SSTEMP and TEMP by calling subroutine TCONF. In addition, MUAP-07011-P R(0) states that uncertainty of the fuel thermal conductivity has already been partly considered in the uncertainty of stored energy in ASTRUM and claims that the same treatment of the stored energy uncertainty in the ASTRUM methodology is applicable to the US-APWR fuel.

Demonstrate that the fuel properties model used in WCOBRA/TRAC(M1.0) accounts adequately for changes in thermal properties over the fuel burnup range applicable to the US-APWR core design. Provide any additional data in support of the applicability of the model to the US-APWR design. Identify all individual parameters related to the US-APWR fuel design that have been treated in the uncertainty analysis related to the initial stored energy in the US-APWR core. For each parameter, provide and justify the corresponding range, including its lower and upper limits as well as any assumed probability distribution, if such parameters were applied in the uncertainty analysis in the US-APWR best-estimate large break LOCA analyses performed with WCOBRA/TRAC(M1.0).

RESPONSE

(1) Applicability of Pellet Thermal Conductivity Model to US-APWR Analysis

WCOBRA/TRAC(M1.0) incorporates the same pellet thermal conductivity model as that in the FINE code (Ref. 43-1). This thermal conductivity model takes into consideration the degradation effect with burnup. The model is described in Section 4.2.1.5 and Appendix B.1.1.5 of Reference 43-1. The thermal conductivity degradation with burnup is developed based on the fuel center temperature measurement data which local burnup are up to 80GWd/t (Ref. 43-2). Therefore, US-APWR fuel design in which the maximum rod average burnup is 62GWd/t satisfies the applicability range of the model. Then, the pellet thermal conductivity model can be applied to US-APWR fuels.

(2) Additional Pellet Thermal Conductivity Data for US-APWR Design

The US-APWR fuel design with the maximum rod average burnup of 62GWd/t satisfies the applicability range of the model. Section 4.2.1.5 of Reference 43-1 describes pellet thermal conductivity data to support the applicability of the model to the US-APWR design.

(3) Uncertainties related to Initial Stored Energy

The average and 95% probability fuel average temperature calculated using the above probability distributions by the Monte Carlo calculation with the HOTSPOT code are shown in Figure 43-1 through Figure 43-4. The calculated temperatures with HOTSPOT are always greater than the temperatures obtained from the FINE code predictions and the uncertainties shown in Table 43-1 for any burnup.

Adequate contributions for the uncertainties related to the fuel initial stored energy are considered and the uncertainty ranges are conservatively considered in US-APWR LBLOCA analysis.

References

- 43-1 Shimomura, T., et al., "Fuel System Design Criteria and Methodology", MUAP-07008-P(R1), Mitsubishi Heavy Industries, 2009.
- 43-2 Wiesenack, W., "Assessment of UO₂ Conductivity Degradation Based on In-Pile Temperature Data", ANS 1997 International Topical Meeting on LWR Fuel Performance, Portland, Oregon, March 1997.
- 43-3 MHI's complementary Information regarding LOCA initialization on Topical Report MUAP-07008-P(0) "Mitsubishi Fuel Design Criteria and Methodology", UAP-HF-09571, December 25, 2009.
- 43-4 U.S. Nuclear Regulatory Commission, Regulatory Guide 1.126.

- 43-5 Bajorek, S. M., et al., 1998, "Code Qualification Document for Best Estimate LOCA Analysis", WCAP-12945-P-A, Volume 1, Revision 2, and Volumes 2 through 5, Revision 1, and WCAP-14747 (Non-Proprietary).
- 43-6 WCAP-16009-P-A Rev.0 Jan. 2005, Realistic Large Break LOCA Evaluation Methodology Using the Automated Statistical Treatment of Uncertainty Method (ASTRUM).



Figure 43-1 Average and 95% Probability Fuel Average Temperature (BU=0GWd/t)



Figure 43-2 Average and 95% Probability Fuel Average Temperature (BU=2.4GWd/t)



Figure 43-3 Average and 95% Probability Fuel Average Temperature (BU=22.2GWd/t)



Figure 43-4 Average and 95% Probability Fuel Average Temperature (BU=62GWd/t)

Question 44

Explain in details how effects associated with initial fuel energy have been accounted for in the modeling of the US-APWR core using WCOBRA/TRAC(M1.0) for best-estimate large break LOCA analyses. Identify and justify any specific assumptions implemented in specifying the core input model. In particular, consider effects associated with core nodalization, presence of different fuel bundles in each noding region, fuel cycle, and core loading schemes.

RESPONSE

The grouping of fuel assemblies in WCOBRA/TRAC(M1.0) models is determined considering the relative core power distribution and the potential flow delivery from the upper plenum and upper head as follows: a hot assembly, low power peripheral assemblies, other assemblies below guide tubes and support columns. The hot assembly is assumed to reside in a location in which the flow is restricted from above. Initial fuel rod stored energy for each assembly is given dependent on the relative power and burnup.

The initial stored energy of the hot rod affects directly a peak cladding temperature as a major heat source, and the initial stored energy of the hot assembly rod affects fluid enthalpy around the hot rod. Therefore, these are important parameters in the LBLOCA analysis. Fuel temperature is highest early in the fuel cycle. Then, the fuel average temperature for the hot rod and the hot assembly rod is conservatively assumed to be the value for this limiting burnup condition in the US-APWR analysis. The highest fuel average temperature is selected among the fuels with different fuel enrichments. And the applied fuel average temperature is higher than that of the fuel containing gadolinia.

The conservative initial stored energy is applied to the hot rod and the hot assembly rod which covers a range of burnup and fuel specifications. And the initial stored energy is estimated at the limiting radial peaking factor which covers a range of core cycle burnup and core loading schemes. Therefore, estimated initial stored energy covers a range of core cycle burnup and core loading schemes.

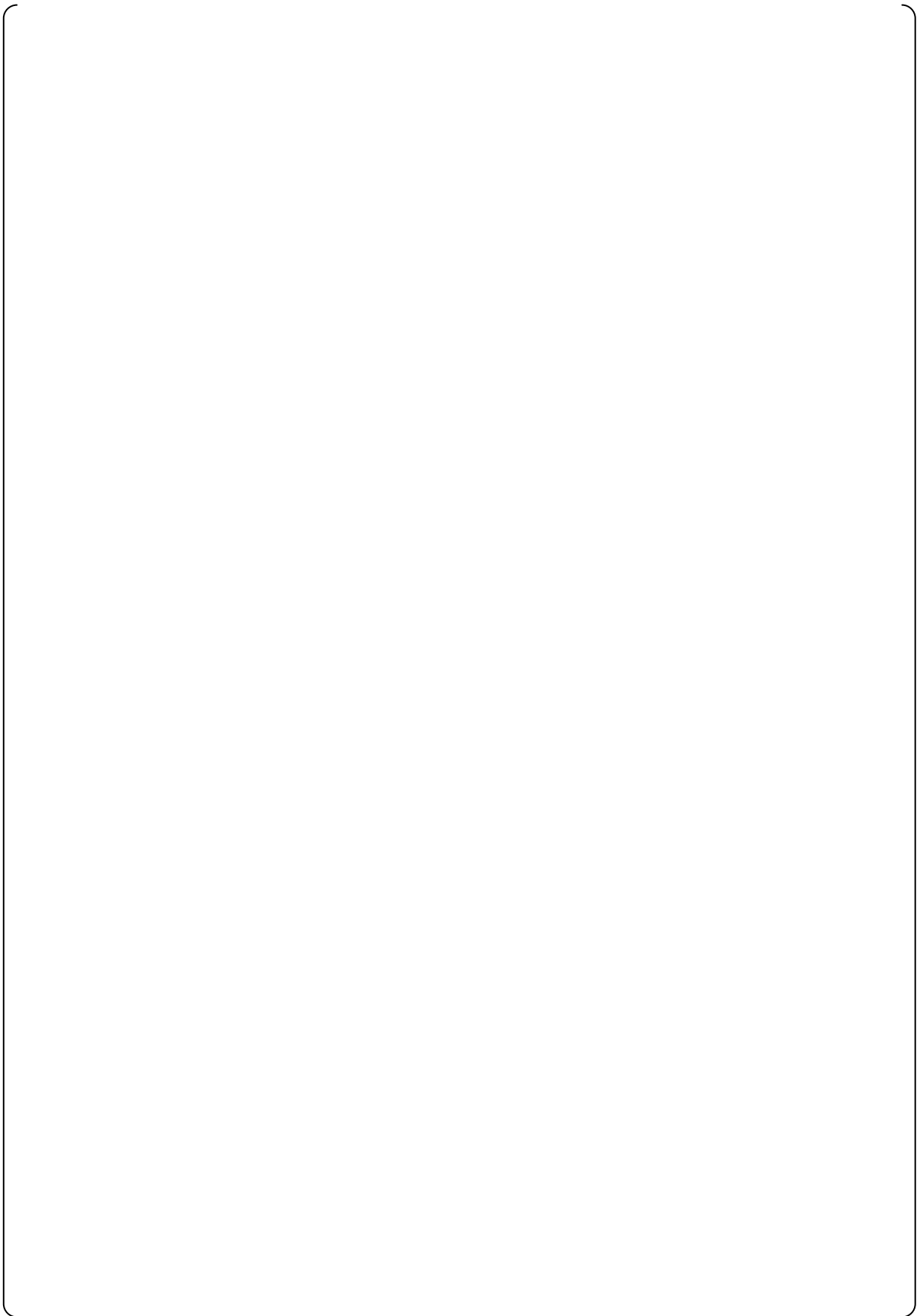
The fuel average temperature for the limiting burnup condition is also assumed for rods in the assemblies residing under support column and guide tube and a rod in the assemblies residing in the periphery of the core. This assumption gives conservative results for the following reasons. The total fuel stored energy in the core affects time to discharge fluid through the break, and cladding temperature is increased during refill for a larger stored energy. The fuel stored energy in the core affects the vapor generation in the core and the steam binding effects is increased during reflood for a larger stored energy.

Rewetting of the fuel rod in the periphery assemblies will affect the flow distribution in the core and the hot assembly flowrate when the downflow through the core occurs during blowdown. However, the fuel rod in the periphery assemblies rewets before core downflow starts even if the fuel average temperature for the limiting burnup condition is applied because a small radial power factor of 0.2 is assumed in the US-APWR analysis. Therefore, the assumption of the fuel stored energy for the fuel rod in the periphery assemblies hardly affects the flow distribution in the core.

Adequate or conservative stored fuel energy which covers the range of the fuel burnup, fuel specifications and core loading schemes is used for every rod in US-APWR analysis.

Question 45

RESPONSE







Question 47

Was the same seed used to generate the random variables in the ASTRUM analyses presented in MUAP-DC001 Revision 1 "Design Control Document for the US-APWR" and MUAP-DC001 Revision 2 "Design Control Document for the US-APWR"?

RESPONSE

Yes, according to the procedure described in the ASTRUM manual, the same seed was used to generate the random variables in the ASTRUM analyses presented in the US-APWR DCD, MUAP-DC001, both Revisions 1 and 2. However, it should be noted that the same seed was used only when the changes are insignificant.

RESPONSES
to
THE THIRD SET OF REQUESTS FOR ADDITIONAL INFORMATION
for
LARGE BREAK LOCA CODE APPLICABILITY REPORT FOR US-APWR
MUAP-07011-P

(Submitted by UAP-HF-10228)

LBLOCA Confirmatory Analysis RAI:

Please provide plotted data for: (1) PCT, (2) fuel rod gap conductance, (3) fuel rod gap width, (4) fuel centerline and surface temperatures, and (5) fuel cladding inner surface temperature at the limiting core location covering the period from 0 to 100 seconds in the WCOBRA/TRAC LBLOCA reference case run. Provide an explanation for the trends and magnitudes of the behavior seen in those plots relative to the various WCOBRA/TRAC fuel rod models documented in WCAP-16009-P-A Section 7-3 and the fuel and fluid conditions in the region during that period. Of particular interest are explanations relative to the onset of cladding heat-up, the cladding heat-up and cooldown rates, and the causes for the blowdown and reflood cladding temperature maxima.

Response

Figures 1 through 5 are the inquired plotted data at the limiting core location covering the period from 0 to 100 seconds of the reference case described in DCD revision 2. Figures 6 through 10 show the additional plots: (6) Hot Assembly Mass Flow Rates, (7) the amounts of heat transfer into the cladding via fuel gap and into the fluid out of cladding, (8) the Heat Transfer Mode Indicator and (9), (10) Heat Transfer Coefficients, for the trends of the cladding temperature during that period. The digital data for these figures is stored in the OSM (see readme.pdf).

In the first one second after break, fluid surrounding the cladding at the limiting location experiences DNB due to the huge coolant discharge from the core and depressurization at the core. At this moment, the cladding is at the onset of the rapid temperature rise.

In the first 10 seconds after the break, the fuel gap width expands exponentially due to the heat flux from the fuel pellet and the decrease of cooling after the DNB. According to the expansion of the gap width, gap conductance decreases as shown in Figure 2 and 3. Although gap conductance decreases, most of the time in this period, the amount of heat transfer to the cladding via fuel gap is far exceeding that to fluid in the cell from cladding as shown in Figure 7. Thus, cladding temperature increases rapidly

(Figure2).

At approximately 12 seconds, the flow reverses the direction to downward, heat transfer mode changes to Dispersed Flow Film Boiling (DFFB) due to the fluid including entrainment. At the moment, cladding temperature is at onset of cooldown, and the Blowdown PCT appears. During this DFFB mode due to the downward flow, the amount of heat transfer into fluid from cladding exceeds the amount of heat transfer into cladding from fuel as seen in Figures 7 and 8. Therefore, cladding temperature keeps decreasing in that period.

According to decreased downward flow from about 20 seconds, fluid in the limiting cell becomes vapor only, therefore, heat transfer is switched to Single Phase Vapor mode (SPV).

As for the gap conductance, h_{gap} increases due to the gap width reduction, temperature difference between cladding inner surface and fuel pellet outer surface decreases, as a result, the amount of heat transfer to cladding decreases. During the period from about 20 to 37 seconds, both of the amount of heat transfer tends to decrease in Figure 7, compared to each other, the amount of heat transfer into cladding is less than that from cladding, then, cladding temperature increases again.

Reflood phase in the DCD reference case starts at 37 seconds. In this phase, the coolant enters from the bottom of the core, the entrainments generated in the lower cells intermittent flow into the limiting cell, as shown in Figure 6. According to the existence of the entrainment, cladding iteratively experiences the DFFB mode and the SPV mode. Repeated cooling of the DFFB mode prevents the cladding temperature rise caused by the increase of gap conductance in Reflood phase. At the 64 seconds, the gap conductance decrease again due to expansion of the gap width, then, cladding temperature trend turns around and experiences the Reflood PCT. After that, cladding temperature is gradually cooled down till the minimum film boiling temperature.

Reference

- Ref-1: M.E., Nissley, et al., "Realistic Large Break LOCA Evaluation Methodology Using Automated Statistical Treatment of Uncertainty Method (ASTRUM)," WCAP-16009-P-A, January 2005.

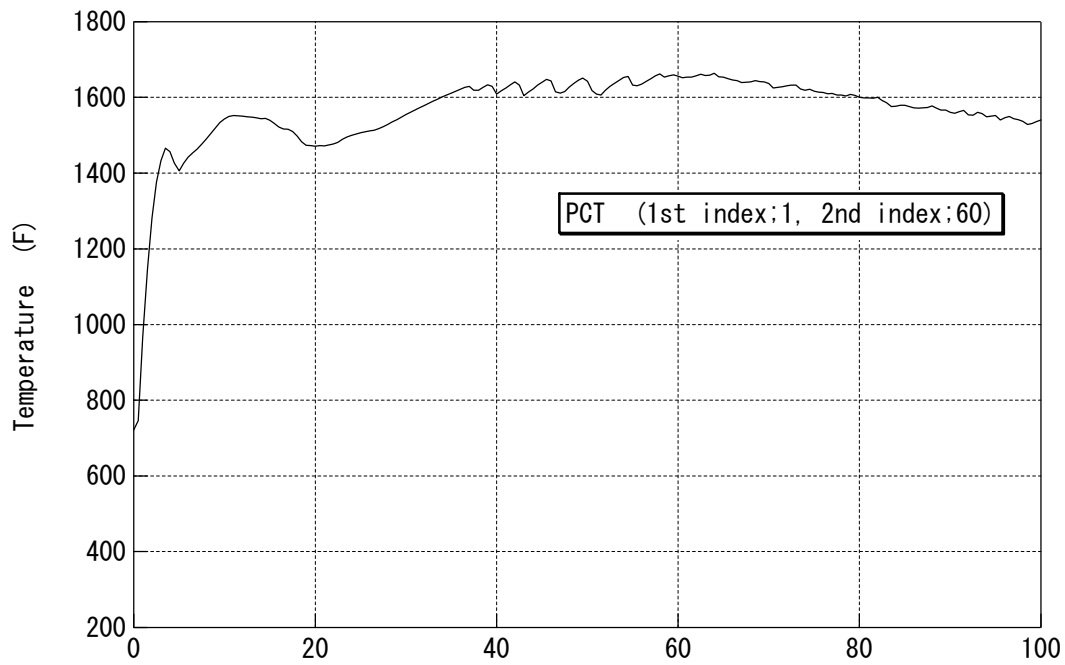


Figure 1-A Peak Cladding Temperature

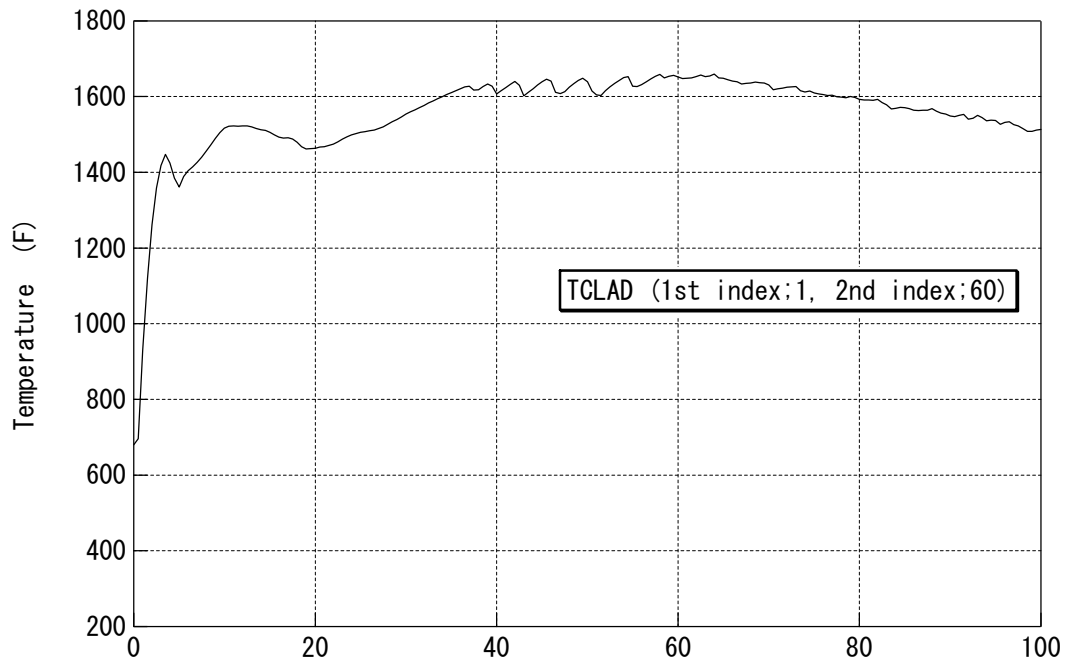


Figure 1-B Cladding Temperature at PCT Location (10.3ft)

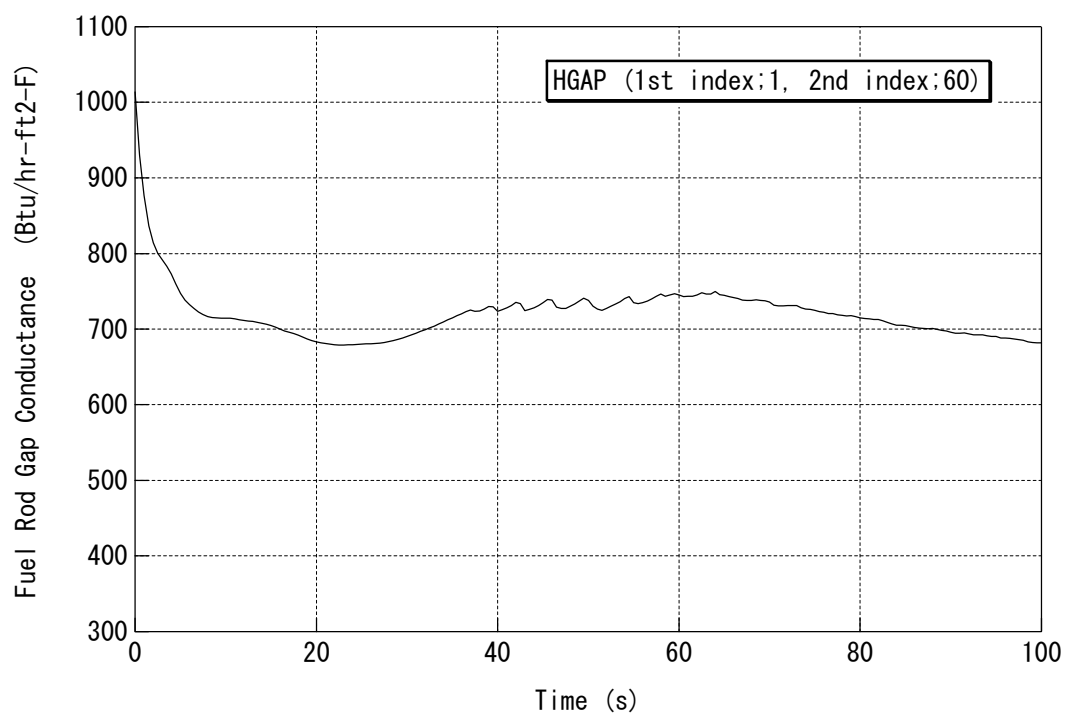


Figure 2 Fuel Rod Gap Conductance at PCT Location (10.3ft)

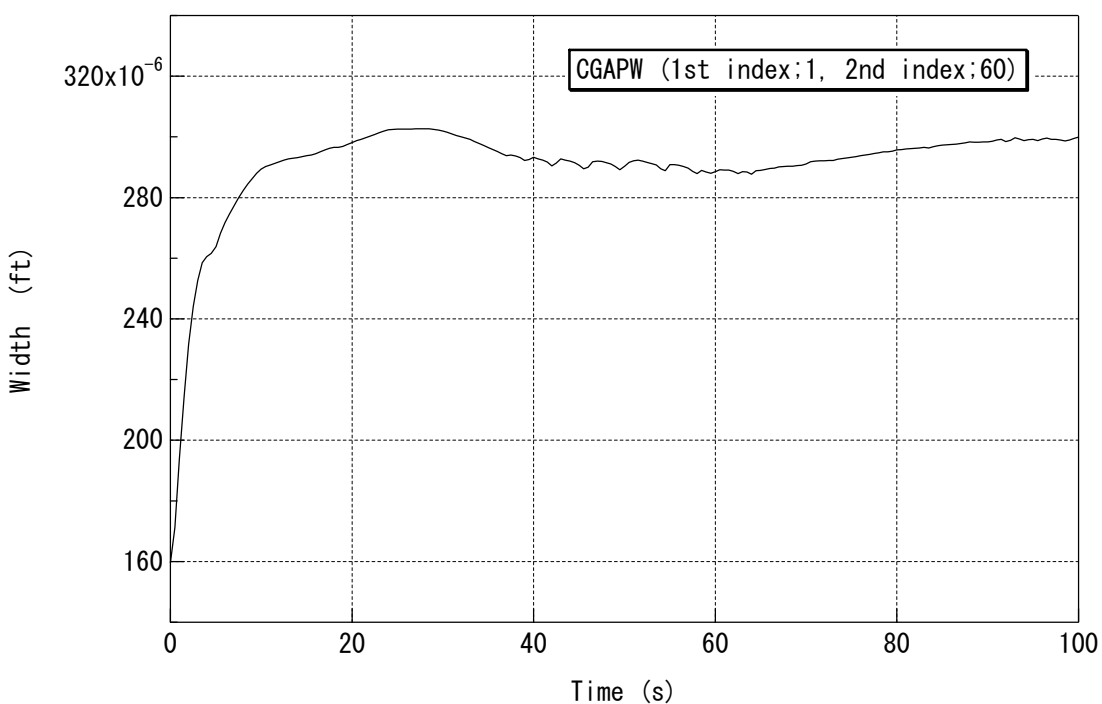


Figure 3 Fuel Rod Gap Width at PCT Location (10.3ft)

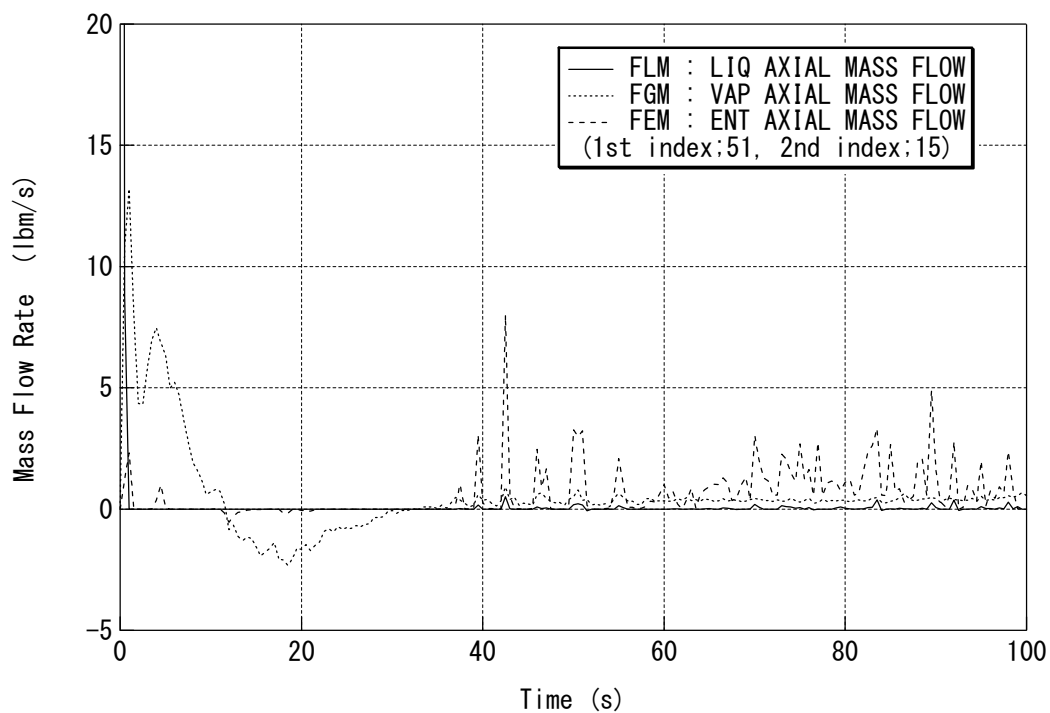


Figure 6 Hot Assembly Mass Flow Rates at PCT Location (cell inlet)



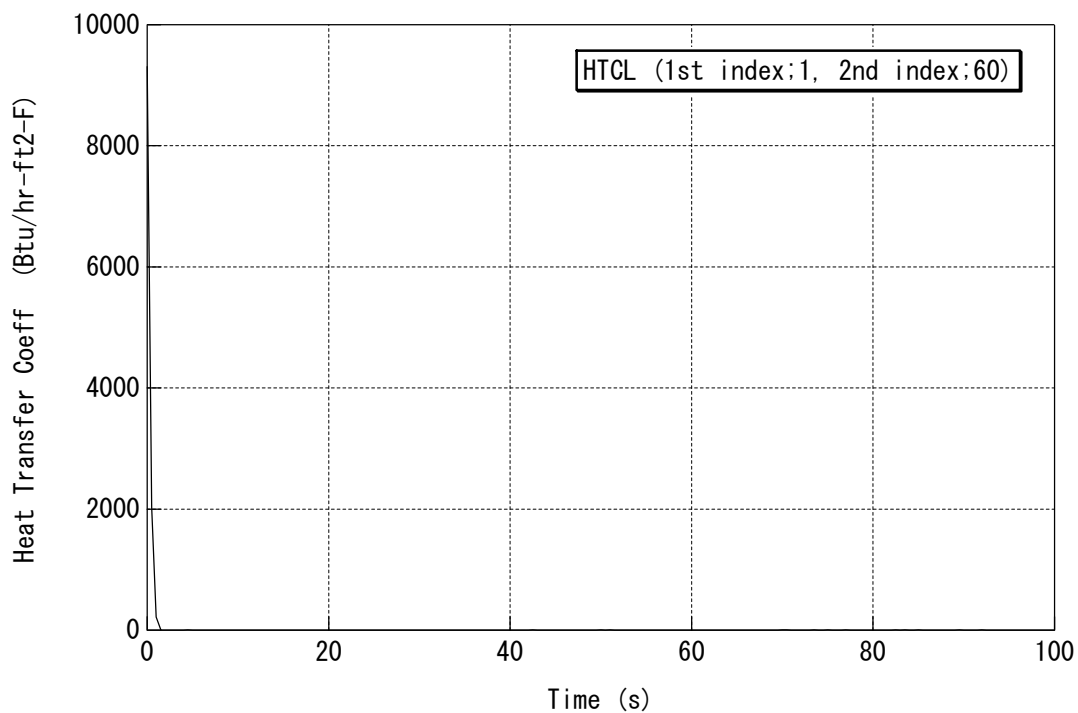


Figure 9 Heat Transfer Coefficient to Liquid

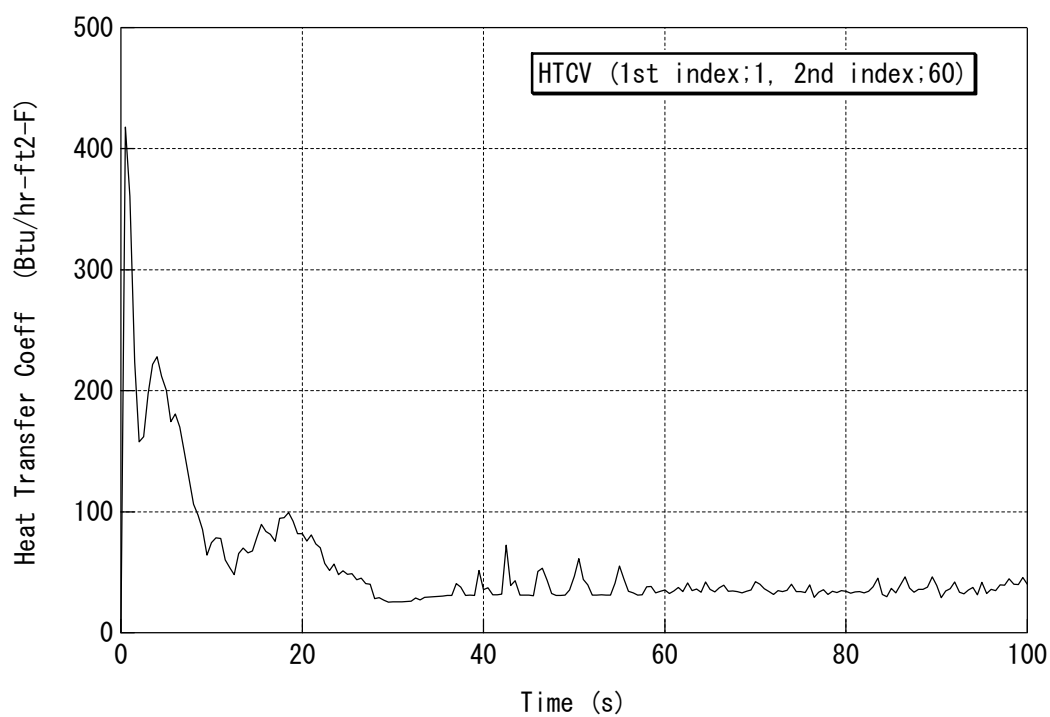


Figure 10 Heat Transfer Coefficient to Vapor